

# CONFERENCE PROCEEDINGS



**ANAND**  
INTERNATIONAL COLLEGE  
OF ENGINEERING

Praveen Agarwal.  
Bhavana Mathur. - Editors

---

# Recent Developments in Engineering & Technology-1

26-27 February, 2021

ISBN 978-81-953996-3-5

# Recent Developments in Engineering & Technology-1

Editor

Praveen Agarwal and Bhavana Mathur

## **Recent Developments in Engineering & Technology-1**

© Praveen Agarwal and Bhavana Mathur

All rights reserved

No part of this publication may be reproduced, stored in a retrieval system or transmitted, in any form or by any means, without prior permission. The views and contents of this book are solely of the authors. Moreover, in the event, the authors have been unable to track any source and if any copyright has been inadvertently infringed, please notify the publisher in writing for corrective action.

ISBN: 978-81-953996-3-5

Second Edition: March 2022

Price: 200 INR

Printed and Published by:

Anand International College of Engineering

Near Kanota, Agra Road, Jaipur

Rajasthan:303012

## Contents

<b>Physicochemical Properties and Sensory Attributes of Hybrid Sweetcorn (<i>Zea Mays L. Var Macho F1</i>) to Different Organic and Inorganic Fertilizers</b> Enrique E. Biñas, Jr. and Ulysses A. Cagasan	1
<b>Efficacy of Rhizome Crude Extracts Organic Pesticide Against Insect-Pests and its Impact on Glutinous Corn (<i>Zea Mays L. Var. Ceratina</i>) Production</b> Enrique E. Biñas Jr.	9
<b>Profitability of Sweet Corn (<i>Zea Mays L. Var Saccharata</i>) Production as Applied with Combined Organic and Inorganic Fertilizers</b> Enrique E. Biñas, Jr. and Ulysses A. Cagasan	19
<b>Prediction Analysis and Forecasting of Stock Price on Google Stocks: An Application</b> Rishabh Singhal and Richa Sharma	28
<b>Soil-Structure Interaction Study on Group Pile over Monopile Foundation</b> Ramesh Gomasa and A.R. Prakash	35
<b>Pushover Analysis of Rc Frame Structure on Sloping Ground Using SAP2000</b> Monika Angral, Manvinder Kingra and Pritpal Kaur	41
<b>Behaviour of Irregular Structures Under Three-Dimensional Earthquake Loading Considering Base Isolation System</b> Raja Suhaib Amin, Amir Hussain Bhat and Hardeep Singh Rai	50
<b>Neonatal Monitoring System: Review and Future Directions</b> Prashant Jani and Seema Mahajan	66
<b>Modeling on Transmission Dynamics of Skin Cancer due to the Exposure of Ultraviolet Radiation</b> Parvin Tahera and Md. Haider Ali Biswas	71
<b>Predicting Employee Turnover with the Modeling of Hybrid Neural Network for Human Resource Management</b> Christopher Francis Britto and Abdul Rahman H Ali	91
<b>Measure Temperature &amp; Humidity on Local Web Server for Home Automation System Using Nodemcu Esp8266 Wi-Fi Module</b> GajendraSinh N. Mori and Priya R. Swaminarayan	97

<b>Internet Of Things: Architecture, Enabling Technologies &amp; Protocols, Applications, Challenges and Future Scope</b> Mahmood Hussain Mir, Sanjay Jamwal and Shahidul Islam	<b>102</b>
<b>Iot Based Remote Monitoring System for Quality Control of Drinking Water at Unmanned Water Stations</b> Tarun Ojha, Jayashri Vajpai and Vinit Mehta	<b>113</b>
<b>Design of Coherent Digital Receiver</b> Jainendra Kumar and Sanjeev Kumar	<b>124</b>
<b>Transfer Learning Based Feature Fusion Approach for Handwritten Digits Recognition of Devanagari Script</b> Danveer Rajpal and Akhil Ranjan Garg	<b>130</b>
<b>Fuzzy Arithmetic Geometric Divergence and its Utility in Pattern Recognition</b> Sapna Gahlot and R. N. Saraswat	<b>138</b>
<b>Analysis of Voltage Stability in Power System: A Research Review</b> Kushketu Kundan Srivastava, Snajiv Kumar and Ajay Kumar	<b>146</b>
<b>Energy Conservation in Educational Institution and Reduction of Electricity Bill by Using IOT.</b> M.Veerasundaram, K. Narmadha and S. Snega	<b>155</b>
<b>Design of Experiment for IOT Based Condition Monitoring and Detection of Hot Spots in Tank of Oil- Immersed Transformers</b> Vinit Mehta, Jayashri Vajpai and Tarun Ojha	<b>169</b>
<b>Application of Deep Learning in Health Informatics: A Review</b> Vinit Mehta and Noopur Shrivastava	<b>181</b>
<b>Application of TOPSIS Optimization Technique in TIG Welding of Mild Steel Plates</b> Prashant Kumar and Bhavana Mathur	<b>190</b>

# **Physicochemical Properties and Sensory Attributes of Hybrid Sweetcorn (*Zea Mays L.* Var Macho F1) to Different Organic and Inorganic Fertilizers**

**Enrique E. Biñas, Jr. and Ulysses A. Cagasan**

**Abstract** Fertilization practices not only influence the growth and yield of sweetcorn but also its physicochemical and sensory attributes. This study was conducted to determine the TSS, TA and pH of sweetcorn and evaluate the sensory qualities of freshly cooked and five 5 - day stored sweetcorn applied with organic and inorganic fertilizers. The experiment was laid out in RCBD with 3 replications. Treatments were as follows :  $T_0$  = Control (without fertilizer applied),  $T_1$  - Inorganic fertilizer at 90-60-60 kg ha<sup>-1</sup> (N, P<sub>2</sub>O<sub>5</sub>, K<sub>2</sub>O),  $T_2$  = 5 t ha<sup>-1</sup> of vermicompost + 45-30-30 kg ha<sup>-1</sup> N, P<sub>2</sub>O<sub>5</sub>, K<sub>2</sub>O,  $T_3$  = 5 t ha<sup>-1</sup> of poultry manure + 45-30-30 kg ha<sup>-1</sup> N, P<sub>2</sub>O<sub>5</sub>, K<sub>2</sub>O,  $T_4$  = 5 t ha<sup>-1</sup> of cow manure + 45-30-30 kg ha<sup>-1</sup> N, P<sub>2</sub>O<sub>5</sub>, K<sub>2</sub>O,  $T_5$  = 5 t ha<sup>-1</sup> of goat manure + 45-30-30 kg ha<sup>-1</sup> N, P<sub>2</sub>O<sub>5</sub>, K<sub>2</sub>O,  $T_6$  = 5 t ha<sup>-1</sup> of mudpress + 45-30-30 kg ha<sup>-1</sup> N, P<sub>2</sub>O<sub>5</sub>, K<sub>2</sub>O,  $T_7$  = Foliar spray (Fermented Golden Snail) + 45-30-30 kg ha<sup>-1</sup> N, P<sub>2</sub>O<sub>5</sub>, K<sub>2</sub>O.

Physicochemical properties of sweetcorn were not affected by the treatments except pH. The pH in sweetcorn grown in all treatments were slightly alkaline. Highest pH of 7.87 was detected from plants applied with combined mudpress and inorganic fertilizers. Lowest pH of 7.17 was detected from plants applied with combined fermented golden snail and inorganic fertilizers. Sensory qualities of sweetcorn either freshly cooked or has been stored for 5 days before cooking were perceived to be “liked moderately” to “like very much”.

**Keywords:** Organic manures, inorganic fertilizer, physicochemical properties, sensory qualities, hybrid sweetcorn

## **1 Introduction**

Corn (*Zea mays L.*) is the second most important cereal crop next to rice grown for human consumption and used as raw materials for different food products. Because of its versatility, it is consumed not only as food for humans and animals but also for industrial and agricultural purposes [1].

Sweetcorn is one of the types of corn, usually grown in smaller scale, but it is becoming popular as snack items and sold in the local markets. The sweet kernels can also be processed into canned products which can be utilized as ingredient for salads, pastries and other processed food products. The sweet kernels contain higher proportions of sugar than starch. Thus, it is boiled “green” which commands reasonably higher price in the local market. It is also the most preferred edible corn because of its nutritional values and health benefits plus its good flavor, aroma and texture [2].

The application of inorganic fertilizer is needed for modern corn varieties to increase yield. However, fertilizers are so expensive nowadays and has a tendency to pollute the environment and decrease production efficiency as well [3]. Hence, combination of organic with the inorganic fertilizer is recommended to minimize the adverse impact on the environment, health, wildlife and water source. A

---

Enrique E. Biñas, Jr.

College of Agriculture and Forestry, Jose Rizal Memorial State University-Tampilisan Campus, ZNAC, Tampilisan, Zamboanga del Norte, PHILIPPINES  
Email Address:enriquebinas@jrmsu.edu.ph

Ulysses A. Cagasan

Department of Agronomy, Visayas State University, Visca, Baybay City, Leyte, PHILIPPINES

sound fertilizer management must attempt to ensure both an enhanced and safe environment; therefore, a balanced fertilization strategy that combines the use of chemical, organic or biofertilizers must be developed and evaluated [4]. Judicious use of organic and inorganic nutrient sources is important to decrease dependence on chemical fertilizers for sustainable high crop production by minimizing nutrient losses to the environment and optimizing nutrient use efficiency [5].

Fertilization practices can influence not only the yield and physical appearance but also the flavor, texture, color, size, shelf life, nutrient and physicochemical content of the crops and product such as total solid soluble (TSS), titratable acidity (TA), pH, etc. [6]. Applying fertilizer materials according to soil test and crop nutrient requirements will provide the basic nutrients needed for high yield and better quality. Nowadays, food quality is influencing the market potential of the commodity as the consumers patronize what is best in their taste [7].

This study uses different organic materials combined with inorganic fertilizers to determine their effects on the total soluble solid (TSS), titratable acidity (TA) and pH of fresh sweetcorn and evaluate the sensory qualities of fresh and five (5) day stored sweetcorn as influenced by organic and inorganic fertilizers.

## 2 Methodology

### 2.1. Experimental Design and Treatments

The experimental area of 857.5 m<sup>2</sup> was prepared to provide good soil condition for seed germination. It was laid out in Randomized Complete Block Design (RCBD) replicated three (3) times with 1 m alleyway between replications and between treatments. There were eight (8) plots measuring 5 m X 4.5 m in each replication. Thus, totaling 24 plots in the experiment with a six rows of sweetcorn in each plot. The treatments were designated as follows:

- T<sub>0</sub> – Control (without fertilizer applied)
- T<sub>1</sub> - Inorganic fertilizer at 90-60-60 kg ha<sup>-1</sup> (N, P<sub>2</sub>O<sub>5</sub>, K<sub>2</sub>O)
- T<sub>2</sub> – 5 t ha<sup>-1</sup> of vermicompost + 45-30-30 kg ha<sup>-1</sup> N, P<sub>2</sub>O<sub>5</sub>, K<sub>2</sub>O
- T<sub>3</sub> – 5 t ha<sup>-1</sup> of poultry manure + 45-30-30 kg ha<sup>-1</sup> N, P<sub>2</sub>O<sub>5</sub>, K<sub>2</sub>O
- T<sub>4</sub> – 5 t ha<sup>-1</sup> of cow manure + 45-30-30 kg ha<sup>-1</sup> N, P<sub>2</sub>O<sub>5</sub>, K<sub>2</sub>O
- T<sub>5</sub> – 5 t ha<sup>-1</sup> of goat manure + 45-30-30 kg ha<sup>-1</sup> N, P<sub>2</sub>O<sub>5</sub>, K<sub>2</sub>O
- T<sub>6</sub> – 5 t ha<sup>-1</sup> of mud press + 45-30-30 kg ha<sup>-1</sup> N, P<sub>2</sub>O<sub>5</sub>, K<sub>2</sub>O
- T<sub>7</sub> – Foliar spray (Fermented Golden Snail) + 45-30-30 kg ha<sup>-1</sup> N, P<sub>2</sub>O<sub>5</sub>, K<sub>2</sub>O

Organic manures were applied in the furrows and incorporated into the soil two (2) weeks before planting at the rate of 5 t ha<sup>-1</sup>. Application of complete fertilizer (14-14-14) was done 10 DAP and urea (46-0-0) 30 DAP. Fermented golden snail were sprayed to plants at 7, 14, 21, 28 and 35 DAP.

Macho F1 hybrid sweetcorn variety was used in the study with 1 seed hill<sup>-1</sup>. Replanting was done 7 DAP. Off-baring 15 DAP, hill-up 30 DAP and handweeding were employed to control weeds. Botanical pesticide derived from tobacco and mild liquid soap was used in controlling insect pests. Diseased plants were uprooted and disposed away from the experimental area.

Sweetcorn ears were detached from the stover during harvest and submitted to the Department of Horticulture and Department of Food Science and Technology, VSU, Visca Baybay City, Leyte for physicochemical analysis and sensory evaluation, respectively. Unhusked and unpacked samples of sweetcorn ears were stored in an ambient condition for 5 days before cooking.

### 2.2. Data Gathered

#### 2.2.1. Evaluation of Physicochemical Properties of Sweetcorn

Five (5) sample of fresh ears were taken from each treatment plot. These were submitted to the Department of Horticulture, VSU, Baybay City, Leyte for the analysis of total soluble solid (TSS), titratable acidity (TA) and pH. Analyses were done using the following procedure:

1. Take 50 grams of fresh kernels and add with 50-100 ml distilled water and homogenized in a blender.
2. Filter the homogenate through a small wad of cotton.
3. Measure pH of the filtrate using the digital pH meter.
4. Measure TSS of the filtrate using a hand refractometer.
5. Calculate actual TSS by multiplying the readings with the dilution factor as follows:

$$\text{Dilution factor} = \frac{\text{Volume of water added (ml)}}{\text{Weight of sample (g)}}$$

6. Pipet 10 ml filtrate to an Erlenmeyer flask or beaker and add 2 drops of 1% phenolphthalein indicator.
7. Titrate with 0.1 N sodium hydroxide (NaOH) to faint pink color. Record the volume of the NaOH and calculate TA using the formula:

$$\% \text{ TA of predominant acid} = \frac{V \times N \times M}{W} \times 100$$

Where: V – volume of NaOH added, ml

N – concentration of NaOH, normality (N)

M – milliequivalent weight of predominant acid g/meq

W – weight equivalent of aliquot, g

$$\frac{\text{Weight of sample, g}}{\text{Weight of sample, g} + \text{vol. of water added, ml}} \times \text{vol. of aliquot}$$

1. **Total Soluble Solid (TSS)** – the amount of solids dissolved within a substance. It is commonly used to measure sugar content in drinks, medicines, fruits and vegetables. Refractometer equipped with a scale, based on the relationship between refractive indices at 20°Bx and the percentage by mass of total soluble solids of a pure aqueous sucrose solution.
2. **Titratable Acidity (TA)** – the total amount of acid in the solution as determined by the titration using a standard solution of sodium hydroxide (titrant). TA is determined by neutralizing the acid present in a known quantity (weight or volume) of food sample.
3. **pH** – measures the levels of acid and alkaline in a substance on a scale from 0 to 14. A high pH value indicates higher alkaline content, and a low pH value signals higher acidity. The higher the pH, it turns fruits sweeter [8].
4. **Statistical Tool Used** – means of the physicochemical data gathered were computed and analysis of variance (ANOVA) was done using the Statistical Tool for Agricultural Research (STAR). Treatment mean comparison was done using Tukey's or Honestly Significant Difference (HSD) test.

## 2.2.2. Sensory Analysis

### 1. Cooking of sweetcorn samples

- 1.a. Five (5) sample ears were cooked freshly after harvest at 2:1/2 kg to liter of water for 20 minutes. Sensory evaluation was done 15 minutes after cooking.
- 1.b. Another 5 samples were stored for 5 days and cooked at 2:1/2 kg to liter of water for 20 minutes. Sensory testing was done ½ hour after cooking. Sample ears were submitted to the Department of Food Science and Technology for sensory evaluation.
2. **Sensory Evaluation** – sensory evaluation of freshly harvested and 5 day stored cooked corn were carried out by employing 42 food technology students as panelist. Each panelist was given 4 samples to be tested. The samples were arranged randomly in each presentation to equalize sample sequence effect on preference. The color, aroma, texture and taste were evaluated using a combination of quality description as perceived by the panelist I combination with 9-point Hedonic Scale particularly for the acceptability evaluation. Samples were served at an ambient temperature in coded plastic cups. Potable drinking water was provided for rinsing the mouth of the panelists in between testing of samples. Incomplete Block Design (IBD) set plan by [9] was used during the sensory evaluation. Since there are 8 treatments tested, the plan of t=8, k=4, r=7, b= 14, λ=3, E= 0.86 Type I was followed. Of these, **t** stands for treatments, **k** refers to the number of units per block or panelist, **r** refers to the number of replications based on IBD, **b** refers to the block, **λ** is the times a block be repeated, and **E** is the efficiency factor.

3. **Statistical Analysis** – the sensory scores was subjected to statistical analysis. One-way analysis of variance was used to test the significant difference between treatments. Treatment comparison

among significant parameters was done through Duncan's Multiple Range Test. The analysis of data was ran through IBM SPSS Statistics 8.0.

### 3. Results and Discussion

#### 3.1. Physicochemical Properties of Sweetcorn

Physicochemical properties of sweetcorn applied with different organic materials combined with inorganic fertilizers is presented in Table 1. Results revealed that only the pH of hybrid sweetcorn ears were affected by the different combinations of organic and inorganic fertilizers. The TSS and TA were comparable in all treatment combinations.

Highest pH value (7.87) was obtained from plants applied with combined mudpress and inorganic fertilizers ( $T_6$ ) comparable to other combinations of organic manures and inorganic fertilizers ( $T_2$ ,  $T_3$ ,  $T_4$  and  $T_5$ ) relative to the controls ( $T_0$ ,  $T_1$ ). On the other hand, plants applied with combined fermented golden snail and inorganic fertilizers ( $T_7$ ) got the lowest pH value (7.17). [10] also found that application of combined fermented golden snail and inorganic fertilizers gave the lowest pH value on yellow corn compared to other combinations of organic and inorganic fertilizers. This is because of the extra acidity in muscovado sugar mixed to golden snail during fermentation thus, resulted in corn ears with low pH value. The significant increase in pH of sweetcorn applied with combined mudpress and inorganic fertilizers ( $T_6$ ) contributed to the better taste of sweetcorn (Table 2). [11] mentioned that the higher the pH, the sweeter is the taste.

**Table 1. Physicochemical properties of hybrid sweetcorn applied with different organic materials combined with inorganic fertilizers**

Treatment	TSS (°Brix)	TA (%)	pH
$T_0$ - Control (without fertilizer applied)	1.90	0.0017	7.47ab
$T_1$ - 90-60-60 kg ha <sup>-1</sup> N, P <sub>2</sub> O <sub>5</sub> , K <sub>2</sub> O	1.67	0.0013	7.67ab
$T_2$ - 5 t ha <sup>-1</sup> vermicompost + 45-30-30 kg ha <sup>-1</sup> N, P <sub>2</sub> O <sub>5</sub> , K <sub>2</sub> O	1.87	0.0013	7.57ab
$T_3$ - 5 t ha <sup>-1</sup> poultry manure + 45-30-30 kg ha <sup>-1</sup> N, P <sub>2</sub> O <sub>5</sub> , K <sub>2</sub> O	1.67	0.0010	7.37ab
$T_4$ - 5 t ha <sup>-1</sup> cow dung + 45-30-30 kg ha <sup>-1</sup> N, P <sub>2</sub> O <sub>5</sub> , K <sub>2</sub> O	1.87	0.0023	7.27ab
$T_5$ - 5 t ha <sup>-1</sup> goat manure + 45-30-30 kg ha <sup>-1</sup> N, P <sub>2</sub> O <sub>5</sub> , K <sub>2</sub> O	2.03	0.0010	7.77ab
$T_6$ - 5 t ha <sup>-1</sup> mudpress + 45-30-30 kg ha <sup>-1</sup> N, P <sub>2</sub> O <sub>5</sub> , K <sub>2</sub> O	2.10	0.0020	7.87a
$T_7$ - Fermented golden snail (foliar spray) + 45-30-30 kg ha <sup>-1</sup> N, P <sub>2</sub> O <sub>5</sub> , K <sub>2</sub> O	2.10	0.0027	7.17b
C.V. (%)	16.65	35.86	3.20

Treatment means with the same and without letter designations are not significantly different at 0.05, HSD and ANOVA, respectively.

#### 3.2. Sensory Evaluation of Sweetcorn

The sensory attributes of hybrid sweetcorn (freshly cooked and stored for 5 days before cooking) are presented in Tables 2 and 3. Results revealed that sensory attributes of sweetcorn either in freshly cooked or after 5 days storage were not affected significantly by the application of organic materials combined with inorganic fertilizers. Thus, the color, taste, aroma and texture of cooked sweetcorn as perceived by the respondents and reflected on the acceptability scores did not differ significantly among treatments.

Both freshly cooked sweetcorn and 5-day stored before cooking were closely perceived to be "liked moderately" to "like very much". This implies that it is acceptable to the consumers and advantageous for traders who will engage in marketing boiled sweetcorn.

**Table 2. Sensory attributes of hybrid sweetcorn applied with different organic materials combined with inorganic fertilizers**

Treatment	Color <sup>ns</sup>	Taste <sup>ns</sup>	Aroma <sup>ns</sup>	Texture <sup>ns</sup>
Freshly cooked sweetcorn				
T <sub>0</sub>	Golden yellow to yellow	Slightly sweet to sweet	With pleasant odor	Slightly hard
T <sub>1</sub>	Golden yellow to yellow	Slightly sweet	With pleasant odor	Slightly hard
T <sub>2</sub>	Golden yellow	Slightly sweet	With pleasant odor	Slightly hard
T <sub>3</sub>	Golden yellow	slightly sweet	With pleasant odor	Slightly hard
T <sub>4</sub>	Golden yellow	Sweet to slightly sweet	With pleasant odor	Slightly hard
T <sub>5</sub>	Golden yellow	Slightly sweet to sweet	With pleasant odor	Slightly hard
T <sub>6</sub>	Golden yellow	Sweet	With pleasant odor	Slightly hard
T <sub>7</sub>	Golden yellow	Slightly sweet	With pleasant odor	Slightly hard
5-day stored cooked sweetcorn				
T <sub>0</sub>	Golden yellow	Slightly sweet	With pleasant odor	Slightly hard
T <sub>1</sub>	Golden yellow	Bland to slightly sweet	With pleasant odor	Slightly hard
T <sub>2</sub>	Golden yellow	Slightly sweet	With pleasant odor	Slightly hard
T <sub>3</sub>	Golden yellow	slightly sweet	With pleasant odor	Slightly hard
T <sub>4</sub>	Golden yellow	Slightly sweet	With pleasant odor	Slightly hard
T <sub>5</sub>	Golden yellow	Slightly sweet	With pleasant odor	Slightly hard
T <sub>6</sub>	Golden yellow	Sweet to slightly sweet	With pleasant odor	Slightly hard
T <sub>7</sub>	Golden yellow	Slightly sweet	With pleasant odor	Slightly hard

**Sensory Description:**

Color	Taste	Aroma	Texture
1 – slightly yellow	1 – bland	1 – with unpleasant odor	1 – hard
2 – yellow	2 – slightly sweet	2 – with pleasant odor	2 – slightly hard
3 – golden yellow	3 – sweet	3 – with strong pleasant odor	3 – sticky 4 – slightly sticky 5 – soft

**Legend:**

T<sub>0</sub> = Control (without fertilizer applied)

T<sub>1</sub> = 90-60-60 kg ha<sup>-1</sup> N, P<sub>2</sub>O<sub>5</sub>, K<sub>2</sub>O

T<sub>2</sub> = 5 t ha<sup>-1</sup> vermicompost + 45-30-30 kg ha<sup>-1</sup> N, P<sub>2</sub>O<sub>5</sub>, K<sub>2</sub>O

T<sub>3</sub> = 5 t ha<sup>-1</sup> poultry manure + 45-30-30 kg ha<sup>-1</sup> N, P<sub>2</sub>O<sub>5</sub>, K<sub>2</sub>O

T<sub>4</sub> = 5 t ha<sup>-1</sup> cow dung + 45-30-30 kg ha<sup>-1</sup> N, P<sub>2</sub>O<sub>5</sub>, K<sub>2</sub>O

T<sub>5</sub> = 5 t ha<sup>-1</sup> goat manure + 45-30-30 kg ha<sup>-1</sup> N, P<sub>2</sub>O<sub>5</sub>, K<sub>2</sub>O

T<sub>6</sub> = 5 t ha<sup>-1</sup> mudpress + 45-30-30 kg ha<sup>-1</sup> N, P<sub>2</sub>O<sub>5</sub>, K<sub>2</sub>O

T<sub>7</sub> = Fermented golden snail (foliar spray) + 45-30-30 kg ha<sup>-1</sup> N, P<sub>2</sub>O<sub>5</sub>, K<sub>2</sub>O

Table 3 shows that acceptability ratings in all aspects of sensory of freshly cooked sweetcorn were relatively the same with the 5-day stored before cooking. It implies that storing unhusked and unpacked sweetcorn for 5 days in an ambient condition maintains its color, taste, aroma and taste. However, it is advisable not to dehusk the sweetcorn during harvest to preserve its marketing potential especially when it is to be stored. If it is stored longer than 5 days, it may become bland because sugar will turn into starch especially when it is dehusked [12].

**Table 3. Acceptability ratings from sensory evaluation of sweetcorn applied with different organic materials combined with inorganic fertilizers**

Treatment	Color <sup>ns</sup>		Taste <sup>ns</sup>		Aroma <sup>ns</sup>		Texture <sup>ns</sup>		General Acceptability <sup>ns</sup>	
	Freshly cooked	5-day stored cooked	Freshly cooked	5-day stored cooked	Freshly cooked	5-day stored cooked	Freshly cooked	5-day stored cooked	Freshly cooked	5-day stored cooked
T <sub>0</sub>	7.77	7.70	7.67	6.60	7.37	7.20	7.50	7.13	7.47	7.20
T <sub>1</sub>	7.73	7.47	7.60	6.43	7.47	6.80	7.40	6.93	7.30	6.83
T <sub>2</sub>	8.07	7.90	7.60	7.07	7.60	7.50	7.37	7.37	7.53	7.70
T <sub>3</sub>	8.00	7.77	7.73	6.70	7.53	6.97	7.50	7.03	7.63	7.33
T <sub>4</sub>	8.03	7.70	7.60	6.80	7.50	6.97	7.40	6.87	7.63	7.20
T <sub>5</sub>	7.77	7.77	7.60	7.03	7.60	6.97	7.50	6.80	7.50	7.17
T <sub>6</sub>	7.97	7.67	7.61	7.17	7.39	7.03	7.29	6.90	7.52	7.17
T <sub>7</sub>	7.90	7.43	7.72	6.97	7.55	6.93	7.34	7.33	7.41	7.13
Sig.	0.55	0.89	1.00	0.65	1.00	0.77	1.00	0.65	0.89	0.16

Acceptability ratings

1-dislike extremely	4-dislike slightly	7-like moderately
2-dislike very much	5- neither like nor dislike	8-like very much
3-dislike moderately	6-like slightly	9-like extremely

Legend:

T<sub>0</sub> = Control (without fertilizer applied)T<sub>1</sub> = 90-60-60 kg ha<sup>-1</sup> N, P<sub>2</sub>O<sub>5</sub>, K<sub>2</sub>OT<sub>2</sub> = 5 t ha<sup>-1</sup> vermicompost + 45-30-30 kg ha<sup>-1</sup> N, P<sub>2</sub>O<sub>5</sub>, K<sub>2</sub>OT<sub>3</sub> = 5 t ha<sup>-1</sup> poultry manure + 45-30-30 kg ha<sup>-1</sup> N, P<sub>2</sub>O<sub>5</sub>, K<sub>2</sub>OT<sub>4</sub> = 5 t ha<sup>-1</sup> cow dung + 45-30-30 kg ha<sup>-1</sup> N, P<sub>2</sub>O<sub>5</sub>, K<sub>2</sub>OT<sub>5</sub> = 5 t ha<sup>-1</sup> goat manure + 45-30-30 kg ha<sup>-1</sup> N, P<sub>2</sub>O<sub>5</sub>, K<sub>2</sub>OT<sub>6</sub> = 5 t ha<sup>-1</sup> mudpress + 45-30-30 kg ha<sup>-1</sup> N, P<sub>2</sub>O<sub>5</sub>, K<sub>2</sub>OT<sub>7</sub> = Fermented golden snail (foliar spray) + 45-30-30 kg ha<sup>-1</sup> N, P<sub>2</sub>O<sub>5</sub>, K<sub>2</sub>O

Figure 1 shows the appearance of freshly cooked and 5-day stored sweetcorn before cooking. It was observed that there is a noticeable difference in color between freshly cooked and 5-day stored green corn before cooking. Freshly cooked sweetcorn was slightly lighter than those stored for 5 days. [13] reported that the longer the storage, the darker is the color of sweetcorn.



**Figure 1. Appearance of freshly cooked and 5-day stored sweetcorn before cooking**

Legend:

T<sub>0</sub> = Control (without fertilizer applied)

T<sub>1</sub> = 90-60-60 kg ha<sup>-1</sup> N, P<sub>2</sub>O<sub>5</sub>, K<sub>2</sub>O

T<sub>2</sub> = 5 t ha<sup>-1</sup> vermicompost + 45-30-30 kg ha<sup>-1</sup> N, P<sub>2</sub>O<sub>5</sub>, K<sub>2</sub>O

T<sub>3</sub> = 5 t ha<sup>-1</sup> poultry manure + 45-30-30 kg ha<sup>-1</sup> N, P<sub>2</sub>O<sub>5</sub>, K<sub>2</sub>O

T<sub>4</sub> = 5 t ha<sup>-1</sup> cow dung + 45-30-30 kg ha<sup>-1</sup> N, P<sub>2</sub>O<sub>5</sub>, K<sub>2</sub>O

T<sub>5</sub> = 5 t ha<sup>-1</sup> goat manure + 45-30-30 kg ha<sup>-1</sup> N, P<sub>2</sub>O<sub>5</sub>, K<sub>2</sub>O

T<sub>6</sub> = 5 t ha<sup>-1</sup> mudpress + 45-30-30 kg ha<sup>-1</sup> N, P<sub>2</sub>O<sub>5</sub>, K<sub>2</sub>O

T<sub>7</sub> = Fermented golden snail (foliar spray) + 45-30-30 kg ha<sup>-1</sup> N, P<sub>2</sub>O<sub>5</sub>, K<sub>2</sub>O

## Conclusion

Application of different organic materials combined with inorganic fertilizers did not give significant differences among TSS and TA of sweetcorn. However, pH of sweetcorn was affected significantly by the combination of organic and inorganic fertilizers. All plants applied with different combinations of organic manures and inorganic fertilizers had pH values above neutral but relatively higher than those in T<sub>7</sub> (combined fermented golden snail and inorganic fertilizers). However, plants applied with combined mudpress and inorganic fertilizers (T<sub>6</sub>) had significantly higher pH than those applied with combined fermented golden snail and inorganic fertilizers (T<sub>7</sub>).

Likewise sensory qualities (color, taste, aroma, and texture) of sweetcorn either freshly cooked or had undergone storage for 5 days before cooking were not affected by the application of different organic materials combined with inorganic fertilizers. All cooked sweetcorn were perceived to be “liked moderately” to ‘like very much’.

## Recommendation

A similar study may be conducted to verify further the physicochemical properties and sensory qualities of sweetcorn and to vary the levels of organic and inorganic fertilizers. Likewise, longer storage period before cooking sweetcorn may be done for further checking of the physicochemical properties and sensory evaluation.

## Acknowledgment

The Authors thank and acknowledge the Department of Science and Technology for funding this research.

## References

- [1] Sailer, L. 2012. The Importance of Corn Journal. Industry News. The Field Position. Retrieved from <http://www.thefieldposition.com/2012/06/the-importance-of-corn/>
- [2] Makhlof, J., J. Zee, N. Tremblay, A. Bélanger, M. H. Michaud and Gosselin, A. 1995. Some nutritional characteristics of beans, sweet corn and peas (raw, canned and frozen) produced in the province of Quebec. Food research international, 28(3), 253-259.
- [3] Fageria, N. K. 2007. Green manuring in crop production. J Plant Nutrition 30: 691-719.
- [4] Chen, J. H. 2006. The combined use of chemical and organic fertilizers and/or biofertilizer for crop growth and soil fertility. In International workshop on sustained management of the soil-rhizosphere system for efficient crop production and fertilizer use. Vol. 16, p. 20.
- [5] Akhtar, M., A. Naeem, J. Akhter, S. A. Bokhari and Ishaque, W. 2011. Improvement in nutrient uptake and yield of wheat by combined use of urea and compost. Soil & Environment, 30: 45-49.
- [6] Hornick, S. B. 1992. Factors affecting the nutritional quality of crops. American Journal of Alternative Agriculture, 7(1-2), 63-68.
- [7] Hornick, S. B. 1992. Factors affecting the nutritional quality of crops. American Journal of Alternative Agriculture, 7(1-2), 63-68.
- [8] Barrett, D. M., J. C. Beaulieu and R. Shewfelt. 2010. Color, flavor, texture, and nutritional quality of fresh-cut fruits and vegetables: desirable levels, instrumental and sensory measurement, and the effects of processing. Critical reviews in food science and nutrition, 50(5), 369-389.
- [9] Cochran, W. G. and Cox, G. M. 1957. Experimental Designs, second edition. ISBN: 978-0-471-54567-5. 640 pp.
- [10] Deocampo, J. B. 2014. Physicochemical properties of yellow corn (*Zea mays* L.) as influenced by the application of different organic materials combined with inorganic fertilizers. Unpublished undergraduate thesis. Capiz State University. Pp 107.
- [11] Barrett, D. M., J. C. Beaulieu and R. Shewfelt. 2010. Color, flavor, texture, and nutritional quality of fresh-cut fruits and vegetables: desirable levels, instrumental and sensory measurement, and the effects of processing. Critical reviews in food science and nutrition, 50(5), 369-389.
- [12] Theuer, R. C. 2006. Do organic fruits and vegetables taste better than conventional fruits and vegetables? State of Science Review, The Organic Center. 50.
- [13] Christensen, E. 2008. Food science: When sweetcorn is not sweet. Retrieved from <http://www.thekitchn.com/food-science-when-sweet-corn-is-60006>.

# **Efficacy of Rhizome Crude Extracts Organic Pesticide against Insect-pests and its Impact on Glutinous Corn (*Zea mays* L. var. *ceratina*) Production**

**Enrique E. Biñas Jr.**

**Abstract** The intractable increasing cost of synthetic pesticides is certainly intense in the coming production years. Looking into this viewpoint the farmers have to look for alternative actions to withstand their farming business profitability. Rhizome crude extracts can be an alternative for synthetic pesticides. This study was conducted to assess the effect of rhizome crude extracts against glutinous corn seedling maggots, corn earworm, corn borer, armyworm, and aphids; evaluate the effect of rhizome crude extracts on the growth and yield of glutinous corn, and determine the profitability of glutinous corn production using rhizome plants as a source of organic pesticide. The treatments were as follows: T<sub>0</sub> – No pesticide applied; T<sub>1</sub> – Potable water alone; T<sub>2</sub> – Ginger crude extracts; T<sub>3</sub> – Turmeric crude extracts; T<sub>4</sub> – Galangal crude extracts; and T<sub>5</sub> – Shampoo ginger crude extracts. Results revealed that insect-pests and their damage on glutinous corn crop were significantly lessened by the application of rhizome crude extracts regardless of sources. This contributed to the significant growth performance of treated plants with rhizome crude extracts thus obtained a profitable yield compared to those plants without any pesticide applied.

**Keywords:** Glutinous Corn, Growth and Yield, Pesticide, Profitability, Rhizome Crude Extracts

## **1. Introduction**

Corn is one of the most important cereal grains in the world [1]. It is considered a versatile crop because it is not only consumed by humans and animals but also used as raw materials for industrial and agricultural purposes [2].

Glutinous corn is one of the types of corn. It is considered as one of the main sources of income of the farmers [3]. However, glutinous corn is prone to common corn insect-pests. It might be the reason why glutinous corn decreased its production thus led the farmers to have a problem raising this crop [4; 5].

The trending insect-pest in corn nowadays is the fall armyworm. This pest brought serious damage to the corn crop [6]. Other insect-pests such as corn seedling maggots, corn earworm, corn borer, etc. also contributed to the reduction of corn production [7]. There are many recommended synthetic pesticides for corn [8], however, it is expensive and there is a tendency to pollute the environment and may be dangerous to human health.

Proper crop protection is important to attain better yields while eliminating the negative effects on the environment and human health. Many articles revealed that there are a lot of organic pesticides as an alternative for synthetic pesticides, one of which is botanical crude extracts from plants that have pesticidal properties. Rhizome plants are discovered to be the best sources of botanical pesticides [9; 10]. [11] studied the insecticidal constituents of rhizome plants. He found that there are compounds that have contact toxicity against larvae of the polyphagous insect-pest *Spodoptera littoralis*. Nine compounds including the most active sesquiterpenoids xanthorrhizol and furanodienone showed pronounced toxicity against neonate larvae of *S. littoralis* in a contact residue bioassay. It means to say that rhizome plants have strong pesticidal properties and has been proven that could control insect-pests (12; 13; 14]. This can be proof that rhizome crude extracts can be used as an organic pesticide for crops.

Enrique Elisan Biñas, Jr.

College of Agriculture and Forestry, Jose Rizal Memorial State University, Znac, Tampilisan, Zamboanga del Norte, PHILIPPINES

Email Address: [enriquebinas@jrmsu.edu.ph](mailto:enriquebinas@jrmsu.edu.ph)

The intractable increasing cost of synthetic pesticides is certainly intense in the coming production years. Looking into this viewpoint the farmers have to look for alternative actions to withstand their farming business profitability. President Gloria Macapagal Arroyo signed Executive Order 481 on the Promotion and Development of Organic Agriculture in the Philippines on December 27, 2005. Then, Former Agriculture Secretary Domingo F. Panganiban signed Administrative Order No. 9 series of 2006 or the Implementing Rules and Regulations (IRR) of EO 481 [15]. The Department of Agriculture has come up with programs and projects in support of EO 481. Thus, the application of bio-organic inputs such as botanical pesticides on crops is highly encouraged in response to the said program.

Since there are limited studies on rhizome crude extracts as an alternative organic pesticide, hence this study was conducted to (1) assess the effect of rhizome crude extracts against glutinous corn seedling maggots, corn earworm, corn borer, armyworm, and aphids; (2) evaluate the effect of rhizome crude extracts on the growth and yield of glutinous corn, and (3) determine the profitability of glutinous corn production using rhizome plants as a source of organic pesticide.

## **2. Materials and methods**

### **2.1. Land Preparation**

An area of 647.5 m<sup>2</sup> was plowed and harrowed twice at the weekly interval to pulverize the soil. This was done to incorporate the weeds in the soil and provide good soil conditions for seed germination. Furrows were made at a distance of 0.75 m between rows after the second harrowing.

### **2.2. Experimental Design and Treatments**

The experimental area of 647.5 m<sup>2</sup> was laid out in Randomized Complete Block Design (RCBD) with three replications. Each replication was divided into six (6) plots to measure 5 m x 4.5 m each. There were 18 plots in the experiment. Each plot had six rows. Each row had 20 hills of glutinous corn. An alleyway of 1 m was provided between replications and between treatment plots including at the outside portions of the plots to facilitate farm operations and data gathering. The treatments were designated as follows:

T<sub>0</sub> – No pesticide applied

T<sub>1</sub> – Potable water alone

T<sub>2</sub> – Ginger extracts (*Zingiber officinale*)

T<sub>3</sub> – Turmeric extracts (*Curcuma longa*)

T<sub>4</sub> – Galangal extracts (*Alpinia galanga*)

T<sub>5</sub> – Shampoo ginger extracts (*Zingiber zerumbet*)

### **2.3. Application of Treatments**

The rhizome crude extracts were applied as foliar spray diluted at a ratio of 5 tablespoons to 1 liter of water and sprayed to plants at weekly intervals. This was done at 7, 14, 21, 28, 35, 42, and 49 days after planting (DAP). The dilution rate of rhizome crude extracts varies in each application schedule by increasing the amount as the plant grew. The older the plants, the higher is the dilution rate of the treatments. The actual amount of treatments is 1L per plot at the start of the application and this was increased by adding another liter in every week of application.

### **2.4. Application of Fertilizer**

The organic fertilizer used in the experiment was fully decomposed chicken dung. It was applied uniformly in the furrows and were incorporated into the soil in each treatment plot two weeks before planting (WBP) at the rate of 10 t ha<sup>-1</sup> [16].

### **2.5. Identification of Insect-pests**

Before the actual experiment, an area of 500 m<sup>2</sup> was planted with glutinous corn crop purposely to observe and identify the common insect-pests and their damage on glutinous corn. This was conducted until the boiling stage. Five (5) insect-pests were commonly observed attacking the crop. These are corn maggot, earworm, corn borer, armyworm, and aphids. These insect-pests and their damage on glutinous corn crops were identified by the Entomologists.

## 2.6. Data Gathered and Statistical Tool Used

Data on insect-pests incidence and their damage on glutinous corn, agronomic characteristics, harvest index, and yield of glutinous corn crop were gathered. Analysis of variance (ANOVA) was done using the Statistical Tool for Agricultural Research (STAR). Treatment means comparison was done using the Tukey's or Honestly Significant Difference (HSD) test. Return on investment (ROI) was also computed to determine the profitability of glutinous corn production with the use of rhizome crude extracts as an alternative pesticide.

## 3. Results and discussion

### 3.1. Insect-pests Incidence

Table 1 shows the effects of rhizome crude extracts on insect-pests incidence. Insect-pests on glutinous corn were affected by different rhizome crude extracts. Statistical analysis revealed that continuous application of rhizome crude extracts from 7 DAP up to 49 DAP at weekly intervals reduced the incidence of insect-pests on glutinous corn compared to those plants without any pesticides applied.

Incidence of corn seedling maggots had significantly decreased at a range of 79 – 85 % (**Table 1**) in plants applied with rhizome extracts from 1 day before and 3 days after the first application of treatments (6 and 10 DAP, respectively) regardless of sources. On the other hand, those plants without any pesticides applied, corn seedling maggots increased their population at a range of 25 – 30 % (**Table 1**). Maggots occurred in an early season. They rapidly attacked the crop most likely during the damp, and cool seasons [17]. This pest can easily be controlled by organic pesticides [18]. [19] reported that rhizome crude extracts also controlled maggots and larvae on crops. This result is the same with the findings of [20] that rhizome crude extracts also controlled the wrigglers and to the findings of [21] that rhizome extracts controlled corn grain weevils and other destructive larvae and insects. Apparently, the application of rhizome crude extracts could effectively control the population of maggots [22].

Moreover, rhizome extracts regardless of sources significantly controlled the incidence of earworms, corn borers, armyworms and minimized the occurrence of aphids on glutinous corn from 30 DAP to harvest at a range of 43 – 46 %, 33 – 38 %, 36 – 46 %, and 25 – 39 %, respectively (**Table 1**). However, these insects rapidly multiplied in plants without pesticides applied at a range of 75 – 78 %, 32 – 47 %, 51 – 59 %, and 19 – 21 %, respectively (**Table 1**). Earworm, corn borer, armyworm, and aphids are common insect pests in corn. They occurred and attacked corn even at the whorl stage. Their later generations are mostly found in corn ears and leaves [23]. The result of this study proves the findings of [24] that biopesticides including rhizome extracts can lessen their population at any stage of crops. This is also supported by [25] that pest management using organic inputs like rhizome is effective to reduce the population of insect-pests. Furthermore, [26] revealed that the bioactivity of rhizome extracts can minimize the incidence of the common insect-pests of various crops including corn. Proper

**Table 1. Effect of rhizome extracts on percent (%) change of corn seedling maggots from 6 DAP to 10 DAP and earworms, corn borer, armyworm incidence, and plants with aphids occurrence on glutinous corn from 30 DAP to harvest**

Insect-pest	Original No. of population (6 DAP)	New No. of Population (10 DAP)	Population Change (%)
Corn seedling maggots			
T <sub>0</sub>	32.00	41.67b	30.22b
T <sub>1</sub>	33.67	42.00b	24.74b
T <sub>2</sub>	34.00	5.33a	-84.32a
T <sub>3</sub>	34.67	7.33a	-78.86a
T <sub>4</sub>	35.67	5.00a	-85.98a
T <sub>5</sub>	35.33	7.00a	-80.19a
Earworm (30 DAP)			
T <sub>0</sub>	24.33b	43.33b	78.09b
T <sub>1</sub>	24.00b	42.00b	75.00b
T <sub>2</sub>	12.33a	7.00a	-43.23a
T <sub>3</sub>	12.33a	7.00a	-43.23a
T <sub>4</sub>	12.33a	6.67a	-45.90a
T <sub>5</sub>	24.33a	5.67a	-54.01a
Corn borer			

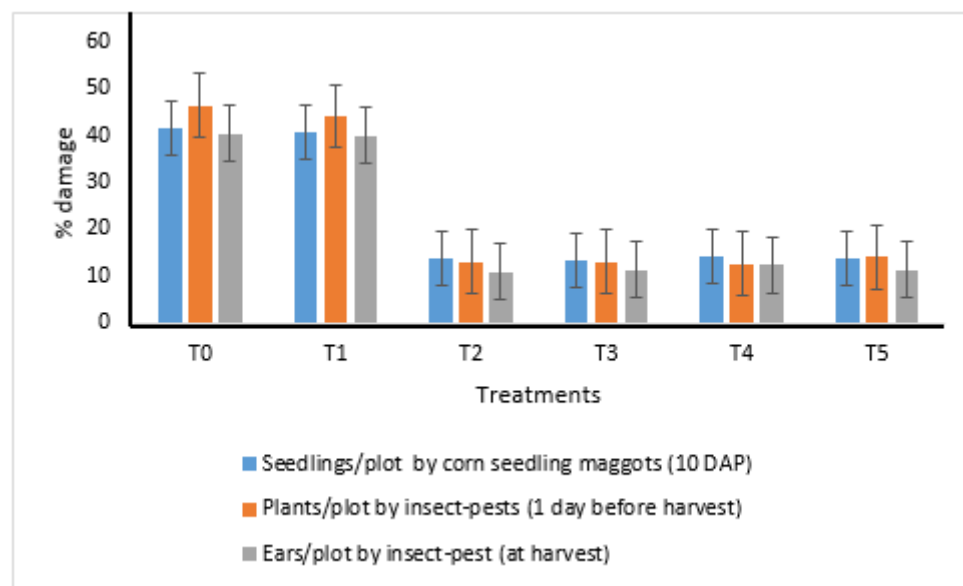
T <sub>0</sub>	12.67b	18.33b	44.67b
T <sub>1</sub>	13.67b	18.00b	31.68b
T <sub>2</sub>	8.00a	5.00a	-37.50a
T <sub>3</sub>	8.00a	5.00a	-37.50a
T <sub>4</sub>	8.00a	5.33a	-33.38a
T <sub>5</sub>	7.67a	5.00a	-34.81a
<hr/>			
Armyworm			
T <sub>0</sub>	23.67b	37.67b	59.15b
T <sub>1</sub>	25.33b	38.33b	51.32b
T <sub>2</sub>	15.00a	9.67a	-35.53a
T <sub>3</sub>	14.33a	9.00a	-37.19a
T <sub>4</sub>	15.33a	9.00a	-41.29a
T <sub>5</sub>	14.33a	7.67a	-46.48a
<hr/>			
Plants with aphids			
T <sub>0</sub>	14.33b	17.33b	20.94b
T <sub>1</sub>	13.67b	16.33b	19.46b
T <sub>2</sub>	6.67a	5.00a	-25.04a
T <sub>3</sub>	7.67a	4.67a	-39.11a
T <sub>4</sub>	7.33a	4.67a	-36.29a
T <sub>5</sub>	8.00a	5.67a	-29.13a

Means with the same letter designations are not significant to each other.

application of botanical pesticides at the right amount can eliminate the occurrence of pests [27; 28]. In addition, proper application of rhizome crude extracts is one of the bests control measures against corn insect-pests [29]. This result proves that rhizome plants are the best sources of organic pesticide to control insect-pests. Thus, the use of rhizome extracts is recommended for controlling insect-pests occurrence to attain better yields [30].

### 3.2. Percent (%) Damage of Plants and Ears Plot<sup>-1</sup> by Insect-Pests

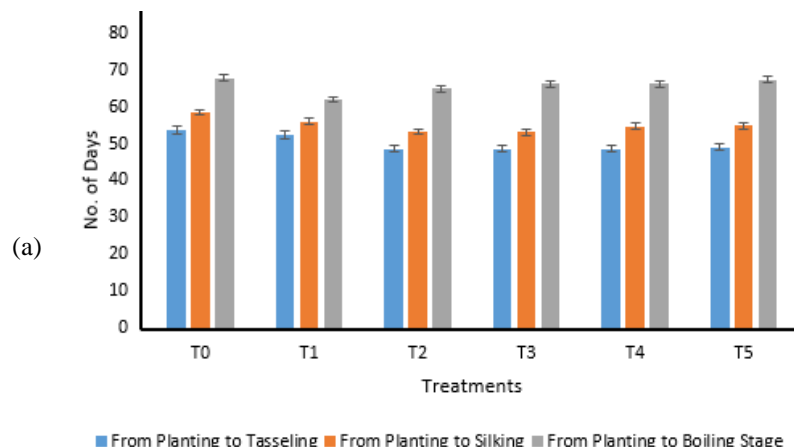
**Figure 1** shows the results of % damage of plants and ears due to the attack of insect pests. Statistical analysis revealed that there was less damage of seedlings, plants and ears applied with rhizome extracts regardless of sources compared to those plants without any pesticides applied at 10 DAP, a day before harvest and harvest, respectively. Insect-pests damage was 41 – 45% from seedlings to ears to those plants applied with rhizome crude extracts regardless of sources. This was significantly lower than those plants without pesticides applied (41 – 45 % damage). This might be due to the less insect-pests incidence in all plants treated with rhizome extracts. Expectedly, the incidence of pests can bring damage to crops. It tends to the loss of yield and economic improvement of crops [31]. To minimize the damage of crops, insect-pests must be controlled. [32] also reported that botanical pesticides lessened the incidence of pests thus minimized crop damage.



**Figure 1. Percent damage by insect-pests on glutinous corn as applied with different rhizome crude extracts**

### 3.3. Agronomic Characteristics and Harvest Index

**Figure 2** shows that the application of different rhizome crude extracts affected the growth and harvest index of the glutinous corn crop. All plants applied with rhizome crude extracts were significantly taller, reached maturity earlier except at the boiling stage. It may be due to the recovery of plants without rhizome extracts applied at the boiling stage. It can be contributed by the favorable condition and the fertilizer applied. Moreover, plants applied with rhizome crude extracts regardless of sources had obtained stover yield and harvest index significantly higher than those plants without any pesticides applied. This might be due to the incidence of insect-pests on the plants (**Table 1**) that affects the growth and harvest index development of glutinous corn crop. This result conforms to the report of [33] that insect-pests occurrence and their damage have significant effects on the growth of crops. Furthermore, [34] reported that crops attacked by pests will result in growth stagnant and expectedly affect the yield.



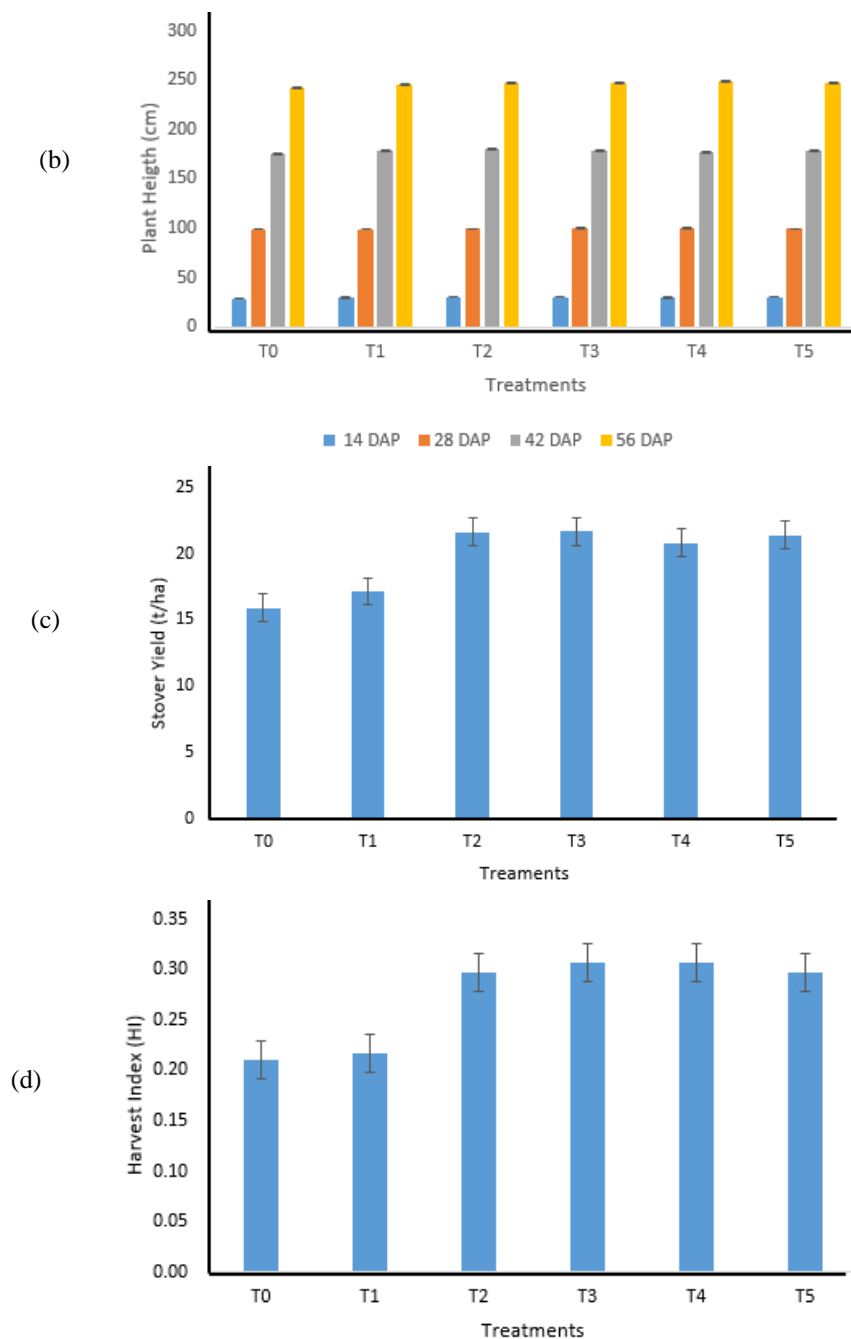


**Figure 2.** Agronomic characteristics of glutinous corn: (a) number of days from planting to tasseling, silking, and boiling stage; (b) plant height (cm); (c) stover yield ( $t\text{ ha}^{-1}$ ); and (d) harvest index (HI) as applied with rhizome crude extracts.

### 3.4. Yield and Yield Components

**Figure 3** revealed that the ear yield of the glutinous corn crop was affected by the application of different rhizome crude extracts except for ear diameter (**Fig. 3b**) and the number of non-marketable ears (**Fig. 3c**). All treated plants

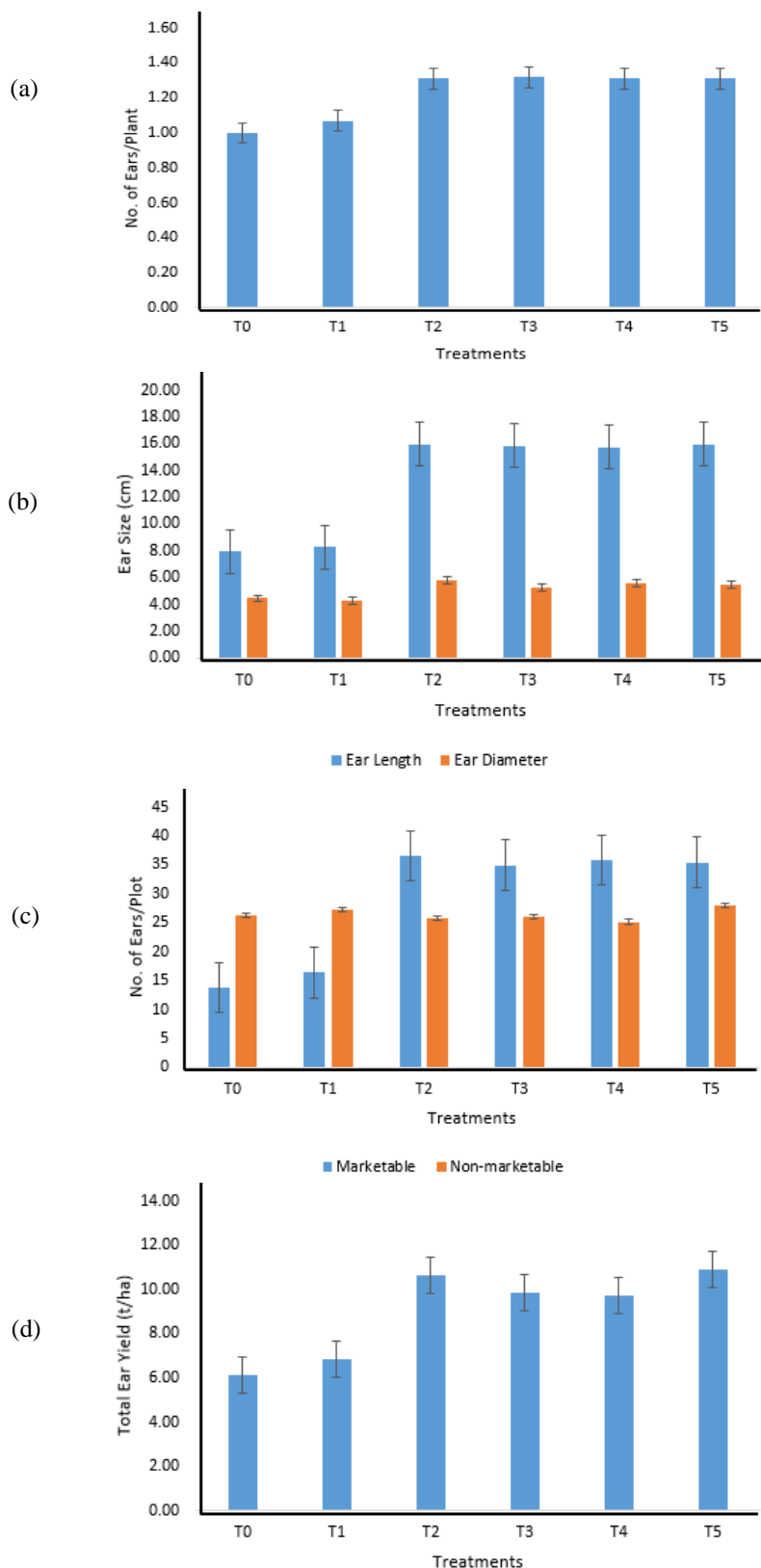


**Figure 3. Yield and yield components of glutinous corn: (a) number of ears plant<sup>-1</sup>; (b) ear size (cm); (c) number of marketable and non-marketable ears plot<sup>-1</sup>; and (d) total ear yield (t ha<sup>-1</sup>) as applied with different rhizome crude extracts**

with rhizome crude extracts regardless of sources had significantly produced more (Fig. 3a) and longer (Fig. 3b) ears. This contributed to the higher number of marketable ears (Fig. 3c), thus attained a total ear yield (Fig. 3d) significantly higher than those plants without any pesticides applied. All of these might be due to the influence of insect-pests incidence (Table 1), % damage (Fig. 1), and the growth performance of

glutinous corn (**Fig. 2**). [35] reported that pest incidence on maize can affect the yield. The higher the pest incidence, the lower is the yield of maize [36; 37].

### 3.5. Production Cost and Return Analysis

All plants applied with rhizome crude extracts obtained higher gross income, net income, and return on investment (ROI) compared to plants without any pesticides applied (**Table 2**). Results revealed that the higher marketable ear yield greatly contributed to the increase in gross income.

The highest net income of PHP 49,213.00 ha<sup>-1</sup> was obtained from plants applied with shampoo ginger (*Zingiber zerumbet*) extracts (T<sub>5</sub>) followed by plants applied with galangal (*Alpinia galanga*) extracts (T<sub>4</sub>) (PHP 47,874.00 ha<sup>-1</sup>) and plants applied with turmeric (*Curcuma longa*) extracts (T<sub>3</sub>) (PHP 47,624.00 ha<sup>-1</sup>) due to their high marketable ear yield obtained and slightly lower production cost. Plants applied with ginger (*Zingiber officinale*) extracts also performed well, however it gained slightly lower than shampoo ginger, galangal, and turmeric. It is due to the higher amount of incurred gingers.

*ROI* is a profitability ratio that calculates the profits of an investment as a percentage of the original cost. For example, the plants applied with shampoo ginger (*Zingiber zerumbet*) extract (T<sub>5</sub>) got the highest ROI of 53.18 %; it means that in every 1 peso invested, there is a gain of PHP 0.5318.

Glutinous corn plants applied with different rhizome crude extracts were profitable except T<sub>0</sub> and T<sub>1</sub>. This might be due to the lesser incidence of insect-pets and better growth that contributed to the marketable ear yield of treated plants with rhizome crude extracts organic pesticide.

**Table 2. Cost and return analysis of glutinous corn crop as applied with different rhizome crude extracts organic pesticide**

Treatment	Marketable Ear Yield (t ha <sup>-1</sup> )	Gross Income* (PHP ha <sup>-1</sup> )	Production Cost (PHP ha <sup>-1</sup> )	Net Income (PHP ha <sup>-1</sup> )	ROI (%)
T <sub>0</sub>	2.15b	53,750.00	65,785.00	-12,035.00	-18.29
T <sub>1</sub>	2.85b	71,250.00	86,347.00	-15,097.00	-17.48
T <sub>2</sub>	5.62a	140,500.00	93,485.00	47,015.00	50.29
T <sub>3</sub>	5.04a	138,500.00	90,876.00	47,624.00	52.41
T <sub>4</sub>	5.55a	138,750.00	90,876.00	47,874.00	52.68
T <sub>5</sub>	5.67a	141,750.00	92,537.00	49,213.00	53.18

Gross income was computed based on the current wholesale/farm gate price of glutinous corn at PhP 25.00 kl<sup>-1</sup> in the locality.

## Conclusions

Based on the results, this can be concluded that the application of rhizome crude extracts as organic pesticide lessened the incidence of insect-pests and their damage on glutinous corn crop; enhanced the growth and yield and improved the profitability of glutinous corn crop production. Therefore, it has a positive and profitable impact on glutinous corn production. This can likewise be a basis of proof that rhizome crude extracts can address the problems on the cost and environmental adverse effects of synthetic pesticides face by farmers nowadays.

## References

- [1] Arnarson, A. 2019. Corn 101. Nutrition Facts and Health Benefits. Retrieved from <https://www.healthline.com/nutrition/foods/corn>, accessed 2019
- [2] Duong, A. 2020. The Versatility of Corn. Retrieved from <https://www.southeastiowaunion.com/subject/news/the-versatility-of-corn-20200110>, accessed 2020
- [3] Cabrido, A. 2018. Planting Glutinous Corn. Retrieved from <https://businessdiary.com.ph/2483/planting-glutinous-corn/>
- [4] Estes, K. 2016. Corn Earworm, European Corn Borer, Fall Armyworm, or Western Bean Cutworm: Which One Is Causing the Injury I'm Finding on My Corn Ears? Department of Crop Sciences, University of Illinois at Urbana-Champaign. Retrieved from <https://farmdoc.illinois.edu/field-crop-production/uncategorized/corn-earworm-european-corn-borer-fall-armyworm-or-western-bean-cutworm-which-one-is-causing-the-injury-im-finding-on-my-corn-ears.html>

- [5] Food and Agriculture Organization 2009. Corn farmers in Ilocos Norte [Philippines] received very low income from corn due to low yield and high production costs. *Journal Article*. Volume p. 160-161
- [6] Chimweta, M., Nyakudya, I.W., Jimu, L. and Bray Mashingaidze, A., 2020. Fall armyworm [*Spodoptera frugiperda* (JE Smith)] damage in maize: management options for flood-recession cropping smallholder farmers. *International Journal of Pest Management*, 66(2), pp.142-154.
- [7] Kumar, P., Singh, R., Suby, S.B., Kaur, J., Sekhar, J.C. and Soujanya, P.L., 2018. An overview of crop loss assessment in maize.
- [8] Bessin and Johnson. 2007, Insecticide Recommendations for Corn. UK Cooperative Extension Service. University of Kentucky-College of Agriculture. Retrieved from [http://www.uky.edu/Ag/PAT/recs/crop/pdf/ENT-16\\_Field\\_Corn.pdf](http://www.uky.edu/Ag/PAT/recs/crop/pdf/ENT-16_Field_Corn.pdf)
- [9] Hossain, M.S., Zaman, S., Haque, A.B.M.H., Bhuiyan, M.P., Khondkar, P. and Islam, M.R., 2008. Chemical and pesticidal studies on *Acorus calamus* rhizomes. *Journal of Applied Sciences Research*, 4(10), pp.1261-1266.
- [10] Khan, A., Islam, M.H., Islam, M.E., Al-Bari, M.A.A., Parvin, M.S., Sayeed, M.A., Islam, M.N. and Haque, M.E., 2014. Pesticidal and pest repellency activities of rhizomes of *Drynaria quercifolia* (J. Smith) against *Tribolium castaneum* (Herbst). *Biological research*, 47(1), p.51.
- [11] Pandji, C., Grimm, C., Wray, V., Witte, L. and Proksch, P., 1993. Insecticidal constituents from four species of the Zingiberaceae. *Phytochemistry*, 34(2), pp.415-419.
- [12] Chaubey, M.K., 2011. Insecticidal properties of *Zingiber officinale* and *Piper cubeba* essential oils against *Tribolium castaneum* Herbst (Coleoptera: Tenebrionidae). *Journal of Biologically Active Products from Nature*, 1(5-6), pp.306-313.
- [13] Singh, K.M., Singh, M.P., Sureja, A.K. and Bhardwaj, R., 2012. Insecticidal activity of certain plants of Zingiberaceae and Araceae against *Spodoptera litura* F. and *Plutella xylostella* Saunders in cabbage. *Indian Journal of Entomology*, 74(1), pp.62-68.
- [14] de Souza Tavares, W., Akhtar, Y., Gonçalves, G.L.P., Zanuncio, J.C. and Isman, M.B., 2016. Turmeric powder and its derivatives from *Curcuma longa* rhizomes: insecticidal effects on cabbage looper and the role of synergists. *Scientific reports*, 6, p.34093.
- [15] Promotion and Development of Organic Agriculture In The Philippines 2005. Retrieved From <Https://Www.Officialgazette.Gov.Ph/2005/12/27/Executive-Order-No-481-S-2005/>, accessed 2015.
- [16] Biñas Jr, E. and Cagasan, U. 2018. Growth and Yield of Sweetcorn (*Zea mays* L. var. Macho F1) as Influenced by Different Combination of Organic and Inorganic Fertilizers. *Science and Humanities Journal*. Vol. 12, 2018. Pp 79-91.
- [17] Broatch, J.S., Dodsall, L.M., Clayton, G.W., Harker, K.N. and Yang, R.C., 2006. Using degree-day and logistic models to predict emergence patterns and seasonal flights of the cabbage maggot and seed corn maggot (Diptera: Anthomyiidae) in canola. *Environmental Entomology*, 35(5), pp.1166-1177.
- [18] Barry, J.D., Sciarappa, W.J., Teixeira, L.A. and Polavarapu, S., 2005. Comparative effectiveness of different insecticides for organic management of blueberry maggot (Diptera: Tephritidae). *Journal of economic entomology*, 98(4), pp.1236-1241.
- [19] Nondo, R.S., Mbwambo, Z.H., Kidukuli, A.W., Innocent, E.M., Mihale, M.J., Erasto, P. and Moshi, M.J., 2011. Larvicidal, antimicrobial and brine shrimp activities of extracts from *Cissampelos mucronata* and *Tephrosia villosa* from coast region, Tanzania. *BMC complementary and alternative medicine*, 11(1), p.33.
- [20] Ningrum, D.S., Wijayanti, S.P.M. and Kuswanto, K., 2019. Mosquito Larvacidal Activity of *Zingiber Montanum* Rhizome Extract Against *Aedes Aegypti* Larvae. *BALABA: Jurnal Litbang Pengendalian Penyakit Bersumber Binatang Banjarnegeara*, pp.33-40.
- [21] Aryani, D.S. and Auamcharoen, W., 2016. Repellency and contact toxicity of crude extracts from three Thai plants (Zingiberaceae) against maize grain weevil, *Sitophilus zeamais* (Motschlusky)(Coleoptera: Curculionidae). *Journal of Biopesticides*, 9(1), p.52.
- [22] Pengsook, A., Puangsomchit, A., Yooboon, T., Bullangpoti, V. and Pluempanupat, W., 2020. Insecticidal activity of isolated phenylpropanoids from *Alpinia galanga* rhizomes against *Spodoptera litura*. *Natural Product Research*, pp.1-5.
- [23] Čamprag, D., Sekulić, R., Kereši, T. and Bača, F., 2004. Corn earworm (*Helicoverpa armigera* Hübner) and measures of integrated pest management. *Corn earworm (*Helicoverpa armigera* Hübner) and measures of integrated pest management*.
- [24] Manandhar, R. and Wright, M.G., 2016. Effects of interplanting flowering plants on the biological control of corn earworm (Lepidoptera: Noctuidae) and thrips (Thysanoptera: Thripidae) in sweet corn. *Journal of Economic Entomology*, 109(1), pp.113-119.
- [25] Moore, V.M. and Tracy, W.F., 2020. Survey of organic sweet corn growers identifies corn earworm prevalence, management and opportunities for plant breeding. *Renewable Agriculture and Food Systems*, pp.1-4.

- [26] Adedire, C.O. and Akinkurolere, R.O., 2005. Bioactivity of four plant extracts on coleopterous pests of stored cereals and grain legumes in Nigeria.
- [27] Pimentel, D., 2009. Pesticides and pest control. In *Integrated pest management: innovation-development process* (pp. 83-87). Springer, Dordrecht.
- [28] Hikal, W.M., Baeshen, R.S. and Said-Al Ahl, H.A., 2017. Botanical insecticide as simple extractives for pest control. *Cogent Biology*, 3(1), p.1404274.
- [29] Pant, M., Dubey, S. and Patanjali, P.K., 2016. Recent advancements in bio-botanical pesticide formulation technology development. In *Herbal insecticides, repellents and biomedicines: effectiveness and commercialization* (pp. 117-126). Springer, New Delhi.
- [30] Rahman, S., Biswas, S.K., Barman, N.C. and Ferdous, T., 2016. Plant extract as selective pesticide for integrated pest management. *Biotechnological Research*, 2(1), pp.6-10.
- [31] Oliveira, C.M., Auad, A.M., Mendes, S.M. and Frizzas, M.R., 2014. Crop losses and the economic impact of insect pests on Brazilian agriculture. *Crop Protection*, 56, pp.50-54.
- [32] Tembo, Y., Mkindi, A.G., Mkenda, P.A., Mpumi, N., Mwanauta, R., Stevenson, P.C., Ndakidemi, P.A. and Belmain, S.R., 2018. Pesticidal plant extracts improve yield and reduce insect pests on legume crops without harming beneficial arthropods. *Frontiers in plant science*, 9, p.1425.
- [33] Donatelli, M., Magarey, R.D., Bregaglio, S., Willocquet, L., Whish, J.P. and Savary, S., 2017. Modelling the impacts of pests and diseases on agricultural systems. *Agricultural systems*, 155, pp.213-224.
- [34] Friedrich, T. and Kassam, A., 2011. Plant Production and Protection Division, Food and Agriculture Organization (FAO) of the United Nations, Rome, Italy. *Low-Input Intensification of Developing Countries 'Agriculture—Opportunities and Barriers*, p.115.
- [35] Sulong, Y., Mohamed, S., Sajili, M.H. and Ngah, N., 2019. Survey on Pest and Disease of Corn (*Zea Mays Linn*) grown at BRIS Soil Area. *Journal of Agrobiotechnology*, 10(1S), pp.75-87.
- [36] Cock, M., 2011. Plant pests: The biggest threats to food security?. *BBC News, Science and Environment*, 8.
- [37] Assefa, B.T., Chamberlin, J., Reidsma, P., Silva, J.V. and van Ittersum, M.K., 2020. Unravelling the variability and causes of smallholder maize yield gaps in Ethiopia. *Food Security*, 12(1), pp.83-103.

# **Performance of Hybrid Sweet Corn (*Zea mays* L. var Macho F1) as applied with Combined Organic and Inorganic Fertilizers**

**Enrique E. Biñas, Jr. and Ulysses A. Cagasan**

**Abstract** Organic manures can be used as an alternative for inorganic fertilizers. However, the application of organic inputs alone cannot meet the nutritional requirements of the crop. There is a need to combine them with inorganic fertilizers to attain better yield. This study was conducted to evaluate the effects of organic and inorganic fertilizers on the growth and yield performance of sweetcorn and assess the profitability of the combined application of organic and inorganic fertilizers on sweetcorn production. The experiment was laid out in RCB design with 3 replications. Treatments were as follows: T<sub>0</sub> = Control (without fertilizer applied), T<sub>1</sub> - Inorganic fertilizer at 90-60-60 kg ha<sup>-1</sup> (N, P<sub>2</sub>O<sub>5</sub>, K<sub>2</sub>O), T<sub>2</sub> = 5 t ha<sup>-1</sup> of vermicompost + 45-30-30 kg ha<sup>-1</sup> N, P<sub>2</sub>O<sub>5</sub>, K<sub>2</sub>O, T<sub>3</sub> = 5 t ha<sup>-1</sup> of poultry manure + 45-30-30 kg ha<sup>-1</sup> N, P<sub>2</sub>O<sub>5</sub>, K<sub>2</sub>O, T<sub>4</sub> = 5 t ha<sup>-1</sup> of cow manure + 45-30-30 kg ha<sup>-1</sup> N, P<sub>2</sub>O<sub>5</sub>, K<sub>2</sub>O, T<sub>5</sub> = 5 t ha<sup>-1</sup> of goat manure + 45-30-30 kg ha<sup>-1</sup> N, P<sub>2</sub>O<sub>5</sub>, K<sub>2</sub>O, T<sub>6</sub> = 5 t ha<sup>-1</sup> of mudpress + 45-30-30 kg ha<sup>-1</sup> N, P<sub>2</sub>O<sub>5</sub>, K<sub>2</sub>O, T<sub>7</sub> = Foliar spray (Fermented Golden Snail) + 45-30-30 kg ha<sup>-1</sup> N, P<sub>2</sub>O<sub>5</sub>, K<sub>2</sub>O.

Sweetcorn plants applied with organic + inorganic fertilizers regardless of sources gave a significant growth and yield compared to those plants without fertilizer applied.

The highest net income and ROI were obtained from plants applied with combined goat manure and inorganic fertilizers at PhP 62,086.00 ha<sup>-1</sup> and 72 %, respectively.

Keywords: combined applications, growth and yield performance, inorganic fertilizer, organic manures, profitability, hybrid sweetcorn

## **1. Introduction**

Corn (*Zea mays* L.) is the second most important cereal crop next to rice grown for human consumption and used as raw materials for different food products. Because of its versatility, it is consumed not only as food for humans and animals but also for industrial and agricultural purposes [1].

One of the management practices under intensive cultivation is through the application of fertilizers. Organic fertilizers, such as animal manure and crop residues can be used as an alternative for inorganic fertilizers [2]. However, recent studies revealed that the application of organic inputs alone cannot meet the nutritional requirements of the crop that there is a need to integrate with inorganic fertilizers to achieve better yields. The supply of nutrients from organic materials can be complemented by enriching them with inorganic nutrients that will be readily released and utilized by the crop to compensate for the slow release of organic nutrients.

The application of inorganic fertilizer is needed for modern corn varieties to increase yield. However, fertilizers are so expensive nowadays and have a tendency to pollute the environment and decrease production efficiency as well [3]. Hence, a combination of organic and inorganic fertilizer is

---

Enrique E. Biñas, Jr.

College of Agriculture and Forestry, Jose Rizal Memorial State University-Tampilisan Campus, ZNAC, Tampilisan, Zamboanga del Norte, PHILIPPINES  
Email Address: [enriquebinas@jrmsu.edu.ph](mailto:enriquebinas@jrmsu.edu.ph)

Ulysses A. Cagasan

Department of Agronomy, Visayas State University, Visca, Baybay City, Leyte, PHILIPPINES

recommended to minimize the adverse impact on the environment, health, wildlife, and water source. Sound fertilizer management must attempt to ensure both an enhanced and safe environment; therefore, a balanced fertilization strategy that combines the use of chemical, organic, or biofertilizers must be developed and evaluated [4]. Judicious use of organic and inorganic nutrient sources is important to decrease dependence on chemical fertilizers. This will also lead to sustainably high crop production due to minimal nutrient losses to the environment and optimum nutrient use efficiency [5].

Several researches on fertilization have been studied on the yield performance and profitability of corn. However, most of the practices only used either organic or inorganic inputs alone. Hence, this study was conducted to evaluate the effects of combined organic and inorganic fertilizer application on the growth and yield performance of hybrid sweetcorn and to assess its profitability on hybrid sweetcorn production.

## 2. Methodology

### 2.1. Land Preparation

An experimental area of 857.5 m<sup>2</sup> was plowed and harrowed twice at the weekly intervals to pulverize the soil. This was done to incorporate the weeds in the soil and provide good soil conditions for seed germination. Furrows were made at a distance of 0.75 m between rows after the second harrowing.

### 2.2. Experimental Treatments

The treatments used in the study were designated as follows:

- T<sub>0</sub> – Control (without fertilizer applied)
- T<sub>1</sub> – Inorganic fertilizer at 90-60-60 kg ha<sup>-1</sup> (N, P<sub>2</sub>O<sub>5</sub>, K<sub>2</sub>O)
- T<sub>2</sub> – 5 t ha<sup>-1</sup> of vermicompost + 45-30-30 kg ha<sup>-1</sup> N, P<sub>2</sub>O<sub>5</sub>, K<sub>2</sub>O
- T<sub>3</sub> – 5 t ha<sup>-1</sup> of poultry manure + 45-30-30 kg ha<sup>-1</sup> N, P<sub>2</sub>O<sub>5</sub>, K<sub>2</sub>O
- T<sub>4</sub> – 5 t ha<sup>-1</sup> of cow manure + 45-30-30 kg ha<sup>-1</sup> N, P<sub>2</sub>O<sub>5</sub>, K<sub>2</sub>O
- T<sub>5</sub> – 5 t ha<sup>-1</sup> of goat manure + 45-30-30 kg ha<sup>-1</sup> N, P<sub>2</sub>O<sub>5</sub>, K<sub>2</sub>O
- T<sub>6</sub> – 5 t ha<sup>-1</sup> of mudpress + 45-30-30 kg ha<sup>-1</sup> N, P<sub>2</sub>O<sub>5</sub>, K<sub>2</sub>O
- T<sub>7</sub> – Foliar spray (Fermented Golden Snail) + 45-30-30 kg ha<sup>-1</sup> N, P<sub>2</sub>O<sub>5</sub>, K<sub>2</sub>O

### 2.3. Soil Sampling and Analysis

Ten (10) soil samples were randomly collected from the experimental area at 20 cm depth before the conduct of the experiment. These were composited, air-dried, and sieved using 2.0 mm wire mesh. These were submitted to the Central Analytical Service Laboratory (CASL), Philippine Root Crops Research Center (PhilRootcrops), VSU, Visca, Baybay City, Leyte for the determination of soil pH, organic matter (%) [6], total N (%) [6], available phosphorous [6] and exchangeable potassium content (Ammonium Acetate Meth).

After harvest, soil samples were gathered for final analysis. Samples were collected per treatment plot at 20 cm depth and composited for the determination of the same soil parameters mentioned above.

### 2.4. Data Gathered and Statistical Tool Used

The data on agronomic characteristics, yield and yield components, and harvest index were gathered. Analysis of variance (ANOVA) was done using the Statistical Tool for Agricultural Research (STAR). Treatment means comparison was done using the Tukey's or Honestly Significant Difference (HSD) test. Total weekly rainfall (mm), average daily minimum and maximum temperatures (°C), and relative humidity (%) throughout the conduct of the study were taken from the records of Philippine Atmospheric Geophysical and Astronomical Services (PAGASA) Station, Visayas State University, Visca, Baybay City, Leyte. The gross income, net income, and return on investment were also determined.

## 3. Results and Discussion

### 3.1. Weather Observations

The total weekly rainfall (mm), average daily minimum, and maximum temperatures (°C), and relative humidity (%) throughout the study are presented in Figure 1 and Appendix Table 4. Data showed that the

rainfall fall on an average of 116.9 mm. This result substantially sufficient for the growth and development of sweetcorn because it conformed to the optimum requirement of the crop at more or less 60 mm per week from planting to harvesting [7]. The rainfall was increased in week 6 at 441.0 mm due to typhoon Paolo that brought heavy rainfall. The minimum and maximum temperature range from 22.3 to 30.1 °C respectively which gave favor to sweetcorn for normal growth and development. The [7] reported that the optimum temperature required for normal growth and development of corn stands is 24 to 28 °C.

[8] also reported that sweetcorn needs a temperature of 20 to 30 °C for germination. The relative humidity of 81-89 % was also favorable for the growth and development of sweetcorn.

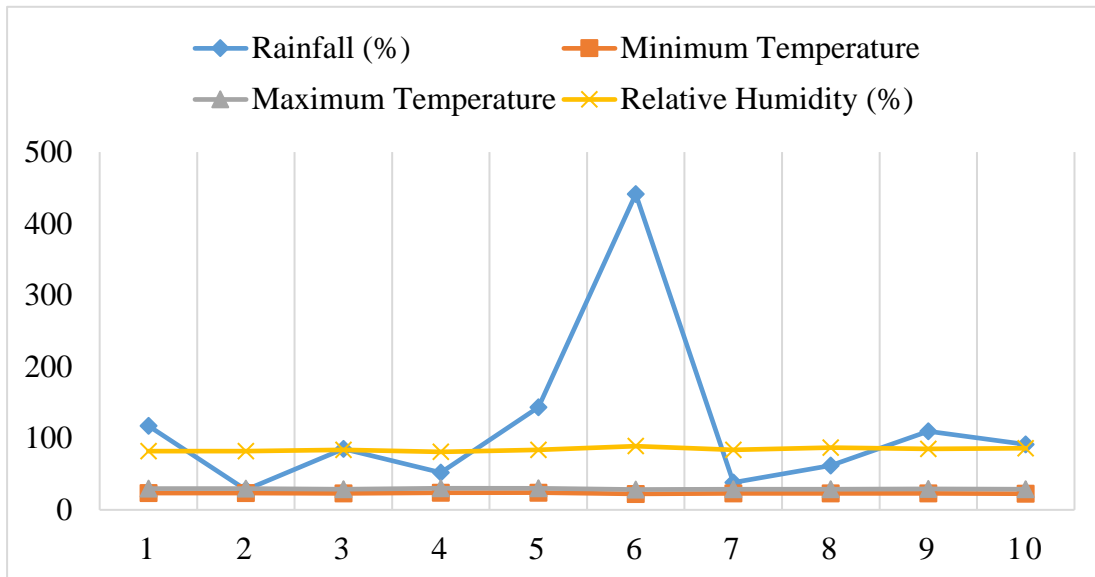


**Figure 1. Total weekly rainfall (mm), average daily minimum and maximum temperatures (°C) and relative humidity (%) from planting to harvesting of sweetcorn.**

### 3.2. Soil Chemical Properties

Soil test results are presented in Table 1. Initial results revealed that the experimental area had a slightly acidic soil (6.51) with adequate organic matter content (5.478 %) and potassium (330.000 mg kg<sup>-1</sup>) content, low total nitrogen (0.206 %) and phosphorous (6.955 mg kg<sup>-1</sup>) based on the indices on soil nutrient availability by [9]. After harvesting the crop, results of the soil analyses indicated that soil nutrients were not affected by the treatments except pH and available P (mg kg<sup>-1</sup>). The highest pH value (6.27) was recorded in plots applied with combined poultry manure and inorganic fertilizers (T<sub>3</sub>) comparable to plots not applied with any fertilizers (T<sub>0</sub>), combined cow dung and inorganic fertilizers (T<sub>4</sub>), combined goat manure and inorganic fertilizers (T<sub>5</sub>), combined with fermented golden snail and inorganic fertilizers (T<sub>7</sub>). This result could be contributed to the higher pH value of these organic manures applied (Table 4). On the other hand, the lowest pH value (5.56) was recorded from plots applied with pure inorganic fertilizers (T<sub>1</sub>). This could be attributed to the high pH from urea hydrolysis and ammonium content of inorganic fertilizer. [10] mentioned that fertilizer containing ammonium acidifies the soil. He added that inorganic fertilizer can be easy to be leached its nitrate and sulfate which loss some base cations causing acidification.

**Table 1. Soil analysis before planting and after harvesting applied with different organic materials combined with inorganic fertilizers**

Treatment	pH (1:2.5)	OM (%)	Total N (%)	Available P (mg kg <sup>-1</sup> )	Exchangeable K (mg kg <sup>-1</sup> )
<b>A. Initial (before planting)</b>					
	6.51	5.478	0.206	6.955	330.000
<b>B. Final (after harvest)</b>					

T <sub>0</sub>	6.08ab	1.510	0.111	8.113b	338.333
T <sub>1</sub>	5.57c	1.364	0.119	33.565a	292.917
T <sub>2</sub>	5.80bc	1.233	0.119	15.817ab	230.000
T <sub>3</sub>	6.27a	1.273	0.128	31.057a	376.250
T <sub>4</sub>	5.98ab	1.346	0.115	13.587ab	271.250
T <sub>5</sub>	6.01ab	1.551	0.129	9.304b	382.708
T <sub>6</sub>	5.84bc	1.278	0.105	16.637ab	237.500
T <sub>7</sub>	6.01ab	1.482	0.104	7.254b	266.667
Mean	5.94	1.380	0.116	16.920	299.450
CV (%)	2.04	18.69	15.78	43.30	22.49

Treatments with the same and without letter designations are not significantly different at 0.05 (HSD) and ANOVA, respectively.

Legend:

- T<sub>0</sub> = Control (without fertilizer applied)
- T<sub>1</sub> = 90-60-60 kg ha<sup>-1</sup> N, P<sub>2</sub>O<sub>5</sub>, K<sub>2</sub>O
- T<sub>2</sub> = 5 t ha<sup>-1</sup> vermicompost + 45-30-30 kg ha<sup>-1</sup> N, P<sub>2</sub>O<sub>5</sub>, K<sub>2</sub>O
- T<sub>3</sub> = 5 t ha<sup>-1</sup> poultry manure + 45-30-30 kg ha<sup>-1</sup> N, P<sub>2</sub>O<sub>5</sub>, K<sub>2</sub>O
- T<sub>4</sub> = 5 t ha<sup>-1</sup> cow dung + 45-30-30 kg ha<sup>-1</sup> N, P<sub>2</sub>O<sub>5</sub>, K<sub>2</sub>O
- T<sub>5</sub> = 5 t ha<sup>-1</sup> goat manure + 45-30-30 kg ha<sup>-1</sup> N, P<sub>2</sub>O<sub>5</sub>, K<sub>2</sub>O
- T<sub>6</sub> = 5 t ha<sup>-1</sup> mudpress + 45-30-30 kg ha<sup>-1</sup> N, P<sub>2</sub>O<sub>5</sub>, K<sub>2</sub>O
- T<sub>7</sub> = Fermented golden snail (foliar spray) + 45-30-30 kg ha<sup>-1</sup> N, P<sub>2</sub>O<sub>5</sub>, K<sub>2</sub>O

The relative increase in P after harvest could be attributed to the mineralization of organic fertilizers. Nutrient analyses of different manures (Table 4) revealed that poultry manure had the highest P content (2.226 %), thus plots applied with poultry manure and inorganic fertilizers (T<sub>3</sub>) obtained the highest P content after harvest relative to the plots applied with pure inorganic fertilizers (T<sub>1</sub>) comparable to those with vermicompost (T<sub>2</sub>), cow dung (T<sub>4</sub>) and mudpress (T<sub>6</sub>) combined with inorganic fertilizers.

### 3.3. Organic Fertilizers Chemical Properties

The chemical properties of organic fertilizers are presented in Table 2. Different organic fertilizers contained an adequate amount of nutrients. These contributed to the significant number, bigger, longer and marketable ears of sweetcorn than those not applied with any of these organic fertilizers. Thus, resulted in the crop obtained significant growth and yield.

**Table 2. Chemical properties of different organic fertilizers**

	pH (1:2.5)	OM (%)	Total (%)			Moisture Content (%)
			N	P	K	
Vermicompost	6.20	4.691	1.890	0.546	0.175	2.041
Poultry dung	8.73	4.342	3.049	2.226	3.513	2.041
Cow dung	8.49	5.090	2.018	0.446	1.363	4.167
Goat manure	8.61	5.586	2.448	0.304	2.200	7.527
Mudpress	6.66	5.844	2.276	0.967	0.225	3.093
FGS	6.50	nd	0.258	trace	0.130	nd

### 3.4. Agronomic Characteristics of Sweetcorn

The number of days from planting to emergence, tasseling, silking and boiling stages, stover yield (t ha<sup>-1</sup>) and plant height (cm) of sweetcorn applied with different organic materials combined with inorganic fertilizers are presented in Tables 3, 4. Statistical analyses revealed that all agronomic characteristics of sweetcorn except the stover yield were significantly affected by the treatments.

All plants applied with organic and inorganic fertilizers regardless of nutrient sources (T<sub>1</sub>, T<sub>2</sub>, T<sub>3</sub>, T<sub>4</sub>, T<sub>5</sub>, T<sub>6</sub> and T<sub>7</sub>) reached the boiling stage earlier compared to those plants not applied with any fertilizers (T<sub>0</sub>). This could be attributed to the early tasseling and silking of fertilized plants. [11] found that unfertilized corn developed slower compared to fertilized plants. This result confirmed the findings of [12] that corn in less

fertile soil delays boiling stage and maturity. [13] also reported that the application of combined organic manure and inorganic fertilizers enhances the growth and development of corn, thus the crop matured earlier.

Plants applied with combined poultry manure and inorganic fertilizers ( $T_3$ ) and combined goat manure and inorganic fertilizers ( $T_5$ ) were similarly taller than other treatments ( $T_0$ ,  $T_1$ ,  $T_2$ ,  $T_4$ ,  $T_6$  and  $T_7$ ) at 14 DAP. This might be due to the high nutrient content of these organic fertilizers (Table 4). However, at 28 DAP up to harvest, plants applied with combined organic and inorganic fertilizers regardless of nutrient sources ( $T_2$ ,  $T_3$ ,  $T_4$ ,  $T_5$ ,  $T_6$  and  $T_7$ ) were statistically similar to plants applied with pure inorganic fertilizers ( $T_1$ ) and were taller than plants not applied with any fertilizers ( $T_0$ ). This result suggests that nutrients were already released and absorbed by the plants, thus, increasing plant height. This conforms to the findings of [14] that the application of combined organic and inorganic fertilizers significantly increased the height of glutinous corn during the early vegetative up to the reproductive stage. This result can be attributed to the adequate amount of nutrients from the fertilizers applied, thus elongates the internode of sweetcorn. As the internodes elongate, the stalks increased their length.

**Table 3. Number of days from planting to emergence, tasseling, silking and boiling stages of hybrid sweetcorn applied with different organic materials combined with inorganic fertilizers**

Treatment	Number of days from planting to			
	Emergence	Tasseling	Silking	Boiling Stage
$T_0$	5.00	50.67a	57.66a	69.00a
$T_1$	5.00	48.67abc	55.00ab	67.00ab
$T_2$	3.00	48.00abc	51.33d	67.00ab
$T_3$	3.00	46.00c	53.33bcd	66.00b
$T_4$	3.00	48.00abc	52.66cd	66.67b
$T_5$	4.00	47.33bc	54.66abc	66.67b
$T_6$	4.00	49.00ab	54.66abc	67.33ab
$T_7$	5.00	49.33ab	53.66bcd	67.67ab
C.V. (%)	0.00*	2.13	1.67	1.20

Treatment means with the same and without letter designations are not significantly different at 0.05 HSD and ANOVA, respectively.

Legend:

$T_0$  = Control (without fertilizer applied)

$T_1$  = 90-60-60 kg ha<sup>-1</sup> N, P<sub>2</sub>O<sub>5</sub>, K<sub>2</sub>O

$T_2$  = 5 t ha<sup>-1</sup> vermicompost + 45-30-30 kg ha<sup>-1</sup> N, P<sub>2</sub>O<sub>5</sub>, K<sub>2</sub>O

$T_3$  = 5 t ha<sup>-1</sup> poultry manure + 45-30-30 kg ha<sup>-1</sup> N, P<sub>2</sub>O<sub>5</sub>, K<sub>2</sub>O

$T_4$  = 5 t ha<sup>-1</sup> cow dung + 45-30-30 kg ha<sup>-1</sup> N, P<sub>2</sub>O<sub>5</sub>, K<sub>2</sub>O

$T_5$  = 5 t ha<sup>-1</sup> goat manure + 45-30-30 kg ha<sup>-1</sup> N, P<sub>2</sub>O<sub>5</sub>, K<sub>2</sub>O

$T_6$  = 5 t ha<sup>-1</sup> mudpress + 45-30-30 kg ha<sup>-1</sup> N, P<sub>2</sub>O<sub>5</sub>, K<sub>2</sub>O

$T_7$  = Fermented golden snail (foliar spray) + 45-30-30 kg ha<sup>-1</sup> N, P<sub>2</sub>O<sub>5</sub>, K<sub>2</sub>O

**Table 4. Plant height (cm) and stover yield (t ha<sup>-1</sup>) of hybrid sweetcorn applied with different organic materials combined with inorganic fertilizers**

Treatment	Plant Height (cm) DAP					Stover Yield (t ha <sup>-1</sup> )
	14	28	42	56	At harvest	

T <sub>0</sub>	30.72b	79.72b	124.85b	184.20b	189.03b	12.42
T <sub>1</sub>	31.00b	100.25ab	187.57a	245.35a	248.37a	19.81
T <sub>2</sub>	31.57b	100.40ab	182.28a	245.47a	250.12a	21.95
T <sub>3</sub>	36.61a	113.18a	193.93a	246.02a	248.30a	20.69
T <sub>4</sub>	30.27b	100.72a	185.35a	245.15a	247.43a	19.93
T <sub>5</sub>	33.53ab	102.10a	184.31a	242.63a	251.30a	21.76
T <sub>6</sub>	31.65b	99.22ab	177.42a	245.88a	247.90a	20.27
T <sub>7</sub>	30.07b	93.43ab	175.07a	237.45a	240.27a	22.51
C.V. (%)	5.34	7.29	6.31	4.40	4.52	17.36

Treatment means with the same and without letter designations are not significantly different at 0.05 HSD and ANOVA, respectively.

#### Legend:

- T<sub>0</sub> = Control (without fertilizer applied)
- T<sub>1</sub> = 90-60-60 kg ha<sup>-1</sup> N, P<sub>2</sub>O<sub>5</sub>, K<sub>2</sub>O
- T<sub>2</sub> = 5 t ha<sup>-1</sup> vermicompost + 45-30-30 kg ha<sup>-1</sup> N, P<sub>2</sub>O<sub>5</sub>, K<sub>2</sub>O
- T<sub>3</sub> = 5 t ha<sup>-1</sup> poultry manure + 45-30-30 kg ha<sup>-1</sup> N, P<sub>2</sub>O<sub>5</sub>, K<sub>2</sub>O
- T<sub>4</sub> = 5 t ha<sup>-1</sup> cow dung + 45-30-30 kg ha<sup>-1</sup> N, P<sub>2</sub>O<sub>5</sub>, K<sub>2</sub>O
- T<sub>5</sub> = 5 t ha<sup>-1</sup> goat manure + 45-30-30 kg ha<sup>-1</sup> N, P<sub>2</sub>O<sub>5</sub>, K<sub>2</sub>O
- T<sub>6</sub> = 5 t ha<sup>-1</sup> mudpress + 45-30-30 kg ha<sup>-1</sup> N, P<sub>2</sub>O<sub>5</sub>, K<sub>2</sub>O
- T<sub>7</sub> = Fermented golden snail (foliar spray) + 45-30-30 kg ha<sup>-1</sup> N, P<sub>2</sub>O<sub>5</sub>, K<sub>2</sub>O

#### 3.5. Yield and Yield Components of Sweetcorn

The yield and yield characteristics of sweetcorn applied with different organic materials combined with inorganic fertilizers are presented in Tables 5, 6. Results indicated that plants applied with combined poultry manure and inorganic fertilizers (T<sub>3</sub>) had significantly more number of ears comparable to those with combined cow dung and inorganic fertilizers (T<sub>4</sub>). As expected, unfertilized plants obtained the least ear due to insufficient nutrients for ear development. Different applications of various organic materials combined with inorganic fertilizers on hybrid sweetcorn had significantly longer and larger ears (cm), had more marketable ears, heavier marketable ears (kg ha<sup>-1</sup>) and total ear yield (t ha<sup>-1</sup>) than the untreated control.

**Table 5. Number of ears, ear length and diameter and number of marketable and non-marketable ears of hybrid sweetcorn applied with different organic materials combined with inorganic fertilizers**

Treatments	Ear (cm)			No. of Ears (plot <sup>-1</sup> )	
	No. of Ears plant <sup>-1</sup>	Length	Diameter	Marketable	Non-Marketable
T <sub>0</sub>	1.00c	7.88b	4.06b	0.57b	42.28
T <sub>1</sub>	1.20b	16.82a	4.98a	24.99ab	28.61
T <sub>2</sub>	1.27b	16.80a	4.79a	24.40ab	32.42
T <sub>3</sub>	1.47a	17.78a	4.86a	18.48ab	42.72
T <sub>4</sub>	1.33ab	16.76a	4.78a	25.82ab	32.74
T <sub>5</sub>	1.27b	16.07a	4.85a	30.00a	28.37
T <sub>6</sub>	1.23b	16.60a	4.79a	24.24ab	30.36
T <sub>7</sub>	1.27b	17.07a	4.80a	31.35a	32.78
C.V. (%)	4.48	7.15	4.14	42.97	25.35

Treatment means with the same and without letter designations are not significantly different at 0.05 HSD and ANOVA, respectively.

#### Legend:

- T<sub>0</sub> = Control (without fertilizer applied)
- T<sub>1</sub> = 90-60-60 kg ha<sup>-1</sup> N, P<sub>2</sub>O<sub>5</sub>, K<sub>2</sub>O
- T<sub>2</sub> = 5 t ha<sup>-1</sup> vermicompost + 45-30-30 kg ha<sup>-1</sup> N, P<sub>2</sub>O<sub>5</sub>, K<sub>2</sub>O
- T<sub>3</sub> = 5 t ha<sup>-1</sup> poultry manure + 45-30-30 kg ha<sup>-1</sup> N, P<sub>2</sub>O<sub>5</sub>, K<sub>2</sub>O
- T<sub>4</sub> = 5 t ha<sup>-1</sup> cow dung + 45-30-30 kg ha<sup>-1</sup> N, P<sub>2</sub>O<sub>5</sub>, K<sub>2</sub>O

$T_5 = 5 \text{ t ha}^{-1}$  goat manure + 45-30-30 kg ha $^{-1}$  N, P<sub>2</sub>O<sub>5</sub>, K<sub>2</sub>O

$T_6 = 5 \text{ t ha}^{-1}$  mudpress + 45-30-30 kg ha $^{-1}$  N, P<sub>2</sub>O<sub>5</sub>, K<sub>2</sub>O

$T_7 =$  Fermented golden snail (foliar spray) + 45-30-30 kg ha $^{-1}$  N, P<sub>2</sub>O<sub>5</sub>, K<sub>2</sub>O

The significantly longer and bigger ears contributed to the significant weight of marketable ears of fertilized plants regardless of nutrient sources. Thus, the fertilized plants significantly obtained a higher total ear yield compared to the untreated control ( $T_0$ ). This could be attributed to the adequate amount of nutrients from different organic fertilizers (Table 4) + inorganic fertilizers applied. [15] reported that sweetcorn required a minimum rate of 90-60-60 kg N, P<sub>2</sub>O<sub>5</sub>, K<sub>2</sub>O. Sweetcorn without fertilizer applied had the lowest yield. The result implies the benefits of the combination of organic and inorganic fertilizers plus the favorable atmospheric condition on the significant increase yield in green cob of sweetcorn. [16] also reported that the combination of organic and inorganic fertilizers can improve the yield of corn crops significantly. With inorganic fertilizer applied though half of the recommended rate could have provided readily available plant nutrients which improved corn yield and productivity. Likewise, [17] found that the combination of organic fertilizers to soil improves corn yield and its quality.

### 3.6. Production Cost and Return Analysis

The profitability of sweetcorn production ha $^{-1}$  applied with different organic materials combined with inorganic fertilizers is presented in Table 7. All fertilized plants obtained higher gross income, net income and return on investment (ROI) compared to plants without fertilizer applied. Results show that the higher marketable ear yield greatly contributed to the increase in gross income. It also depicts that the higher the production cost, the lower is the net income.

The highest net income of PHP 62,086.00 ha $^{-1}$  was obtained from plants applied with combined goat manure and inorganic fertilizers ( $T_5$ ) followed by plants applied with combined cow dung and inorganic fertilizers ( $T_4$ ) (PHP 52,786.00 ha $^{-1}$ ) and plants applied with pure inorganic fertilizer ( $T_1$ ) (PHP 47,594.00 ha $^{-1}$ ) due to their high marketable ear yield obtained and slightly lower production cost.

ROI is a profitability ratio that calculates the profits of an investment as a percentage of the original cost. For example, the plants applied with combined goat manure and inorganic fertilizers ( $T_5$ ) got the highest ROI of 72 %; it means that in every 1 peso invested, there is a gain of PHP 0.7206.

**Table 6. Ear yield and harvest index of hybrid sweetcorn**

Treatment	Ear Yield (t ha $^{-1}$ )			Harvest Index (HI)
	Marketable	Non-Marketable	Total	
$T_0$	0.05b	2.35	2.40b	0.20
$T_1$	5.07a	3.87	8.94a	0.32
$T_2$	3.33a	4.97	8.30a	0.20
$T_3$	4.03a	4.90	8.93a	0.27
$T_4$	5.55a	3.09	8.64a	0.32
$T_5$	5.93a	3.33	9.26a	0.27
$T_6$	3.38a	3.71	7.09a	0.23
$T_7$	4.95a	3.63	8.58a	0.26
CV (%)	26.89	27.16	25.04	31.76

Treatment means with the same and without letter designations are not significantly different at 0.05, HSD and ANOVA, respectively.

Legend:

$T_0$  = Control (without fertilizer applied)

$T_1$  = 90-60-60 kg ha $^{-1}$  N, P<sub>2</sub>O<sub>5</sub>, K<sub>2</sub>O

$T_2$  = 5 t ha $^{-1}$  vermicompost + 45-30-30 kg ha $^{-1}$  N, P<sub>2</sub>O<sub>5</sub>, K<sub>2</sub>O

$T_3$  = 5 t ha $^{-1}$  poultry manure + 45-30-30 kg ha $^{-1}$  N, P<sub>2</sub>O<sub>5</sub>, K<sub>2</sub>O

$T_4$  = 5 t ha $^{-1}$  cow dung + 45-30-30 kg ha $^{-1}$  N, P<sub>2</sub>O<sub>5</sub>, K<sub>2</sub>O

$T_5$  = 5 t ha $^{-1}$  goat manure + 45-30-30 kg ha $^{-1}$  N, P<sub>2</sub>O<sub>5</sub>, K<sub>2</sub>O

$T_6$  = 5 t ha $^{-1}$  mudpress + 45-30-30 kg ha $^{-1}$  N, P<sub>2</sub>O<sub>5</sub>, K<sub>2</sub>O

$T_7$  = Fermented golden snail (foliar spray) + 45-30-30 kg ha $^{-1}$  N, P<sub>2</sub>O<sub>5</sub>, K<sub>2</sub>O

Sweetcorn plants applied with different organic materials in combination with inorganic fertilizers were profitable except T<sub>2</sub> and T<sub>6</sub>. This might be due to the higher amount of nutrients of these organic fertilizers applied that contributed to the marketable ear yield but low production cost.

The cost of organic materials differs among treatments. The highest cost was incurred from the combination of vermicompost and inorganic fertilizers (T<sub>2</sub>) because of the high price of vermicompost but since it has a low amount of nutrients (Table 4) relative to mudpress (T<sub>6</sub>), thus the returns were negative. The combination of goat manure and inorganic fertilizers (T<sub>5</sub>) was more profitable and advantageous because of the low price of goat manure yet with a high amount of nutrients (Table 4) thus, high yield. The combination of poultry manure and inorganic fertilizers (T<sub>3</sub>) got the lowest net income because of its relatively higher price.

**Table 7. Cost and return analysis of hybrid sweetcorn production applied with different organic materials combined with inorganic fertilizers**

Treatment	Marketable Ear Yield (t ha <sup>-1</sup> )	Gross Income* (PHP ha <sup>-1</sup> )	Production Cost (PHP ha <sup>-1</sup> )	Net Income (PHP ha <sup>-1</sup> )	ROI (%)
T <sub>0</sub>	0.05b	1,250.00	51,620.00	-50,370.00	-97.56
T <sub>1</sub>	5.07a	126,750.00	79,156.00	47,594.00	60.13
T <sub>2</sub>	3.33a	83,250.00	117,304.00	-34,054.00	-25.03
T <sub>3</sub>	4.03a	100,750.00	87,484.00	13,266.00	15.16
T <sub>4</sub>	5.55a	138,750.50	85,964.00	52,786.00	61.40
T <sub>5</sub>	5.93a	148,250.00	86,164.00	62,086.00	72.06
T <sub>6</sub>	3.38ab	84,500.00	84,724.00	-224.00	-0.26
T <sub>7</sub>	4.95a	123,750.00	86,134.00	37,616.00	43.67

Gross income was computed based on the current wholesale/farmgate price of sweetcorn at PHP 25.00 kl<sup>-1</sup> in the locality.

#### Legend:

- T<sub>0</sub> = Control (without fertilizer applied)
- T<sub>1</sub> = 90-60-60 kg ha<sup>-1</sup> N, P<sub>2</sub>O<sub>5</sub>, K<sub>2</sub>O
- T<sub>2</sub> = 5 t ha<sup>-1</sup> vermicompost + 45-30-30 kg ha<sup>-1</sup> N, P<sub>2</sub>O<sub>5</sub>, K<sub>2</sub>O
- T<sub>3</sub> = 5 t ha<sup>-1</sup> poultry manure + 45-30-30 kg ha<sup>-1</sup> N, P<sub>2</sub>O<sub>5</sub>, K<sub>2</sub>O
- T<sub>4</sub> = 5 t ha<sup>-1</sup> cow dung + 45-30-30 kg ha<sup>-1</sup> N, P<sub>2</sub>O<sub>5</sub>, K<sub>2</sub>O
- T<sub>5</sub> = 5 t ha<sup>-1</sup> goat manure + 45-30-30 kg ha<sup>-1</sup> N, P<sub>2</sub>O<sub>5</sub>, K<sub>2</sub>O
- T<sub>6</sub> = 5 t ha<sup>-1</sup> mudpress + 45-30-30 kg ha<sup>-1</sup> N, P<sub>2</sub>O<sub>5</sub>, K<sub>2</sub>O
- T<sub>7</sub> = Fermented golden snail (foliar spray) + 45-30-30 kg ha<sup>-1</sup> N, P<sub>2</sub>O<sub>5</sub>, K<sub>2</sub>O

#### Conclusion

Sweetcorn applied with organic and inorganic fertilizers regardless of sources gave favorable growth and yield performance. Application of combined goat manure and inorganic fertilizers (T<sub>5</sub>) was greatly profitable for it gained higher net income and ROI of PHP 62,086.00 ha<sup>-1</sup> and 72.06 %, respectively. While, application of combined inorganic fertilizers with either vermicompost (T<sub>2</sub>) or mudpress (T<sub>6</sub>) got a negative net income.

#### Acknowledgment

The Author thanks the Department of Science and Technology for funding this research.

## References

- [1] Sailer, L. 2012. The Importance of Corn Journal. Industry News. The Field Position. (<http://www.thefieldposition.com/2012/06/the-importance-of-corn/>)
- [2] Sharma, A. R. And B. N. Mittra. Effect of different rates of application of organic and nitrogen fertilizers in a rice-based cropping system. J. Agr. Sci. (Camb.) 1991; 117: 313-318.
- [3] Fageria, N. K. 2007. Green manuring in crop production. J Plant Nutrition 30: 691-719.
- [4] Chen, J. H. 2006. The combined use of chemical and organic fertilizers and/or biofertilizer for crop growth and soil fertility. In *International workshop on sustained management of the soil-rhizosphere system for efficient crop production and fertilizer use* (Vol. 16, p. 20). Land Development Department Bangkok, Thailand.
- [5] Akhtar, M., A. Naeem, J. Akhter, S. A. Bokhari and W. Ishaque. 2011. Improvement in nutrient uptake and yield of wheat by combined use of urea and compost. Soil & Environment, 30: 45-49.
- [6] PCARR. 1980. Standard Methods of Analysis for Soil, Plant Tissue, Water and Fertilizer. Los Baños, Laguna. vii, 194 p. : ill. ; 28 cm.
- [7] Department of Agriculture and Fisheries 1980. Weather condition requirements for sweetcorn. Retrieved from  
<https://www.google.com.ph/search?dcr=0&ei=UQHTWtfmBoO80ATnp4TYBg&q=Department+of+agriculture+and+fisheries+weather+requirement+for+sweetcorn&oq=Department+of+agriculture+and+fis>heries+weather+requirement+for+sweetcorn&gs
- [8] Jacobson, G. 2016. Sweetcorn growth and storage temperature requirements. Retrieved from <https://www.theseedcollection.com.au/blog/our-blog/sweet-corn-growth-storage/>
- [9] Landon, J.R. 1991. Booker tropical soil manual: A Handbook for Soil Survey and Agricultural Land Evaluation in the Tropics and Subtropics. Longman Scientific and Technical, Essex, New York. 474p.
- [10] Jenkins, T. 2015. How does chemical fertilizers affect the soil pH in acid, neutral and slightly alkaline soil? Indian Institute of Soil Science. Retrieved from [www.researchgate.net](http://www.researchgate.net).
- [11] Joyo, J. W. 2007. Growth and yield performance of corn as influenced by different organic fertilizers. Unpublished undergraduate thesis. Visayas state university, visca, Baybay City, Leyte. Pp. 29.
- [12] Catingan, B. D. 1982. Growth, yield and yield components of flint corn as influenced by varying nitrogen levels and tow spacing. Unpublished Undergraduate Thesis. Visayas State College of Agriculture, Bayay City, Leyte. 69 pp.
- [13] Chen, J. H. 2006. The combined use of chemical and organic fertilizers and/or biofertilizer for crop growth and soil fertility. In *International workshop on sustained management of the soil-rhizosphere system for efficient crop production and fertilizer use* (Vol. 16, p. 20). Land Development Department Bangkok, Thailand.
- [14] Elisan, B. 2015. Growth and yield of glutinous corn (*Zea mays* L.) as influenced by the application of different combinations of organic and inorganic fertilizers. Unpublished undergraduate thesis. Capiz state University, pontevedra, Capiz. Pp 79.
- [15] Burr, J., N. S. Mansour, E. H. Gardner, H. J. Mack and T. L. Jackson .1979. Sweet corn: eastern Oregon, east of Cascades. Retrieved from [http://oregonstate.edu/dept/hermiston/sites/default/files/sweet\\_corn\\_fg62-e2.pdf](http://oregonstate.edu/dept/hermiston/sites/default/files/sweet_corn_fg62-e2.pdf)
- [16] Ojeniyi, S. O. 2002. Soil management, national resources and environment. Oke-Ado: Adeniran press. Pp 24.
- [17] Motavalli, P.P., R. P. Singh and M. M. Anders. 1994. Perception and management of farmyard manure in the semi-Arid tropics of India. Agricultural systems. 46: 189-204.

# Prediction Analysis and Forecasting of Stock Price on Google Stocks

Rishabh Singhal and Richa Sharma

**Abstract** Stock prediction is one of the widely studied topic in the field of computation, statistics, trading, and finance. Stock values differ daily according to their market analysis. Each information gathered through stock trades will have missing information focuses because of occasions and different issues. In this paper, Google stock price analysis has been carried out using an interpolation approach to identify the missing values from the data. Moreover, the result is carried out using python. At last, the conclusion is given.

**Keywords-** Google Stocks, Stock Price, Interpolation, Lagrange's Interpolation, Time Series.

## 1. Introduction

Stock price means the current price of the stock in the market. When shares are issued to a company, it is given a price that tells the value of the company. The stock price goes up and down based on different factors as there is a change in the industry, political events, environmental change, and many other factors. Mainly stock price depends on the company supply, demand, management, and production. When the company shares its stock in the market they are first determined by the company's initial public offering. Investors use a variety of measures as the number of shares offered also, they look in up and down of the stocks in history.

Google is one of the trending multinational company which provides internet related services and products including hardware, software, search engine, etc. It was founded in 1998 by Larry Page and Sergey Brin in California, U.S.A. Google mostly has a high stock price, and the value mostly increases (see, Figure 1.1) because of the value of the company in the market as investors have the confidence to invest in it.



Figure. 1.1 Google Stocks Data vs Various Months

---

Rishabh Singhal  
Department of Computer Science, JK Lakshmi pat University, Jaipur, India  
e-mail: rishabhsinghal@jklu.edu.in

Richa Sharma  
Department of Science and Liberal Arts, JK Lakshmi pat University, Jaipur, India  
e-mail: richasharma@jklu.edu.in

Stock market provides information to client slants, less steady because of creating news and inclined to attacks. Stock market is like a weighing machine in short term it is not having so much commotion but rather more consistency [1]. Stock prediction is highly in demand in the market and it's not an easy task as investing in stocks market involves high risk. This research shows a systematic approach for developing a methodology for stock prediction and forecasting also tells us about the existing methods [2]. Brokers mostly use fundamental methods to examine different stocks for doing the right investment. This analysis is one of the old methodologies as it involves the study of industry fundamentals such as incomes and costs, rank in the market, yearly development rate, etc. [3].

Technical analysis accepts that the historical performance of contents and markets are pointers of future prediction. Primarily the development of technical analysis looks at the four measurements, specifically value, volume, time, and expansiveness. Changes in cost reflect changes in financial backer disposition. Also, value, the first measurement shows the disposition level of financial backers. It is useful to notice value pointers, for example, value propels versus decreases and value examples of offers contrasted with the market file. Volume, the subsequent measurement, mirrors the force of changes in financial backer perspectives [4]. There is a deep connection between stock value and industry which is sometimes used to decide when to enter or leave the market [5]. Analysis and forecasting of the stock are some of the trending topics to work on. There are different methods for analysis and forecasting. A different approach, scaling from very unofficial process to official. These methods are classified as Traditional Time Series analysis, Fundamental Analysis Methods, Technical Analysis Methods, and Machine Learning Methods. The norm to this classification is the sort of instruments and the kind of data that this method is utilizing to forecast the market [6].

Data mining is how we can use data in a better way. There are different methods to predict the closing price of stock data. They have used multiple algorithms like SMI, CMI, and Bollinger Band for the accuracy of results for the net price. The algorithm was able to predict the trend of the market if it will increase or decrease [7]. Different methods are used like RNN and LSTM to forecast the stock price and analyze how machine learning can improve to find the changes with time [8]. This research is based on forecasting different stock prices for multiple companies. They used RNN, LSTM, and CNN for the forecasting and calculated the error percentage obtained for each model. CNN gave more accurate results [9]. This research involves an algorithm which uses least square support vector machine (LS-SVM) and Particle swarm optimization (PSO) algorithm for better optimization of the model [10].

In this study, we have applied Lagrange's Interpolation method using python programming language to determine the missing values in the google stock data. It is an appropriate method for unequal time intervals or irregularity in the time series dataset and to handle higher degree polynomials. As it converges to exact solution very quickly thereby leading to more accurate results. Less missing values in a dataset will lead to greater efficiency in further results. In section 2, we describe the methodology. Section 3 contains the algorithmic analysis which includes the algorithm which is used for predicting the stock data. In section 4, results are shown which we have obtained using manual calculations and python implementations. At last, in section 5, we conclude that Lagrange's interpolation is a better approach and it's very important to find missing values for forecasting.

## 2. Methods

### 2.1 Basic Concepts of Interpolation

Interpolation method is used to determine the function  $f(x)$  that passes through the given set of data points and use that function to get the value of  $x$ . Using Interpolation method one can find the value between the known data points. Technically it is a method that finds the value of the equation for any middle value which is missing.

Lagrange's Interpolation is a method to find polynomial which accepts a specific value at discrete points. The polynomial of degree  $\leq (n-1)$  that passes through the  $n$  points.

$$(x_1, y_1 = f(x_1)), (x_2, y_2 = f(x_2)), \dots, (x_n, y_n = f(x_n))$$

and is given by

$$P(x) = \sum_{j=0}^n P_j(x)$$

Where,

$$P_j(x) = y_j \prod_{k=1}^n \frac{x - x_k}{x_j - x_k}$$

written explicitly

$$P(x) = \frac{(x - x_2)(x - x_3) \dots (x - x_n)}{(x_1 - x_2)(x_1 - x_3) \dots (x_1 - x_n)} y_1 + \frac{(x - x_1)(x - x_3) \dots (x - x_n)}{(x_2 - x_1)(x_2 - x_3) \dots (x_2 - x_n)} y_2 + \dots \\ + \frac{(x - x_2)(x - x_3) \dots (x - x_{n-1})}{(x_n - x_1)(x_n - x_2) \dots (x_n - x_{n-1})} y_n$$

Here  $P(x)$  be a function defined on a domain containing definite numbers  $x_1, x_2, \dots, x_n$ . Following algorithm compute the missing value,  $S' = P_n(x')$ , for a given a number  $x'$ , where  $P_n(x)$  is the  $n^{\text{th}}$  interpolating polynomial of  $P(x)$ .

### 3. Algorithmic Analysis

Python is a widely used high level programming language. It was created by Guido van Rossum in 1991 and further developed by the Python Software Foundation. Python can be used to handle big data and perform complex mathematics and can work on different platforms. Due to its ease of learning and usage, python codes can be easily written and executed much faster than other programming languages.

The algorithm takes raw data as input. The algorithm consists of 3 major part where in the first part the data is pre-processed in which the algorithm find outs the missing dates and values and after that, the prediction part starts in which there is a function to find out the missing values in the interval of every 7 days so that the predicted results are more accurate and match to the nearest data. At last, the main function of Lagrange's interpolation is used to calculate the missing data points which are as follows:

```
for i=0 to n {
    Yi = f(xi)
}
for i=1 to n {
    for j=n to i{
        Yj = [(x - xj)yj-1 - (x - xj-1)yj] / (xj-1 - xj)
    }
}
S' = Yn
```

where,

$x$  denotes the dates from the data available.

$y$  denotes the volume from the data available.

At last, the calculated data points are inserted in the data and a final data is created and given as output which is further used for the visualization and forecasting.

### 4. Results

Using Lagrange's interpolation formula as shown in equation (1), we have obtained missing values. We have also calculated the missing values in the whole dataset starting from 1<sup>st</sup> August 2019 till 1<sup>st</sup> September 2020 using python implementation of Lagrange's interpolation and obtained certain result (see, Table 4.1). After visualizing the table, we can verify that the results we have obtained from the manual calculations and the results obtained by the software implementation are matching which shows the accuracy of our model.

**Table-4.1 Comparison Between Manual Calculation and Python Output**

Dates	Volumes	
	Manual Calculation	Python Output
8/1/2019	1771271	1771271
8/2/2019	1745450	1745450
8/3/2019	2049913	2049913
8/4/2019	2370230	2370230
8/5/2019	2391972	2391972
8/6/2019	1800707	1800707

So, as we can see in the scatter plots before prediction(see, figure 4.1) and after prediction(see, figure 4.2) the scattered values are in the same region, and there we can analyse the number of days has increased as the scattered plot after prediction contains the values of missing data too and the scatter graph is better

than the previous one.

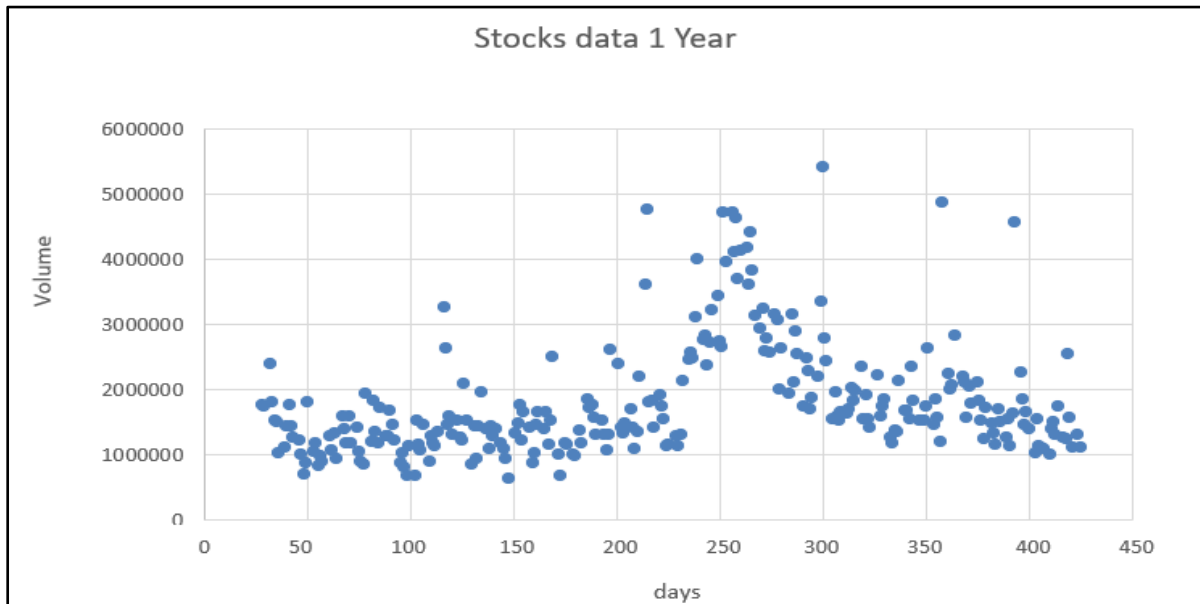


**Figure. 4.1 Scatter Plot for Volume vs Days Before Prediction**

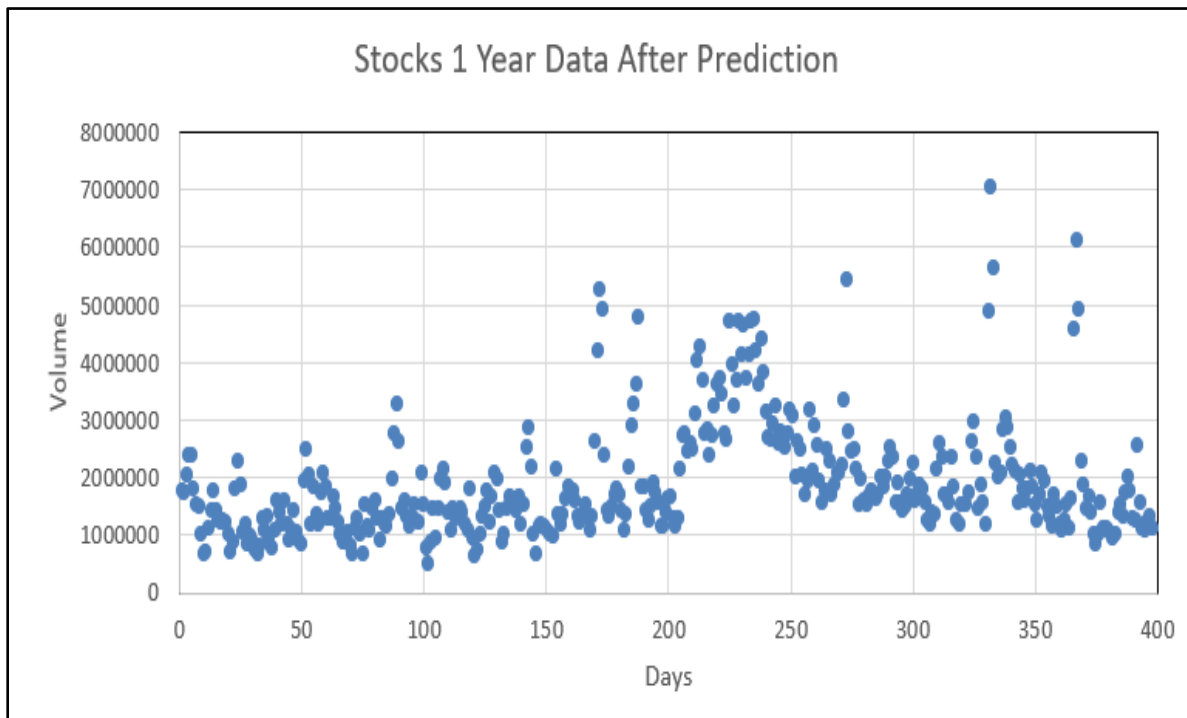


**Figure. 4.2 Scatter Plot for Volume vs Days After Prediction**

In both the curves below (see, figure 4.3 and figure 4.4) which are nearly matching which states that the values we have predicted using interpolation lie in the same range after prediction which tells that the accuracy of our model is good, and predictions are correct.

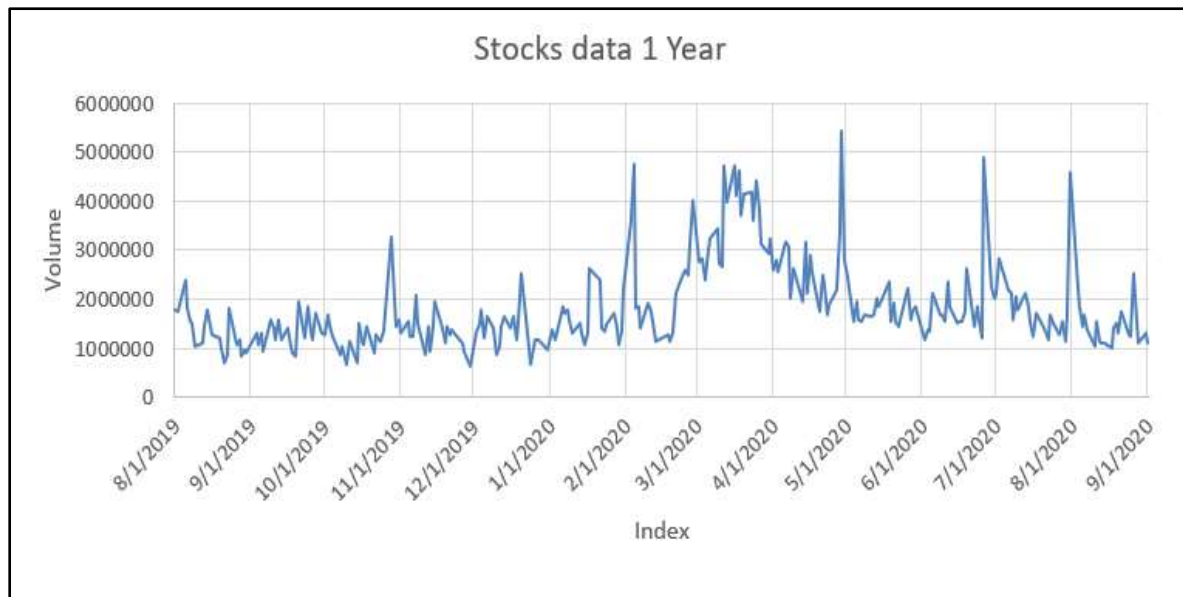


**Figure. 4.3 Line Curve of Volume vs Various Months Before Prediction**

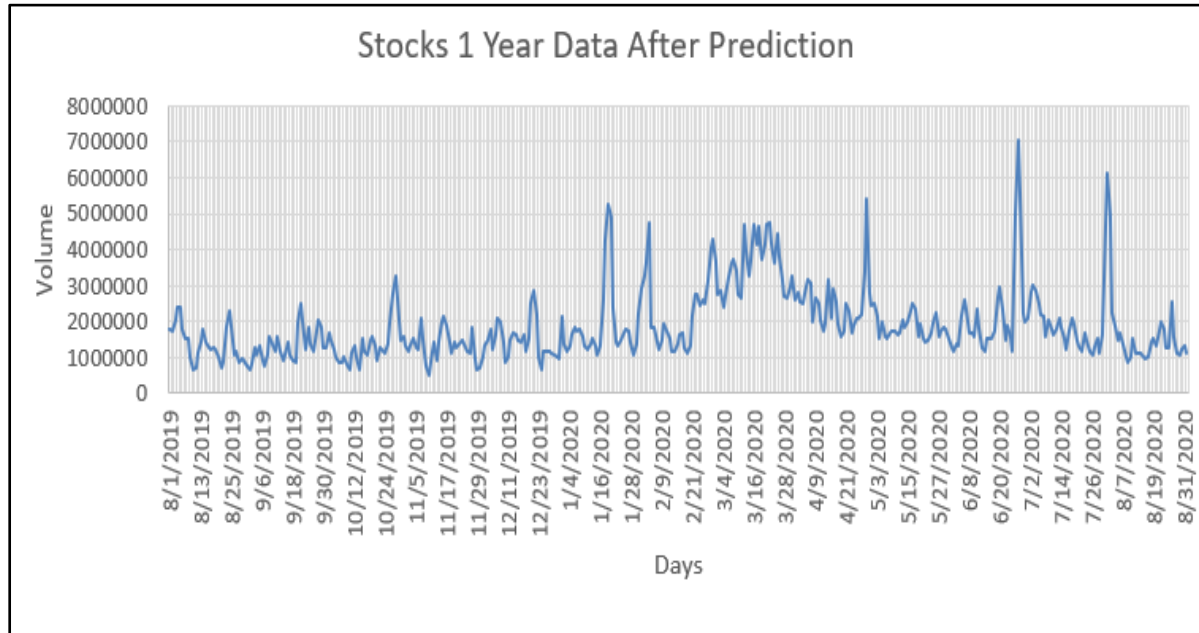


**Figure. 4.4 Line Curve of Volume vs Various Months After Prediction**

So, after all analysis and visualization we came to the result that our model can predict all the values. The interpolation function is working properly with a good accuracy.

Then, we have forecasted Data for next one month September 2020(see, figure 4.5) after the data prediction the values we have obtained while forecasting gives us a view that the values can go up and down according to the market trend.

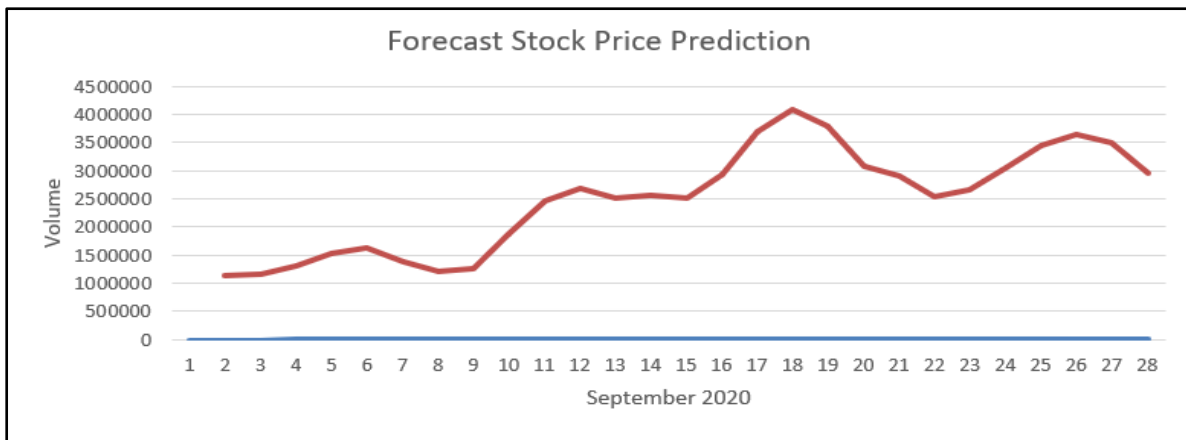


**Figure. 4.5 Forecasted Stock Market Trend of a Month: Volume vs Days**

## Conclusion

In this study, we have applied Lagrange's interpolation to predict the missing data of Google Stocks. After visualization, we concluded that for Google Stocks, Lagrange's interpolation is better as it can be applied to the dataset with unequal intervals. It is very important to find missing value to do accurate forecasting on the data also making the data complete for any further analysis. Lagrange's interpolation has good accuracy in predicting the missing values. The need of finding the missing values increases when we must forecast the statistical model and predict results based upon that. Less missing values means greater accuracy in the prediction of further results.

Another parameter that was studied in our paper was adjusted closing price. It is a graphical representation that gives the idea about the value of stocks at a certain period. It is a very important factor considered by investors before investing in any company. It gives an idea about how stocks of a particular company are performing over a while and then investors can decide whether their investment in the company will be fruitful to them or not. In this model, we have forecasted the stock prices of the upcoming month using the collected data for better insight on the google stocks. This modelling approach is successful on our data having unequal intervals and this method can be applied to any company's stock price dataset giving the desired results.

## Acknowledgments

The author would like to express our deepest appreciation to all those who provided us the possibility to complete this research. Special gratitude to my project manager, Dr. Richa Sharma for her valuable time, encouragement, invaluable guidance, support and for providing me with her valuable advice for implementing my research. The author wishes deeply thankful to his beloved parents who fulfill whatever he needs and gives him never-ending encouragement which have been helpful in my research to attain the destination without any trouble.

## References

- [1] Murphy.: Technical Analysis of The Financial Markets: A Comprehensive Guide to Trading Methods and Applications, Volume 2. Prentice Hall Press, (1999).
- [2] Turner.: A Beginner's Guide to Day Trading Online, Adams Media, Massachusetts, USA, (2007).
- [3] Dev Shah, Haruna Isah and Farhana Zulkernine.: Stock Market Analysis: A Review and Taxonomy of Prediction Techniques, International Journal of Financial Studies (IJFS) Vol. 7, No. 2, (2019).
- [4] Gourav Kumar, Sanjeev Jain and Dr. Uday Singh.: Stock Market Forecasting Using Computational Intelligence: A Survey. Archives of Computational Methods in Engineering. 28. 10.1007/s11831-020-09413-5, (2020).
- [5] K. Senthamarai Kannan, P. Sailapathi Sekar, Mohamed Sathik and P. Arumugam.: Financial Stock Market Forecast Using Data Mining Techniques, Proceedings of The International Multiconference of Engineers and Computer Scientists (IMECS) Vol I, Hong Kong, (2010).
- [6] Sudheer, V.: Trading Through Technical Analysis: An Empirical Study from Indian Stock Market, International Journal of Development Research, Vol. 5, Issue 08, pp. 5410-5416, (2015).
- [7] Zabir Haider Khan, Tasnim Sharmin Alin, Md. Akter Hussain.: Price Prediction of Share Market Using Artificial Neural Network (Ann), International Journal of Computer Applications (0975 – 8887) Vol. 22, No. 2, (2011).

- [8] Adil Moghara, Mhamed Hamicheb.: Stock Market Prediction Using LSTM Recurrent Neural Network, Procedia Computer Science, Vol. 170, pp. 1168-1173, (2020).
- [9] Sreelekshmy Selvin, Vinayakumar Ravi, E. A. Gopalakrishnan, Vijay Menon, Soman Kp.: Stock price prediction using LSTM, RNN, and CNN-Sliding Window Model, International Conference on Advances in Computing, Communications and Informatics (ICACCI), pp. 1643-1647, (2017).
- [10] Hegazy, Osman & Soliman, Omar S. & Abdul Salam, Mustafa.: A Machine Learning Model for Stock Market Prediction, International Journal of Computer Science and Telecommunications, Vol. 4, pp. 17-23, (2013).

# A Study on Soil-Structure Interaction of Engineered Structures: A Review

Ramesh Gomasa and A.R. Prakash

**Abstract** Soil structures are critical for reinforced concrete constructions to have adequate strength and durability. Bridges, turbines, dams, industrial structures, and other large constructions are all made of it. Seismic reactions to structures are frequently based on soil-structure interactions. It's typically employed in pile foundation geotechnical studies. The reaction of soil and structure, which determines ground and structure motion, is the most important aspect of soil-structure interaction. Knowing the interactions between the soil and the earth is one of the most significant components. If the soil interactions are favourable, the structure will be safe and sturdy, and it will be able to endure earthquakes. As a result, understanding soil interaction is critical for any structure's safety and serviceability. The focus of this work is on group piles as opposed to the monopile basis of soil interaction. This illustrates why a monopile foundation is preferable than a group pile foundation. Monopile foundations are a common and basic form of foundation nowadays. The major focus of this work is on soil structure and interaction, as well as monopile foundation and its relevance.

**Keywords-** Soil-Structure Interaction, Strength, Durability, Properties.

## 1. Introduction

The components or particles that make up the soil structure are diverse. Sand, clay, and silt are all part of this category. To make a soil mix, these ingredients are mixed together. Soil structure refers to the combination of the ingredients. From a geotechnical standpoint, the mixture is referred to as aggregates. Geotechnical engineering defines it in a variety of ways. We can tell if a building is sturdy or not, as well as whether the soil is weak or strong, using this information.

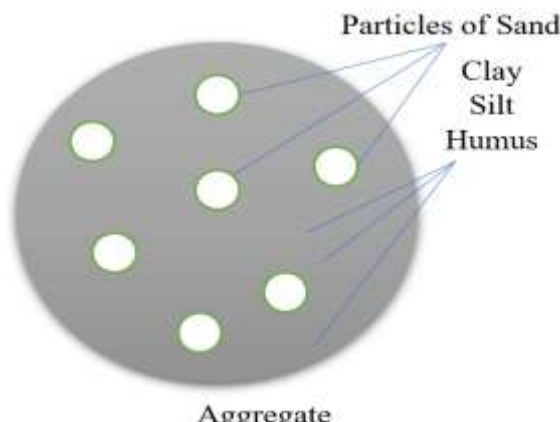


Fig.1 Aggregate

---

Ramesh Gomasa

Department of Civil Engineering, Vaagdevi College of Engineering, Warangal, Telangana, India  
e-mail: rameshgomasa@gmail.com

A.R. Prakash

Department of Civil Engineering, Vaagdevi College of Engineering, Warangal, Telangana, India

Diverse sorts of compositions, as well as different types of patterns, make up the soil structure. Water can travel through the structure depending on this. As a result, it is one of the most crucial aspects of soil interactions to understand. These professionals are needed in the geotechnical laboratory to test soil interactions. Soil samples were examined by specialized professionals. Following the tests, technicians or qualified individuals discuss whether the soil is excellent or not, as well as water circulation and permeability of the building. Soil structure is classified into grades and classes in general. Some instances of excellent and terrible structure are shown below.

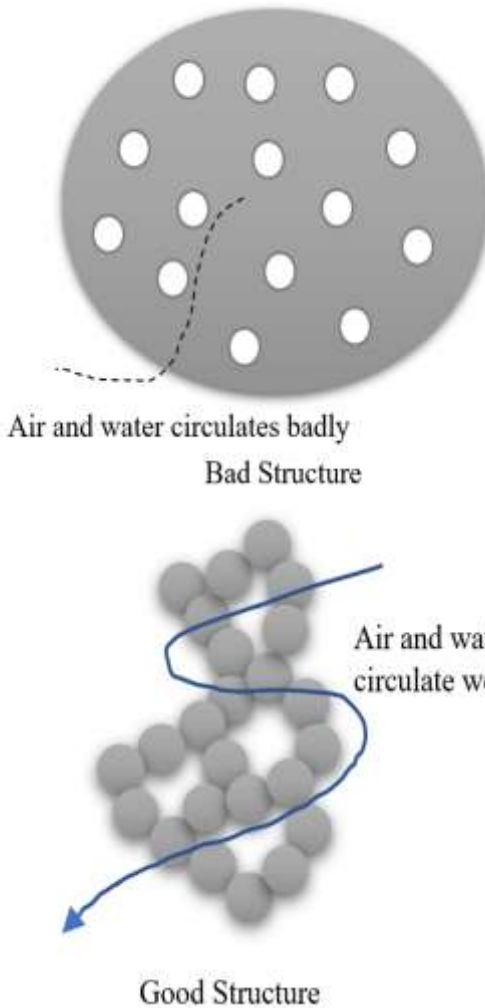
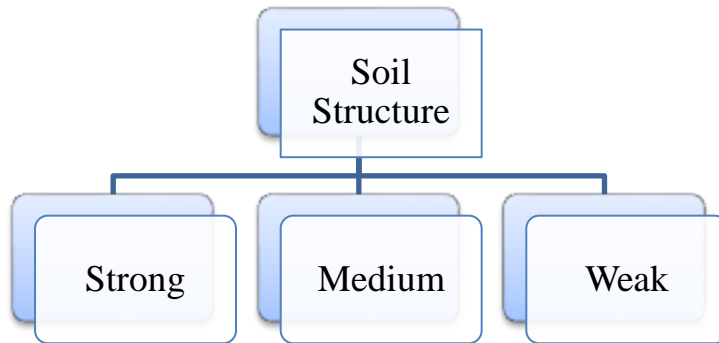


Fig. Good Structure

## II. Soil Structure

Soil structures are frequently described in terms of grades, classes, and aggregates. Aggregates, as well as their kinds and sizes, play a significant role in gaining a better understanding of the soil structure and profile. This soil structure is mostly determined by the soil's properties.

### Grades of Soil Structure



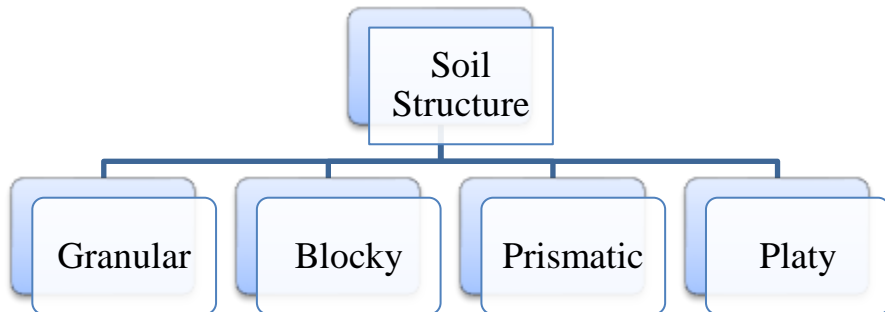
**Strong structure:** These are more durable and stronger. The soil is well-structured. Large and tiny aggregates, as well as shattered components, make up this mixture.

**Medium structure:** These are more powerful and long-lasting. The soil structure is excellent. It is made up of big and tiny aggregates, as well as fragmented elements.

**Weak structure:** The strength and durability of them are quite low. The structure of the soil is quite flimsy. It also incorporates non-aggregate components as well as aggregates.

### Classification of Soil Structure

There are four types of structures used for soil structure. they are as follows.



### III. Literature Review

#### Yang (2006) et al.

Direct integration of ground acceleration data supplied for seismic soil–structure interaction analysis frequently creates implausible drifts in the calculated displacement, according to experience. The drifts might have a big impact on large-scale interaction analysis that uses displacement excitation as a parameter. This work presents a straightforward method for integrating acceleration in order to get a realistic displacement–time series. The acceleration data is baseline-corrected in the time domain using the least-square curve fitting technique, and then processed in the frequency domain using a windowed filter to eliminate the components that generate long-period oscillations in the resulting displacement. The suggested approach's practicality is evaluated.

#### Harte 2012 et al.

The along-wind driven vibration response of an onshore wind turbine is investigated in this work. Because softer soils might affect the dynamic response of wind turbines, the study incorporates dynamic interaction effects between the foundation and the underlying soil. An Euler–Lagrangian technique is used to build a

Multi-Degree-of-Freedom (MDOF) horizontal axis onshore wind turbine model for dynamic analysis. A rotor blade system, a nacelle, and a flexible tower are coupled to a foundation system utilizing a sub structuring technique in the model. Three spinning blades make up the rotor blade system, which incorporates the impact of centrifugal stiffening due to rotation.

#### **Kausel, E. (2010) et al.**

Soil–structure interaction is a multidisciplinary area that combines soil and structural mechanics, soil and structural dynamics, earthquake engineering, geophysics and geomechanics, material science, computational and numerical techniques, and a variety of other technical disciplines. Its roots can be traced back to the late 1800s, and it gradually evolved and matured over the following decades and during the first half of the twentieth century, before accelerating in the second half, fueled primarily by the needs of the nuclear power and offshore industries, as well as the introduction of powerful computers and simulation tools such as finite elements, and the need for seismic safety improvements.

#### **Kocak 2000 et al.**

The authors suggest a basic three-dimensional soil–structure interaction (SSI) model. To begin, a model for a layered soil media is created. The layered soil medium is separated into thin layers in that model, with each thin layer represented by a parametric model. The parameters of this model are determined in terms of the thickness and elastic properties of the sublayer by comparing the actual dynamic stiffness matrices of the sublayer with those predicted by the parametric model developed in this study in frequency–wave number space when the sublayer is thin and subjected to plane strain and out-of-plane deformations. A three-dimensional finite element model for the soil–structure system is then built by adding the structure to the soil model.

#### **Pitilakis 2008 et al.**

The numerical modelling of soil–structure interaction (SSI) phenomena examined in a shaking table facility is described in this study. The shaking table test was created to verify the numerical substructure technique's capacity to reproduce the SSI phenomena. In a dry bed of sand put within a specially built shaking-table soil container, a model foundation–structure system with high SSI potential is implanted. A significant ground motion is applied to the experimental system. The substructure technique is used to numerically simulate the entire soil–foundation–structure system in the linear viscoelastic domain. In both the frequency and temporal domains, there is a good agreement between the experimental and numerical responses. Many key characteristics of SSI that emerge from the experiment are recorded.

#### **Nakhaei, M 2008 et al.**

In a Bilinear-SDOF model under seismic stress, the influence of Soil–Structure Interaction (SSI) on Park and Ang Damage Index is explored. An detailed parametric analysis is used to achieve this. The severity of SSI is controlled by two non-dimensional parameters: (1) a non-dimensional frequency referred to as the structure-to-soil stiffness ratio index, and (2) the structure's aspect ratio. Cone Models are used to simulate the soil beneath the building, which is thought to be a homogenous elastic half space. Three separate earthquake ground movements as representative motions recorded on different soil conditions are then used to the system.

#### **Yazdchi 1999 et al.**

The transient response of an elastic structure contained in a homogeneous, isotropic, and linearly elastic half-plane is investigated in this research. The study takes into account transient dynamic and seismic forces. The linked Finite-Element–Boundary-Element methodology (FE–BE) is the numerical method used. The near field is discretized using the finite element technique (FEM), whereas the semi-infinite distant field is modelled using the boundary element method (BEM). At the soil–structure interface, these two techniques are linked by equilibrium and compatibility requirements. The transient boundary element formulation takes into account the effects of non-zero starting conditions caused by pre-dynamic loads and/or the structure's self-weight.

## ADVANTAGES OF SSI

<b>Advantages</b>	Single Foundation
	Range of Diameter up to 6m
	Structure More Flexible
	More Natural Period

## DESIGN METHODOLOGY OF SSI

<b>Design Methodology</b>	Pile Dimensions
	Site Location
	Load Carrying Capacity
	Geometry of Pile
	Installation
	Materials

## V. CONCLUSION

The findings of the monopile foundation against the group foundation are as follows. In which the outcomes of acceleration, velocity, and displacement are determined. We can determine acceleration, velocity, and displacement responses based on the following answers involving time and depth.

## REFERENCES

- [1]. Yang, J., Li, J. B., & Lin, G. (2006). A simple approach to integration of acceleration data for dynamic soil-structure interaction analysis. *Soil dynamics and earthquake engineering*, 26(8), 725-734.
- [2]. Harte, M., Basu, B., & Nielsen, S. R. (2012). Dynamic analysis of wind turbines including soil-structure interaction. *Engineering Structures*, 45, 509-518.
- [3]. Kausel, E. (2010). Early history of soil-structure interaction. *Soil Dynamics and Earthquake Engineering*, 30(9), 822-832.
- [4]. Kocak, S., & Mengi, Y. (2000). A simple soil-structure interaction model. *Applied Mathematical Modelling*, 24(8-9), 607-635.
- [5]. Pitilakis, D., Dietz, M., Wood, D. M., Clouteau, D., & Modaressi, A. (2008). Numerical simulation of dynamic soil-structure interaction in shaking table testing. *Soil dynamics and earthquake Engineering*, 28(6), 453-467.
- [6]. Anand, V., & Kumar, S. S. (2018, November). Seismic soil-structure interaction: a state-of-the-art review. In *Structures* (Vol. 16, pp. 317-326). Elsevier.
- [7]. Nakhaei, M., & Ghannad, M. A. (2008). The effect of soil-structure interaction on damage index of buildings. *Engineering Structures*, 30(6), 1491-1499.
- [8]. Yazdchi, M., Khalili, N., & Valliappan, S. (1999). Dynamic soil-structure interaction analysis via coupled finite-element-boundary-element method. *Soil Dynamics and Earthquake Engineering*, 18(7), 499-517.
- [9]. Wang, Q., Wang, J. T., Jin, F., Chi, F. D., & Zhang, C. H. (2011). Real-time dynamic hybrid testing for soil-structure interaction analysis. *Soil Dynamics and Earthquake Engineering*, 31(12), 1690-1702.
- [10]. Tongaonkar, N. P., & Jangid, R. S. (2003). Seismic response of isolated bridges with soil-structure interaction. *Soil Dynamics and Earthquake Engineering*, 23(4), 287-302.

- [11]. Todorovska, M. I. (2009). Seismic interferometry of a soil-structure interaction model with coupled horizontal and rocking response. *Bulletin of the Seismological Society of America*, 99(2A), 611-625.
- [12]. Su, J., & Wang, Y. (2013). Equivalent dynamic infinite element for soil-structure interaction. *Finite elements in analysis and design*, 63, 1-7.
- [13]. Spyros, C. C., Koutromanos, I. A., & Maniatakis, C. A. (2009). Seismic response of base-isolated buildings including soil-structure interaction. *Soil Dynamics and Earthquake Engineering*, 29(4), 658-668.
- [14]. Sáez, E., Lopez-Caballero, F., & Modaressi-Farahmand-Razavi, A. (2013). Inelastic dynamic soil-structure interaction effects on moment-resisting frame buildings. *Engineering structures*, 51, 166-177.
- [15]. Shakib, H., & Fuladgar, A. (2004). Dynamic soil-structure interaction effects on the seismic response of asymmetric buildings. *Soil Dynamics and Earthquake Engineering*, 24(5), 379-388.
- [16]. Ülker-Kaustell, M., Karoumi, R., & Pacoste, C. (2010). Simplified analysis of the dynamic soil-structure interaction of a portal frame railway bridge. *Engineering structures*, 32(11), 3692-3698.
- [17]. Ülker-Kaustell, M., Karoumi, R., & Pacoste, C. (2010). Simplified analysis of the dynamic soil-structure interaction of a portal frame railway bridge. *Engineering structures*, 32(11), 3692-3698.
- [18]. Wang, H. F., Lou, M. L., Chen, X., & Zhai, Y. M. (2013). Structure-soil-structure interaction between underground structure and ground structure. *Soil Dynamics and Earthquake Engineering*, 54, 31-38.
- [19]. Soneji, B. B., & Jangid, R. S. (2008). Influence of soil-structure interaction on the response of seismically isolated cable-stayed bridge. *Soil Dynamics and Earthquake Engineering*, 28(4), 245-257.
- [20]. Spyros, C. C., Maniatakis, C. A., & Koutromanos, I. A. (2009). Soil-structure interaction effects on base-isolated buildings founded on soil stratum. *Engineering Structures*, 31(3), 729-737.
- [21]. Allotey, N., & El Naggar, M. H. (2008). Generalized dynamic Winkler model for nonlinear soil-structure interaction analysis. *Canadian Geotechnical Journal*, 45(4), 560-573.
- [22]. Bhattacharya, S., Nikitas, N., Garnsey, J., Alexander, N. A., Cox, J., Lombardi, D., ... & Nash, D. F. (2013). Observed dynamic soil-structure interaction in scale testing of offshore wind turbine foundations. *Soil Dynamics and Earthquake Engineering*, 54, 47-60.
- [23]. Wegner, J. L., Yao, M. M., & Zhang, X. (2005). Dynamic wave-soil-structure interaction analysis in the time domain. *Computers & structures*, 83(27), 2206-2214.
- [24]. Amorosi, A., Boldini, D., & Di Lernia, A. (2017). Dynamic soil-structure interaction: a three-dimensional numerical approach and its application to the Lotung case study. *Computers and Geotechnics*, 90, 34-54.
- [25]. Ghandil, M., & Behnamfar, F. (2017). Ductility demands of MRF structures on soft soils considering soil-structure interaction. *Soil Dynamics and Earthquake Engineering*, 92, 203-214.
- [26]. Raychowdhury, P. (2011). Seismic response of low-rise steel moment-resisting frame (SMRF) buildings incorporating nonlinear soil-structure interaction (SSI). *Engineering Structures*.
- [27]. Bhattacharya, S., & Adhikari, S. (2011). Experimental validation of soil-structure interaction of offshore wind turbines. *Soil Dynamics and Earthquake Engineering*, 31(5-6), 805-816.
- [28]. Krishnamoorthy, A., & Anita, S. (2016, February). Soil-structure interaction analysis of a FPS-isolated structure using finite element model. In *Structures* (Vol. 5, pp. 44-57). Elsevier.
- [29]. Behnamfar, F., & Banizadeh, M. (2016). Effects of soil-structure interaction on distribution of seismic vulnerability in RC structures. *Soil Dynamics and Earthquake Engineering*, 80, 73-86.
- [30]. de Silva, F. (2020). Influence of soil-structure interaction on the site-specific seismic demand to masonry towers. *Soil Dynamics and Earthquake Engineering*, 131, 106023.

# **Pushover Analysis of RC frame structure on sloping ground using SAP2000**

**Monika Angral, Manvinder Kingra and Pritpal Kaur**

**Abstract** From the past few years, large-scale research has been going on, on the performance of the structures during earthquake. In the course of earthquake, the structure went through many elastic zones. Performance based seismic design is a leading edge to anticipate the capability of the structure by using the non-linear static analysis. As the name describes it, non-linear static analysis is a process in which the structure is pushed horizontally with the increasing loading pattern and the structure is pushed until its failure. It is the easiest method to consider the post elastic behavior of the structure. In this paper, 2types of models are modeled and analyzed. On the plane ground and the other on the sloping ground with step-back structure. G+10 models are considered in the seismic zone III. Modeling and analysis was executed on SAP2000 software. IS 1893(part1):2016 was considered for seismic analysis. It was carried out that the structures on the plane ground are safer than on the sloping ground. Also, the failures are earlier in the step-back structures and more hinges were there.

**Keywords-** Non-linear static analysis, Pushover analysis, RCC frame structure, Step-back structure, SAP2000 v 21.

## **1. Introduction**

In the contemporary world, the demand of high-rise structures increased day by day. Due to the inadequacy of land, the constructions on the hilly or sloping areas are prominent these days. Different type of structures can be constructed on sloping areas such as step-back structures, set-back structures and set-back step-back structures. Also, the short columns can be considered.

In case of hilly areas, the construction of high-rise buildings is dangerous as they do not have same foundation level. The base of building must be strong enough to take all the structure load and transfer it to the ground. Same happens with the vibrations produced during the earthquake events. The shaking produced during seismic events provide vibrations in the structure which leads in failure of structure members. Columns are affected more than beams as they are vertical members in the structure which transfer loads to the others floors up to the ground. Different methods can be used to identify these failures while designing the structure in hilly areas. Non-linear static analysis is one which is easiest method to locate failures earlier. Non-linear static analysis also known as pushover analysis can be performed on software. Sap2000 is the software which we are used in this paper to perform pushover analysis on the structure. It has been noticed that changes have been required in the design based on linear elastic analysis. Nowadays the structures are designed according to the codes and they designed and analyzed earlier to check the failures in the structure. Pushover analysis is basically done to check the seismic capacity of any structure. Two dimensional or three-dimensional structures can be modeled in Sap200 to analyze the structure. Lateral loads are applied on the structure and they increased monotonically until the various

---

Monika Angral

PG Student M.Tech Structural Engineering, Guru Nanak Dev Engineering College, Ludhiana, India.  
Email Address :monikaangral0@gmail.com

Er. Manvinder Kingra

Assistant Professor, Department of Civil Engineering, Guru Nanak Dev Engineering College, Ludhiana, India.

Er. Pritpal Kaur

Assistant Professor, Department of Civil Engineering, Guru Nanak Dev Engineering College, Ludhiana, India.

members of the structure fails. The loads are applied continuously until the structure fails. After that a curve is plotted between base shear and roof top displacement if the structure.

## 2. PUSHOVER ANALYSIS

Pushover analysis is basically an easiest method to perform analysis on the structure as it keeps all the records of each step applied on the structure. It keeps the record of the yielded members and the failure members. The curve is plotted with these failures by the software itself. Some changes have been made in the structure to reduce the stiffness in the structure. This process continues until total collapse occurs or control movement at peak reaches to the point of damage. Then a graph is plotted between base and displacement which is basically global curve. Different load combinations are applied on the model. These load combinations are from the Indian Standard code. With the pushover curve the hinges are located. There are various plastic range for hinges such as

1. Point A to B is the elastic area.
2. Point B to IO is the instant occupancy area.
3. Point IO to LS is the life safety area.
4. Point LS to CP is the collapse prevention area.

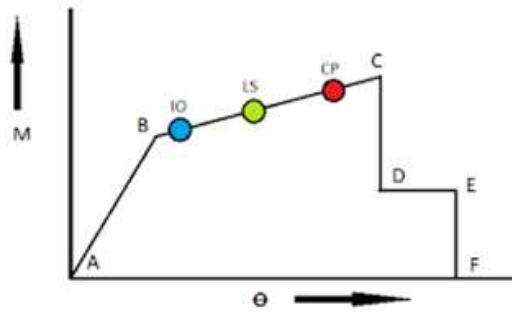


**Fig. 2.1 Non-linear static analysis curve**

As the hinges reaches at point D, the hinge stopped to drop the load. After that all the forces are removed and the elements are unloaded. When the hinge reached at point D, the pushover magnitude is again amplified and the displacements increases again. If the hinges are upto CP zone then the structure is safe but after IO zone, the retrofitting for the structure is required. The earlier failures are due to some basic reasons such as the material quality, workmanship, different load patterns and the structural member's capability. Pushover analysis is the impressive tool to estimate damages in structural and non-structural members which occurs due to future shaking. There are different characteristics in the structure which can be

1. Capacity curve helps us to estimate structure capacity.
2. The distribution of plastic hinges at ultimate load can be found.
3. The structure's lateral resistance.
4. The retrofitting of the existing structures.
5. The different drifts at the top of the structure and its distribution along the vertical height of the structure.

Pushover consists of two types of procedures:

1. Estimation of target displacement for the structure:- The process included that the top displacement of the structure is fixed and pushover analysis is provided to meet that displacement. The fixed displacement is the target displacement.
2. Force controlled method:- The procedure includes that the forces occurred on the structure are calculated first and then applied on the structure and then the analysis is carried out to get the desired results.

## 3. Methodology

With the increase in the population the scarcity and demand of land occurs. To fulfil the requirement of land the construction in the hilly areas are required these days. In this paper the analysis is carried out

considering rc structure in seismic zone III, importance factor 1.5, Response reduction Factor 5, Zone factor 0.16 and type II soil. Non-linear static analysis is done on plane and sloping ground. Different seismic load patterns are applied on the structure according to IS 1893:2016 (part1). The analysis is carried out on SAP2000 which is based upon finite element. A G+10 high structure is designed and analysed in SAP2000 on plane and sloping ground. And their comparison is made to get the results. Indian standard codes are used for load patterns and combinations and loads. Fe415 is used for reinforcement and M25 is used for cement.

**Table-3.1 Details of the structure**

<b>Zone</b>	III
<b>Soil type</b>	Medium
<b>Plan area</b>	(24×36)m <sup>2</sup> -4@6m×6@6m
<b>Floor to floor height</b>	3.5m
<b>Number of storey</b>	G+10
<b>Grade of concrete</b>	M25
<b>Grade of steel</b>	HYSD415
<b>Size of beam</b>	450×300mm
<b>Size of column</b>	450×450mm
<b>Depth of slab</b>	125mm
<b>Dead load</b>	Auto calculated by SAP2000
<b>Live load</b>	3kN/m <sup>2</sup>
<b>Roof live load</b>	1.5kN/m <sup>2</sup>
<b>Importance factor</b>	1.5
<b>Response reduction factor</b>	5
<b>Time period</b>	Auto calculated by SAP2000
<b>Outer wall(230mm thick)load</b>	9.42816kN/m(considering 30% opening)
<b>Parapet wall(1m height)load</b>	2.208kN/m(considering 30% opening)
Earthquake load	IS1893:2016
Design code	IS456:2000

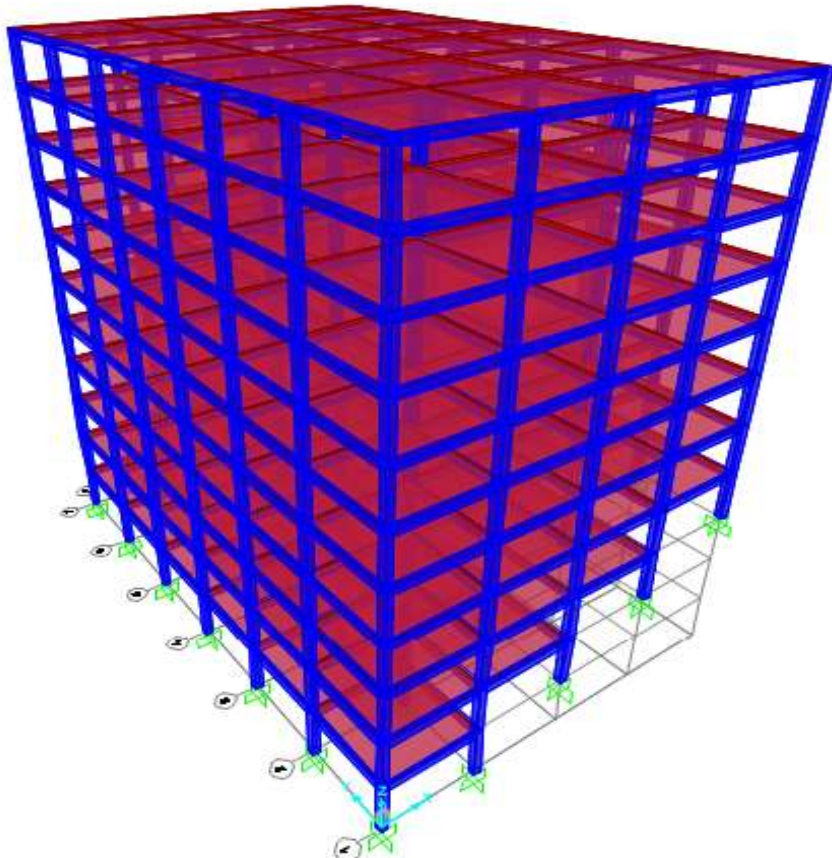


Fig. 3.1 G+10 structure on plane ground (model 1)

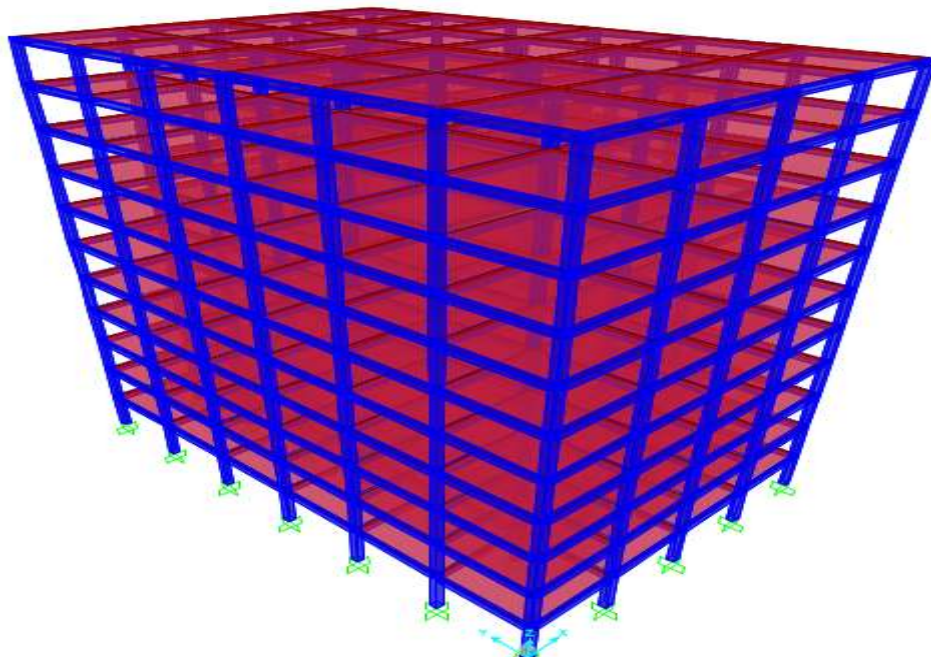


Fig. 3.2 G+10 structure on plane ground (model 2)

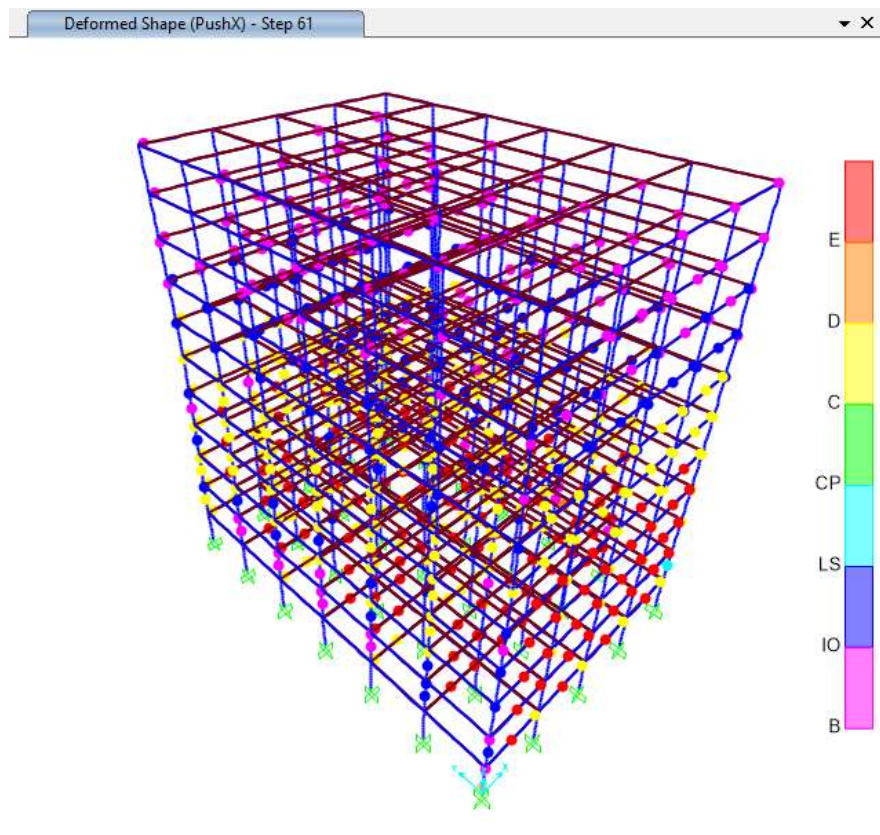


Fig. 3.3 Hinges results of model 1 in pushx direction

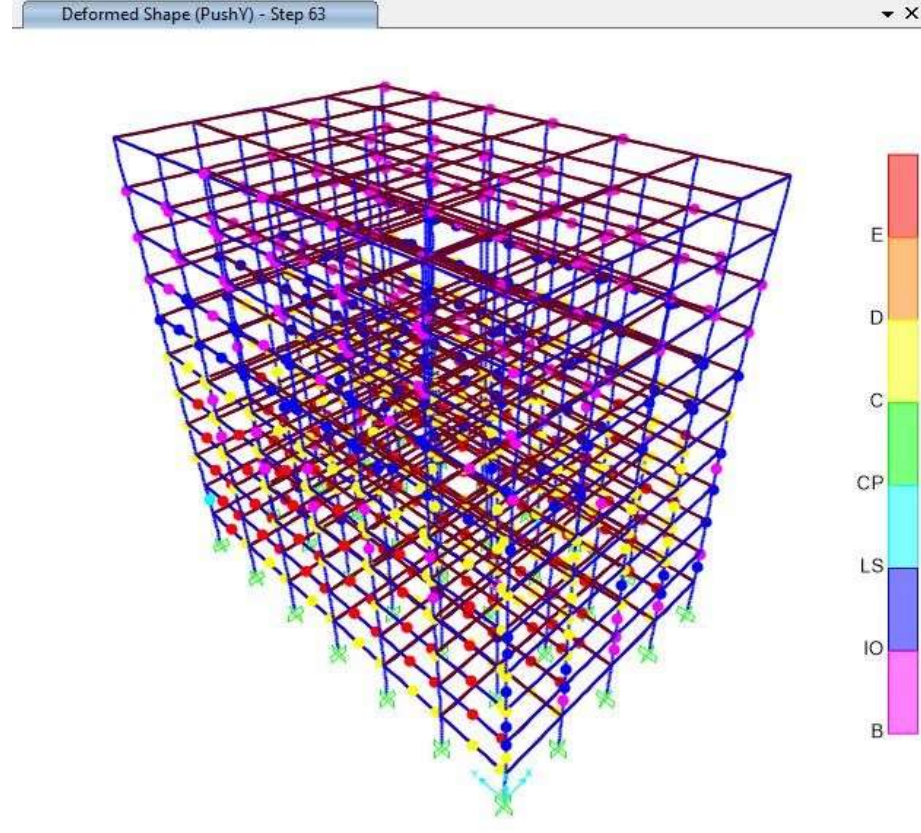
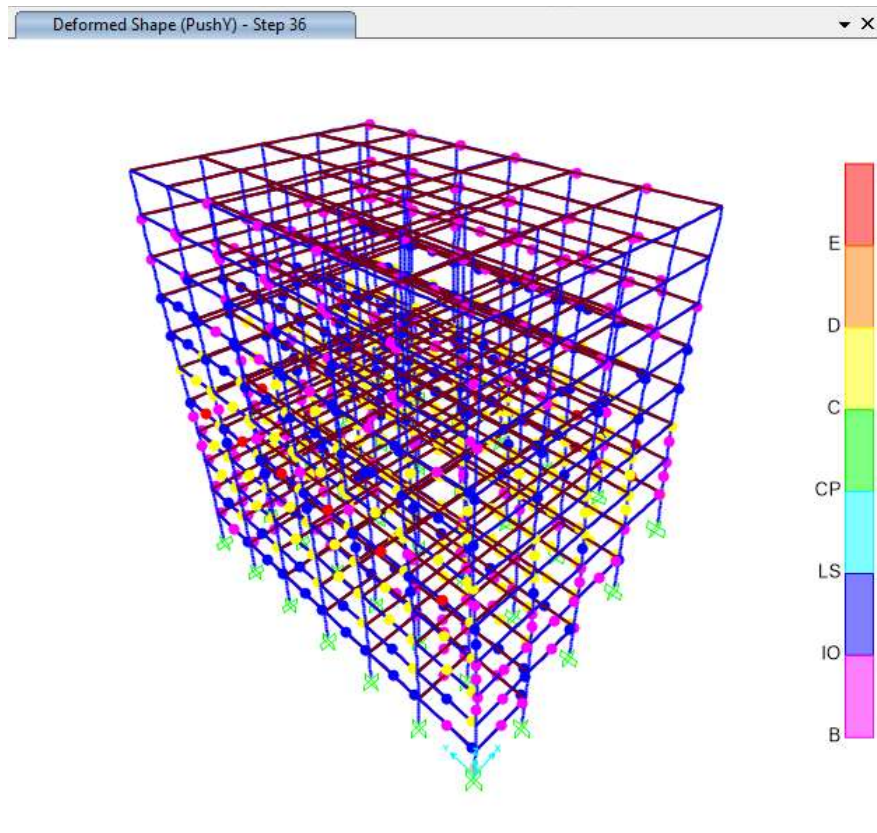
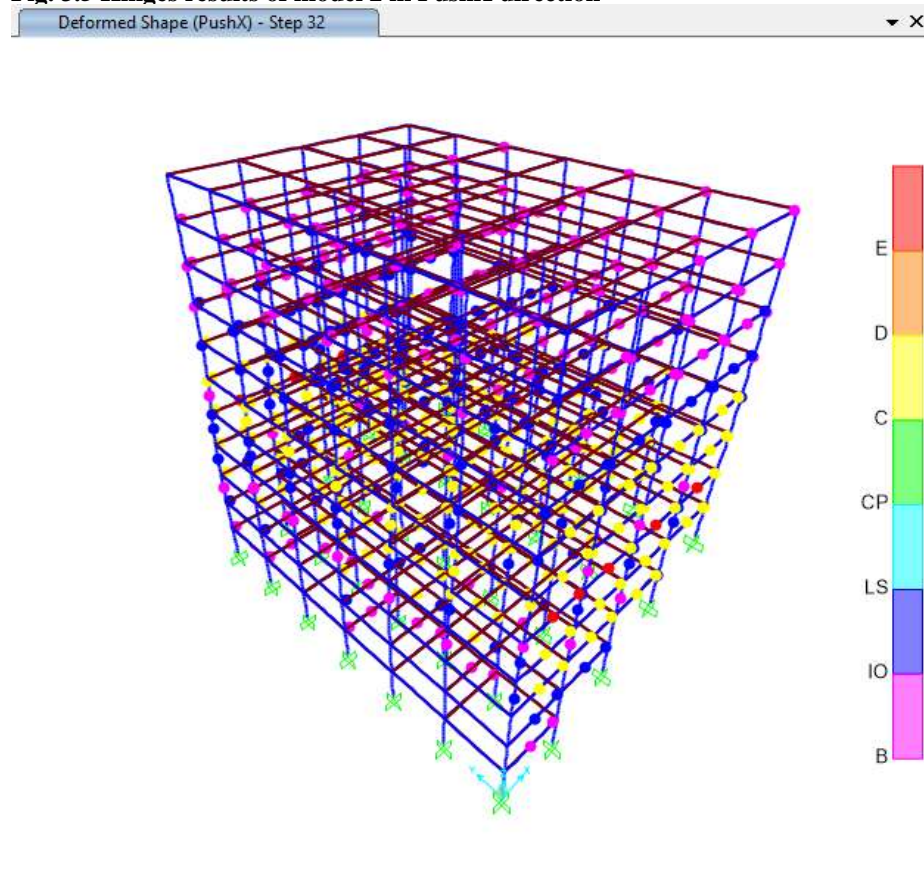


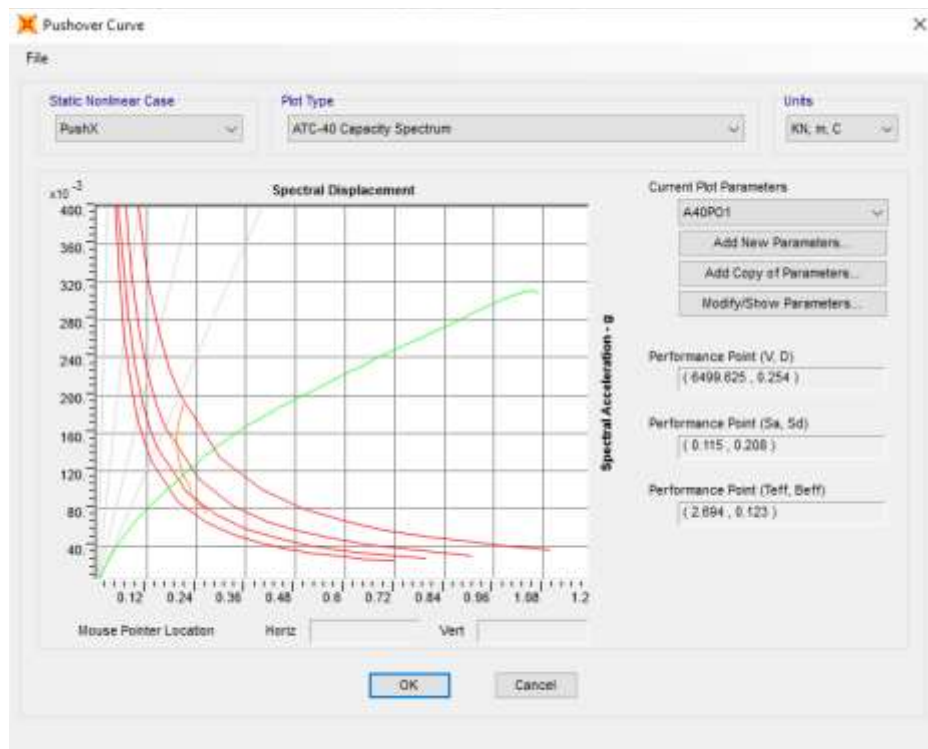
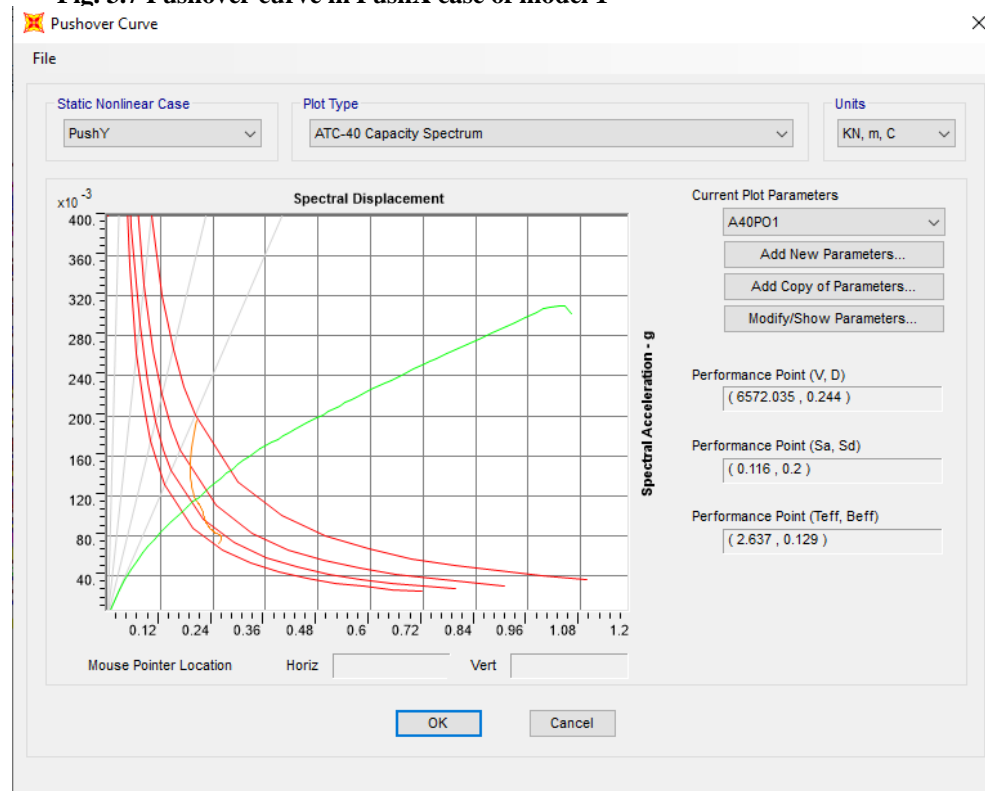
Fig. 3.4 Hinge results of model 1 in PushY direction



**Fig. 3.5 Hinges results of model 2 in PushX direction**



**Fig. 3.6 Hinges results of model 2 in PushY direction**

**Fig. 3.7 Pushover curve in PushX case of model 1****Fig. 3.8 Pushover curve in PushY case of model 1**

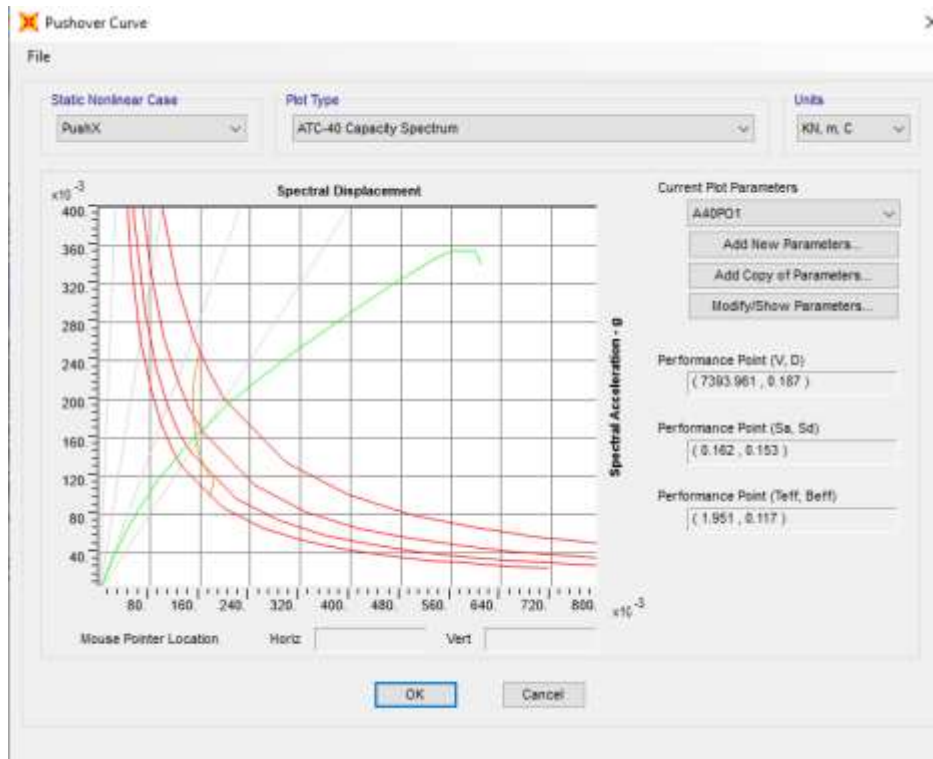


Fig. 3.9 Pushover curve in PushX case of model 2

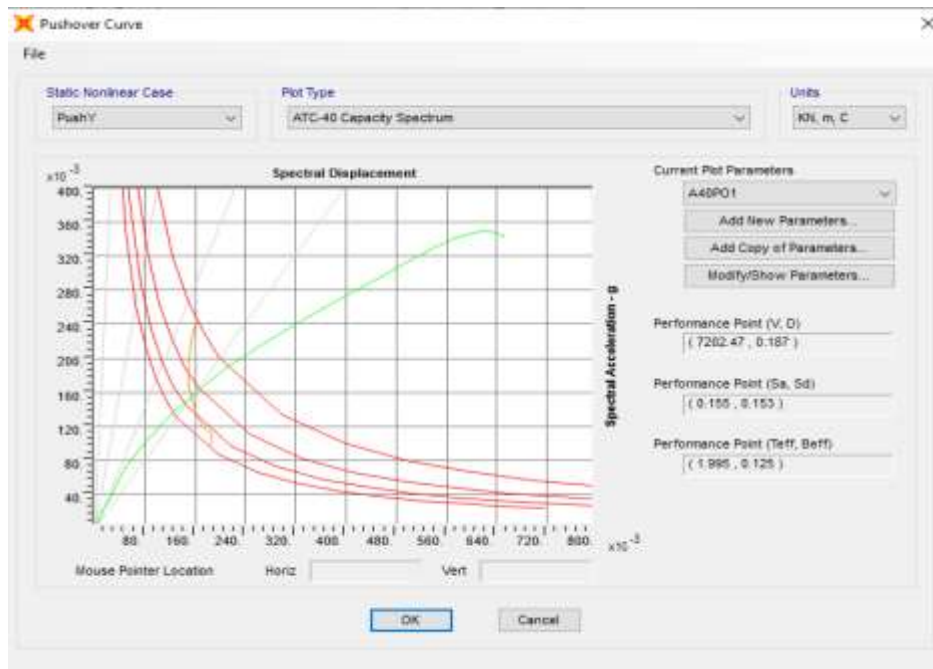


Fig. 3.10 Pushover curve in PushY case of model 2

Table-3.2 Pushover result of model 1

	V(kN)	D(m)	Sa	Sd	Teff	Beff
<b>PushX</b>	6499.625	0.254	0.115	0.208	2.694	0.123
<b>PushY</b>	6572.035	0.244	0.116	0.2	2.637	0.1229

**Table-3.3 Pushover result of model 2**

	V(kN)	D(m)	Sa	Sd	Teff	Beff
<b>PushX</b>	7393.961	0.187	0.162	0.153	1.951	0.177
<b>PushY</b>	7202.47	0.187	0.155	0.153	1.995	0.125

## Conclusion

1. It was concluded that most of the hinges were formed in the beams as compared to the columns.
2. Beams are weaker than columns.
3. On sloping ground the structure seismic capacity is less as they have steep ground where as the structure on the plane ground can bear more seismic forces.
4. The structural seismic capacity depends upon the element properties, material properties and the seismic zone.
5. The structure on the plane ground was more resistance to base shear as compared to the sloping ground.
6. From the curve it was concluded that the RCC frame on the plane ground are more able to resist and withstand forces as compared to the models on the sloping ground.

## Acknowledgments

The author would like to extend her deepest gratitude and gratefulness to teachers for providing with the right ways of thinking and concepts of this research. The author wishes deeply thankful to her beloved parents and friends who fulfill whatever she needs and gives her never-ending love and encouragement which have been helpful in my research to attain the destination without any trouble.

## References

- [1] Azaz, M., Sohailuddin, S., Ansari, A., Atif, M., Ameenuddin, M., (2017), "Pushover Analysis on RCC Structures for Zone IV and Zone V", International Journal for Research in Applied Science & Technology, 5(12), 243-252.
- [2] Clerk Maxwell, J. (1892). *A Treatise on Electricity and Magnetism*, 3rd ed., vol. 2. Oxford: Clarendon, pp.68–73.
- [3] Baitule, S., Dalawi, T., (2018), "A review on Non-linear Pushover Analysis of Flat Slab Building", International Journal of Innovative Research in Science, Engineering and Technology, 7(4), 3903-3906.
- [4] Bento, R., Falcao, S., Rodrigues, F., (2004), "Non-linear static procedures in performance based seismic design", 13th World Conference on Earthquake Engineering, Vancouver, B.C., Canada, 2(2522), 1-9.
- [5] Chopra, A.K., Goel, A.K., (2004), "A modal pushover analysis procedure for estimating seismic demands for buildings", Earthquake engineering and structure dynamics, 33(8), 903- 927.
- [6] Deep, V.M., Raju, P.P., (2017), "Pushover Analysis of RC building: Comparative study on seismic zones of India", International Journal of Civil Engineering and Technology, 8(4), 567- 578.
- [7] Daniel, D.M., John, S.T., (2016)," Pushover Analysis of RC Building", International Journal of Scientific & Engineering Research, 7(10), 2229-5518.
- [8] El-Fotoh, G.A., Aly, A.S., Attabi, M.M.H., (2018), "Pushover Analysis for Reinforced Concrete Portal Frames", International Journal of Scientific & Engineering Research, 9(3), 347-355.
- [9] Ganapati, S.K., Mangalgi, S., (2017), "Pushover Analysis of RC Frame Structure with Floating Column on Sloping Ground", International Research Journal of Engineering and Technology, 4(8), 1751-1759.
- [10] Ghosh, R., Debbarma, R., (2019), "Effect of slope angle variation on the structures resting on hilly region considering soil-structure interaction", International Journal of Advanced Structural Engineering, 11:67-77.
- [11] Hakim, R.A., Alama, M.S., Ashour, S.A., (2014), "Seismic Assessment of an RC Building Using Pushover Analysis", Engineering, Technology & Applied Science Research, 4(3), 631- 635.

# **Behaviour of Irregular Structures Under Three-Dimensional Earthquake Loading Considering Base Isolation System**

**Raja Suhaib Amin, Amir Hussain Bhat and Hardeep Singh Rai**

**Abstract:-** Irregular configuration either in plan or in elevation is recognised as one of the main causes of earthquake failure of structures. There is therefore concern regarding irregular structures, especially in seismic zones. Structures usually possess a combination of irregularities and therefore may not result in accurate prediction of seismic response if single irregularity is taken into account. The choice, type and location of irregularity in the design of earthquake resistant structures is important as it helps in improving the utility and aesthetics of the structure. To prevent the irregular structures during earthquake various techniques can be used and one of the most important technique is base isolation technique. This research therefore focuses on the seismic response of reinforced concrete irregular buildings taking cracked section property into account with distinct irregularity combinations consisting of fixed base and lead rubber bearing base isolator. A 9 storey RC frame is analysed for seismic behaviour with and without taking cracked section property into account and then the cracked section regular RC frame model is modified by integrating vertical irregularities in different combinations and a total of 23 cases are studied. Lead rubber bearing (LRB) is analytically devised following the guidelines of UBC-97 for the case which gives maximum response and then compared. After Response spectrum analysis it is found that cracked section property shows more displacement and drift than gross section model thus showing less factor of safety and more realistic behaviour. And also, it is found that irregularity affects the seismic response considerably. The irregularity of stiffness has a maximal impact on seismic response among all the different forms of single irregularities analyzed. The structure having both mass and stiffness irregularities shows maximum seismic response. After using lead rubber bearing (LRB) base isolator in the structure where irregularities are present in combination it is observed that the irregular structure response towards earthquake force gets reduced. The findings of this analysis will be of

---

**Raja Suhaib Amin**

Department of Civil Engineering, Guru Nanak Dev Engineering College, Ludhiana, India  
Email Adress: [subysuhaib1@gmail.com](mailto:subysuhaib1@gmail.com)

**Amir Hussain Bhat**

Department of Civil Engineering, Guru Nanak Dev Engineering College, Ludhiana, India  
Email Adress: [abhat966@gmail.com](mailto:abhat966@gmail.com)

**Hardeep Singh Rai**

Department of Civil Engineering, Guru Nanak Dev Engineering College, Ludhiana, India  
Email Adress: [hardeep.rai@gmail.com](mailto:hardeep.rai@gmail.com)

wise use in designing of irregular structures without compromising their basic performance.

**Keywords:** - Irregular Structures; Base Isolation; Seismic Behaviour; Lead Rubber Bearing; Earthquake; Stiffness Irregularity; Mass Irregularity

## 1. INTRODUCTION

Earthquake happens when two sections of the surface or tectonic plates, abruptly shift along the fault lines because of tectonic movements. Tremors and movements like earthquakes discharge a colossal amount of energy which can cause serious damage to the structures. Its strength depends on the distance between the earthquake and its focus. The degree of damage around the epicenter is greater, which lies immediately above the focus on the surface of earth. Earthquakes causes serious damages to the structures. Figure 1.1 shows a building damaged due to earthquake situated in Tohoku region of Japan. Structures react dynamically to the earthquake forces which causes creation of excessive stress in the RC structural frame members and therefore it is important to consider earthquake effects while designing the structures. All structures have a natural frequency or resonance which is usually defined as no. of seconds the structure will take to vibrate to and fro. The ground beneath the structure also has a specific resonant frequency. In the event when time period of ground movement coordinates with the natural frequency of a structure, it will go through the biggest motions conceivable and endure the greatest harm. Structures of different height will react differently to the horizontal ground motion. A tall building will respond to very low frequency oscillations of the ground. A medium height building responds to medium frequency oscillations while tall and short buildings might not get affected. A short building responds to high frequency oscillations and in this situation intermediate and tall building will not show any serious response. During strong ground motions the structural configuration decides what will be the behavior of a building. During earthquake the major causes of failure of a structure is its irregular configurations which can happen to be either in plan or in elevation. Therefore, those structures which are irregular in configuration and are located in seismic zones are a matter of concern. Considering single irregularity in a structure will not give accurate prediction of seismic response, because generally in structures irregularities are present in combinations. Therefore, while considering the aesthetics and utility of a structure it is important to predict correctly the type, choice and location of irregularity. Structures present in “zone-V” are more prone to earthquake than the structures present in other seismic zones.



Fig 1 Total Collapse of Building Due to Earthquake in Tohoku Region of Japan

Table 1 Irregularity Limits Prescribed by IS 1893:2016 (Part I)

Type of Irregularity	Classification	Limits
Mass (M)	Vertical Irregularity	$M_i < 1.5M_a$
Stiffness (S)	Vertical irregularity	$S_i < S_{i+1}$
Vertical geometry (VG)	Vertical irregularity	$VG < 1.25 V_{G_a}$
Re-entrant Corner (R)	Horizontal irregularity	$R_i \leq 15\%$
Torsion (T)	Horizontal irregularity	$\Delta_{max} \leq 1.5\Delta_{avg}$

### A. Types of Irregularity

In IS 1893:2016 (Part 1) different types of irregularity are mentioned which can be present in a structure. These irregularities are major causes of failure of structures during strong ground motions. Failures like soft storey failure, plan irregularity failure, Mass irregularity failure, shear failure are the results of irregularities present in a structure.

### B. Concept of Base Isolation

Base isolation or seismic isolation is a method where the structure above the ground is isolated by introducing a mechanism that will permit the structure to stay at one spot. With base isolation system, when the ground moves, it will cause no impact on the structure consequently making it more secure. Earthquake loads are the most predominant that demands lateral design of loads. Earthquake cannot be controlled and we cannot design a structure to withstand indefinitely high intensity earthquake demands. The only thing we can do is to accept this demand and make sure that earthquake bearing capacity is more than that demand. But base isolation takes an opposite approach i.e., to reduce the seismic demand instead of increasing the capacity. The idea of base isolation is that the response of the structure is adjusted to such an extent that ground underneath the structure moves without moving the structure.

### C. Lead Rubber Bearing Base Isolation System (LRB)

The most commonly used base isolation system is lead-rubber bearing (LRB) isolators. It has the capability to combine isolation function and energy dissipation in a single compact unit. Such LRB isolator devices provide vertical load support, horizontal flexibility, supplemental damping, and centering force to the structure from earthquake attack. In addition, the cost of installation and maintenance as compared to other passive vibration control devices is very less. Base Isolation LRB lead rubber bearings work on the principle of base isolation and it minimizes the energy transferred from the ground to the structure during earthquake. It consists of a laminated rubber and steel bearing with steel flange plates for mounting to the structure. All isolators have an energy dissipating lead core. The rubber in the isolator acts as a spring. It is very soft laterally but very stiff vertically so that it supports vertical load. The high vertical stiffness is achieved by having thin layers of rubber reinforced by steel shims. These two characteristics allow the isolator to move laterally with relatively low stiffness yet carry significant axial load due to their high vertical stiffness. The lead core provides damping by deforming plastically when the isolator moves laterally in an earthquake.

## 2. METHODOLOGY

In the present study, seismic behavior of G+9 storey RC frame structure with single and combination of mass and stiffness irregularities taking cracked section property into

account is studied and their seismic response is contemplated numerically using a finite element-based software, ETABS. The structure is first modelled as Regular building with fixed base and then mass and stiffness irregularities are introduced in single and in combinations in a regular building to make it an irregular building. A total of 23 different models including a regular model are studied using finite element-based software in which 7 cases consists of mass irregularity, 7 cases consist of stiffness irregularity, 7 cases consist of combination of mass and stiffness irregularity at different storey levels. All the 22 models are modelled with fixed base. Lead Rubber Bearing (LRB) base isolator is then numerically designed for the model which gives maximum response and then its fixed base is replaced by LRB base isolator. All the 23 models are designed and analysed by Response Spectrum Analysis. The results are obtained in terms of structural response like Storey drift and Storey Displacement.

### 3. VALIDATION

Moehle (1984) has led probed a limited scale nine-storeyed test structure exposed to El-Centro North-South 1940 ground movement (scaled). The outcomes announced are utilized to approve the model created for the current research. Two RCC frames having nine stories and three bays were set opposite and parallel to one another. The frames together convey a complete load of 460 kg at each floor level. The average distance between floors is 0.229 m. The casing has three bays towards length and one bay towards width. The span of each bay in the direction of length and width are 0.305 m and 0.914 m separately. At the base, the frames were exposed to simulated seismic tremor base movement in the direction parallel to the plane of the frame. A similar test structure is demonstrated and studied mathematically utilizing ETABS. The initial three natural frequencies and the top storey displacement of the frame obtained mathematically are compared with the exploratory outcomes detailed by Moehle (1984). The equivalent is organized in Table 2.

Table 2 Validation of Software

S.No.	Response	Literature	Obtained
1	1 <sup>st</sup> Natural frequency (Hz)	45	3.1
2	2 <sup>nd</sup> Natural frequency (Hz)	14	15.3
3	3 <sup>rd</sup> Natural frequency (Hz)	28.3	26.5
4	4 <sup>th</sup> Natural frequency (Hz)	16.4	18.5

### 4. Modelling and Analysis of frames with regular and irregular configuration

A (G+9) storey RC frame structure having storey height of 3.35 m is studied. The RC frame has 6 bays in X-direction and 6 bays in Y-direction. The length of each bay in X-direction is 4m and that of Y- direction is 3m. The irregularities are incorporated in terms of mass and by changing the vertical configurations of the regular structure. Table 3 shows the building parameters like structure type, floor height, frame size, number of bays etc.

Table 3 Building Parameters

S. No.	PARAMETER	VALUES
1.	Structure Type	Special RC moment resisting frame
2.	No. of Storey	G+9
3.	Floor Height	3.35m for regular building and 5.5m for stiffness irregularity

4.	Materials	M30 concrete and HYSD 500 reinforcement.
5.	Frame Size	20m X 15m
6.	No. of Bays	6 bays each of 4m in X direction and 6 bays each of 3m in Y direction
7.	Size of Columns	750mm X 500mm
8.	Size of Beams	500mm X 350mm
9.	Depth of Slab	150mm and 250mm for mass irregularity
10.	For mass irregularity	25 kN/m <sup>2</sup> (swimming pool load)
10.	Cracked Moment of Inertia	1.7 I <sub>gross</sub> for columns, and 0.35 I <sub>gross</sub> for beams

## 5. CONFIGURATION OF CASES HAVING SINGLE AND COMBINATION OF IRREGULARITIES AND THEIR LOCATION

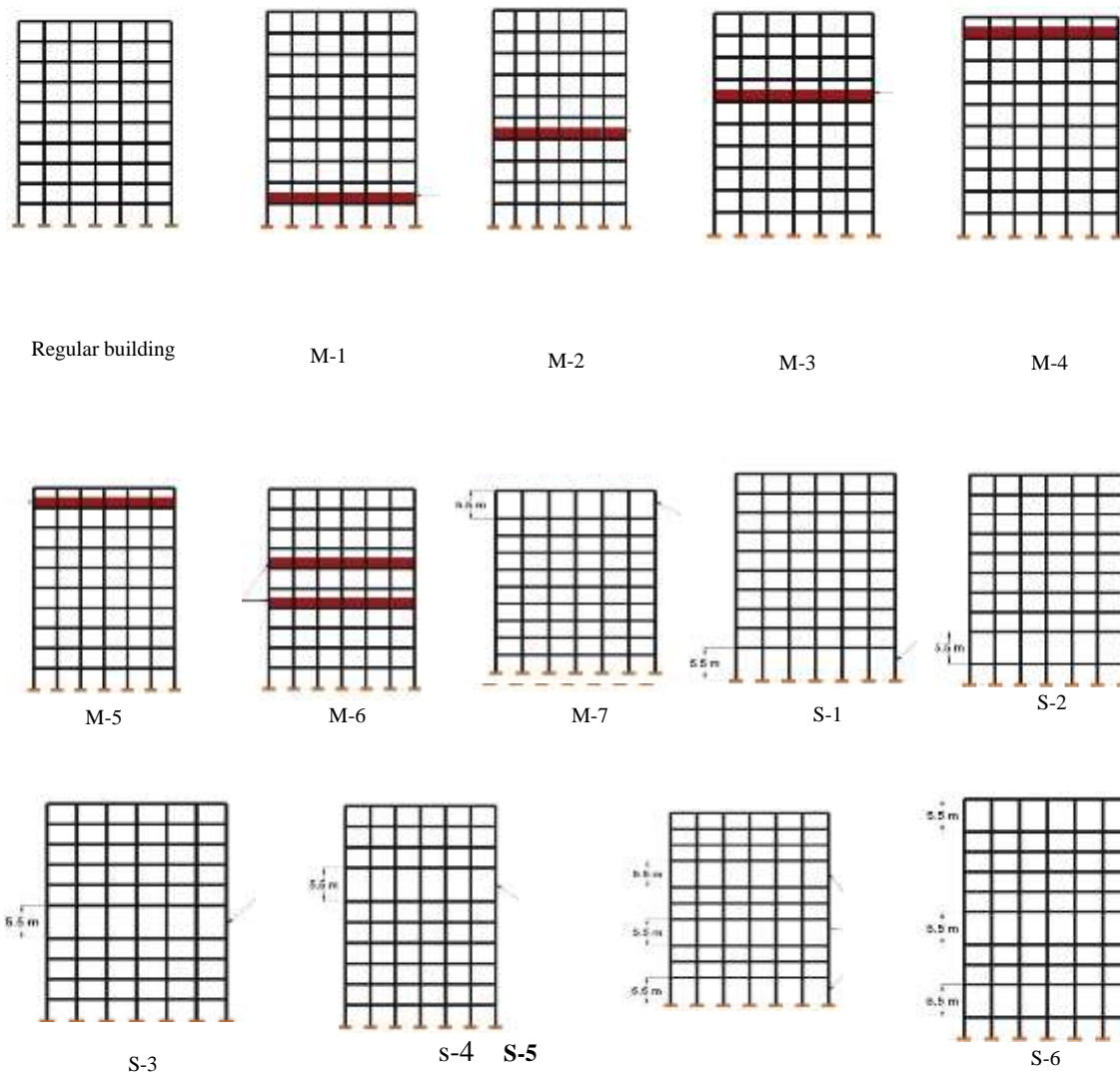
The details of all the twenty-three cases which consists of one regular RC frame structure, twenty-one Irregular RC frame structures with fixed bases and one Irregular RC frame structure with LRB base isolation system is shown in Table 4.

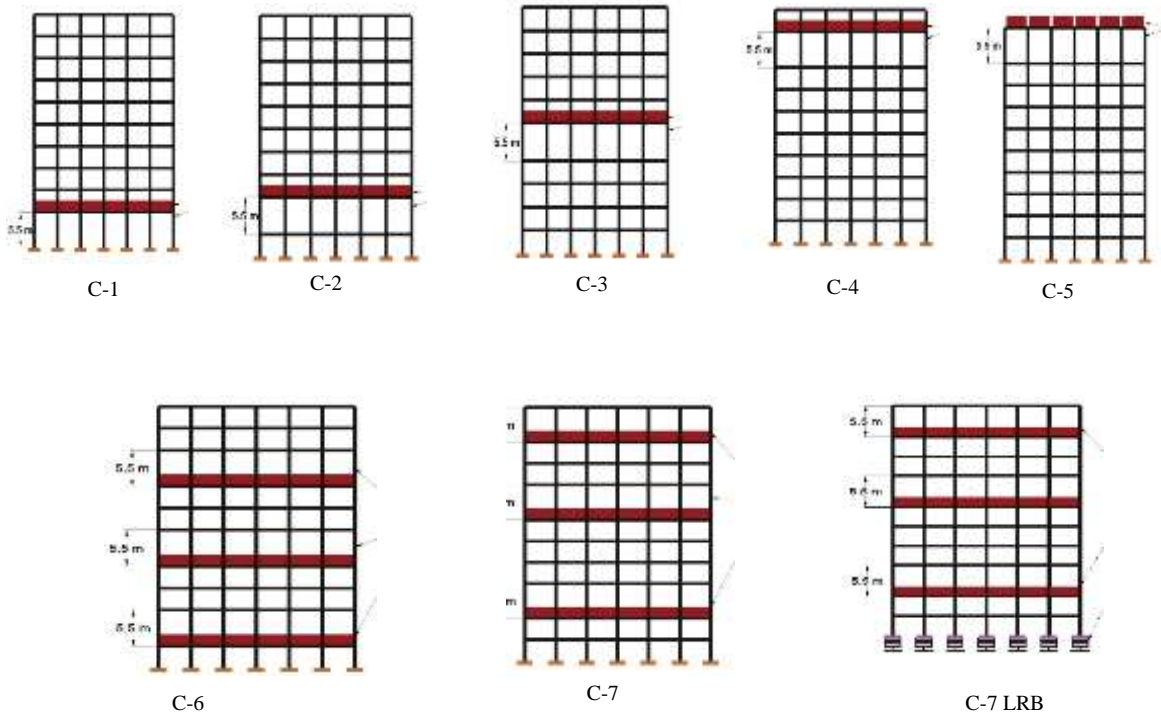
Table 4 Details of Cases Having Single and Combination of Irregularities

Model No.	Type of Irregularity	Location of Irregularity
1.	Regular Building (R)	Nil
2.	Mass Irregularity (MI-1)	Ist storey
3.	Mass Irregularity (MI-2)	4 <sup>th</sup> storey
4.	Mass Irregularity (MI-3)	6 <sup>th</sup> storey
5.	Mass Irregularity (MI-4)	9 <sup>th</sup> storey
6.	Mass Irregularity (MI-5)	1 <sup>st</sup> & 3 <sup>rd</sup> storey
7.	Mass Irregularity (MI-6)	4 <sup>th</sup> & 6 <sup>th</sup> storey
8.	Mass Irregularity (MI-7)	4 <sup>th</sup> , 6 <sup>th</sup> & 10 <sup>th</sup> storey
9.	Stiffness irregularity (SI-1)	Ground storey
10.	Stiffness irregularity (SI-2)	1 <sup>st</sup> storey
11.	Stiffness irregularity (SI-3)	4 <sup>th</sup> storey
12.	Stiffness irregularity (SI-4)	6 <sup>th</sup> storey
13.	Stiffness irregularity (SI-5)	9 <sup>th</sup> storey
14.	Stiffness irregularity (SI-6)	Ground 3 <sup>rd</sup> & 6 <sup>th</sup> storey

<b>15.</b>	Stiffness Irregularity (SI-7)	1 <sup>st</sup> , 4 <sup>th</sup> & 9 <sup>th</sup> storey
<b>16.</b>	Combinational irregularity (CI-1)	Stiffness at ground storey with mass irregularity at storey 1 <sup>st</sup>
<b>17.</b>	Combinational irregularity (CI-2)	Stiffness at 1 <sup>st</sup> storey with mass irregularity at storey 2 <sup>nd</sup>
<b>18.</b>	Combinational irregularity (CI-3)	Stiffness at 4 <sup>th</sup> storey with mass irregularity at storey 5 <sup>th</sup>
<b>19.</b>	Combinational irregularity (CI-4)	Stiffness at 8 <sup>th</sup> storey with mass irregularity at storey 9 <sup>th</sup>
<b>20.</b>	Combinational irregularity (CI-5)	Stiffness at 9 <sup>th</sup> storey with mass irregularity at storey 10 <sup>th</sup>
<b>21.</b>	Combinational irregularity (CI-6)	Stiffness at 1 <sup>st</sup> , 4 <sup>th</sup> and 7 <sup>th</sup> with mass irregularity at 1 <sup>st</sup> , 4 <sup>th</sup> and 7 <sup>th</sup>
<b>22.</b>	Combinational irregularity (CI-7)	Stiffness at 2 <sup>nd</sup> , 6 <sup>th</sup> and 9 <sup>th</sup> with mass irregularity at 2 <sup>nd</sup> , 6 <sup>th</sup> and 9 <sup>th</sup> storey
<b>23.</b>	Combinational irregularity (CI-7) with lead rubber bearing base isolation	Stiffness at 2 <sup>nd</sup> , 6 <sup>th</sup> and 9 <sup>th</sup> with mass irregularity at 2 <sup>nd</sup> , 6 <sup>th</sup> and 9 <sup>th</sup> storey

## 6. CONFIGURATION AND LOCATION OF IRREGULARITIES





## Results and Discussion

The results are compared graphically and in tabular form showing Displacement and Storey Drift graphs for different configuration and combination of Mass and Stiffness Irregularities with fixed base and LRB base isolation system in order to have a better understanding how irregular structures behave during earthquake.

### A. Seismic Behavior of Gross and Cracked Section Models

The Maximum displacement and the maximum base shear were computed and tabulated in Table 4. It is clear from the table that there is a decrease of 27% of base shear when cracked section is considered. Also, there was seen an increase in the maximum displacement by about 47% when cracked section was considered.

Table 5. Maximum displacement and the maximum base shear in Gross and cracked section model

Gross Section Model	Max Displacement (mm)	35
	Max Base Shear (KN)	6099.23
Cracked Section Model	Max Displacement (mm)	51
	Max Base Shear (KN)	4452.38
	Percentage Decrease of Base Shear in Cracked Section	27%
	Percentage increase of displacement in Cracked Section	47%

The seismic behavior of gross and cracked section models is shown in fig 2. Their Seismic behavior is analysed by comparing story shear with story displacement as shown in fig. It can be seen from the fig that the ultimate seismic capacity of the cracked section

model towards earthquake motion is smaller than the gross section model. This is because, when same earthquake load is applied to both models, cracked section model triggers displacement response and absorbs the earthquake load thus showing greater story displacement than gross section model and in case of gross section model it absorbs the load by showing higher initial stiffness thus showing greater story shear.

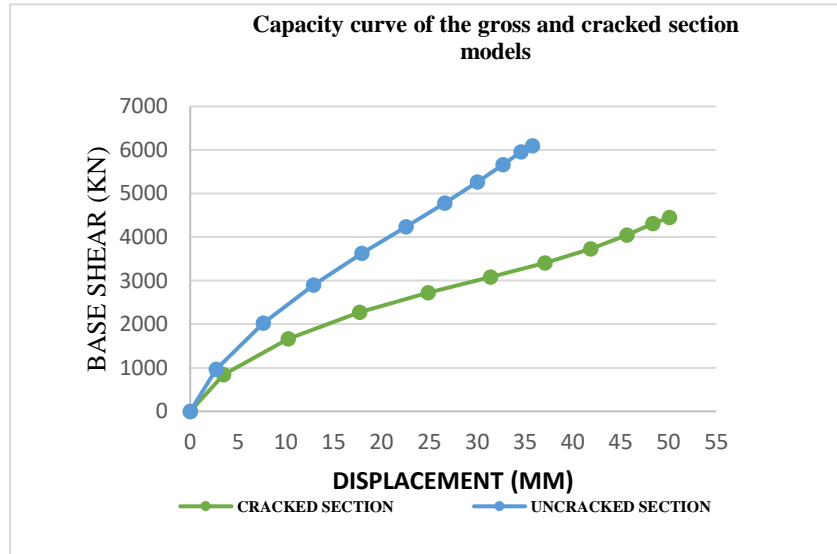


Fig 2. Capacity curve

Considering Base shear, cracked section model shows a decrease of 27.04% when compared with gross section model and with regard to displacement response, cracked section model shows an increase of 47 % when compared with gross section model.

The drift response of cracked and gross section model is shown in fig. 3. From the fig it can be clearly stated that the drift response of cracked section is more as compared to the gross section model. This is because of low cracked moment of inertia considered in cracked model. In cracked section we reduced the moment of inertia to 70% for columns and 35% for beams to analyse with the concept of strong column weak beam. It can be concluded from the result that the safety factor for the gross section is higher than the cracked section when it is concerned with design base shear i.e., gross section overestimates the ultimate seismic capacity of the structure.

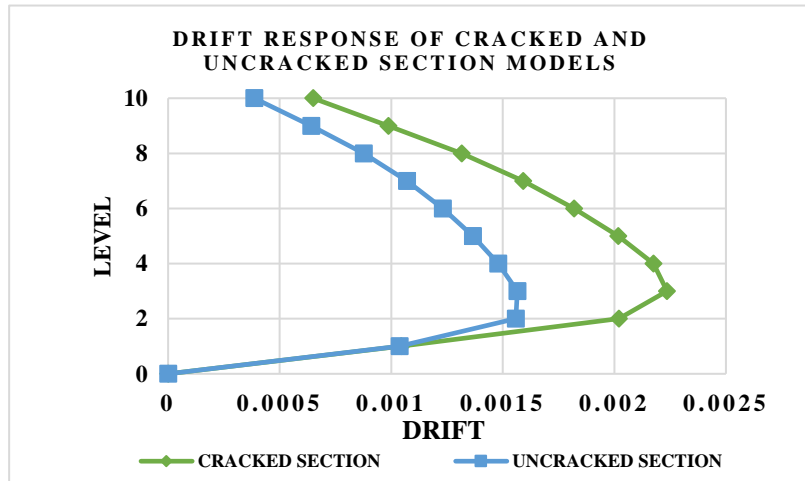


Fig 3. Drift response

## B. For Mass Irregularity cases

Max displacement response for mass irregularity cases is shown in tabulated form and in graphical form.

TABLE 5. Maximum displacement and drift values in Mass irregularity Cases

Case	Max Displacement (mm)	Max Drift
Regular	45.115	0.002236
M1	51.8	0.002668
M2	52.5	0.002478
M3	55.5	0.002623
M4	65.0	0.002816
M5	66.2	0.003173
M6	67.2	0.003655
M7	70.4	0.004297

Among the various cases the max displacement response is shown by MI-7 case, as shown in fig 4. where mass irregularity is present at 4<sup>th</sup>, 6<sup>th</sup> & 10<sup>th</sup> storey. The result is then compared with regular RC frame structure and it is found that the displacement response goes on increasing by increasing the mass and by increasing the elevation of mass irregularity. In comparison to regular structure case M1-1, MI-2, MI-3, MI-4, MI-5, MI-6, MI-7 shows an increase in displacement response by 15%, 17%, 20%, 44.5%, 47%, 50%, 56.12% respectively when compared with the regular RC frame structure.

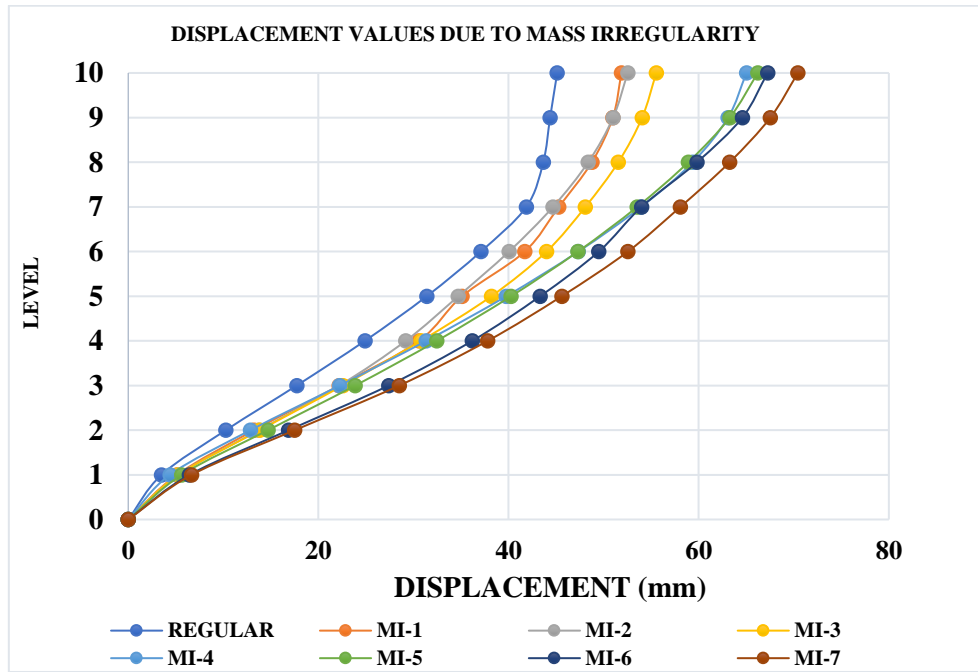


Fig 4. Displacement Response of Mass irregularity cases

The Response spectrum Storey Drift responses of mass irregularity cases is shown in fig 5. Among the various cases the max storey drift response is shown by MI-7 case, where mass irregularity is present at 4th, 6th & 10th storey. It is found that when we introduced mass irregularity at 4th, 6th & 10th storey in a regular RC frame structure the increase of

92.17% is observed in Storey Drift response of RC frame structure when compared with the regular RC frame structure.

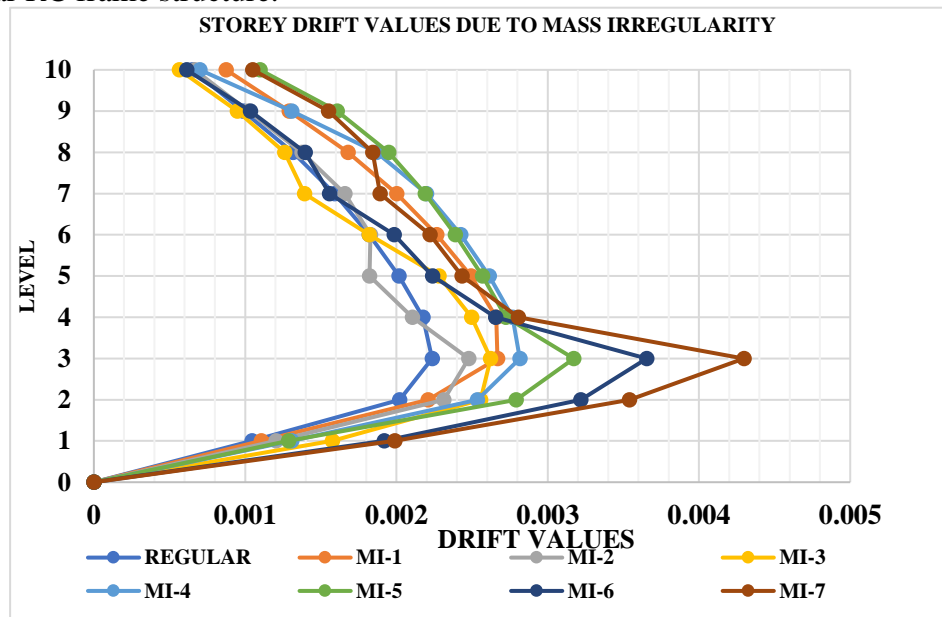


Fig 5. Drift Response of Mass Irregularity cases

### C. For Stiffness Irregularity cases

Table 6 shows the maximum displacement and maximum drift in case of stiffness irregularity.

Table 6 Maximum displacement and drift values in Mass irregularity Cases

Case	Maximum Displacement (mm)	Maximum Drift
Regular	45.115	0.002236
SI-1	59.775	0.002235
SI-2	65.523	0.002585
SI-3	60.922	0.002278
SI-4	59.785	0.002297
SI-5	56.384	0.002861
SI-6	87.542	0.003928
SI-7	95.044	0.004643

The Response spectrum analysis of Stiffness irregularity cases is shown in fig 6. Among the various cases the maximum displacement response is shown by SI-7 case, where stiffness irregularity is present at 1<sup>st</sup>, 4<sup>th</sup> & 9<sup>th</sup> storey. The result is then compared with regular RC frame structure. In comparison to regular structure SI-1, SI-2, SI-3, SI-4, SI-5, SI-6, SI-7 shows an increase in displacement response when compared with regular building by 52.45 %, 45.23%, 35.12%, 31.23%, 25%, 94%, 110.67% respectively.

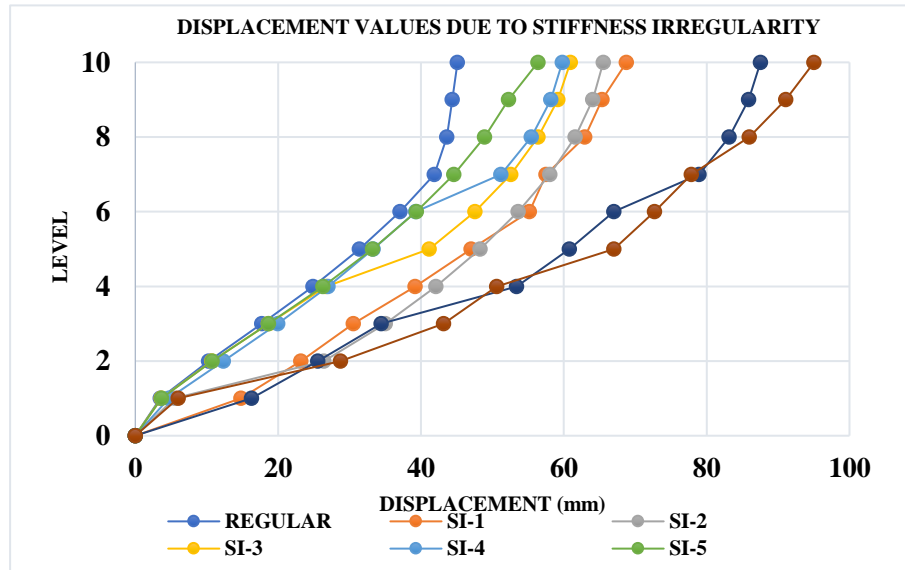


Fig 6. Displacement Response of Stiffness Irregularity cases

The Response spectrum Storey Drift responses of Stiffness irregularity cases is shown in fig 7. Among the various cases the max drift response is shown by SI-7 case, where stiffness irregularity is present at 1<sup>st</sup>, 4<sup>th</sup> & 9<sup>th</sup> storey. The result is then compared with regular RC frame structure. It is found that when we introduced Stiffness irregularity together at 1<sup>st</sup>, 4<sup>th</sup> & 9<sup>th</sup> storey in a regular RC frame structure the increase of 107.64 % is observed in Drift response of RC frame structure when compared with the regular RC frame structure. It is clear from the observation and the result that if we increase the Stiffness irregularity in a structure, it will become more irregular and shows greater Storey Drift response towards earthquake forces

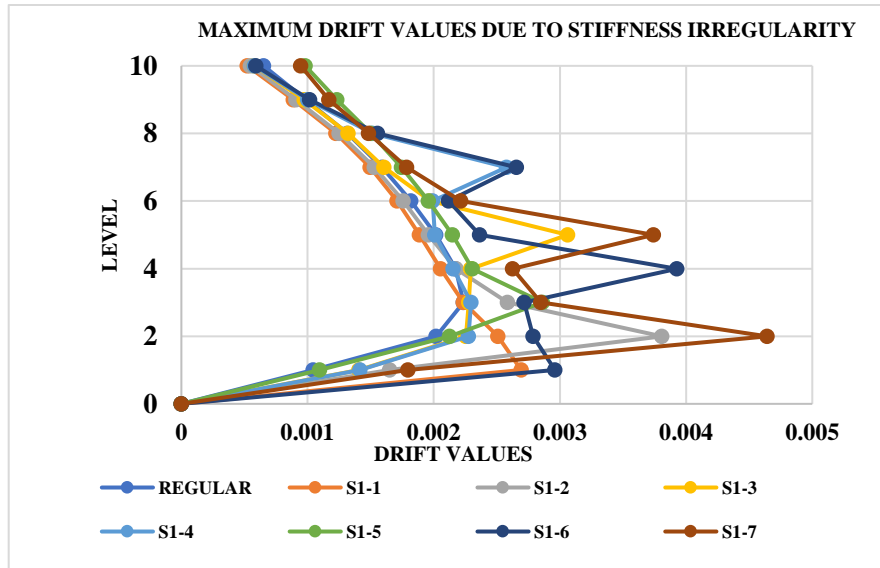


Fig 7. Drift response of Stiffness Irregularity Cases

#### D. For Combinational Irregularity cases

Table 7. shows the maximum displacement and maximum drift in case of combinational irregularity.

Table 7. Max displacement and Drift values for stiffness irregularity cases

The Response spectrum Displacement responses of combined Mass and Stiffness irregularity cases is shown in fig 8. The result is then compared with regular RC frame structure. CI-1, CI-2, CI-3, CI-4, CI-5 CI-6, CI-7. shows an increase in displacement

Case	Maximum Displacement (mm)	Maximum Drift
Regular	45.115	0.002236
CI-1	59.229	0.002677
CI-2	66.057	0.002870
CI-3	67.915	0.003385
CI-4	70.132	0.002690
CI-5	71.079	0.002703
CI-6	116.937	0.00532
CI-7	125.263	0.005937

response by 31.30 %, 46.41%, 50%, 55.15%, 58.12%, 160%, 178.12% when compared with regular building.

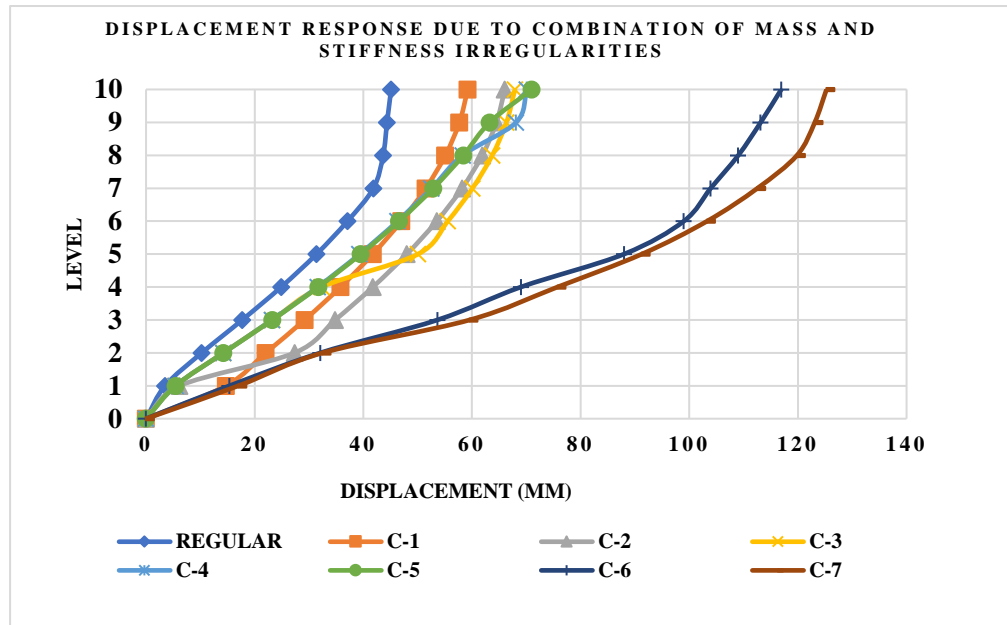


Fig 8. Displacement Response of combinational irregularity case

The Response spectrum Story Drift responses of combined Mass and Stiffness irregularity cases is shown in fig 9. It is found that when we introduce mass and Stiffness irregularities in combination at 2<sup>nd</sup>, 6<sup>th</sup> & 9<sup>th</sup> storey in a regular RC frame structure the increase of 165.51 % is observed in Storey Drift response of RC frame structure when compared with the regular RC frame structure.

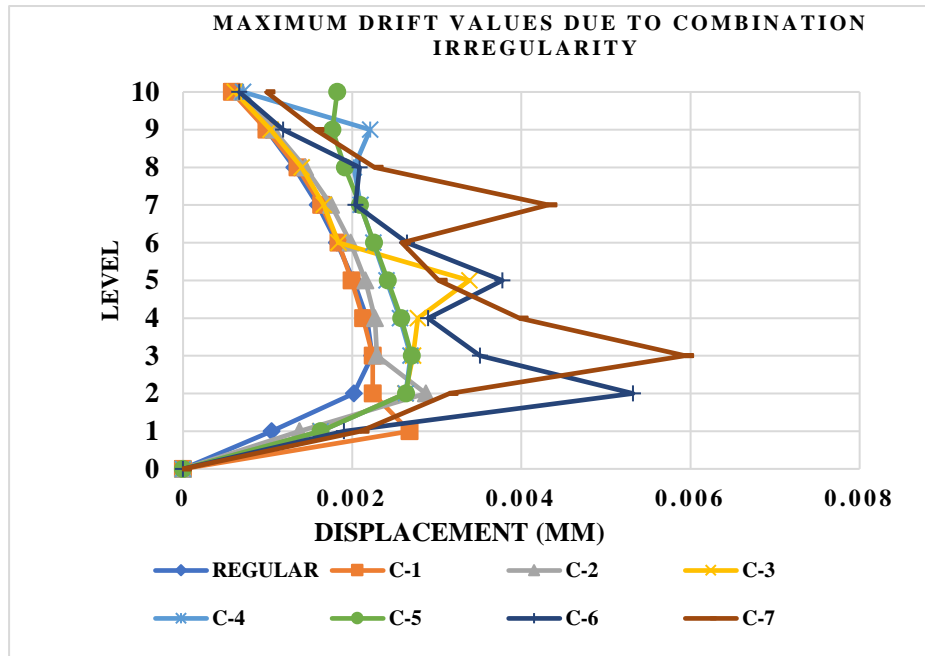


Fig 9. Drift Response of combinational irregularity case

#### E. For Worst Combinational Irregularity Case Having LRB and Fixed Base.

Table 8 shows max relative displacement and drift values in case of worst case of combinational irregularity with fixed base and lead rubber bearing base isolator.

Table 8 shows the maximum relative displacement and maximum drift

Case	Maximum relative Displacement (mm)		Maximum Drift
	Bottom	Top	
Regular	0	45.115	0.002236
CI-7 With Fixed Base	0	125.263	0.005937
CI-7 With LRB	92.443	99.82	0.00114

The Response spectrum Displacement responses of worst combinational irregularity case Mass and Stiffness irregularity with FIXED BASE and with LEAD RUBBER BEARING is shown in fig. 10.

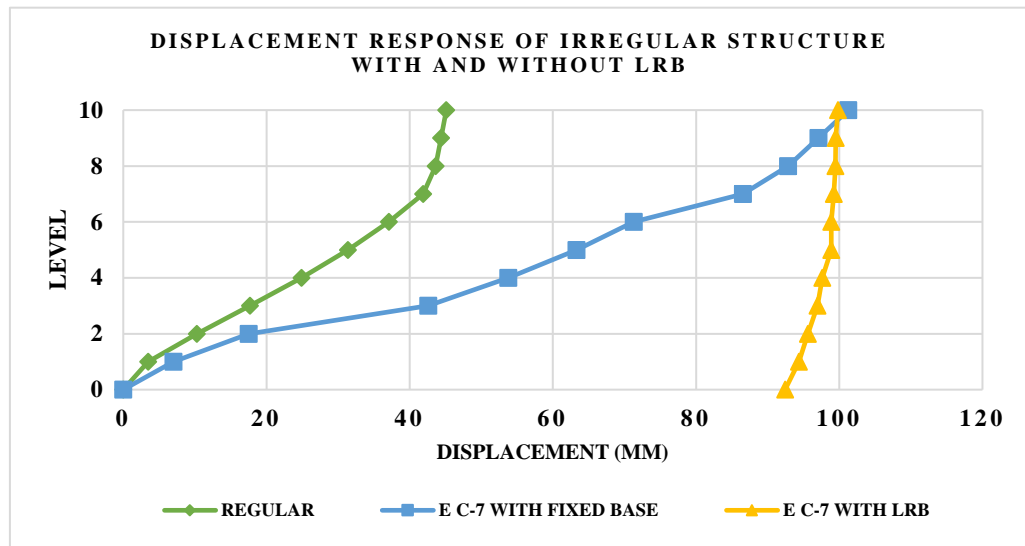


Fig 10. Displacement Response of fixed and LRB cases

It is found that when we introduce LEAD RUBBER BEARING base isolation system in a structure (CI-7 case), there is very little relative displacement between top and bottom of structure. The base isolator relatively moves with the ground but upper storeys shows no relative increase in displacement.

The Response spectrum Story Drift responses of combined Mass and Stiffness irregularity cases with FIXED BASE and with LEAD RUBBER BEARING is shown in fig 11. It is found that when we introduce LEAD RUBBER BEARING base isolation system the storey drift decreases to a greater extent and thus making the structure stable because no seismic force is permitted to enter into the structure. Though the structure moves but structure retains its shape and making the structure stable.

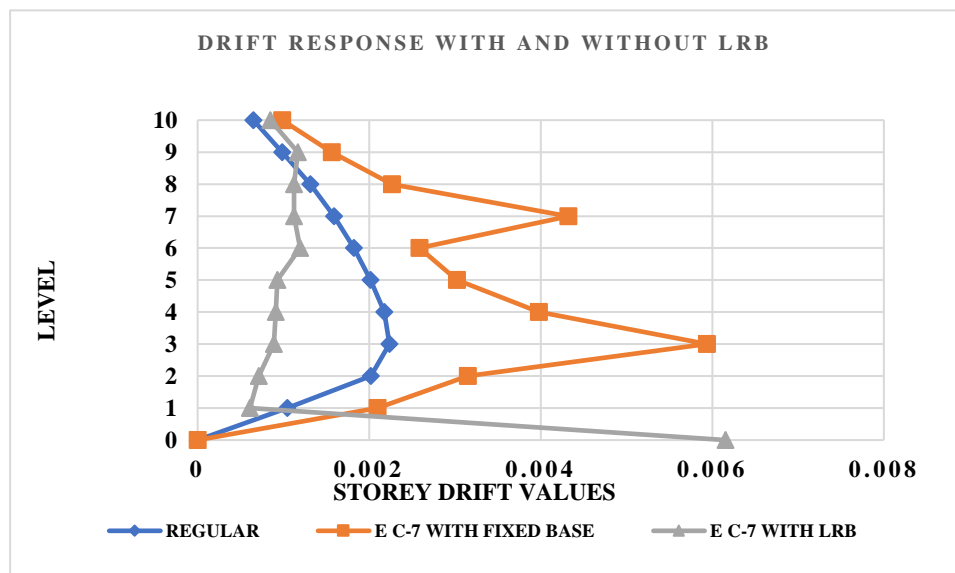


Fig 11. Drift Response of fixed and LRB cases

## 7. CONCLUSION

The conclusions made are;

1. The ultimate seismic capacity of the cracked section model towards earthquake motion is smaller than the gross section model. This is because, when same earthquake load is applied to both models, cracked section model triggers displacement response and cracked section model shows an increase of 47 % in displacement response when compared with gross section model.
2. Considering Base shear, cracked section model shows a decrease of 27.04% when compared with gross section model by showing lower initial stiffness.
3. The RC frame structure with fixed base where mass irregularity is introduced shows more response towards earthquake forces than the structures where mass irregularity is absent. From the response spectrum analysis, the mass irregularity shows an increase of nearly 57 % in displacement and 92.17 % increase in inter-storey drift.
4. The RC frame structure with fixed base where stiffness irregularity is introduced shows an increase of nearly 110% in displacement and 107% increase in inter-storey drift.
5. The RC frame structure consisting of stiffness irregularity shows a decreasing trend in displacement and drift response when stiffness irregularity is present at upper levels. Nearly 27% decrease in displacement response is noted when stiffness irregularity is present at upper levels.
6. From the response spectrum analysis, the worst case is when both mass and stiffness irregularities are present in combination in RC frame structure with fixed base. From the analysis it is noted that about 179.12% increase in displacement response and 165.7% increase in inter-storey drift is recorded in the worst case when compared with the regular building.
7. After replacing the fixed base with lead rubber bearing base isolation system in the RC frame structure consisting of worst combination of irregularity, the displacement and drift response decreases to a greater extent. From the response spectrum analysis of RC frame structure with LRB it is noted that nearly 82.5% decrease in displacement response and 71.2% decrease in inter storey drift is recorded.

## REFERENCES

- [1.] Naveen, S. E., Abraham, N. M., & Kumari, A. S. D. (2019). Analysis of irregular structures under earthquake loads. *Procedia Structural Integrity 2nd International Conference on Structural Integrity and Exhibition 2018*, 14(2019), 806–819.
- [2.] Firoj, M. K., Singh, S. K. (2019). *Response Spectrum Analysis for Irregular Multi-Storey Structure in Seismic Zone V*. January.
- [3.] Sahoo, D. N., Parhi, P. K. (2018). *Base Isolation of Residential Building using Lead Rubber Bearing Technique*. 7(05), 122–131.
- [4.] Oyguc, R., Toros, C., & Abdelnaby, A. E. (2018). Seismic behavior of irregular reinforced-concrete structures under multiple earthquake excitations. *Soil Dynamics and Earthquake Engineering*, vol 104(issueFebruary 2017), 15–32.
- [5.] Titiksh, A. (2017). Effects of irregularities on the seismic response of a medium rise structure. *Asian Journal of Civil Engineering*, 18(8), 1307–1314
- [6.] Bello, M., Adedeji, A. A., & Rahmon, R. (2017). Dynamic Analysis of Multi-Storey Building under Seismic Excitation by Response Spectrum Method using ETABS Dynamic Analysis of Multi-Storey Building under Seismic Excitation by Response Spectrum Method using ETABS. *USEP: Journal of Research*

- Information in Civil Engineering, Vol.14, No 4, 2017 Dynamic, December.*
- [7.] Varadharajan, S., Sehgal, V. K., Saini, B., (2015). *Seismic behaviour of Multistorey RC Frames with vertical mass irregularities Seismic behaviour of Multistorey RC Frames with vertical mass irregularities. March*, 20–39.
  - [8.] Georgoussis, G., Tsompanos, A., & Makarios, T. (2015). Approximate seismic analysis of multi-story buildings with mass and stiffness irregularities. *Procedia Engineering*, 125, 959–966.
  - [9.] Moehle, B. J. P., Asce, A. M., & Alarcon, L. F. (2013). *Seismic Analysis Methods For Irregular Buildings ASCE*. 112(1), 35–52.
  - [10.] Ravikumar, C. M., S, B. N. K., Sujith, B. V, & D, V. R. (2012). *Effect of Irregular Configurations on Seismic Vulnerability of RC Buildings*. 2(3), 20–26. <https://doi.org/10.5923/j.arch.20120203.01>
  - [11.] Sharbatdar, M. K., Vaez, S. R. H., Amiri, G. G., & Naderpour, H. (2011). Seismic Response of Base-Isolated Structures with LRB and FPS under near Fault Ground Motions. *Procedia Engineering*, 14, 3245–3251.
  - [12.] Kadid, A., Yahiaoui, D., & Chebili, R. (2010). Behaviour of reinforced concrete buildings under simultaneous horizontal and vertical ground motions. *Asian Journal of Civil Engineering*, VOL. 11(issue (Aug-2010)), 463–476.
  - [13.] Hwang, J. S. (2008). Experimental Study of Isolated Building under Triaxial Ground Excitations. *ASCE, August*, 879–886

# **Survey on various techniques for IOT based Neonatal Incubators**

**Prashant Jani and Seema Mahajan**

**Abstract** A lots of premature babies' loss their lives due to Improper monitoring inside the neonatal Incubator worldwide. An Incubator is an electrical equipment in which any premature infant kept and monitored on certain bio-logical parameters and these parameters ensure baby's safety rate as well as death rate too. For monitoring these parameters health centers use some sensors which are directly connected with infant and represent it on display. Any irregularity and abnormal activity will be detected via alarm. In this Survey, we are focusing on existing biological parameters in incubator, analysis technique used for that, alarm system for attention in real time system and transmission technique for the same.

**Keywords:** IoT, Incubator, Neonate, Premature Baby

## **1.Introduction:**

The recent emerging in IoT technology for numerous applications [1, 2] crushes the traditional sensing of adjoining environments. It is developing very rapidly and attractive a major source for discussion of communication among different sensors including dream sensors over smart devices such as smartphones, smart cities etc. The neonatal period is the most vulnerable period for child survival and a critical phase for later development [3]. Maintaining a normal body temperature (BT) is thus a critical function for the survival of the newborn baby (NB). However, especially for preterm, lowbirth weight, and sick NBs, utensils for temperature instruction may easily be stunned, leading to hypothermia, cold stress, metabolic deterioration, and, ultimately, death [4]. Improving temperature solidity for sick and preterm infants, thus, continues to be an area of precedence in the neonatal intensive care unit (NICU).

A cool incubator system has been projected in [5] that continuously monitors and sends the measurements to the cloud. The system involves of Arduino controller, several sensors, Wi-Fi connection, and cloud storing and processing system. A wireless smart sensor system has been proposed in [6] for infant incubator system to remotely screen the infants utilizing different sensors, ZigBee wireless protocol and IEEE 1451 communication edge.

Currently, Most of NICU are well-resourced with progressive machines and devices to monitor which are designed for the special condition of the infants. Some of the checking equipment often used in NICU are cardiorespiratory monitor, blood pressure monitor, temperature, pulse oximeter, transcutaneous oxygen and carbon-di-oxide monitor, Ultrasound, X-Ray, etc. With Internet of Things, medical occupation has listed and technologists are trying to merge the various situation together to build a strong monitoring system. Connecting things to internet with standard rules and suitable architectural variations expedites continuous health monitoring for all day and any place. In this context several incubator monitoring classification for neonatal care are argued in literature review.

---

Prashant Jani  
Department of Computer Science, Indus University, Gujarat, INDIA  
Email Address : janiprashant9@gmail.com

Seema Mahajan  
Department of Computer Science, Indus University, Gujarat, INDIA  
Email Address : ce.hod@indusuni.ac.in

## 2. Literature Review:

There are so many factors that should have to be considered in baby's nourishment and specially health centers and NICU has to monitored some parameters as far as baby's health concerned. Few of them are listed here:

Sr. No.	1	2	3	4	5
Investigator	[7]	[8]	[9]	[10]	[11]
Input Parameters Used	Temperature, Humidity	Body Temperature	Temperature, Heart beat	Temperature, Pulse rate	weight, temperature, and head circumference.
Findings of the study	This paper that would enable the medical specialist to monitor and control temperature and humidity of incubator.	In this Paper, Author using Arduino, temperature sensor, monitoring or controlling the Temperature of the baby's body.	Raspberry Pi is used for monitoring and controlling the whole system. LCD is used to display humidity, temperature, heart beat and respiration of neonatal.	The Neonatal Health Monitoring System is a tool that can measure, display and record human features such as body temperature, pulse rate and other health-related criteria.	A Growth parameters that parents often pay attention and monitoring for their infants are weight and temperature to determine the health condition of the infant.

**Table 1: Literature Review**

### 2.1 Various Parameters for infant monitoring in incubator:

After reviewing existing study, here are some parameters that has to be monitored by every NICU through IoT are listed below:

#### 1. Infant Body Temperature

Constantly taking infant's body temperature and giving notification if any abnormal activity detected.

#### 2. Pulse Rate

Through Pulse sensor it returns infant's heart rate continuously and it is monitored on display.

#### 3. Infant Body Weight

Body weight of the premature plays a vital role in early days because it helps to predict or understand the overall wealth progress of an infant

#### 4. Infant Humidity

Real time monitoring system is used to measure a humidity of an infant.

#### 5. Incubator Temperature

This temperature is purely depending and set after infant's body temperature measured. Generally, NICU kept it around 82-86 Degree F.

#### 6. Blood Oxygen Level

It can be read by small probe putting in newborn's hand or foot and generally, it can be kept 95% to 98%.

#### 7. Sound Recognition

Through sound recognition sensor NICU can recognize the infant's sound response and detection ability.

### 3. Analysis technologies Used:

Incubators all over the globe were made using different technologies. These technologies are responsible for data storage, data transmission.

#### a) Wireless Transmission

In this system [11] The skin temperature of child, temperature and humidity of the incubator, Oxygen and Carbon-di- Oxide concentration in incubator weight, heartbeat, Blood pressure and oxygen saturation are monitored. All these are conveyed to computer via network (internet). Infant Folks can spot their infant's nursing situation in their office or family by the network. A processer is official to browse and download the vision-frequency picture and monitoring data. Author [12] has designed a method to display the new-born infant's biological data remotely outside NICU. It is finished by providing a modest mobile application where data can be supervised live. To create communication between vital sign monitor and the remote server Wi-Fi and 3G used.

#### b) Wireless PLC System

Author Eugene T. Puzio [13] has intended an incubator wherever the Temperature and humidity of the incubator and Skin temperature of infant is dignified. The Mechanisms used are Blue light lamps, Ventilation holes, controller, display screen, control buttons and buzzer with PLC system and Wireless Transmission module.

#### c) Cloud Storage Based Technology

Cloud computing uses Virtual Machine storage or an application in its place of building computer substructures. An improved system designed by Mr. Soukaina Brangui [14] the author monitors the temperature and weight data in real-time. Cloud server is used to store the data. A variety of data being uploaded on cloud like Weight, Pulse rate, Temperature. Alarm or notification also has been generated using cloud server.

#### d) Bluetooth technology

Wei Chen [15] has deliberate system with wireless transmission technology. BlueSMiRF and Arduino pro mini were used. An infant jacket is considered for the baby to monitor in non-invasively. The system data are conveyed and traditional from multiple sensors within specific range. For this system temperature sensor and display LCD were used.

#### e) Respiratory sensor using fiber optics technology

Author Arika Dhia [16] has created a design of respiratory sensor using fiber optics technology for this incubator presentation. This sensor functions based on the light intensity change due to the thorax movement. This movement is happened during the respiration. The data is handled in Arduino Uno microcontroller and it is measured real time and showed in LCD.

#### f) Fuzzy Inference System

In 2019, Authors [17] introduces the optimization of the egg incubator system using fuzzy inference and based on Internet of Things (IoT). So the egg hatching system is more steady when it warms up the

temperature at the incubator and can be measured via the internet network. The results gained by running IoT-based incubator system on the 38 0C set point, system are successively optimally.

#### **4. Abnormal neonatal Activity detection:**

Mostly, Incubator system were designed to read the data and monitor the data. If any abnormal activity happen in between it indicates notifications using alarm detection system. Different types of alert system used for indication. If any irregularity occurs, alarm is directed through Short-Message Transmitting module (SMS) to hospital staff's phone. In this system [18] Real time monitoring of temperature and humidity of the incubator is measured. The Modules used are WIFI, Camera, Battery, Micro Controller, Captive touch screen. In some abnormal situation data is also reported on family members mobile phone too using Internet via Arduino. Some image based algorithm constantly sending Neonatal images to decided cell phones or computers for monitoring purpose. Any of the parameters falls down or goes to beyond limits then alarm ringed on doctor's or respective NICU staff members phone or device.

#### **Conclusion & Future Scope:**

A design of incubator is most important thing as far as infant's health concerned. So design must be well structured and efficient enough. The system design must be affordable and effective manner. All the parameters and technologies used inside incubator must be worked efficiently to maintain infant's health records.

In future, more health parameters can be added and analyzed for better health prediction of an infant. Also, any classification technique will be applied on infant's data for health prediction.

#### **References:**

- [1] S. Khan, K. Muhammad, S. Mumtaz, S. W. Baik, and V. H. C. de Albuquerque, "Energy-efficient deep CNN for smoke detection in foggy IoT environment," *IEEE Internet of Things Journal*, (2019)
- [2] T. Hussain, K. Muhammad, J. Del Ser, S. W. Baik, and V. H. C. de Albuquerque, "Intelligent Embedded Vision for Summarization of Multi-View Videos in IIoT," *IEEE Transactions on Industrial Informatics* (2019)
- [3] D. Askin, "The high-risk newborn and family. Wong's nursing care of infants and children, ong DL, Hockenberry MJ, and Wilson D. St. Louis: Mosby," ed: Elsevier (2007)
- [4] A. R. Laptook and M. Watkinson, "Temperature management in the delivery room," (in eng), *Semin Fetal Neonatal Med*, vol. 13, no. 6, pp. 383-91, (Dec 2008)
- [5] D Sivamani, R Sagayaraj, R Jai Ganesh and A. Nazar Ali. "Smart incubator using internet of things." *International Journal for Modern Trends in Science and Technology*, Vol. 4, no. 9, pp 23-27, (2018)
- [6] Wu, Guoguang, and Shangwen Chen. "Design of wireless smart sensor module for infant incubator test." In *2016 5th International Conference on Measurement, Instrumentation and Automation (ICMIA 2016)*. Atlantis Press, (2016)
- [7] Shehla Inam, Muhammad Farrukh Qureshi, Faisal Amin, Muhammad Akmal, Muhammad Ziaur Rehman "Android based Internet Accessible Infant Incubator." *IEEE 978-1-7281-2334-9/19*, (2019)
- [8] Megha Koli , Purvi Ladje, Bhavpriya Prasad, Ronak Boria, Prof. Nazahat J. Balur" INTELLIGENT BABY INCUBATOR" *Proceedings of the 2nd International conference on Electronics, Communication and Aerospace Technology (ICECA, 2018)*
- [9] Pravin Kshirsgar, Varsha More, Vaibhav Hendre, Pranav Chippalkatti and Krishan Paliwal "IOT Based Baby Incubator for Clinic" *ICCCE* , (2019)
- [10] Sheril Amira O.1, Nor Asmira H.1, Tengku Nadzlin T. I.2, Mohd Helmy A. W.1, Omar A.H.3, Muhammad Shukri A.2 & Ahmad Alabqari M.R. "Neonatal Health Monitoring System with IOT Application" *Journal of Physics: Conference Series, JICETS* (2019)
- [11] "Network monitoring device for nursing baby";2006-06-14; Patent no:CN200960246Y
- [12] Robert Greer, Chris Olivier., "Remote Real-Time Monitoring and Analysis of Neonatal Graduate Infants",,
- [13] Anthony McClain, 364 Shadetree La., "Incubator system with monitoring and communication capabilities"; (Jun. 25, 2002)

- [14] "Cloud-based monitoring system and risk management for premature new-borns",, José Ilton de Oliveira Filho and Otacilio da Mota Almeida Electrical Engineering Department Federal University of Piauí Teresina, Brazil
- [15] Wei Chen, Son Tung Nguyen, Roland Coops., "Wireless Transmission Design for Health Monitoring at Neonatal Intensive Care Units"; Department of Industrial design, Eindhoven University of Technology, Den Dolech 2,5612 AZ, The Netherlands.
- [16] Arika Dhia, Kresna Devara., "Design of Fiber Optic Based Respiratory Sensor for New-born Incubator Application", API Conference Proceedings 1933,040018 (2018)
- [17] Renny Rakhmawati, Irianto, Farid Dwi Murdianto, Atabik Luthfi, Aviv Yuniar Rahman "Thermal Optimization on Incubator using Fuzzy Inference System based IoT" 978-1-5386-8448-1/19 (2019)

# **Modeling on Transmission Dynamics of Skin Cancer due to the Exposure of Ultraviolet Radiation**

**Tahera Parvin and Md. Haider Ali Biswas**

**Abstract** Many kinds of cancers occur in human body. Among them skin cancer is a malignant cancer of the skin. Skin cancer is the uncontrol growth of abnormal cells in the epidermis. It is the most common type of cancer in fair-skinned populations in many parts of the world. But recent reports show people of all colors get skin cancer. In present world ultraviolet radiation is the main risk factor of skin cancer. So, it is a matter of concern also for dark skin people. This paper deals with nonlinear dynamical systems in the form of mathematical modeling to elucidate the relationship between ultraviolet radiation and skin cancers. In our study, we observe the equilibria of our model and find the basic reproduction number for DFE point. We show the involved local and global stability analysis for the equilibria points under some conditions. The main aim is to show the effect of over exposure of UV radiation on skin cancer. Finally, numerical simulation of the proposed model is performed to justify the analytical finding.

**Keywords**-Ultraviolet radiation, skin cancer, stability, basic reproduction number, Lyapunov function, mathematical model and numerical analysis.

## **1. Introduction**

Biological scheme is inherently complicated. Fortunately, mathematical models are uniquely positioned to provide a tool flexible for appropriate analysis, hypothesis the whole organism studies. Cancer has become the second main cause of death in the world. About 2 to 3 million cases of non-melanoma skin cancers and 132,000 cases of melanoma skin cancers occur worldwide each year [1] If we diagnose three cancers affected people then one parson is skin cancer affected, one American among five Americans develop skin cancer in their life. It greatly affects quality of life, and it can be disfiguring or even deadly. Medical treatment for skin cancer creates massive health care costs for the nation. In 2018, 287,723 cases of melanoma skin cancer and 1,042,056 of non-melanoma skin cancer were diagnosed globally. 60,712 people died of melanoma skin cancer and 65,155 of non-melanoma skin cancer [2]. Melanoma skin cancer deaths in Bangladesh reached 320 among 472 new cases [3].

---

Tahera Parvin  
Mathematics Discipline, Khulna University, Khulna-9208, Bangladesh  
Email Address : moly151245@gmail.com

Md. Haider Ali Biswas  
Mathematics Discipline, Khulna University, Khulna-9208, Bangladesh  
Email Address : mhabiswas@yahoo.com

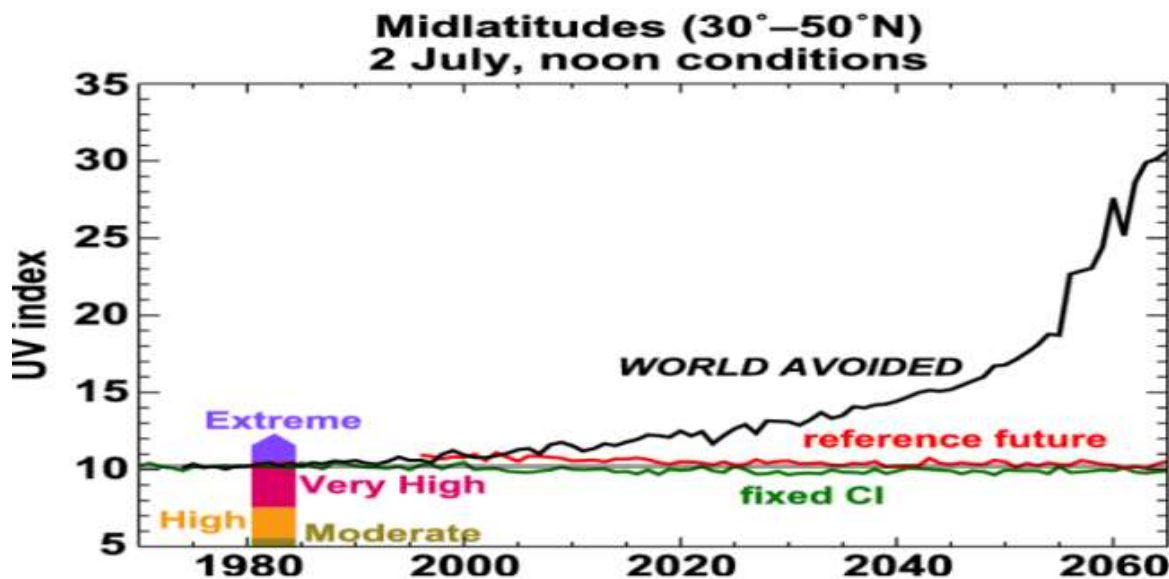


**Fig 1.1.** Global reduction in ozone levels would lead to a huge Increase in dangerous UV (Source: Newman et al. ,2009)

Stratospheric ozone layer is decreasing 0.4 to 0.8 percent each year from 2012 [4], the atmosphere loses more and more of its protective filter function and more solar UV radiation reaches the Earth's surface. Newman et al. [5] predicted that due to global reduction of stratospheric ozone layer dangerous UV index will be increased three times of its standard scale. Additional 300,000 non-melanoma and 4,500 melanoma skin cancer cases are caused by the 10 percent decay of ozone layer [1]. Average temperature of Bangladesh will raise by  $1.0^{\circ}\text{C}$  to  $1.5^{\circ}\text{C}$  by 2050 even if resistant methods are taken by us. If we do not take any measure, then the country's average temperatures will increase by  $1.0^{\circ}\text{C}$  to  $2.5^{\circ}\text{C}$  [6].

Ultraviolet radiation (UVR) is part of electromagnetic spectrum with wavelengths 100-400 nm emitted by the sun and by artificial sources (e.g., sunbeds, tanning devices). Reductions in stratospheric ozone ( $O_3$ ) are expected to allow more solar ultraviolet-B to reach the earth surface. Consequently, more UV radiation that come from sun and sunbeds can harm the DNA in the skin cells. If enough DNA damage increases day by day, it can cause skin tumor, which can lead to skin cancer. Considering all the fatalities of skin cancer as well as the effect of ultraviolet radiation on skin cancer, theory based as well as statistics study on skin cancer was discussed by many researchers. A mathematical model was formulated by Fears et al. [7] considering the effect of age and UV on the outbreak of skin cancer among fair skinned people in the United States. A dose-response model was constructed by De Grilil and Leun [8], based on the results of animal experiments, presented for skin cancer induction in a human population by chronic exposure to ultraviolet radiation. The effects of ultraviolet radiation were represented by Moan and Dahlback [9] on skin cancer in their theory-based study. Shore [10] discussed the radiation-induced skin cancer in humans. He also discussed the treatment options for skin cancer. The impact of climate change on skin cancer was represented by Bharath and Turner [11]. The relationship between sun exposure and melanoma risk for tumors in different body sites in a large case-control study in a temperate climate was explained by Bishop et al. [12]. The effects of ultraviolet radiation on cancer were explored by Greinert et al. [13]. The ultraviolet radiation-induced non-melanoma skin cancer as well as regulation of DNA damage repair and inflammation was represented by the research study of Kim and He [14]. The solar UV exposure and mortality from skin tumors was discussed by Berwick and Garcia [15]. Mathematical modeling is playing an incredible role for providing quantitative insight into multiple fields. It has already contributed to a better understanding of the mechanisms of various non-communicable diseases. Mathematical modeling has gotten attention because modeling and simulation of any physical phenomena allows us for rapid assessment. Biswas et al., [16] investigated and analyzed the transmission of most devastating infectious diseases independently in which mathematical modeling was the key tool (see also Biswas et al., [17]. Agarwal and Verma [18] studied the modeling and analysis of the spread of an infectious disease cholera with environmental fluctuations. Dubey et al [19] showed the dynamics of an SIR model with nonlinear incidence and treatment rate in their study. Taking the above discussions into account, we propose a model

to study the dynamics of skin cancer transmission. Many theoretical as well as statistics models of skin cancer have been proposed by researchers. But this is a newly proposed differential equation mathematical model of skin cancer on the basis of some basic assumptions. Our goal is to study the disease dynamics of skin cancer due to the over exposure of ultraviolet radiation.

## 2. Mathematical model of skin cancer

There is no clinical documentation that close contact can spread skin cancer from one people to another. It is a non-communicable disease. Mathematical model is the most significant tools to analyze the transmission dynamics of non-communicable disease. Mathematical model of non-communicable disease helps us to understand the mechanisms of different cell population. Our aim is to formulate a mathematical model of skin cancer and investigate the effect of ultraviolet radiation on skin cells.

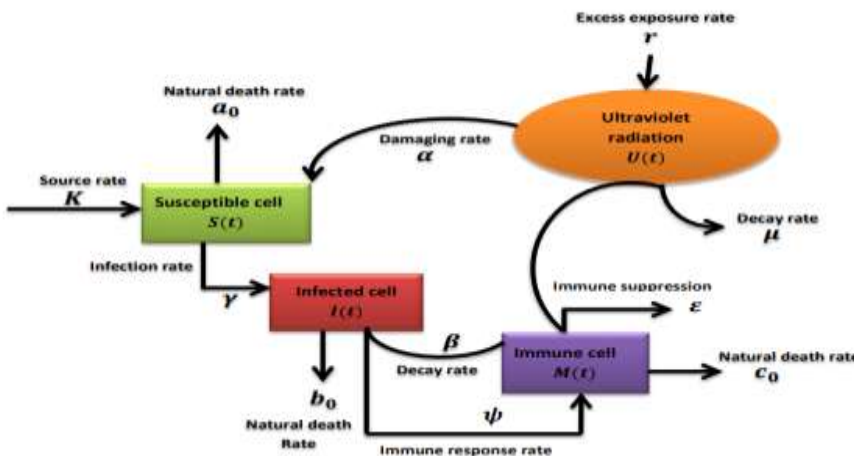


**Fig 2.1.** Transmission diagram of skin cancer due to ultraviolet radiation and infected cell.

In this study, we represent a four compartmental model of skin cancer. Among them the first three compartments are cell population and the last one is environmental risk factor (ultraviolet radiation). Susceptible cells are denoted by  $S(t)$  which are mainly epidermis, the outer layer of our skin. Infected cells are denoted by  $I(t)$  which are mainly skin cancer stem cells and the immune cells are denoted by  $M(t)$ . Natural Killer (NK) cells, CD4+ T and CD8+ T cells are the main immune cells for this cancer which are created in bone marrow and matured in thymus gland. The main risk factor of skin cancer ultraviolet radiation is denoted by  $U(t)$ . Let  $K$  is the recruitment rate of susceptible cells,  $r$  is the excess exposure rate of Ultraviolet radiation that at first damage skin cell and then create cancer. The parameter  $\gamma$  is the rate at which ultraviolet light infecting or damaging the susceptible cells,  $\alpha$  is the rate at which susceptible cell infected in contact with infected cells,  $\beta$  is decay rate of infected cells in contact with immune cells,  $\psi$  is Immune response rate due to infected cells,  $\epsilon$  is immunosuppression rate due to ultraviolet radiation and  $\mu$  is decay rate of ultraviolet radiation. Also, the parameters  $a_0$ ,  $b_0$  and  $c_0$  are the natural death rate of susceptible, infected and immune cells.

According to the model diagram in **Fig 2.1** and parameters described above, the mathematical model of skin cancer can be written in the form of following nonlinear system of ordinary differential equations:

$$\begin{aligned}
 \frac{dS}{dt} &= K - (\alpha U + \gamma I)S - a_0 S \\
 \frac{dI}{dt} &= (\alpha U + \gamma I)S - \beta IM - b_0 I \\
 \frac{dM}{dt} &= \psi I - \epsilon MU - c_0 M \\
 \frac{dU}{dt} &= r - \mu U
 \end{aligned}$$

(2.1)

With  $S(0) = S_0 > 0$ ,  $I(0) = I_0 \geq 0$ ,  $M(0) = M_0 \geq 0$  and  $U(0) = U_0 > 0$ .

## 2.1. non-periodicity and limiting behavior

**Lemma 2.1.** Let  $X$  be a solutions of model (2.1). If  $X(0) \in \mathbb{D}_+^4$  then the limit of  $X(t)$  exists when  $t \rightarrow \infty$ . In particular,  $X$  is periodic if only if  $X$  is stationary.

**Proof:** Let  $X(t) = S(t) + I(t) + M(t) + U(t)$

From 1<sup>st</sup> equation of model (2.1) we get,

$$\frac{dS}{dt} = K - (\alpha U + \gamma I)S - a_0 S$$

$$\text{i.e., } \frac{dS}{dt} + a_0 S \geq K$$

$$\text{i.e., } S \leq \frac{K}{a_0} \left(1 - e^{-a_0 t}\right) + S_0 e^{-a_0 t}$$

At  $t \rightarrow 0, S(t) > 0$

And also,  $t \rightarrow \infty, S(t) > 0$ .

From second equation of model (2.1) we get,

$$\frac{dI}{dt} = (\alpha U + \gamma I)S - \beta IM - b_0 I$$

$$\Rightarrow \frac{dI}{I} \geq R dt : \text{where, } R = (\gamma S - b_0)$$

$$\Rightarrow \frac{dI}{I} \geq R dt$$

$$\text{i.e., } I(t) \geq I(0) e^{Rt}$$

At  $t \rightarrow 0, I(t) > 0$

And also,  $t \rightarrow \infty, I(t) > 0$ .

Similarly, we can verify the positivity of  $M(t)$  and  $U(t)$  under the initial conditions.

Therefore, the solutions  $S(t), I(t), M(t), U(t)$  of the model (1) exist when  $t \rightarrow \infty$ . So,  $X$  is periodic.

Hence, the **Lemma 2.1** is proved.

## 2.2. Existence of the equilibrium points of the system

The equilibrium points of the model (2.1) are obtained by equating  $\frac{dS}{dt} = \frac{dI}{dt} = \frac{dM}{dt} = \frac{dU}{dt} = 0$ .

Thus, we have,

$$(2.2) \quad K - (\alpha U + \gamma I)S - a_0 S = 0$$

$$(\alpha U + \gamma I)S - \beta IM - b_0 I = 0$$

$$(2.3)$$

$$\psi I - \varepsilon MU - c_0 M = 0$$

$$(2.4)$$

$$r - \mu U = 0$$

$$(2.5)$$

### (i) Ultraviolet Radiation free equilibrium:

Trivial equilibrium point:  $E_0^1: (0, 0, 0, 0)$

At disease free equilibrium point (DFE),  $I = M = U = 0$ .

Thus, the system (2.2) -(2.5) reduces to

$$K - a_0 S = 0$$

$$\text{i.e. } S = \frac{K}{a_0}$$

So, disease free equilibrium point (DFE):  $E_0^2 : \left( \frac{K}{a_0}, 0, 0, 0 \right)$

$$E_0^3 : (S^0, I^0, M^0, 0)$$

where,

$$S^0 = \frac{-\beta P + \sqrt{P^2 - 4QX} + 2b_0 c_0 \gamma}{2c_0 \gamma}; [P = (b_0 c_0 \gamma + a_0 \beta \psi), Q = c_0, X = (a_0 b_0 \psi - K \psi \gamma)]$$

$$I^0 = \frac{-P + \sqrt{P^2 - 4QX}}{2\gamma\psi}$$

$$M^0 = \frac{-P + \sqrt{P^2 - 4QX}}{2c_0 \gamma}$$

$$E_0^4 : (S_0, I_0, M_0, 0)$$

where,

$$S_0 = \frac{-\beta P + \sqrt{P^2 - 4QX} + 2b_0 c_0 \gamma}{2c_0 \gamma}$$

$$I_0 = \frac{-P + \sqrt{P^2 - 4QX}}{2\gamma\psi}$$

$$M_0 = \frac{-P + \sqrt{P^2 - 4QX}}{2c_0 \gamma}$$

#### (ii) The immune free equilibrium point:

The immune free equilibrium point:  $E_0 : (\bar{S}, \bar{I}, \bar{M}, 0)$

Thus, the system (2.2)-(2.5) reduces to

$$K - (\alpha \bar{U} + \gamma \bar{I}) \bar{S} - a_0 \bar{S} = 0 \quad (2.6)$$

$$(\alpha \bar{U} + \gamma \bar{I}) \bar{S} - b_0 \bar{I} = 0 \quad (2.7)$$

$$\psi \bar{I} = 0 \quad (2.8)$$

$$r - \mu \bar{U} \quad (2.9)$$

But in this case, we consider  $\bar{I} \neq 0$ .

Then from equation (2.9) we get,  $\bar{U} = \frac{r}{\mu}$ .

From (2.6) and (2.7) we get,  $\bar{I} = \frac{K - a_0 \bar{S}}{b_0}$

Putting the values of  $\bar{U}$  and  $\bar{I}$  in (2.6)

$$A \bar{S}^2 + B \bar{S} + C = 0$$

$$\text{Here, } A = -\frac{\gamma a_0}{b_0}$$

$$B = \frac{\alpha r}{\mu} + \frac{\gamma K}{b_0} + a_0$$

$$C = -K$$

Using Descartes's rule of sign we get, it has exactly one negative root and 2 or 0 positive root(s).

**(iii) Endemic equilibrium point:**

If all populations exist, the model (2.1) present endemic equilibrium (EE) point given by  $E^* = (S^*, I^*, M^*, U^*)$

Then from equation (2.2) -(2.5), we get,

$$K - (\alpha U^* + \gamma I^*) S^* - a_0 S^* = 0 \quad (2.10)$$

$$(\alpha U^* + \gamma I^*) S^* - \beta I^* M^* - b_0 I^* = 0 \quad (2.11)$$

$$\psi I^* - \varepsilon M^* U^* - c_0 M^* = 0 \quad (2.12)$$

$$r - \mu U^* = 0 \quad (2.13)$$

From equation (2.10), (2.12) and (2.13) we get,

$$U^* = \frac{r}{\mu}$$

$$I^* = \frac{(r\varepsilon + c_0\mu)M^*}{\mu\psi} \quad (2.14)$$

$$S^* = \frac{a_1}{a_2 + r\gamma M^* + a_3}$$

Using system (2.14) in (2.11) we get,

$$A^* M^{*4} + B^* M^{*3} + C^* M^{*2} + D^* M^* + G^* = 0 \quad (2.15)$$

where,

$$A^* = -\beta r\varepsilon\mu^2\gamma^2\psi$$

$$B^* = -[\beta r\varepsilon(2\mu^2\psi a_2 r\gamma + 2\mu^2 r\psi a_3\gamma) + \mu^2 r^2\gamma^2\psi(c_0 r + b_0 r\varepsilon)]$$

$$C^* = \mu^2\psi a_1 r^2\gamma^2 - \beta r\varepsilon(2\mu^2\psi a_2 r\gamma + 2\mu^2 r\psi a_3\gamma) - (c_0 r + b_0 r\varepsilon)$$

$$(2\mu^2\psi a_2 r\gamma + 2\mu^2 r\psi a_3\gamma) - b_0 c_0 r^3 \mu^2 \gamma^2 \psi$$

$$D^* = \psi^2 \mu^2 \alpha r^2 \gamma a_1 + \mu^2 \psi \gamma r a_1 a_2 + \psi \mu^2 r \gamma^2 c_0 r a_1 + \mu^2 \psi \gamma r a_1 a_3 -$$

$$(c_0 r + b_0 r\varepsilon)(\mu^2 \psi \varepsilon^2 + \mu^2 \psi a_3^2 + \mu^2 a_2 a_3 + \mu^2 \psi a_2 a_3)$$

$$- b_0 c_0 r (\mu^2 r \gamma \psi a_2 + 2\mu^2 r \gamma \psi a_3)$$

$$G^* = \psi^2 \mu^2 \alpha r a_1 a_2 + \psi^2 \mu^2 \alpha r a_1 a_3 + \psi \mu^2 \gamma r a_1 a_2 c_0 + \psi \mu^2 \gamma r a_1 a_3 c_0$$

$$- b_0 c_0 r (\varepsilon^2 \mu^2 \psi + a_3^2 \mu^2 \psi + \mu^2 a_2 a_3 + \mu^2 \psi a_1 a_3)$$

Only real positive solutions of the cubic equation (2.15) provide biological relevant steady state. Based on parameters values of model (2.1), we can have between one and four endemic equilibria. Among them at least one will be positive using Descartes's rule of sign if

i)  $C^* < 0, D^* > 0 \& G^* > 0$

ii)  $C^* < 0, D^* < 0 \& G^* > 0$

### 2.3. Basic reproduction number

A very important threshold quantity is the basic reproduction number, sometimes called the basic reproductive number or basic reproductive ratio, which is usually denoted by  $R_0$ . The epidemiological definition of  $R_0$  is the average number of secondary cases produced by one infected individual introduced into a population of susceptible individuals, where an infected individual has acquired the disease, and susceptible individuals are healthy but can acquire the disease. In reality, the value of  $R_0$  for a specific

disease depends on many variables. In our study we use the next generation matrix approach to find the basic reproduction number.

The next generation matrix has rank 2.

Here,

$$F = \begin{pmatrix} \gamma S_0 & \alpha S_0 \\ 0 & 0 \end{pmatrix} \text{ And } V = \begin{pmatrix} b_0 & 0 \\ 0 & \mu \end{pmatrix}$$

$$\text{So, we obtain } V^{-1} = \begin{pmatrix} \frac{1}{b_0} & 0 \\ 0 & \frac{1}{\mu} \end{pmatrix}$$

$$\text{Thus, } FV^{-1} = \begin{pmatrix} \frac{\gamma S_0}{b_0} & \frac{\alpha S_0}{\mu} \\ 0 & 0 \end{pmatrix}$$

Positive eigenvalues of  $FV^{-1}$  is the Basic Reproduction Number  $R_0$ .

So,

$$\text{So, the Basic Reproduction Number } R_0 = \frac{\gamma S_0}{b_0}.$$

The disease-free equilibrium point (DFE) is  $E_0 \left( \frac{K}{a_0}, 0, 0, 0 \right)$ . So,  $S_0 = \frac{K}{a_0}$

$$\text{Thus, we get, } R_0 = \frac{\gamma K}{a_0 b_0}$$

#### 2.4. Stability analysis

##### (a) Stability of zero equilibrium:

**Theorem 2.1.** The zero-equilibrium point  $E_0^1$  of the model (2.1) is stable.

**Proof:** Let,  $\frac{dS}{dt} = P, \frac{dI}{dt} = Q, \frac{dM}{dt} = R, \frac{dT}{dt} = T$

Then the model (2.1) becomes,

$$P = K - (\alpha U + \gamma I)S - a_0 S \quad (2.16)$$

$$Q = (\alpha U + \gamma I)S - \beta IM - b_0 I \quad (2.17)$$

$$R = \psi I - \varepsilon MU - c_0 M \quad (2.18)$$

$$T = r - \mu U \quad (2.19)$$

The Jacobian matrix of the system (2.16) -(2.19) can be written as,

$$J = \frac{\partial(P, Q, R, T)}{\partial(S, I, M, U)} = \begin{bmatrix} \frac{\partial P}{\partial S} & \frac{\partial P}{\partial I} & \frac{\partial P}{\partial M} & \frac{\partial P}{\partial U} \\ \frac{\partial Q}{\partial S} & \frac{\partial Q}{\partial I} & \frac{\partial Q}{\partial M} & \frac{\partial Q}{\partial U} \\ \frac{\partial R}{\partial S} & \frac{\partial R}{\partial I} & \frac{\partial R}{\partial M} & \frac{\partial R}{\partial U} \\ \frac{\partial T}{\partial S} & \frac{\partial T}{\partial I} & \frac{\partial T}{\partial M} & \frac{\partial T}{\partial U} \end{bmatrix} = \begin{bmatrix} -(\alpha U + \gamma I + a_0) & -\gamma S & 0 & -\alpha S \\ \alpha U + \gamma I & \gamma S - \beta M - b_0 & -\beta I & \alpha S \\ 0 & \psi & -(\varepsilon U + c_0) & -\varepsilon M \\ 0 & 0 & 0 & -\mu \end{bmatrix} \quad (2.20)$$

At point  $E_0^1$ ,

$$J_{E_0^1} = \begin{bmatrix} -a_0 & 0 & 0 & 0 \\ 0 & -b_0 & 0 & 0 \\ 0 & \psi & -c_0 & 0 \\ 0 & 0 & 0 & -\mu \end{bmatrix}$$

(2.21)

The characteristic equation of matrix  $J_{E_0^1}$  is  $\det(J_{E_0^1} - \lambda I) = 0$ .

So we get,

$$\begin{vmatrix} -a_0 - \lambda & 0 & 0 & 0 \\ 0 & -b_0 - \lambda & 0 & 0 \\ 0 & \psi & -c_0 - \lambda & 0 \\ 0 & 0 & 0 & -\mu - \lambda \end{vmatrix} = 0$$

So, the eigen values are  $\lambda_1 = -a_0, \lambda_2 = -b_0, \lambda_3 = -c_0, \lambda_4 = -\mu$

Here all of the eigen values are negative. So,  $E_0^1$  is stable. Hence, **theorem 2.1** is proved

### (b) Local stability of DFE point

In this section, we want to found the stability at DFE point is locally stable providing the theorem 2.2.

**Theorem 2.2:** The DFE point  $E_0^2$  of the model (2.1) is locally asymptotically stable if  $R_0 < 1$  and  $R_0 > 1$ , then it is unstable.

**Proof:** At point  $E_0^2 \left( \frac{K}{a_0}, 0, 0, 0 \right)$  the Jacobian matrix becomes,

$$J_{E_0^2} = \begin{bmatrix} -a_0 & -\frac{\gamma K}{a_0} & 0 & -\frac{\alpha K}{a_0} \\ 0 & \frac{\alpha K}{a_0} - b_0 & 0 & \frac{\alpha K}{a_0} \\ 0 & \psi & -c_0 & 0 \\ 0 & 0 & 0 & -\mu \end{bmatrix}$$

(2.22)

Using elementary row operation in equation (2.22) we obtain,

$$J_{E_0^2} = \begin{bmatrix} -a_0 & -\frac{\gamma K}{a_0} & 0 & -\frac{\alpha K}{a_0} \\ 0 & \frac{\alpha K - a_0 b_0}{a_0} & 0 & \frac{\alpha K}{a_0} \\ 0 & 0 & -c_0 & -\frac{\alpha K \psi}{\gamma K - c_0 b_0} \\ 0 & 0 & 0 & -\mu \end{bmatrix}$$

This is an  $4 \times 4$  upper triangular Jacobian matrix.

So, the eigenvalues of  $J_{E_0^2}$  are  $\lambda_1 = -a_0, \lambda_2 = \frac{\gamma K - a_0 b_0}{a_0} = b_0(R_0 - 1), \lambda_3 = -c_0$  and  $\lambda_4 = -\mu$

The equilibrium point  $E_0^2$  will be locally asymptotically stable when all the eigenvalues of  $J_{E_0^2}$  will be negative,

According to cell biology all the parameters of the model (2.1) is positive. So, clearly all the eigenvalues of  $J_{E_0^2}$  is negative except  $\lambda_2$ .

$\lambda_2$  is negative when  $R_0 < 1$ .

So, the equilibrium point  $E_0^2$  is locally asymptotically stable when  $R_0 < 1$ , otherwise unstable.

Hence, the **theorem 2.2** is proved.

**(c) Global Stability of the Disease-Free Equilibrium Point**

In this section, we use the Lyapunov direct method to (Huo and Feng[20], Vargas-De-Leon [21]) show the conditions for the global asymptotic stability of the disease-free equilibrium point.

**Theorem 3.3.** If  $R_0 \leq 1$ , then the disease-free equilibrium point  $E_0^1$  is globally asymptotically stable in  $\mathbb{D}_+^4$ .

**Proof:** Define the global Lyapunov function  $E : \{(S, I, M, U) \in \mathbb{D}_+^4 : S > 0, I > 0, M > 0, U > 0\} \rightarrow \mathbb{D}$  by

$$\begin{aligned} E &= \gamma S + a_0 I \\ i.e. \dot{E} &= \gamma \dot{S} + a_0 \dot{I} \\ \Rightarrow \dot{E} &= \gamma(K - (\alpha U + \gamma I)S - a_0 S) + a_0((\alpha U + \gamma I)S - \beta IM - b_0 I) \\ \Rightarrow \dot{E} &= \gamma K - a_0 b_0 I - (\gamma - a_0)(\alpha U + \gamma I)S - a_0 \gamma S - a_0 \beta IM \\ \Rightarrow \dot{E} &= a_0 b_0 I \left( \frac{R_0}{I} - 1 \right) - (\gamma - a_0)(\alpha U + \gamma I)S - a_0 \gamma S - a_0 \beta IM \end{aligned}$$

Here,  $a_0 < \gamma$ . So,  $\dot{E}$  is negative when  $R_0 \leq 1$ .

Hence, by Lyapunov principle, DFE point is globally asymptotically stable when  $R_0 \leq 1$ .

**(d) Stability of  $E_0^3$  point**

**Theorem 2.4.** The model (2.1) is a saddle point or a stable point at the equilibrium point  $E_0^3$ .

**Proof:** The Jacobian matrix of model (2.1) becomes at equilibrium point  $E_0^3$

$$J_{E_0^3} = \begin{bmatrix} a_{11} & a_{12} & 0 & a_{14} \\ 0 & a_{22} & a_{23} & a_{24} \\ 0 & 0 & a_{33} & a_{34} \\ 0 & 0 & 0 & -\mu \end{bmatrix}$$

where,

$$\begin{aligned} a_{11} &= \frac{P - \sqrt{P^2 - 4QX} - 2a_0\psi}{2\psi} \\ a_{12} &= \frac{\beta P - \beta \sqrt{P^2 - 4QX} + 2b_0 c_0 \gamma}{2c_0} \\ a_{14} &= \frac{\alpha \beta P - \alpha \beta \sqrt{P^2 - 4QX} + 2b_0 c_0 \alpha \gamma}{2c_0 \gamma} \\ a_{22} &= \frac{2a_0 \beta P \psi - 2a_0 \beta \psi \sqrt{P^2 - 4QX} + 4a_0 b_0 c_0 \gamma \psi}{2c_0 (P - \sqrt{P^2 - 4QX} - 2a_0 \psi)} \\ a_{23} &= \frac{\beta P - \beta \sqrt{P^2 - 4QX}}{2\gamma \psi} \\ a_{24} &= \frac{2\alpha a_0 \beta P \psi - 2\alpha a_0 \beta \psi \sqrt{P^2 - 4QX} + 4a_0 b_0 c_0 \alpha \gamma \psi}{2c_0 \gamma (P - \sqrt{P^2 - 4QX} - 2a_0 \psi)} \\ a_{33} &= \frac{(\beta P - \beta \sqrt{P^2 - 4QX})[-2c_0 \psi (P - \sqrt{P^2 - 4QX} - 2a_0 \psi)] - 2c_0 \gamma \psi}{2\gamma \psi (2a_0 \beta P \psi - 2a_0 \beta \psi \sqrt{P^2 - 4QX} + 4a_0 b_0 c_0 \gamma \psi)} \\ a_{34} &= \frac{2c_0 \alpha + \varepsilon P - \varepsilon \sqrt{P^2 - 4QX}}{2c_0 \gamma} \end{aligned}$$

Similarly, the characteristic equation  $|J_{E_0^3} - \lambda I| = 0$  gives the eigenvalues

$$\lambda_1 = a_{11}, \lambda_2 = a_{22}, \lambda_3 = a_{33}, \lambda_4 = -\mu.$$

Now,  $E_0^3$  will be stable if  $\lambda_1, \lambda_2, \lambda_3 < 0$ , otherwise unstable.

**(e) Stability of  $E_0^4$  point**

**Theorem 2.5.** The model (2.1) is a saddle point or a stable point at the equilibrium point  $E_0^4$ .

**Proof:** The Jacobian matrix of model (2.1) becomes at equilibrium point  $E_0^4$

$$J_{E_0^4} = \begin{bmatrix} b_{11} & b_{12} & 0 & b_{14} \\ 0 & b_{22} & b_{23} & b_{24} \\ 0 & 0 & b_{33} & b_{34} \\ 0 & 0 & 0 & -\mu \end{bmatrix}$$

where,

$$\begin{aligned} b_{11} &= \frac{P + \sqrt{P^2 - 4QX} - 2a_0\psi}{2\psi} \\ b_{12} &= \frac{\beta P + \beta \sqrt{P^2 - 4QX} - 2b_0c_0\gamma}{2c_0} \\ b_{14} &= \frac{\alpha\beta P + \alpha\beta \sqrt{P^2 - 4QX} - 2b_0c_0\alpha\gamma}{2c_0\gamma} \\ b_{22} &= \frac{(\beta P + \beta \sqrt{P^2 - 4QX} - 2b_0c_0\gamma)(P + \sqrt{P^2 - 4QX} - 2a_0\psi)}{2c_0\gamma(P + \sqrt{P^2 - 4QX} - 2a_0\psi)} \\ b_{23} &= \frac{\beta P + \beta \sqrt{P^2 - 4QX}}{2\gamma\psi} \\ b_{24} &= \frac{2\alpha a_0 \beta P \psi + 2\alpha a_0 \beta \psi \sqrt{P^2 - 4QX} - 4a_0 b_0 c_0 \alpha \gamma \psi}{2c_0 \gamma (P + \sqrt{P^2 - 4QX} - 2a_0\psi)} \\ b_{33} &= \frac{-2c_0 (\beta P + \beta \sqrt{P^2 - 4QX}) + 2b_0 c_0^2 \gamma}{(\beta P + \beta \sqrt{P^2 - 4QX} - 2b_0 c_0 \gamma)} \\ &\quad - \psi \left( 2\alpha a_0 \beta P \psi + 2\alpha a_0 \beta \psi \sqrt{P^2 - 4QX} - 4a_0 b_0 c_0 \alpha \gamma \psi \right) + \\ &\quad \left( \varepsilon P + \varepsilon \sqrt{P^2 - 4QX} \right) \left( \beta P + \beta \sqrt{P^2 - 4QX} - 2b_0 c_0 \gamma \right) \\ b_{34} &= \frac{(P + \sqrt{P^2 - 4QX} - 2a_0\psi)}{2c_0\gamma(\beta P + \beta \sqrt{P^2 - 4QX} - 2b_0 c_0 \gamma)(P + \sqrt{P^2 - 4QX} - 2a_0\psi)} \end{aligned}$$

Similarly, the characteristic equation  $|J_{E_0^4} - \lambda I| = 0$  gives the eigenvalues

$$\lambda_1 = b_{11}, \lambda_2 = b_{22}, \lambda_3 = b_{33}, \lambda_4 = -\mu.$$

Now,  $E_0^4$  will be stable if  $\lambda_1, \lambda_2, \lambda_3 < 0$ , otherwise unstable.

**(f) Local stability of endemic equilibrium point  $E^*$**

Here, we investigate the stability of endemic equilibrium point  $E^*$  using theorem 2.6.

**Theorem 2.6.** The endemic equilibrium point  $E^*(S^*, I^*, M^*, U^*)$  is locally asymptotically stable when

$$(\gamma S^* - \beta M^* - b_0)(\alpha U^* + \gamma I^* + a_0) < \gamma S^* (\alpha U^* + \gamma I^*) \quad \text{and}$$

$$\psi \beta I^* (\alpha U^* + \gamma I^* + a_0) < (\varepsilon U^* + c_0) ((\gamma S^* - \beta M^* - b_0)(\alpha U^* + \gamma I^* + a_0) - \gamma S^* (\alpha U^* + \gamma I^*)) \quad \text{otherwise}$$

unstable.

**Proof:** Using equation (2.20) the Jacobian matrix at endemic equilibrium point  $E^*(S^*, I^*, M^*, U^*)$  becomes,

$$J_{E^*} = \begin{bmatrix} -(\alpha U^* + \gamma I^* + a_0) & -\gamma S^* & 0 & -\alpha S^* \\ \alpha U^* + \gamma I^* & \gamma S^* - \beta M^* - b_0 & -\beta I^* & \alpha S^* \\ 0 & \psi & -(\varepsilon U^* + c_0) & -\varepsilon M^* \\ 0 & 0 & 0 & -\mu \end{bmatrix} \quad (2.23)$$

Using elementary row operation in equation (2.23) we obtain,

$$J_{E^*} = \begin{bmatrix} -(\alpha U^* + \gamma I^* + a_0) & -\gamma S^* & 0 & -\alpha S^* \\ 0 & C_2 & -\beta I^* & C_3 \\ 0 & 0 & D_2 & D_3 \\ 0 & 0 & 0 & -\mu \end{bmatrix}$$

The characteristic equation of this Jacobian matrix is,

$$|J_{E^*} - \lambda I| = \begin{vmatrix} -(\alpha U^* + \gamma I^* + a_0) - \lambda & -\gamma S^* & 0 & -\alpha S^* \\ 0 & C_2 - \lambda & -\beta I^* & C_3 \\ 0 & 0 & D_2 - \lambda & D_3 \\ 0 & 0 & 0 & -\mu - \lambda \end{vmatrix} = 0$$

So, the eigenvalues of  $J_{E^*}$  are  $\lambda_1 = -(\alpha U^* + \gamma I^* + a_0)$ ,  $\lambda_2 = C_2$ ,  $\lambda_3 = D_2$  and  $\lambda_4 = -\mu$ .

Now,  $J_{E^*}$  will be stable if  $C_2 < 0$  and  $D_2 < 0$

Here,

$$C_2 = \frac{(\gamma S^* - \beta M^* - b_0)(\alpha U^* + \gamma I^* + a_0) - \gamma S^*(\alpha U^* + \gamma I^*)}{(\alpha U^* + \gamma I^* + a_0)}$$

So, when

$$C_2 < 0$$

$$\frac{(\gamma S^* - \beta M^* - b_0)(\alpha U^* + \gamma I^* + a_0) - \gamma S^*(\alpha U^* + \gamma I^*)}{(\alpha U^* + \gamma I^* + a_0)} < 0$$

$$(\gamma S^* - \beta M^* - b_0)(\alpha U^* + \gamma I^* + a_0) < \gamma S^*(\alpha U^* + \gamma I^*)$$

Then,  $J_{E^*}$  will be stable.

Here,

$$D_2 = \frac{-(\varepsilon U^* + c_0)((\gamma S^* - \beta M^* - b_0)(\alpha U^* + \gamma I^* + a_0) - \gamma S^*(\alpha U^* + \gamma I^*)) + \psi \beta I^*(\alpha U^* + \gamma I^* + a_0)}{(\gamma S^* - \beta M^* - b_0)(\alpha U^* + \gamma I^* + a_0) - \gamma S^*(\alpha U^* + \gamma I^*)}$$

So, when

$$D_2 < 0$$

$$D_2 = \frac{-(\varepsilon U^* + c_0)((\gamma S^* - \beta M^* - b_0)(\alpha U^* + \gamma I^* + a_0) - \gamma S^*(\alpha U^* + \gamma I^*)) + \psi \beta I^*(\alpha U^* + \gamma I^* + a_0)}{(\gamma S^* - \beta M^* - b_0)(\alpha U^* + \gamma I^* + a_0) - \gamma S^*(\alpha U^* + \gamma I^*)} < 0$$

$$\psi \beta I^*(\alpha U^* + \gamma I^* + a_0) < (\varepsilon U^* + c_0)((\gamma S^* - \beta M^* - b_0)(\alpha U^* + \gamma I^* + a_0) - \gamma S^*(\alpha U^* + \gamma I^*))$$

Then,  $J_{E^*}$  will be stable otherwise, unstable.

Hence the **Theorem 2.6** is proved.

**(g) Global Stability of the Endemic Equilibrium Point**

In this section, we use the Lyapunov direct method to establish sufficient conditions for the global asymptotic stability of the endemic equilibrium point.

**Theorem 2.7.** The endemic equilibrium point of the model (2.1) is globally asymptotically stable if  $i < 0$  in the interior of the feasible region, otherwise it is unstable.

**Proof:** Actually, by using a Lyapunov function (Buonomo and Vargas-De-León (2012)), we will prove that the equilibrium point  $E^*$  is globally asymptotically stable when  $i < 0$ . Here by the word “globally”, we mean the whole positive invariant domain. For convenience, we make a translation of variables,  $S = \bar{S}, I = \bar{I}, M = i - \bar{M}, U = \bar{U}$ . The model becomes

$$\begin{aligned} \frac{d\bar{S}}{dt} &= K - (\alpha\bar{U} + \gamma\bar{I})\bar{S} - a_0\bar{S} \\ \frac{d\bar{I}}{dt} &= (\alpha\bar{U} + \gamma\bar{I})\bar{S} - \beta\bar{I}i + \beta\bar{I}\bar{M} - b_0\bar{I} \\ \frac{d\bar{M}}{dt} &= -\psi\bar{I} - \varepsilon\bar{M}\bar{U} + \varepsilon i\bar{M} + c_0i - c_0\bar{M} \\ \frac{d\bar{U}}{dt} &= r - \mu\bar{U} \end{aligned} \quad (2.24)$$

we consider the following nonlinear Lyapunov function,

$$\begin{aligned} L &= \left( \bar{S} - S^* - S^* \ln \frac{\bar{S}}{S^*} \right) - \left( \bar{I} - I^* - I^* \ln \frac{\bar{I}}{I^*} \right) + \bar{M} \\ i.e. \dot{L} &= \left( 1 - \frac{S^*}{\bar{S}} \right) \dot{\bar{S}} - \left( 1 - \frac{I^*}{\bar{I}} \right) \dot{\bar{I}} + \dot{\bar{M}} \\ \Rightarrow \dot{L} &= \left( 1 - \frac{S^*}{\bar{S}} \right) \left( K - (\alpha\bar{U} + \gamma\bar{I})\bar{S} - a_0\bar{S} \right) - \left( 1 - \frac{I^*}{\bar{I}} \right) \\ &\quad \left( (\alpha\bar{U} + \gamma\bar{I})\bar{S} - \beta\bar{I}i + \beta\bar{I}\bar{M} - b_0\bar{I} \right) - \psi\bar{I} - \\ &\quad \varepsilon\bar{M}\bar{U} + \varepsilon i\bar{M} + c_0i - c_0\bar{M} \\ \Rightarrow \dot{L} &= \frac{K}{\bar{S}} \left( S^* - \bar{S} \right) - (\alpha\bar{U} + \gamma\bar{I}) \left( S^* - \bar{S} \right) - a_0 \left( S^* - \bar{S} \right) \\ &\quad - (\alpha\bar{U} + \gamma\bar{I}) \left( S^* - \frac{\bar{S}I^*}{\bar{I}} \right) + \beta\bar{I} \left( \bar{I} - I^* \right) - \beta\bar{M} \left( \bar{I} - I^* \right) + \\ &\quad b_0 \left( \bar{I} - I^* \right) - \psi\bar{I} - \varepsilon\bar{M}\bar{U} + \varepsilon i\bar{M} + c_0i - c_0\bar{M} \end{aligned}$$

Now if  $i < 0$ , and  $\bar{S} = S^*, \bar{I} = I^*, \bar{M} = M^*, \bar{U} = U^*$  then  $\dot{L} < 0$

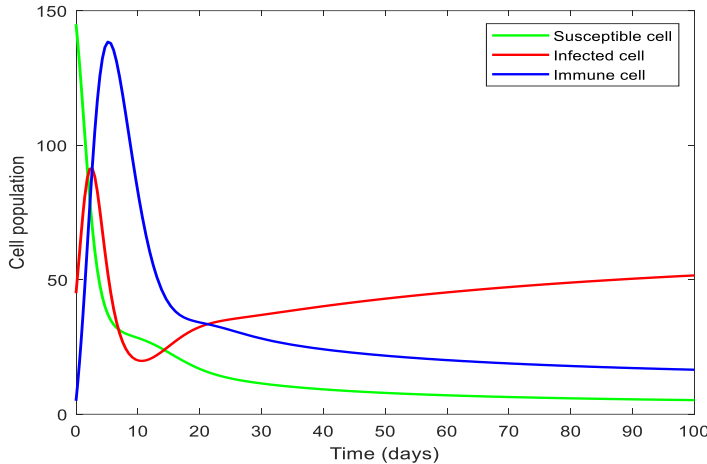
In this case, endemic equilibrium point is globally asymptotically stable.

### 3. Numerical analysis

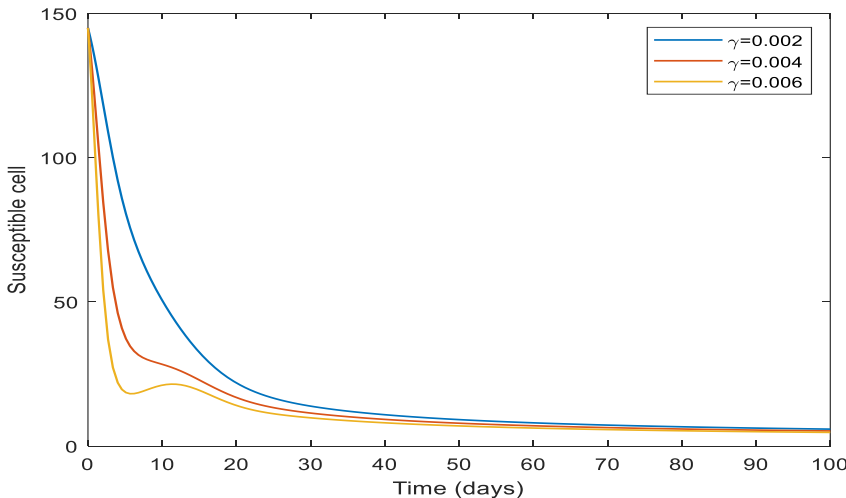
We perform numerical simulations of our model (2.1) by the ODE45-solver using MATLAB programming. To solve the model (2.1), we consider the initial values as  $S(0) = 145, I(0) = 45, M(0) = 5, U(0) = 10$ , and all the parameters showed in Table 3.1. Our goal is to study the effects of two parameters i.e., infection rate  $\gamma$  due to infected cell and excess UV index  $r$ . We perform simulations for the fixed time 100 days. we have solved the model (2.1) for the tabulated values in Table 3.1 representing the initial and parametric values considered for our model. The simulations of the populations are shown in Figs 3.1-3.11.

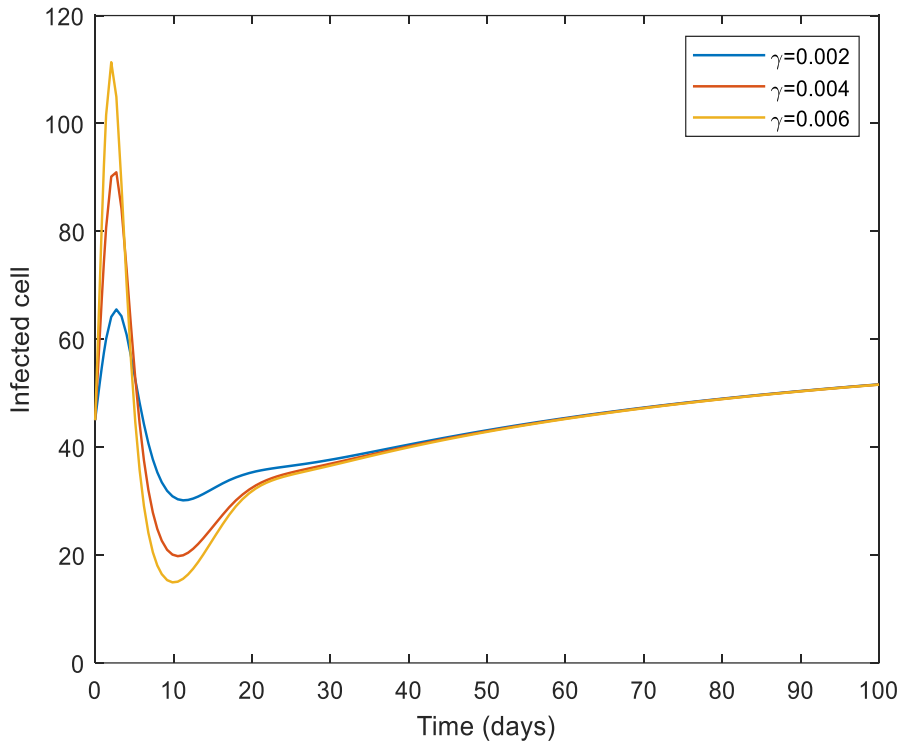
**Table 3.1:** Parameter specifications of model (2.1)

Parameter	Description	Value
$K$	Recruitment rate of susceptible cells	$5.07 \text{ day}^{-1}$
$\alpha$	The rate at which ultraviolet light damaging the susceptible cells	$0.001 \text{ day}^{-1}$
$\gamma$	The rate at which susceptible cells infected due to infected cells	$0.02 \text{ day}^{-1}$
$a_0$	Natural death rate of susceptible cells	$0.003 \text{ day}^{-1}$
$\beta$	Decay rate of infected cells in contact with immune cells	$0.0034 \text{ day}^{-1}$
$b_0$	Natural death rate of infected cells	$0.04 \text{ day}^{-1}$
$\psi$	Immune response rate due to infected cells	$0.5 \text{ day}^{-1}$
$\varepsilon$	Immune Suppression rate due to ultraviolet radiation	$0.002 \text{ day}^{-1}$
$c_0$	Natural death rate of immune cells	$0.039 \text{ day}^{-1}$
$R$	Excess exposure rate of ultraviolet radiation	12 uvindex
$\mu$	Decay rate of ultraviolet radiation	$0.01 \text{ day}^{-1}$

**Fig 3.1.** The disease behaviour of susceptible, infected and immune cell.

**Fig 3.1** shows the state trajectories of the three compartments such as susceptible, infected and immune cell. We have observed that the susceptible cell gradually decreases with time. At initial state the infected cell increases then decreases after sometime later it also increases if no control measure is employed. And the immune cell increases at the at initial stage of infection but sometime later gradually decreases with time.

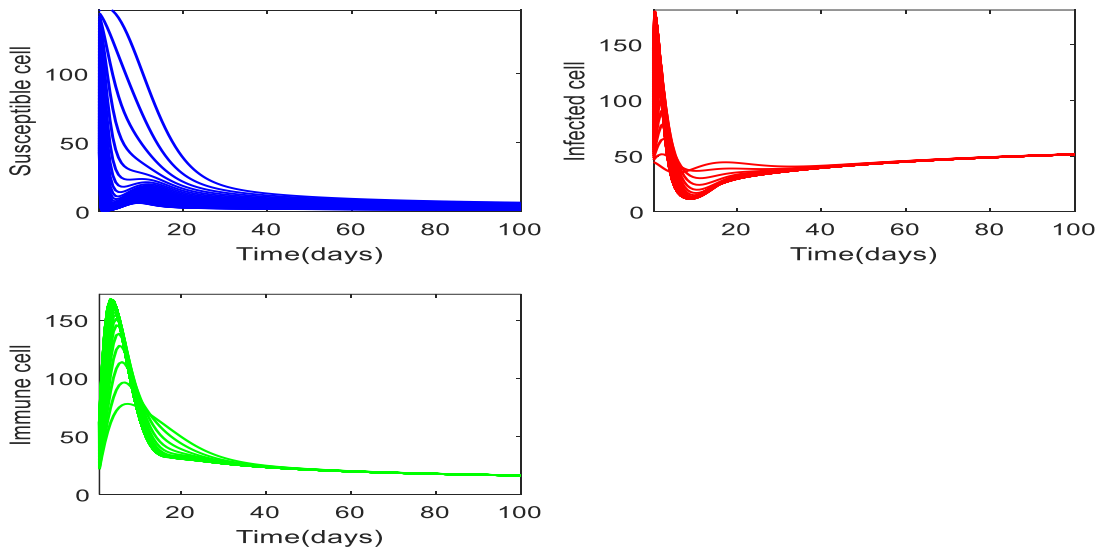
**Fig 3.2.** Effect of  $\gamma$  on susceptible cell.



**Fig 3.3.** Effect of  $\gamma$  on infected cell.

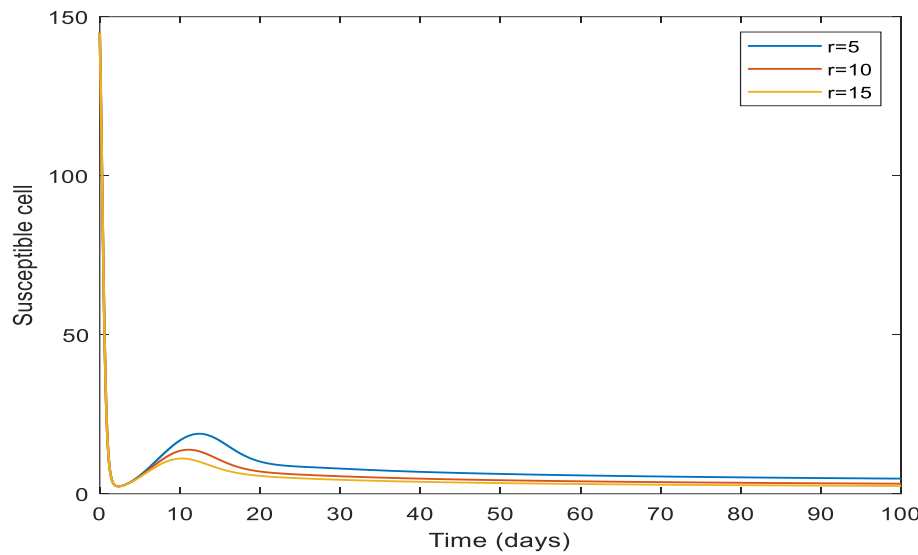
In **Fig 3.2**, we see that in the increase of values of  $\gamma$  (infection rate due to infected cell) the density of susceptible cell decreases respectively.

In **Fig 3.3**, we observe that, 0 to 5 days the density of infected cell increase with increase the values of  $\gamma$  (infection rate due to infected cell), but 5 to 30 days the density decrees with increase the values of  $\gamma$  (infection rate due to infected cell) and 30 to 100 days there is no change in the density of infected cell with the increase the values of  $\gamma$  (infection rate due to infected cell).

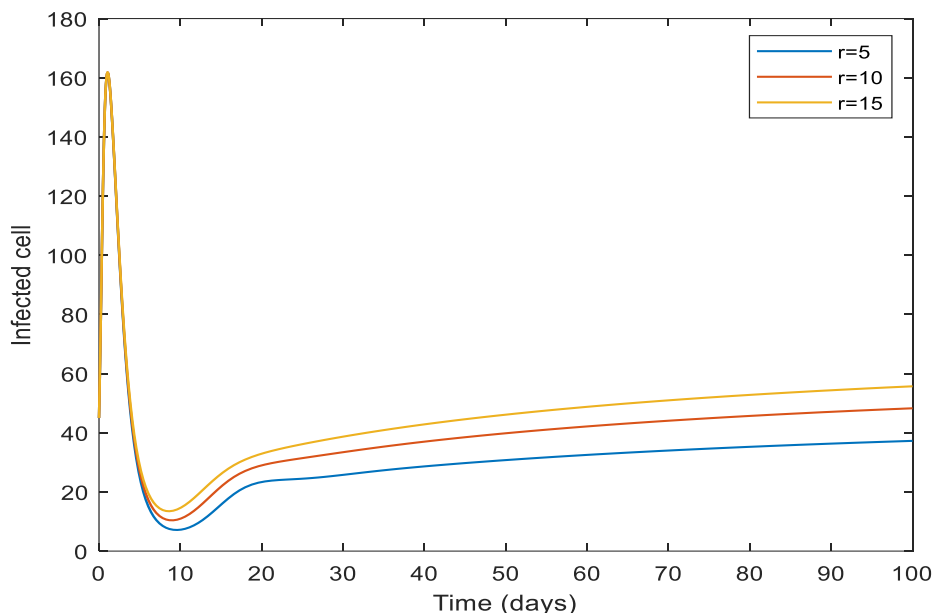


**Fig 3.4.** Effect of  $\gamma$  on susceptible cell, Infected cell and Immune cell.

**Fig 3.4** shows with increase of  $\gamma$  (infection rate due to infected cell) the density of susceptible cell decreases, the density of infected cell increases and the density of immune cell decreases that means skin cancer become more malignant.

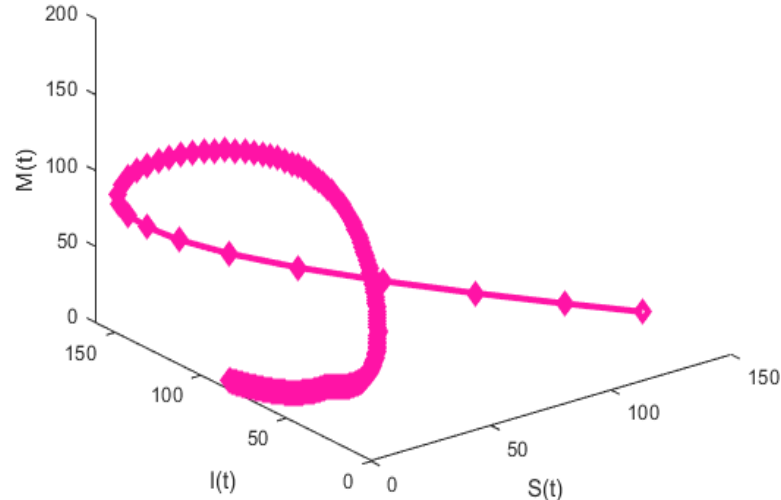
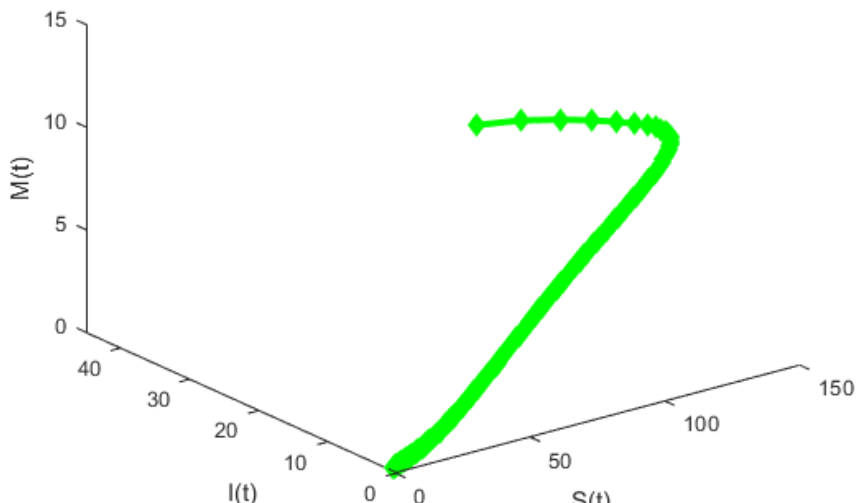


**Fig 3.5.** Effect of  $r$  on susceptible cell.



**Fig 3.6.** Effect of  $r$  on infected cell.

**Fig 3.5** represent if the values of  $r$  (UV index) increases then the density of susceptible cell decreases with time and **Fig 3.6** indicate that with the increasing values of  $r$  (UV index) the density of infected cell increases with time. These two figures justify the clinical and analytical incidence of UV index on skin cancer.

(a)  $R_0 > 1$ (b)  $R_0 < 1$ 

**Fig 3.7.** Variation of Susceptible cells, Infected cells and Immune cells when  $R_0 > 1$  and  $R_0 < 1$ .

In **Fig 3.7** we have shown the variation of susceptible, infected and immune cell. In analytical analysis we have obtained the DFE point is locally asymptotically stable when  $R_0 < 1$  that we have obtained numerically in **Fig 3.7(b)** and **Fig 3.7(a)** shows the instability of DFE point when  $R_0 > 1$

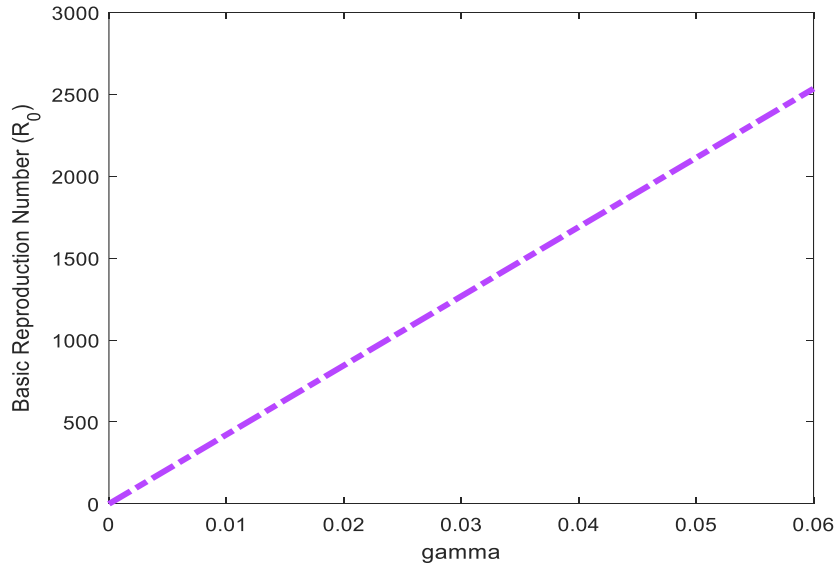


**Fig 3.8.** Using the parameter values of Table 1,  $R_0$  increases as infection rate  $\gamma$  increases.

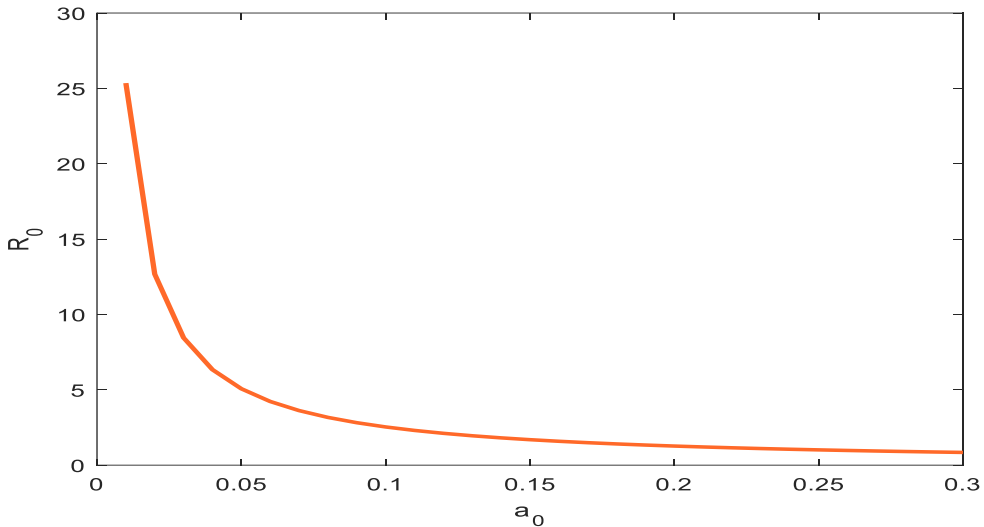


**Fig 3.9.** Using the parameter values of Table 1,  $R_0$  decreases as natural death rate  $a_0$  increases.

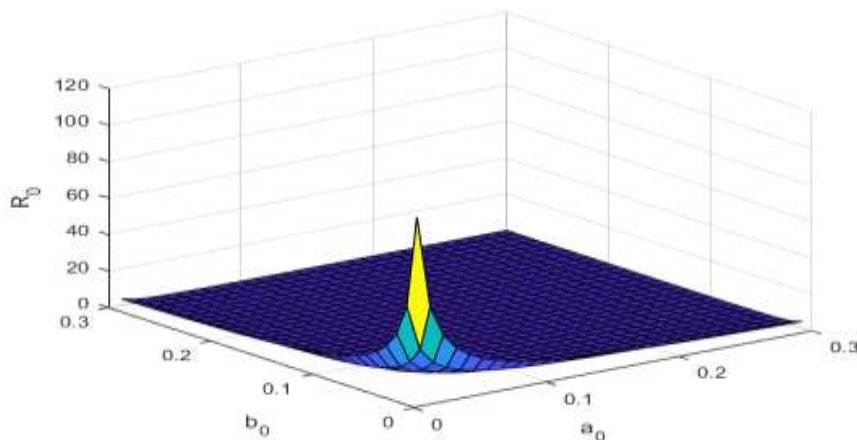


**Fig 3.10.** The graph of basic reproduction number ( $R_0$ ) with respect to the natural death rate ( $a_0$ ) of susceptible populations and natural death rate ( $b_0$ ) of infected populations.

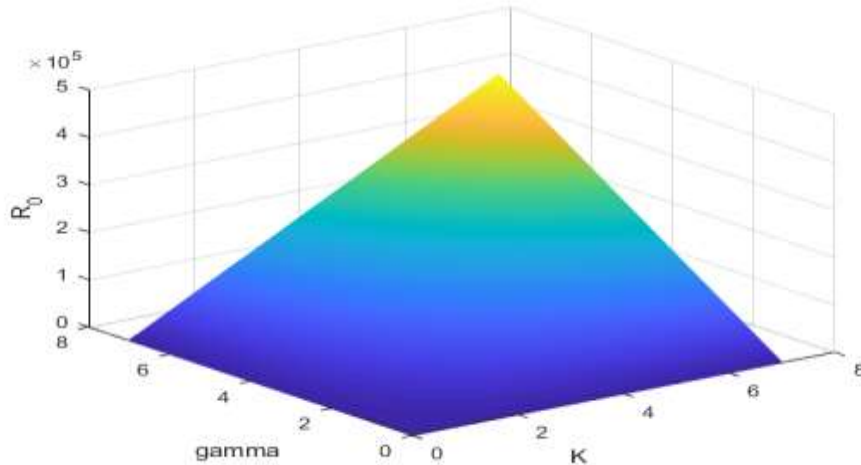


**Fig 3.11.** The graph of basic reproduction number ( $R_0$ ) with respect to the recruitment rate ( $K$ ) of susceptible populations and infection rate ( $\gamma$ ) due to infected populations.

In our study, the disease-free equilibrium point is locally asymptotically stable if  $R_0 < 1$  and unstable if  $R_0 > 1$ . Whereas, the endemic equilibrium point is locally asymptotically stable if  $R_0 > 1$  and unstable if  $R_0 < 1$ . The simulated graphs are represented in Figs. 3.8 and 3.9. Figs 3.10 and 3.11 present a 3-dimensional plot of basic reproduction number.

## Conclusion

In this paper, a four compartmental model has been proposed to study the spread of skin cancer due to the over exposure of ultraviolet radiation. We first determined the non-periodicity and limiting behavior of the solutions and then found the equilibria of the proposed model (2.1). We have observed the basic reproduction number for DFE point. Then we performed the stability analysis of the equilibria. We found that the zero equilibria point is asymptotically stable, disease-free equilibrium point is locally asymptotically stable if  $R_0 < 1$  and unstable if  $R_0 > 1$ . We have also shown the stability of ultraviolet radiation free equilibria and endemic equilibrium point. Using Lyapunov direct method we have shown the global stability of DFE and EE points under some conditions. In our study we found that ultraviolet radiation is one of the main risk factors of skin cancer. It also damages immune cells. Therefore, it is time to take proper steps to aware about the effect of ultraviolet radiation all over the world so that we can protect us from harmful UV radiation and reduce the transmission of skin cancer.

## Acknowledgements

The first author is supported by M.Sc. (NST) fellowship, bearing ID: MSc-201203, Serial: 291, Merit: 77, No: 39.00.0000.012.002.06.21. Session: 2021-2022 which is provided by the Ministry of Science and Technology, Government of the People's Republic of Bangladesh. The NST fellowship is gratefully acknowledged for financial support.

## References

- [1] World Health Organization. (2017, 16 October). " Ultraviolet Radiation (UV) and Skin Cancer " Retrieved from [https://www.who.int/news-room/q-a-detail/radiation-ultraviolet-\(uv\)-radiation-and-skin-cancer](https://www.who.int/news-room/q-a-detail/radiation-ultraviolet-(uv)-radiation-and-skin-cancer)
- [2] World Health Organization International Agency for Research on Cancer (IARC). GLOBOCAN 2020: Non-melanoma skin cancer worldwide in 2020. Available from: <https://gco.iarc.fr/today/data/factsheets/cancers/17-Non-melanoma-skin-cancer-fact-sheet.pdf>.
- [3] World Health Organization International Agency for Research on Cancer (IARC). GLOBOCAN 2020: Melanoma of skin cancer worldwide in 2020. Available from: <https://gco.iarc.fr/today/data/factsheets/cancers/16-Melanoma-of-skin-fact-sheet.pdf>.

- [4] Our World in Data, (2018). Ozone layer. Retrieved from <https://ourworldindata.org/ozone-layer>.
- [5] Newman, P.A., Oman, L.D., Douglass, A.R., Fleming, E.L., Frith, S.M., Hurwitz, M.M., Kawa, S.R., Jackman, C.H., Krotkov, N.A., Nash, E.R., Nielsen, J.E., Pawson, S., Stolarski, R.S. and Velders, G.J.M. (2009). What Would Have Happened to the Ozone Layer if Chlorofluorocarbons (CFCs) Had not been Regulated? *Atmos. Chem. Phys.*, Vol. 9, pp. 2113–2128.
- [6] United Nations / Framework Convention on Climate Change (2015) Adoption of the Paris Agreement, 21st Conference of the Parties, Paris: United Nations.
- [7] Fears, T.R., Scotto, J., Marvin, A. and Schneiderman. (1977). Mathematical Model of Age and Ultraviolet Effects on the Incidence of Skin Cancer among Whites in the United States, *American Journal of Epidemiology*, Vol. 105, pp. 420-427.
- [8] Grulil, F.R.D. and Vander Leun, J. C. (1979). A Dose-response Model for Skin Cancer Induction by Chronic U.V. Exposure of a Human Population, *J. theor. Biol.*, Vol. 83, pp. 487-504.
- [9] Moan, J. and Dahlback, A. (1993). Ultraviolet Radiation and Skin Cancer: Epidemiological Data from Scandinavia, *Environmental UV Photobiology*, Vol. 1, pp. 255-293.
- [10] Shore, R.E. (2001). Radiation-Induced Skin Cancer in Humans, *Medical and Pediatric Oncology*, Vol. 36, pp. 549-554.
- [11] Bharath, A.K. and Turne, R.J. (2009). Impact of Climate Change on Skin Cancer, *Journal of the Royal Society of Medicine*, Vol. 102, No. 6, pp. 215-218.
- [12] Bishop, J.A.N., Chang, Y.M., Elliott, F., Chan, M., Leake, S., Karpavicius, B., Haynes, S., Fitzgibbon, E., Kukalizch, K., Moor, J.R., Elder,D.E., Bishop,D,T. and Barrett, J.H. (2011). Relationship between Sun Exposure and Melanoma Risk for Tumours in Different body sites in a Large Case-control Study in a Temperate Climate, *European Journal of Cancer*, Vol. 47, pp. 732-741.
- [13] Greinert, R., de Vries, E., Erdmann F., Espina, C., Auvinen, A., Kesminiene, A. and Schu, J., (2014). European Code against Cancer 4th Edition: Ultraviolet Radiation and Cancer, *Cancer Epidemiology*, Vol. 39S, pp. 575-583.
- [14] Kim, I.Y., He,Y.Y. (2014). Ultraviolet Radiation-induced Non-melanoma Skin Cancer: Regulation of DNA Damage Repair and Inflammation, *Genes & Diseases*, Vol. 1, pp. 188-198.
- [15] Berwick, M. and Garcia, A. (2020). Solar UV Exposure and Mortality from Skin Tumors: An Update, *Reichrath, J.(ed.), Sunlight, Vitamin D and Skin Cancer*. 3<sup>rd</sup> ed., Advances in Experimental Medicine and Biology, Vol. 1268, pp.143-154.
- [16] Biswas, M.H.A., Islam, M.A., Akter, S., Mondal, S., Khatun, M.S., Samad, S.A., Paul, A.K. and Khatun, M.R. (2020). Modelling the Effect of Self-Immunity and the Impacts of Asymptomatic and Symptomatic Individuals on COVID-19 Outbreak, *CMES-Computer Modeling in Engineering & Sciences*, Vol. 125, No. 3, pp. 1033–1060.
- [17] Biswas, M.H.A. (2014). On the Evaluation of AIDS/HIV Treatment: An Optimal Control Approach, *Current HIV Research*, Vol. 12, No. 1, pp. 1-12.
- [18] Agarwal, M. and Verma, V. (2012). Modeling and Analysis of the Spread of an Infectious Disease Cholera with Environmental Fluctuations, *Applications and Applied Mathematics*, Vol. 7, No. 1, pp. 406-425.
- [19] Dubey, B. Dubey, P. and Dubey. U.S. (2015). Dynamics of an SIR Model with Nonlinear Incidence and Treatment Rate, *Applications and Applied Mathematics*, Vol. 10, No. 2, pp. 718-737.
- [20] Huo, H.F., Feng, L.X. (2012). Global Stability of an Epidemic Model with Incomplete Treatment and Vaccination, *Discrete Dynamics in Nature and Society*, pp. 1–14.
- [21] Vargas-De-Leon, C. (2017). Global Stability of Infectious Disease Models with Contact Rate as a Function of Prevalence Index, *Mathematical Biosciences and Engineering*, Vol. 14, No. 4, pp. 1019–1033.
- [22] Biswas, M.H.A., Paiva L.T. and de Pinho, M.D.R. (2014). A SEIR Model for Control of Infectious Diseases with Constraints, *Mathematical Biosciences and Engineering*, Vol. 11, No. 4, pp. 761-784.
- [23] Allen, B.G., Bhatia, S.K., Anderson, C.M., Gilmore, J.M.E., Sibenaller, Z.A., Mapuskar, K.A., Schoenfeld, J.D., Buatti, J.M., Spitz, D.R. and Fath, M.A. (2014). Ketogenic Diets as an Adjuvant Cancer Therapy: History and Potential Mechanism, *Redox Biol*, Vol. 2, pp. 963–970.
- [24] Arino, J. and Portet, S. (2020). A simple model for COVID-19, *Infectious Disease Modelling*, Vol. 5, pp. 309-315.

- [25] Buonomo, B., Vargas-De-León, C. (2012). Global Stability for an HIV-1 Infection Model Including an Eclipse Stage of Infected cells, *Journal of Mathematical Analysis and Applications*, Vol. 385, No. 2, pp. 709–720.
- [26] Eikenberry, S.E., Mancuso, M., Iboi, E., Phan, T., Eikenberry, K., Kuang, Y., Kostelich, E. and Gumel, A.B. (2020). To mask or not to mask: Modeling the potential for face mask use by the general public to curtail the COVID-19 pandemic, *Infectious Disease Modelling*, Vol. 5, pp. 293-308.
- [27] Lemos-Paião, A.P., Silva, C.J. and Torres, D.F.M. (2020). A New Compartmental Epidemiological Model for COVID-19 with a Case Study of Portugal, *Ecological Complexity*, Vol. 44, N0. 100885.
- [28] Nono, M.K., Ngouonkadi1, E.B.M., Bowong, S. and Fotsin, H.B. (2020). Hopf and backward bifurcations induced by immune effectors in a cancer oncolytic virotherapy dynamics, *International Journal of Dynamics and Control*.

# Predicting Employee Turnover with the Modeling of Hybrid Neural Network for Human Resource Management

Christopher Francis Britto and Abdul Rahman H Ali

**Abstract** In organizations, Human Resource Management (HRM) plays a significant role in providing a high-quality workforce to the organizations' development and in managing and retaining talent resources. The HR department often confronts the uncertainty in employee attrition, which creates a negative impact on the organization in the form of productivity loss, recruitment cost, and training cost. In essence, recruiting new candidates and training them in a particular skill without losing productivity is challenging and time-consuming. Hence, it is essential to predict the attrition or turnover of the employees in advance to gain the potential benefits and avoid the economic and knowledge losses in the organizations. The study focuses on dynamically identifying the determinants of the turnover for the prediction of employee turnover using the hybrid neural network with the consideration of the organization and employee behaviors. This work presents the neural network-based employees' turnover prediction model for effective human resource management. The proposed approach enhances the HR decision-making model in two key processes, such as feature importance extraction and turnover prediction with the help of the hybrid neural networks. Thus, the proposed approach ensures effective HR decision-making in terms of the increased job satisfaction without compromising the organization's benefits, which avoids the knowledge and cost losses to the organization.

**Keywords-** Employee turnover; prediction model; hybrid neural network.

## 1. Introduction

The organization often confronts the high employee turnover that affects both the growth and performance of the organization. The impact of turnover has received considerable attention by senior management, human resources professionals and industrial psychologists. It has proven to be one of the most costly and seemingly intractable human resource challenges confronting several organizations globally [1].

In human resource management, predicting the turnover of the employees based on the significance of the different factors is critical over the time-variant behaviors of the employees as well as the organizations. Analyzing the importance of the factors associated with the decision-making process of the employees' turnover is challenging due to the increased diversity of the factors among the employees. In consequence, assessing and determining the important decision factors on the reasons for the job quit from the current organization is quite a challenging task. The employers lack to identify the uncertain reasons for any individual employee in their organization and make proactive employee retention, which leads to the losses in the knowledge and cost.

---

Christopher Francis Britto  
Department of Computer Science and Information Technology, Mahatma Gandhi University, Meghalaya (India)  
Email Address : brittochris@gmail.com

Abdul Rahman H A  
Department of Electronics, Taibah University, Madinah, Saudi Arabia

However, predicting the factors that influence the turnover of the employees over the dynamic changes in employee behaviors is difficult. Hence, there is an essential need for determining the at-risk employees in the attrition, which is highly demanded by the organizations. The traditional HR analytics models have analyzed several key factors such as age, years of experience, skill level, salary, and professional strength to identify the reasons behind the attrition of each employee [2].

### 1.1 Proposed System

Owing to the huge expenditures in the human resource department, effectively managing the available human resources is crucial without losing potential employees from the organization. Data mining and machine learning methods have extracted the significance of the factors and predicting the employees' turnover, predicting the turnover of the employees when there is increased uncertainty and inherent variations in the employees' behaviors without compromising the organizations' benefits is a critical task. In addition to the shallow learning models, the deep learning of the artificial neural network models overcome the actionable insights extraction-related constraints faced by the employers. However, quantifying the significance of the feature sets over the different dimensions of the employee-organization relationship using the statistical and mining methods misleads the prediction of the attrition rate and reduces the retention rate of the employees. Hence, it is essential to compute the importance of the features and predict the employees' turnover with the assistance of the deep neural network models with the target of balancing both the employees and organization.

### 1.2 Literature Review

Zhang et al [3] have proposed machine learning technique to sort out the characteristics of employee turnover. It adopts the GBDT algorithm and LR algorithm to fit the characteristic model which influences employee turnover. This paper implements the employee turnover prediction in realistic companies, which provides an effective reference for companies to reduce the turnover rate of employees.

Soni et al [4] have proposed a study to investigate the employee characteristics and various organizational variables that may result in employee turnover. The goal of this research is to check application of both ANN, ANFIS models for the prediction of employee turnover in an organization and to recognize the technique which stands the best for the chosen dataset. The results show that ANN model is much better at fitting the output than the ANFIS model for the unseen data set. It was therefore chosen as the technique for the purpose of developing the prediction model.

Alao et al [5] proposes a model that identifies employee related attributes that contribute to the prediction of employees' attrition in organizations. The demographic and job-related records of the employee were the main data which were used to classify the employee into some predefined attrition classes. Waikato Environment for Knowledge Analysis (WEKA) and See5 for Windows were used to generate decision tree models and rulesets. The results of the decision tree model and rulesets generated were then used for developing a predictive model that was used to predict new cases of employee attrition. A framework for a software tool that can implement the rules generated in this study was also proposed. Results obtained from the study shows that employee salary and length of service were determining factors for predicting employee attrition in the institution whose data was used for the case study. Employees who have worked longer in the organization with no reasonable increase in income are likely to be more discouraged which influences their attrition. The findings of this study further support studies that have been carried out in the area of predicting employee attrition. It also supports the findings of Nagadevara, et al (2008) that it is possible to predict employee turnover intentions even before they had made their final decision to leave.

## 2. Material and Method

Zhang et al. [3] have proposed machine learning technique to sort out the characteristics of employee turnover. It adopts GBDT algorithm and LR algorithm to fit the characteristic model which influences employee turnover. This paper implements the employee turnover prediction in realistic companies, which provides an effective reference for companies to reduce the turnover rate of employees. There are many factors affecting employee turnover. According to the analysis of both staff behavior and company experience, employee turnover is impacted by a series of factors, for example, salary, business trip, job environment satisfaction, work commitment, overtime, promotion, salary increase. In this paper, the data for employee turnover is from around 100 companies. Based on data mining technology, this paper mainly analyzes the basic information, work experience, position salary etc. Based on the historical records of employees (especially, leave or not leave), the weights of various factors are fitted by logical regression, adaboost, SVM and other algorithms. The key characteristics of employee turnover will be used in the prediction of future turnover. The overall flowchart is shown in Figure1.

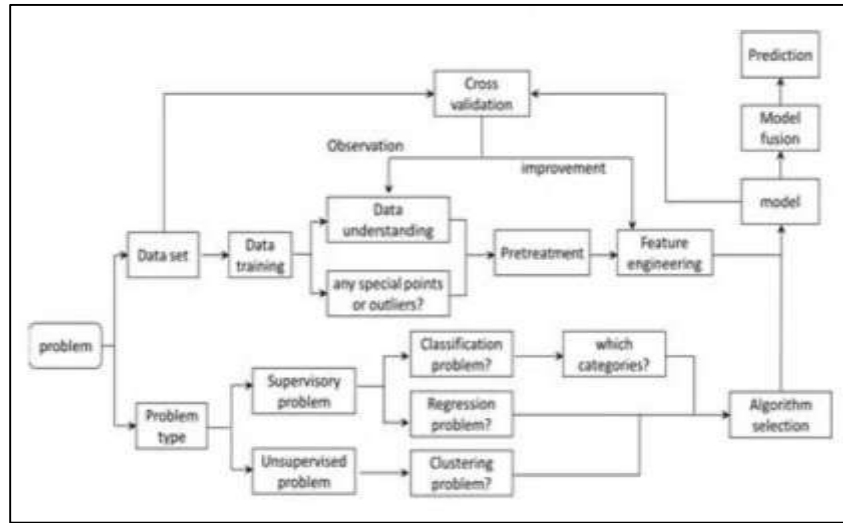


**Figure 1: Overall flowchart of employee turnover characteristics construction**

Soni et al. [4] have proposed a study to investigate the employee characteristics and various organizational variables that may result in employee turnover. The goal of this research is to check application of both ANN, ANFIS models for the prediction of employee turnover in an organization and to recognize the technique which stands the best for the chosen dataset. The results show that ANN model is much better at fitting the output than the ANFIS model for the unseen data set. It was therefore chosen as the technique for the purpose of developing the prediction model.

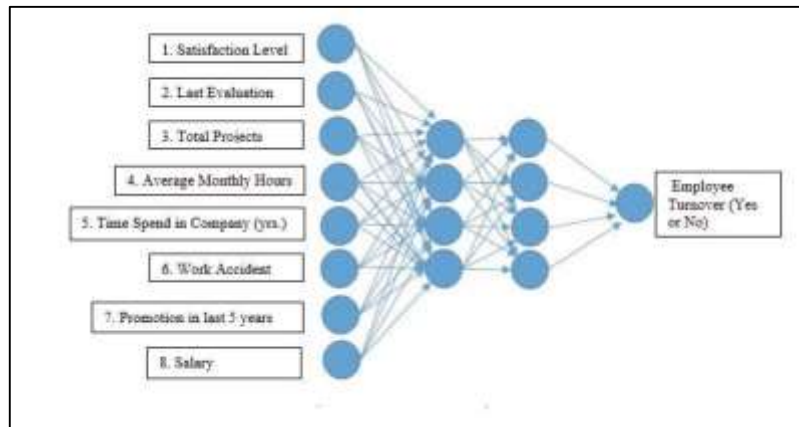


**Figure 2: ANN basic architecture for Employee Turnover**

Alao et al. [5] proposes a model that identifies employee related attributes that contribute to the prediction of employees' attrition in organizations. The demographic and job-related records of the employee were the main data which were used to classify the employee into some predefined attrition classes. Waikato Environment for Knowledge Analysis (WEKA) and See5 for Windows were used to generate decision tree models and rulesets. The results of the decision tree model and rule-sets generated were then used for developing a predictive model that was used to predict new cases of employee attrition.

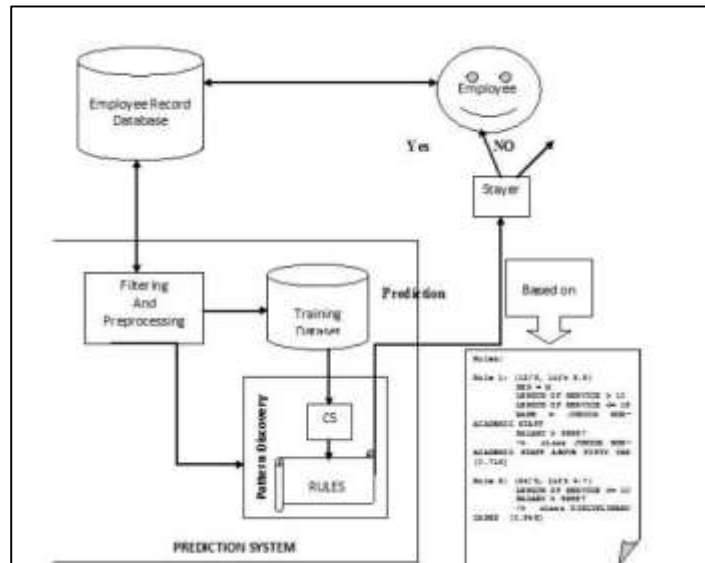


**Figure 3: Framework for Employee Attrition Prediction System**

Wang, X. et al. [6] state that the HR information management should be strengthened by using inside enterprise (i.e. company- and employee-specific information) and outside enterprise information (i.e. economic circumstances) about the employees' situation. A conceptual framework is given for a decision support system based on turnover knowledge. The study provides a very useful evaluation model for employee turnover risk, where both inside and outside factors are taken into account. Because the authors do not elaborate on the methodology and the application of the framework, the study encourages further study of suitable mechanisms. In this paper, the theoretical framework is extended by providing a methodology.

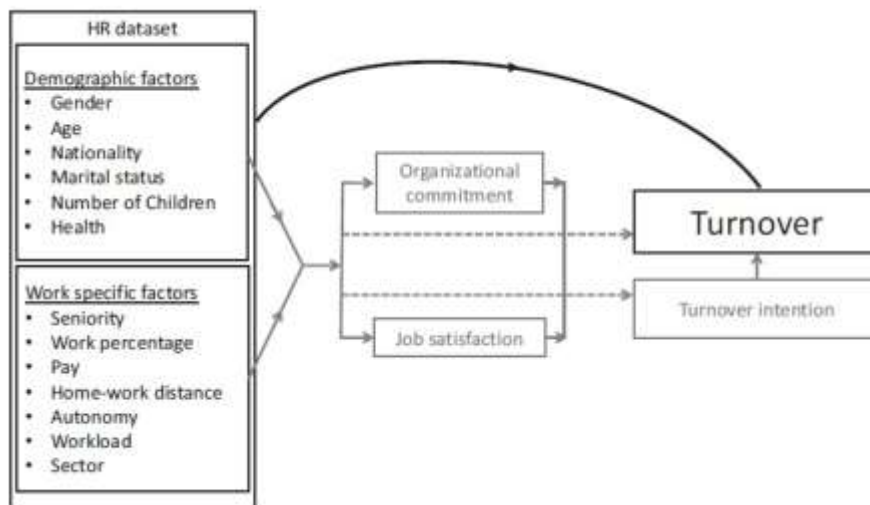


**Figure 4: Indirect relationship to turnover as studied in literature**

Our study “Predicting Employee Turnover with the Modeling of Hybrid Neural Network for Human Resource Management” presents the neural network-based employees’ turnover prediction model for effective human resource management.

The hybrid neural network model involves the modeling of the significant feature sets through the high-level abstraction and the prediction of the consequences on the organization by the employee without compromising either both the quality and profit of the organization or job satisfaction of an employee. By predicting employee turnover based on the behaviors of employees as well as the organization, it enforces the optimal retention of the employees without degrading the performance of the organization.

Thus, it effectively maintains the trade-off between the organization and employee with the assistance of the hybrid neural network model.

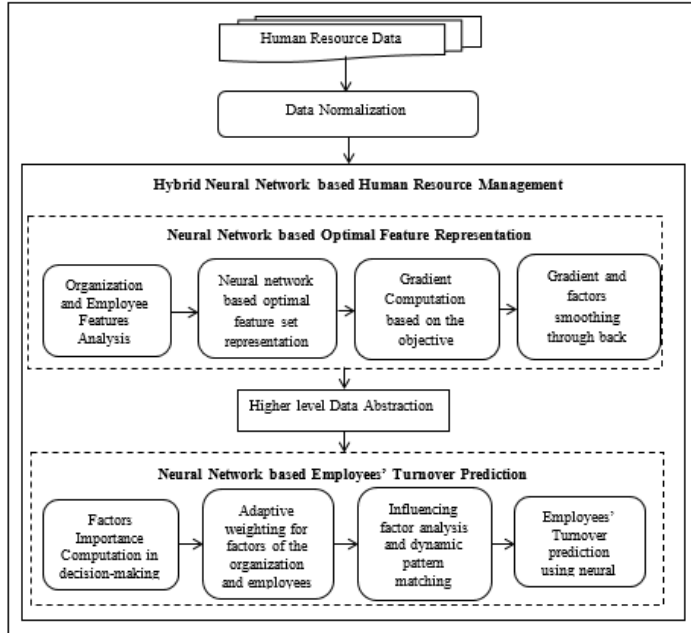


**Figure 5: Hybrid Neural Network-based Human Resource Management Methodology**

The process involved in the proposed HR decision-making model is depicted in Figure 5. The proposed methodology enhances human resource management with the help of the hybrid neural network model. It designs the enhanced human resource management model involving the neural network-based optimal feature representation and the neural network-based employee turnover prediction. Initially, the proposed approach applies the data normalization on the raw human resource data that comprises the multiple factors of the employees and organization from different perspectives. In the phase of optimal feature representation, the proposed approach examines the normalized feature values of both the employees and organization and applies the deep neural network model for optimally generating the reduced representation of the input data. In this case, the term optimal refers that the consideration of the factors influencing the employees' turnover based on pattern extraction in an unsupervised manner. In essence, the proposed approach computes the gradient score for the coarse-grained generated feature set for an individual or group of employees for the analysis of the impact on the job transition. By applying the backpropagation on the neural network model, it smoothens both the gradient value and the factors that influence the turnover of the employees. Owing to the dynamic changes in the behavior of the employees as well as the organization, continuous smoothening through backpropagation becomes an effective solution in human resource management, which results in the transformation of the high-level abstraction of the input data. In the phase of the employees' turnover prediction, the proposed approach computes the significance of the factors in the job transition in addition to the extraction of the high-level data abstraction, which is based on the profile information, organization activities on a particular employee, and employees' behaviors in the organization. By analyzing the factors accumulated in the human resource data, it adaptively assigns the weight for all the factors to the extracted actionable insights of behavior changes and influence probability on the employees' turnover. As a result, the proposed approach accurately predicts the turnover of the employee through effective pattern matching and influence analysis, which balances the benefits of both the employees and the organization. Thus, the enhanced human resource management model facilitates the organization to enforce preventive actions towards the retention of the employees.

#### 4. Findings

Employee turnover is the main reason for organization loss of productivity and profits. Organizations are under constant strain to maintain the level of productivity and provide the right environment and rewards to retain the employees. Employee behaviors are unpredictable, and their needs differ based on circumstances. So, the organization needs to evaluate different conditions to retain their talent in the organization.

In their study, Zhang, H. et al [4] proposes machine learning technique to sort out the characteristics of employee turnover. Furthermore, they adopt GBDT algorithm and LR algorithm to fit the characteristic model which influences employee turnover.

In their study, Soni, U. et al [5] investigate the employee characteristics and various organizational variables that may result in employee turnover. The goal of this research is to check application of both ANN, ANFIS models for the prediction of employee.

In our study “Predicting Employee Turnover with the Modeling of Hybrid Neural Network for Human Resource Management” presents the neural network-based employees’ turnover prediction model for effective human resource management. It designs the enhanced human resource management model involving the neural network-based optimal feature representation and the neural network-based employee turnover prediction. By analyzing the factors accumulated in the human resource data, it adaptively assigns the weight for all the factors to the extracted actionable insights of behavior changes and influence probability on the employees’ turnover. As a result, the proposed approach accurately predicts the turnover of the employee through effective pattern matching and influence analysis, which balances the benefits of both the employees and the organization. Thus, the enhanced human resource management model facilitates the organization to enforce preventive actions towards the retention of the employees.

## 5. Conclusion

This work presented the neural network-based employees’ turnover prediction model for effective human resource management. The proposed approach enhances the HR decision-making model in two key processes, such as feature importance extraction and turnover prediction with the help of the hybrid neural networks. To quantify and identify the significant factors that leverage the employee towards the attrition, it extracts and retains the potential feature sets using the neural network along with the backpropagation. Moreover, to accurately predict the job’s mobility and facilitate the employer in their decision-making, it applies the neural network model based on the analysis of the activities performed by both the employees and the organization. Thus, the proposed approach ensures effective HR decision-making in terms of the increased job satisfaction without compromising the organization’s benefits, which avoids the knowledge and cost losses to the organization.

Employee turnover is the main reason for organization loss of productivity and profits. Organizations are under constant strain to maintain the level of productivity and provide the right environment and rewards to retain the employees. Employee behaviors are unpredictable, and their needs differ based on circumstances. So, the organization needs to evaluate different conditions to retain their talent in the organization.

## References

- [1] Anantha Raj A. Arokiasamy, “A Qualitative Study on Causes and Effects of Employee Turnover in the Private Sector in Malaysia”, Middle-East Journal of Scientific Research, Vol.16, No.11, pp.1532-1541,2013.
- [2] Radant, O., Colomo-Palacios, R. and Stantchev, V., “Factors for the management of scarce human resources and highly skilled employees in IT-departments: a systematic review”, Journal of Information Technology Research (JITR), Vol.9, No.1, pp.65-82, 2016.
- [3] Zhang, H., Xu, L., Cheng, X., Chao, K. and Zhao, X., “Analysis and prediction of employee turnover characteristics based on machine learning”, In IEEE 18th International Symposium on Communications and Information Technologies (ISCIT), pp.371-376, 2018.
- [4] Soni, U., Singh, N., Swami, Y. and Deshwal, P., “A Comparison Study between ANN and ANFIS for the Prediction of Employee Turnover in an Organization”, In IEEE International Conference on Computing, Power and Communication Technologies (GUCON), pp.203-206, 2018.
- [5] Alao, DABA and Adeyemo, AB, “Analyzing employee attrition using decision tree algorithms”, Computing, Information Systems, Development Informatics and Allied Research Journal, Vol.4, No.1, pp.17-28, 2013.
- [6] Wang, X., Wang, H., Wang, H., Zhang, L. and Cao, X. (2011), “Constructing a decision support system for management of employee turnover risk”, Information Technology and Management, Vol. 12 No. 2, pp. 187-196.

# **Measure Temperature & Humidity on Local Web Server for Home Automation System using NodeMCU ESP8266 Wi-Fi Module**

**GajendraSinh N. Mori and Priya R. Swaminarayan**

**Abstract** - Now a day IoT applications become new opportunity for all the domains like home automation, medical diagnosis, agriculture environment, transportation industries and so on and so forth where we can see use of many different IoT devices to measure and manage real time data and gets some insights from it that will be helpful for taking good business decisions. McKinsey Global Institute research and predicted that the IoT domain covered more than \$11.1 trillion market share by 2025. To see this prediction we have great options to dive deep into the IoT domain. In this paper, we measure temperature & humidity on local standalone web server for home automation using NodeMCU ESP8266 Wi-Fi Module that display real time data and additionally display corona case statistics that give latest updates of corona cases worldwide. This concept is inexpensive, efficient and preferable for any home automation. This system has three main components: an ESP8266 NodeMCU Wi-Fi Module, DHT11 Sensor and Standalone web server.

**Keywords** - Home Automation, ESP8266, NodeMCU Wi-Fi Module, DHT11 Sensor, Local Web Server, ESPAsyncTCP Library, ESPAsyncWebServer Library.

## **1. Introduction**

Today's IoT become leading domain for almost all the industries that gives easy and flexible life for human. IoT provides many applications for Home Automation where we can controlled electrical lights, AC, locks and other home appliances to enhanced safety and security of home and also IoT serves to other industries like medical, agriculture, transportation and so on and so forth where we can manage our devices and getting real time data that helps to find out some business insight for future use and take good business decisions. In today's technical world, smart devices likes smart phones, smart tv, smart refrigerators, smart washing machines and so on that involved in every aspect of people's daily lives also these devices are very much powerful for communication and interaction with each other [1].In this paper, we use DHT11 sensor and NodeMCU ESP8266 Wi-Fi module mainly for getting real time temperature and humidity data on local synchronous standalone web server that access using generated IP address also display corona cases statistics that give latest updates of corona cases worldwide. This system will assist and provide real time data of home that will support the needy people [2].

## **2. Related Works**

Internet of things (IoT) is the trending technology now a day that deals with the connection of the different heterogeneous devices and the software applications over the network. The important application of IoT is Home Automation [3]. Then in 2003 after improvement of network, K. Y. Lee and J. W. Choi suggest that a Smart Home become a unit where all the appliances can connect, communicate and monitored remotely [4]. This system enables many heterogeneous devices to be interoperable with different networks, many protocols and different technologies for example,

---

**GajendraSinh N. Mori**  
Email Address : [gajendranmori@gmail.com](mailto:gajendranmori@gmail.com)

**Priya R. Swaminarayan**

Bluetooth, WiFi, ZigBee, 6LowPAN and IEEE 802.15.4 [5]. The current idea helps us that microcontroller sensors is used to predict possibilities centred data rather than strictly tracking the device. As far as economy is concern, a single sensor known as DHT sensor is used by the proposed system for temperature and humidity readings also it used to create the authenticate framework of the climate database [6]. The innovation of the ESP8266 module contributes to the creation of robust and complete systems as opposed to the design methodology that developed the Arduino core under the hegemony of the ESP8266 Wi-Fi based on GitHub ESP8266 core website. This module is a platform for machine learning, incorporating between ESP8266 and NodeMCU[7]. The home automation system offers fast and immediate access of all the home appliances. The physically challenged and elderly people find it difficult to reach the switchboard to turn on and off the appliances. So, a voice-controlled home automation system can be useful for them to access the appliances by sitting in one place [5]. A smartphone for giving user commands by using the Google assistant and NodeMCU microcontroller, with Wi-Fi (ESP8266) connectivity to gain access and control the devices and appliances [8]. The sensor is directly connected with ESP 8266 controller with WiFi Module and Send data through the gateway via internet to the things speak. The things speak can get the signal from the sensor as variable along the value. After processing, controller will send a cooling or heating signal to the system [9]. In 2013, S. V. A. Syed Anwaarullah proposed inexpensive home automation system that monitoring using an Android device and the proposed system uses RESTful web services for communication between home automation system and home appliances [10].

### 3. System Architecture & Working Principles

In this part we will discuss brief idea about system architecture of proposed system like below “Fig. 1”, and how it works.

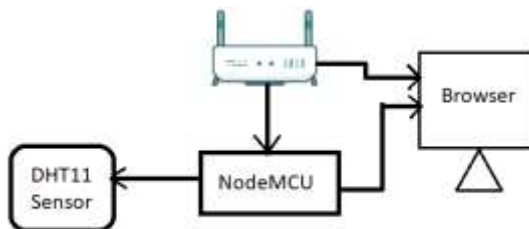


Fig. 1. System Architecture

The Above System Architecture mainly consist of NodeMCU ESP8266 Wi-Fi Module, DHT11 Sensor, and Local Web Server in any working PC with Wi-Fi connectivity, Follow below steps to know the flow of system.

- 1) Connect DHT11 Sensor with NodeMCU ESP8266 Wi-Fi Module using Jumper Wire.
- 2) Connect NodeMCU ESP8266 Wi-Fi Module with PC using USB to OTG cable.
- 3) After setup, NodeMCU and PC getting power from the electric port, DHT11 sensor sends temperature and humidity data to the NodeMCU and at last NodeMCU sends that data to the web server to display.

### 4. Hardware Descriptions

#### A. NodeMCU ESP8266 Wi-Fi Module

The NodeMCU ESP8266 is a microcontroller with inbuilt Wi-Fi connectivity features that developed by the Arduino Company. This module offers an additional Wi-Fi chipset that allows us to communicate through the GPIOs by connecting to the Internet and easily transmitting data over the Internet [11]. This module is used as a platform for machine learning environment. In below “Fig. 2”, we can see that this module operates with networks 802.11n and 802.11b category this means it can be easily used as an access point access point (AP) and Wi-Fi system or both together simultaneously [7].

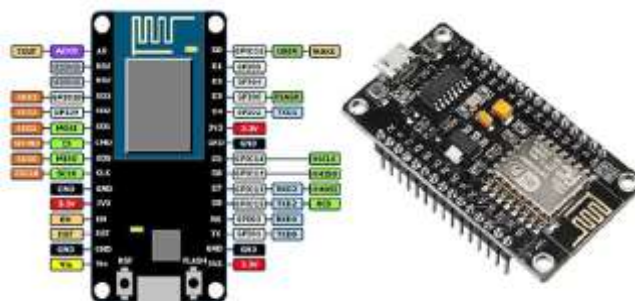


Fig. 2. NodeMCU ESP8266 Wi-Fi Module

### **B. DHT11 Temperature & Humidity Sensor**

DHT11 sensor is used to measure temperature and humidity in easy manners. It captures the value of temperature (T) and humidity (H) using optical signal. It comes with a dedicated Negative Temperature Coefficient (NTC) concept to measure the values of the temperature and humidity as serial data. It can measure temperature from 0 °C to 50 °C and humidity from range 20 % to 90 %. It offers easy installation, reliable quality, fast response, anti interference in terms of measurement and low cost [12] that we can see in below “Fig. 3”.

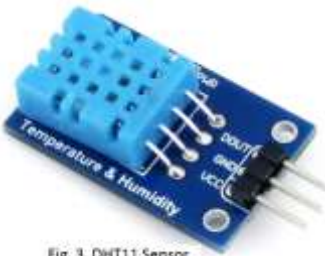


Fig. 3. DHT11 Sensor

## **5. Software Descriptions**

### **Arduino IDE.**

Node MCU ESP8266 has been programmed using the Arduino IDE. The DHT11 sensor sends temperature and humidity to the IDE also during execution it displays data on serial monitor of IDE. The main advantage of using NodeMCU ESP8266 is that once it is connected to the internet it can be controlled remotely from anywhere in the world by using its unique IP address. As far as data visualization is concerned we use local web server to display the temperature and humidity values. Also it shows latest statistics of corona case worldwide.

## **6. Implementation & Working**

To measure temperature and humidity for home automation environment we have to connect all required hardware such as DHT11 Sensor with NodeMCU ESP8266 Wi-Fi Module as per below mapping that mentioned below Then connect both with power supply. Provide Wi-Fi connectivity for both NodeMCU and PC respectively like below “Fig. 4”.

### **DHT11 to NodeMCU Connection Mapping**

VCC	to	3V3
Data Pin	to	D1(GPIO5)
GND	to	GND

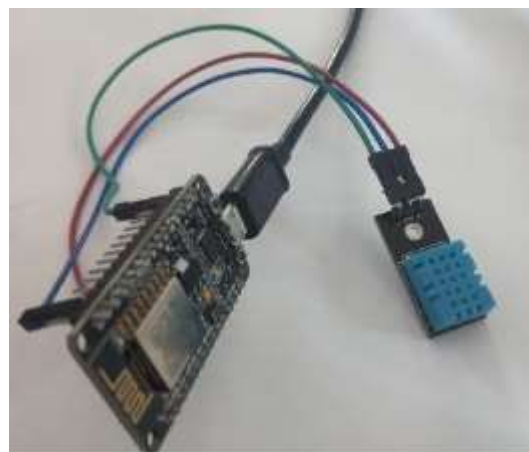


**Fig. 4. Schematic of Connection**

After design circuit, we need to write the code for it in Arduino IDE, for coding we will have include some libraries that are ESP8266WiFi, ESPAsyncTCP, ESPAsyncWebServer and Adafruit\_Sensor, after it set the Wi-Fi credentials, choose port number and write proper code in html with css for displaying temperature and humidity values on local host that will be display like below “Fig. 5”.

192.168.43.37

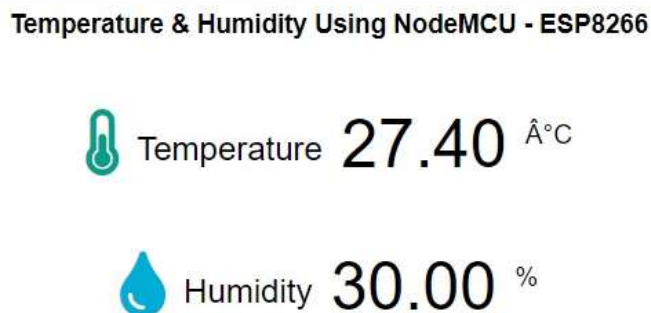


**Fig. 5. Display Temperature & Humidity Data**

## Conclusion

In this paper, we conclude that DHT11 sensor is so cheap and reliable to measure temperature and humidity, easy to install, NodeMCU ESP8266 Wi-Fi Module has inbuilt Wi-Fi cheep so no need to take extra effort for Wi-Fi connectivity. Using this system we can get latest data of temperature and humidity with auto refresh also it display current corona cases statistics worldwide. Overall, this work will helps to the needy peoples who wish to access home live data on the web server. As far as future enhancement is concern we can connect other different sensors like, smoke, radiation, leak gas and many more for home automation also we can store data in database for future use.

## Acknowledgments

I would like to express my gratitude to my Respected Guide, Dr. Priya R. Swaminarayan, who guided me throughout this research work. I would also like to thank my mother who always support and motivate me in right and ethical direction also wish to say thanks to all who directly or indirectly help and support me and offered deep insight into the study.

## **References**

- [1] Waheb a. jabbar 1,2, (senior member, ieee), Tee kok kian1 , Roshahliza m. ramli1 , (member, ieee), Siti nabila zubir1 , Nurthaqifah s. m. zamrizaman1 , Mohammed balfaqih 3,4, (member, ieee), Vladimir shepelev3 , and Sultan alharbi, Design and Fabrication of Smart Home With Internet of Things Enabled Automation System.
- [2] R. piyarel and S.R. Leel,"Smart Home-control and Monitoring System Using Smart Phone", Independent Computer Consultants Association 2013, ASTL vol.24,pp 83-86,2013.
- [3] Saurabh Singh, Harjeet Matharu and Dr. Sangeeta Mishra, "Internet Of Things (Iot) Based Home Automation System", November, 2017, DOI: 10.5281/zenodo.1049436.
- [4] K. Y. Lee, and J. W. Choi, "Remote-Controlled Home Automation System via Bluetooth Home Network" vol. 3, 2003, pp. 2824-2829.
- [5] Sabharwal, N., Kumar, R., Thakur, A., & Sharma, J. (2014). A Low-Cost Zigbee Basedautomatic Wireless Weather Station With Gui And Web Hosting Facility. International Journal of Electrical and Electronics Engineering.
- [6] Krishnamurthi, K., Thapa, S., Kothari, L., & Prakash, A. (2015). Arduino based weather monitoring system, International Journal of Engineering Research and General Science, 3(2), 452-458.
- [7] Sarmad Nozad Mahmood, Sameer Alani, Forat Falih Hasan, Mohammed Sulaiman Mustafa, ESP 8266 Node MCU Based Weather Monitoring System.
- [8] K. Loga Priya1, Mrs. S. Saranya2, Voice-Activated Home Automation using NodeMCU.
- [9] Khin Kyawt Kyawt Khaing, Temperature and Humidity Monitoring and Control System with Thing Speak.
- [10] Amar Pawar1 , Rahul Sharan 2 , Rahul Patil3 , Sandip Chavan 4."Home Automation using Bluetooth and IOT".
- [11] X. Bajrami, I. Murturi, An efficient approach to monitoring environmental conditions using a wireless sensor network and NodeMCU.
- [12] Mouser Electronics Homepage, <https://www.mouser.com/ds/2/758/DHT11> last accessed 2019/05/20.

# **INTERNET OF THINGS: ARCHITECTURE, ENABLING TECHNOLOGIES & PROTOCOLS, APPLICATIONS, CHALLENGES AND FUTURE SCOPE**

**Mahmood Hussain Mir, Sanjay Jamwal and Shahidul Islam**

**ABSTRACT:** Internet of Things is a recent and promising area of mobile and pervasive computing; mobility and pervasiveness are the two most important characteristics of a mobile and pervasive communication system. In technical terms, the Internet of Things can be referred as the Internet of Objects, or Object-Oriented Internetworking (OOI). It focuses on the fact that objects are connected over the Internet rather than people. IoT refers to the internetwork of daily objects, with some sort of intelligence. IoT is opening vast opportunities for many new applications areas that will change the livelihood of the people. During last decade, IoT is attracting more curiosity from researchers and industrialists around the globe. Internet of Things is a made up of two terms Internet and Things; Things refer to physical objects with any inbuilt communication technology such as Infrared, RFID, Bluetooth and Wi-Fi, etc. The Internet refers to the internetworking of objects through which objects are communicating with each other. This aim of this survey is to come up with through extensive survey on the main components such as architecture, enabling technologies and protocols, and applications of IoT. This survey is dedicated to those who want to add up to its development to this developing novel field in such ubiquitous scenario. Furthermore, some challenges, issues, and future scope are also discussed.

**Keywords-** IoT; Protocol; RFID; Sensor; WSN; Actuator; Transducer

## **1. Introduction**

IoT refers to a scenario in which network connectivity and computing capability go beyond the computers to smart devices such as objects, sensors and even everyday items, allowing them to generate, exchange, and consume data with no or less human intervention [1]. The term “Internet of Things” was coined by Peter Lewis in November 1985 at a U.S. Commerce Department conference [2]. After that Conference, the term IoT was not used until late 1990’s. Kevin Ashton of Proctor and Gamble (P&G) uses the Internet of Things later in his presentation in 1999 [3]. He later co-founded the Auto-ID Centre at the Massachusetts Institute of Technology (MIT). Ashton talked in-depth about IoT in RFID Journal in 2009. Ashton embedded IoT in the inventory systems (RFID devices) [4]. There is no general and common definition for IoT, The “Internet of Things” is a global concept and requires common definition. The ITU-T IoT-GSI (IoT Global Standards Initiative) team has formulated the following definition for the Internet

---

Mahmood Hussain Mir

Department of Computer Sciences, Baba Ghulam Shah Badshah University, Rajouri, Jammu and Kashmir  
India- 185234      Email Address : [mahmoodhussain@bgsbu.ac.in](mailto:mahmoodhussain@bgsbu.ac.in)

Sanjay Jamwal

Department of Computer Sciences, Baba Ghulam Shah Badshah University, Rajouri, Jammu and Kashmir  
India- 185234      Email Address : [sanjayjamwal@bgsbu.ac.in](mailto:sanjayjamwal@bgsbu.ac.in)

Shahidul Islam

Department of Computer Sciences, Baba Ghulam Shah Badshah University, Rajouri, Jammu and Kashmir  
India- 185234      Email Address : [shahidulislam@bgsbu.ac.in](mailto:shahidulislam@bgsbu.ac.in)

of Things: “A global infrastructure for the information society, enabling advanced services by interconnecting (physical and virtual) things based on existing and evolving interoperable information and communication technologies” [5]. The IERC definition states that IoT is: “A dynamic global network infrastructure with self-configuring capabilities based on standard and inter-operable communication protocols where physical and virtual “things” have identities, physical attributes, and virtual personalities and use intelligent interfaces, and are seamlessly integrated into the information network” [6].

ITU and IERC define the Internet of Things (IoT) as a dynamic and global network infrastructure with self-configuring capabilities based on standard Communication Technologies and Protocols [7]. IoT involves many technologies such as architecture, transducer (sensor/actuator), communication, identification (addressing) etc. IoT's basic idea is the pervasive presence of various things or objects with a Radio Access Network (RAN) such as Bluetooth, ZigBee, Wi-Fi with RFID tags [8]. RFID tags have a unique identification (unique address) through which objects or things can communicate and cooperate to achieve a common goal.

The number of IoT devices is large than the number of human beings on the planet in 2011, and by 2025, IoT devices are expected to be between 30 billion and 50 billion. There will be more than five other types of devices sold with native Internet connectivity [9].

According to industry analyst firm IDC, the IoT industry will grow to approximately 300 billion devices by 2025, which includes 30 billion connected devices. IDC sees this growth driven mostly by intelligent systems that will be installed and collecting data across both consumer and enterprise applications [10].

IoT can also be considered a global network, that allows the communication between human-to-human, human-to-things, and things-to-things, which is anything in the world by providing a unique identity to each object [11]. In technical terms, device-to-device, device-to-cloud connectivity, and device-to-gateway or interchangeably to anything, anyplace, anytime to anyone. Figure: 1 internet of things depicts the scenario of IoT.

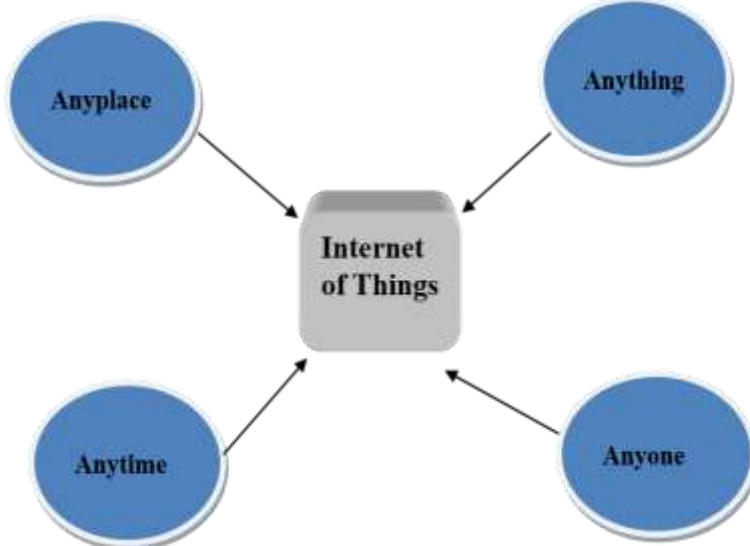


**Figure1. Internet of Things**

## 2. General Architecture

Internet of Things is a novel concept, so there is no standard architecture given by any standardization agency like IEEE, ITU-T, ETSI, IETF, CEN/ISO, GSI etc. Researchers, as well as Industrialists, are focusing on a layered architecture. In layered fashion, IoT mainly consists of three different layers [12]. Most of the IoT work is taken from a wireless sensor networks perspective. The layered architecture has two different divisions with a network or transport layer to serve the purpose of a common media for communication. The sensing layer is for data capturing and the application layer is the uppermost layer responsible for data utilization in applications [13].

Nowadays, the internet and the real world are relatively detached, and the communication between them mostly depends on the human-computer interface. Some applications are also automatically monitoring or controlling the environment objects in an intelligent way in the real world [14]. These intelligent applications can be assumed as the first attempt of IoT applications. The essential features of future IoT are internet of everything, internet of services and internet of networks. IoT is pervasive in nature every object is connected or sensed by ubiquitous sensors [15]. Conceptually, the architecture of IoT is divided into three basic layers. (i) Application Layer (ii) Transport or Network Layer (iii) Sensing or Perception Layer.

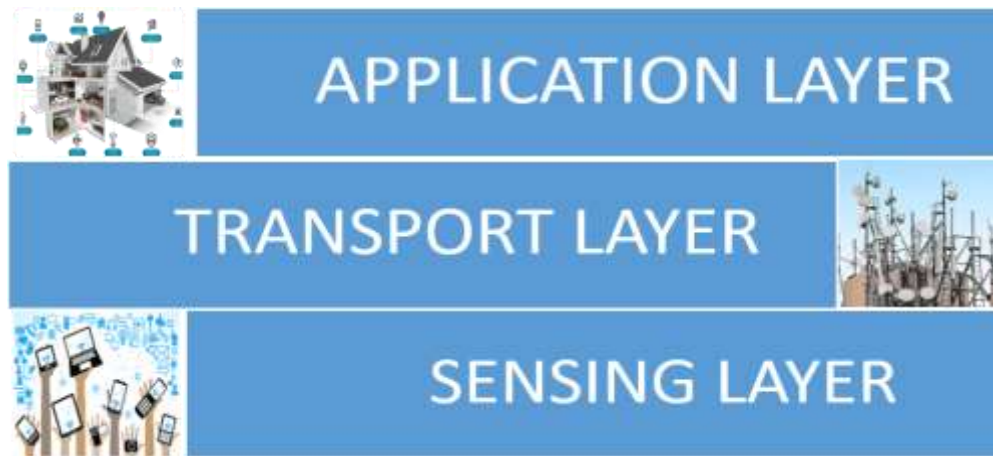


**Figure 2. General Architecture of IoT**

### 2.1 Sensing Layer

Sensing or Perception Layer resides at the bottom of all of the layers in a layered architecture. The sensing layer comprises physical devices and components with inbuilt communicating technology such as smart devices [16] (RFID, sensors, actuators etc.). The perception layer's main objective is to connect things into IoT network and measure, collect, and process the sensed information via deployed smart devices, transmitting the processed information into the upper layer via layer interfaces. There are predefined interfaces between these layers to communicate with each other [17]. Two types of interfaces are explained in this IoT architecture one is between Perception Layer and Transport layer and other is between Transport Layer and Application Layer.

### 2.2 Transport Layer

Transport or Network layer is a basic layer mainly associated with internet as in OSI reference model or in TCP/IP protocol suite [18]. This layer is responsible for transmission of data to and from the above and below layers. Transport Layer is implemented as the middle layer in IoT architecture. This is also called network layer as in TCP/IP network, and Internet are merged herein three-layer architecture network, transport and Internet layer are merged [19]. This is why IoT has adopted layered architecture so that layer can be added or merged easily. Transport layer receives the sensing layer's processed information and determines the routes and paths to transmit the data to the IoT hub, devices, and applications via integrated networks. Transport layer is responsible for routing data packets, which implies routing protocols are implemented in the transport layer. The transport or network layer is the main layer in IoT architecture, because various devices [20] (hub, switch's, gateway etc.), and various communication technologies (ZigBee, Bluetooth, Wi-Fi, 3G, 4G, Long-Term Evolution (LTE), etc.) [21] are merged in this layer. The transport or network layer has two different types of interfaces one is for communicating with layer below it and other is for layer above it. All the logic is implemented to communicate with different types of networks and devices using various communication technologies and protocols.

### 2.3 Application layer

The topmost layer of IoT layered architecture is the Application Layer. The application layer is also called as the business layer because whole logic is applied in this layer [22]. The application layer takes the data as input from the transport layer and uses it to fulfil the required services or operations. The work of an application layer is to provide services to the layer below it. These services are storage service to backup data into a database, or provide the analysis service to evaluate the received data for predicting the future state of physical devices [23]. The application layer receives the data from the layer below it and provides the services to the layer below it [24]. Only one interface is sandwiched with it in the application layer because it only communicates with the layer below it.

## 3. IoT Enabling Technologies and Protocols

Due to IoT devices heterogeneity with different technologies, different vendors have various technologies in the market. The integration of all the enabling technologies is necessary so that devices can communicate with each other. The IoT is a broadband network that uses standard communication

protocols [25]. Transducers (Sensor/Actuator) embedded in physical devices communicate through wired or wireless networks, usually using the same Internet Protocol (IP) that connects to the internet. IoT is not necessarily part of the real internet (local).

### **3.1 Transducer**

A device made up of hardware and software with inbuilt capabilities to convert one form of energy into another form of energy. Transducers may be of many types depending upon need. In IoT, there are two types of transducers, namely Sensor and Actuator [26]. Sensor: a device that converts a physical value to an electrical output, which implies converting sensed information into an electrical signal. Sensors are primary IoT devices with inbuilt communicating technology. Actuator: a device which converts an electrical signal into physical output, in other terms actuator takes input from the sensor (directly/indirectly) to do a physical change [27].

### **3.2 Radio-Frequency Identification (RFID)**

RFID tag is a key technology playing a important role in the field of the IoT. RFID tags are popular for automatically identifying anything and assigning a unique digital identity to each thing or object, to be deployed in the network and related to the digital information and service [28]. RFID tags are of two different versions: active and passive [29]. Passive RFID tags have no battery as they use the power of the reader's interrogation signal to communicate. The passive tags are used in many bank cards and road toll tags, and toll tags are first global deployments. Active RFID readers have an inbuilt battery and can initiate communication such as monitoring tags.

### **3.3 Wireless Sensor Network (WSN)**

WSN works as a network communication medium suitable for data transmission. Wireless Sensor Networks can coordinate with RFID systems to keep track the objects. WSN have many applications and can be used in many areas such as healthcare, government and environmental services and seismic sensing [30]. Furthermore, WSN could be merged with RFID systems to bridge physical and digital devices. They can achieve goals like obtaining information collecting the location, position, movement, temperature, etc. Today's most highly used Wireless Sensor Network is based on IEEE 802.15.4 standard [31] mainly meant for low power devices.

### **3.4 Addressing**

The way to uniquely recognize Things is though for the success of IoT. Addressing is only way by which billions of devices can be identifiable and can be controlled remotely by internet [32]. The most important advantages of uniquely addressing are reliability, uniqueness, scalability and persistence. Every object connected and those that are not connected so far must be identified location and functionalities uniquely. The current protocol IPv4 may not support this large set of objects individually but may identify a group as a single device [33]. The Internet Mobility features in the IPV6 may overcome some of the device identification problems; however, the heterogeneous nature of wireless nodes, different data types, parallel operations and the convergence of data from objects exacerbates the issue. IPv6's [34] addressing protocol scheme provides more address space than water drops in the sea. Some researchers have calculated that it could be as high as 1030 addresses per person. With IPv6, it is much simpler for an IoT device to obtain a global IP address, enabling efficient peer-to-peer communication.

IoT includes all types of connections i.e. device to device, device to person and person to person, which implies a extraordinary interconnection of people [35]. The existing drift in the IoT can similarly provide interconnection of objects and objects to establish smart environments. To this end, the capability of uniquely identifying objects is pivotal for favorable end result of the IoT. This is because uniquely addressing the large array of objects is vital for controlling them via the Internet. The mentioned uniqueness concept, reliability, scalability, and persistence denote the essential requirements to come up with a unique addressing scheme.

### **3.5 Protocols**

There are various protocols already available some of them can be deployed to the IoT devices, but some may not fit in this scenario. The protocol is a set of rules that are used generally for communication in

information and communication technology [36]. The communication in the scenario of IoT can of three types such as:

1. Device to Device (D2D or M2M): In IoT, devices can communicate with devices. Data-Distribution Service for real-time systems [37] (DDS) protocol is used for the purpose.
2. Device to Server (D2S): Data generated by IoT devices should be sent to the server, so need arises for a protocol that can do a task. Message Queuing Telemetry Transport [38] (MQTT) is a protocol which receives data from the device and communicates it with the server. Extensible Messaging and Presence Protocol [39] (XMPP) is also a protocol used to connect devices to people. It is a particular case in D2S pattern.
3. Server to Server (S2S): In IoT scenario, the server's also needed to share the device data with other servers. Advanced Message Queuing Protocol [40] (AMQP) is a protocol designed to connect servers, which implies it defines the standard for middle layer's communication.

#### **4. Summary of Findings**

After reviewing a lot of literature in the field Internet of Things, copious work has been carried out different researchers regarding architectures, applications, Communication Technology, Protocols. We have formulated a tabular form that summarizes the most prominent elements and protocols defined by these groups. The IoT elements are shown with sample and protocols divided into four broad categories: application protocols, service discovery protocols, infrastructure protocols and other influential protocols. Below is Table 1: IoT Elements and Protocols that have given a broad view of IoT architectural elements.

**TABLE 1: IoT Elements and Protocols**

<b>IoT Elements</b>		<b>Samples</b>	<b>Protocols</b>		
<b>Identification</b>	<b>Naming</b>	EPC, uCode	<b>Application Layer</b>	DDS, CoAP, AMQP, MQTT, MQTT-SN, XMPP, HTTP	
	<b>Addressing</b>	IPv4, IPv6			
<b>Sensing</b>		Smart Sensors, Wearables, Sensing devices, Embedded Devices, Sensors, Actuators, RFID tags	<b>Service Discovery</b>		mDNS, DNS-SD
<b>Communication</b>		RFID, NFC, UWB, Bluetooth, BLE, IEEE 802.15.4, Z-Wave, Wi-Fi, WiFiDirect, LTE-A	<b>Infrastructure Protocols</b>	<b>Routing Protocol</b>	RPL
				<b>Network Layer</b>	6LoWPAN, IPv4/IPv6
<b>Computation</b>	<b>Hardware</b>	Smart Things, Arduino, Phidgets, Intel Galileo, Raspberry Pi,		<b>Link Layer</b>	IEEE 802.15.4

		Gadgeteer, BeagleBone, Cubieboard, Smartphones			
	<b>Software</b>	OS (Contiki, TinyOS, LiteOS, RiotOS, Andriod) Cloud (Nimbits, Hadoop etc.)	<b>Physical/ Device Layer</b>	LTE-A, EPCglobal, IEEE 802.15.4, Z- Wave	
	<b>Service</b>	Identity-Related (shipping), Information Aggregation (smart grid), Collaborative- Aware (smart home), Ubiquitous (smart city)	<b>Influential Protocols</b>	IEEE 1888.3, IPSec, IEEE 1905.1	
	<b>Semantic</b>	RDF, OWL, EXI			

## 5. Potential Applications of IoT

The Potential of IoT makes it possible to think about developing a massive number of applications. From an enormous set of applications, only a little part is currently available to our public. There are many application domains and environments in which new IoT based applications would likely improve and ease in the way of our living. For instance, at home, while travelling, in the health sector, in the workplace, in the transport sector etc. The following papers have discussed most of the application areas of IoT [41][17][13][42]. These can be grouped but not limited to the following domains:

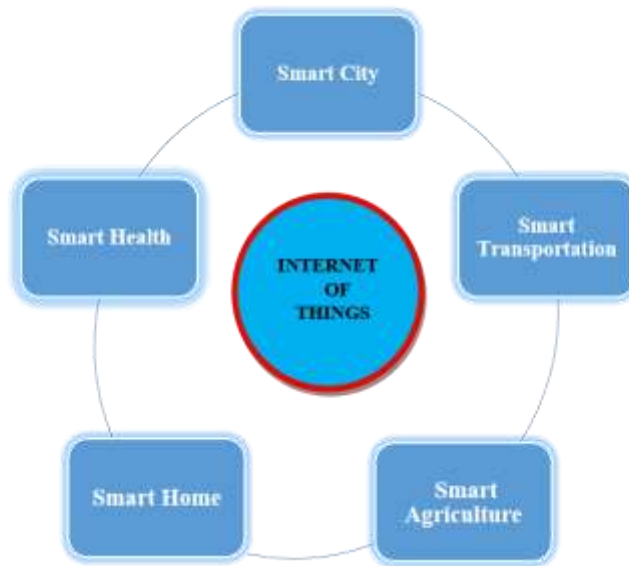


**Figure 3. Applications of IoT**

### **5.1 Smart Cities**

There is no formal and universally acceptable definition of “Smart City”. The mission and aim are to use public resources better and increase the quality of the services provided to the general public while decreasing the public's operational costs. It can be defined as a city that looks and integrates conditions of all of its main infrastructures, including roads, bridges, tunnels, rail/subways, and airports, to utilize its resources better while maximizing services to its citizens [43]. An urban IoT deployment can achieve the smart city's primary objective through a communication infrastructure that provides unique and simple access to a plethora of public services, increasing transparency to the citizens [44]. An urban IoT, indeed, may bring several benefits in optimization of conventional public services, such as transport and parking, lighting, surveillance and maintenance of public areas, preservation of cultural heritage, garbage collection, well-being of hospitals, and schools [45]. Many national governments have planned to adopt ICT solutions to manage public affairs, thus realizing the so-called Smart City concept. India had also come forward in June 2015, a programme launched by Prime Minister Narendra Modi to improve urban cities basic infrastructure [46]. Under this programme, each city will get 1,000 crores central government funding to develop its infrastructure.

### **5.2 Smart Transportation**

Internet of things (IoT) is transforming every field, and smart transportation is one of them. It is a network of connected vehicles, roadways etc. [47] through a wireless network. The intelligent transportation will reshape and automate the roadways, railways and airways. Smart transportation will also optimize cargo services and will create new business opportunities [48]. By implementing IoT in the vehicles, the more excellent safety, reliability can be achieved. Smart parking, vehicle tracking are other applications of the intelligent transportation system [49].

### **5.3 Smart Agriculture**

Most of the population depends on agriculture directly or indirectly. Due to population explosion, agricultural land is decreasing day by day. It is hard to feed the whole population using traditional ways in agriculture [50]. The new ways should be adopted so that production can be increased to provide food to the people. IoT is a promising technology which can be integrated with agriculture to make it smart. Smart agriculture uses the latest information communication tools to increase agricultural products' quality and quantity [51]. Various sensors are available like temperature, humidity, moisture, light, water etc. which can collect data and share it using WSN. Smart irrigation, smart farming, smart monitoring are sub-application domains of smart agriculture [52].

### **5.3 Smart Home**

The rise in information communication technology has given shape to many new domains. The smart home is one of them, in which all electronic devices like lights, AC's, fans, TV's etc. are controlled remotely by using smartphones or computers [53]. Appliances that are deployed in homes almost have at least any communication technology can qualify for smart devices. The radio access (RAN) such as Bluetooth, Wi-Fi, WiMax, 3G, 4G, LTE, 5G etc. [54] are primary building blocks for smart homes. In smart homes, sensors are deployed that sense the environment and share data with applications to respond accordingly [55]. In smart homes even doors and windows are opened using actuators. Smart energy, smart surveillance and smart lighting are sub-application areas of smart homes.

#### **5.4 Smart Health**

The IoT provides feasible solutions to many applications like traffic congestion, waste management, health and emergency services. IoT has redesigned the traditional healthcare system by deploying smart objects and devices everywhere [56]. Electronic health record (EHR) is readily available due to the introduction of technology. Remote health monitoring, elderly care, fitness programs are attractive application areas of smart health. IoT based healthcare setups are expected to reduce the costs, increase and enrich the user's experience. There are a lot of medical devices and sensors available in the market [57]. Temperature sensor, BP sensor, HR sensor, Oxygen saturation sensor etc. are some medical sensors used in patient monitoring. Many applications are available like google fit, health assistant, cardiax etc. available on smartphones [58].

### **6. Challenges and Issues**

The Internet of things (IoT) is the network of physical devices, vehicles, buildings, and other items set in with embedded hardware, software, sensors, actuators, and network connectivity which ultimately allow these things to collect and interchange data [59]. Moreover, it is one of the fast growing technology today and promises a great deal in bringing the virtual world together and making it a waking reality. Therefore, IoT systems can help businesses collect and analyse huge amounts of data that allows better and faster decision making, giving companies a competitive advantage.

However, there are some limitations to it as it presents security challenges in identity management and usability concerns. Other important limitations include privacy concerns, widespread cyber threats and unsolicited intrusions. Of note, privacy concerns are the most concerning issues. The information that is transferred becomes open access to the data collectors, government agencies and hackers. Quite often, personal information gets passed on to non-intended persons and might be misused and finally causes security breach. Moreover challenges and issues in IoT are discussed in [60][61][62][12][13].

### **7. Current Approaches and Future Directions**

The Internet of Things Security Foundation (IoTSF) came into existence on 23 September 2015 at the Digital Catapult in London [63] to take care of increasing concerns over security. To overcome this dangerous issue, network guards and firewalls have been used as network security devices and have been found to solve the issue to a greater extent. Others include, base device platform analysis, network traffic verification, verification of functional security requirements and end-to-end penetration test. However, no complete solution has been put forward so far, therefore, there is a need of competent solutions to privacy concerns. The novel approach to put end to most of the privacy concerns would be targeting encryption of data, network traffic data and end-to-end penetration test. Most of the future directions are elaborated in the articles [64][65][32][66]. IoT can apply any field and can integrate with machine learning, deep learning and artificial intelligence to provide better insights.

### **Conclusion**

This survey paper aims to give detailed view of IoT with the enabling technologies, architecture, applications, etc. In this paper, a latest literature was reviewed to investigate the whole about IoT that has been presented till date, including architectures, enabling technologies, characteristics and applications, issues and challenges, and future directions. Fast growing rate in smart devices, the need for future IoT network architecture arises. The existing network architectures cannot accommodate the current number of smart devices, as expected to be increasing in coming years. Need for new protocols arise as existing protocols are bulky and are taking much of the resources, and new trends of security mechanism should be adopted. This paper has presented application areas of IoT with its potential. IoT is still in infancy lot of

research is to done in this field to fully develop the IoT. Moreover, this paper has presented future scope and open research challenges of IoT. Internet of Things is a novel revolution in the field Internet technology & it has opened lot of new opportunities to researcher's industrialists in embedded, computer science & information technology area due to its very diverse area of application & heterogeneous mixture of various communications and embedded technology in its architecture.

## References

- [1] L. Atzori, A. Iera, and G. Morabito, "The Internet of Things: A survey," *Comput. Networks*, vol. 54, no. 15, pp. 2787–2805, 2010, doi: 10.1016/j.comnet.2010.05.010.
- [2] T. Ladd and O. Groth, "The internet of things," *Econ. (United Kingdom)*, vol. 411, no. 8964, 2015.
- [3] T. Pfeifer, "The Internet of Things - A White Paper," no. July, 2012, [Online]. Available: [http://www.tom-pfeifer.name/academic/publish/Internet\\_of\\_Things\\_White\\_paper\\_Pfeifer.pdf](http://www.tom-pfeifer.name/academic/publish/Internet_of_Things_White_paper_Pfeifer.pdf).
- [4] P. P. Ray, "A survey on Internet of Things architectures," *J. King Saud Univ. - Comput. Inf. Sci.*, vol. 30, no. 3, pp. 291–319, 2018, doi: 10.1016/j.jksuci.2016.10.003.
- [5] I. Of and S. Cities, "ITU-T," 2018.
- [6] S. Vermesan, O., Friess, P., Guillemin, P., Gusmeroli, *Europe's IoT Strategic Research Agenda 2012*, no. August. 2012.
- [7] CERP-IOT, "Internet of Things Strategic Research Roadmap - European Commission," *Aerospace Technol. Appl. Dual Use*, no. January, p. 9, 2008, [Online]. Available: [http://ec.europa.eu/information\\_society/policy/rfid/documents/in\\_cerp.pdf](http://ec.europa.eu/information_society/policy/rfid/documents/in_cerp.pdf).
- [8] V. Bhuvaneswari and R. Porkodi, "The internet of things (IOT) applications and communication enabling technology standards: An overview," *Proc. - 2014 Int. Conf. Intell. Comput. Appl. ICICA 2014*, no. March, pp. 324–329, 2014, doi: 10.1109/ICICA.2014.73.
- [9] A. Ivanov, "The internet of things," *IEEE Des. Test*, vol. 31, no. 3, pp. 4–5, 2014, doi: 10.1109/MDAT.2014.2335314.
- [10] "IoT End User Perceptions , Strategies and Preferences in Hungary," no. April, 2018.
- [11] S. Madakam, R. Ramaswamy, and S. Tripathi, "Internet of Things (IoT): A Literature Review," *J. Comput. Commun.*, vol. 03, no. 05, pp. 164–173, 2015, doi: 10.4236/jcc.2015.35021.
- [12] J. Lin, W. Yu, N. Zhang, X. Yang, H. Zhang, and W. Zhao, "A Survey on Internet of Things: Architecture, Enabling Technologies, Security and Privacy, and Applications," *IEEE Internet Things J.*, vol. 4, no. 5, pp. 1125–1142, 2017, doi: 10.1109/JIOT.2017.2683200.
- [13] K. Singh and D. D. Singh Tomar, "Architecture, enabling technologies, security and privacy, and applications of internet of things: A survey," *Proc. Int. Conf. I-SMAC (IoT Soc. Mobile, Anal. Cloud), I-SMAC 2018*, pp. 642–646, 2019, doi: 10.1109/I-SMAC.2018.8653708.
- [14] S. M. R. Islam, D. Kwak, M. H. Kabir, M. Hossain, and K. S. Kwak, "The internet of things for health care: A comprehensive survey," *IEEE Access*, vol. 3, pp. 678–708, 2015, doi: 10.1109/ACCESS.2015.2437951.
- [15] P. K. D. Pramanik, B. K. Upadhyaya, S. Pal, and T. Pal, *Internet of things, smart sensors, and pervasive systems: Enabling connected and pervasive healthcare*. Elsevier Inc., 2019.
- [16] J. Tervonen, M. Luimula, S. Pieskä, T. Pitkäaho, and J. Alaspää, "RFID and wireless sensor and actuator networks in advanced production applications," *Solid State Phenom.*, vol. 164, no. June, pp. 155–160, 2010, doi: 10.4028/www.scientific.net/SSP.164.155.
- [17] P. Sethi and S. R. Sarangi, "Internet of Things: Architectures, Protocols, and Applications," *J. Electr. Comput. Eng.*, vol. 2017, 2017, doi: 10.1155/2017/9324035.
- [18] A. H. Alhamedi, H. M. Aldosari, V. Snášel, and A. Abraham, "Internet of things communication reference model and traffic engineer system (TES)," *Adv. Intell. Syst. Comput.*, vol. 334, pp. 303–313, 2015, doi: 10.1007/978-3-319-13572-4\_25.
- [19] N. M. Kumar and P. K. Mallick, "The Internet of Things: Insights into the building blocks, component interactions, and architecture layers," *Procedia Comput. Sci.*, vol. 132, pp. 109–117, 2018, doi: 10.1016/j.procs.2018.05.170.
- [20] S. D. Kwelwa, "Please note : Changes made as a result of publishing processes such as copy-editing , formatting and page," pp. 1–5, 2018.
- [21] L. Garcia, J. M. Jiménez, M. Taha, and J. Lloret, "Wireless Technologies for IoT in Smart Cities," *Netw. Protoc. Algorithms*, vol. 10, no. 1, p. 23, 2018, doi: 10.5296/npa.v10i1.12798.
- [22] M. B. Yassein, M. Q. Shatnawi, and D. Al-Zoubi, "Application layer protocols for the Internet of Things: A survey," *Proc. - 2016 Int. Conf. Eng. MIS, ICEMIS 2016*, 2016, doi: 10.1109/ICEMIS.2016.7745303.
- [23] K. S. Mohamed, "The Era of Internet of Things," *Era Internet Things*, pp. 93–111, 2019, doi:

- 10.1007/978-3-030-18133-8.
- [24] L. Nastase, "Security in the Internet of Things: A Survey on Application Layer Protocols," *Proc. - 2017 21st Int. Conf. Control Syst. Comput. CSCS 2017*, no. July 2016, pp. 659–666, 2017, doi: 10.1109/CSCS.2017.101.
- [25] A. Al-Fuqaha, M. Guizani, M. Mohammadi, M. Aledhari, and M. Ayyash, "Internet of Things: A Survey on Enabling Technologies, Protocols, and Applications," *IEEE Commun. Surv. Tutorials*, vol. 17, no. 4, pp. 2347–2376, 2015, doi: 10.1109/COMST.2015.2444095.
- [26] SCME, "Introduction to Transducers, Sensors, and Actuators," *Southwest Cent. Microsystems Educ. Univ. New Mex.*, p. 4, 2014, [Online]. Available: [http://engtech.weebly.com/uploads/5/1/0/6/5106995/more\\_on\\_transducers\\_sensors\\_actuators.pdf](http://engtech.weebly.com/uploads/5/1/0/6/5106995/more_on_transducers_sensors_actuators.pdf).
- [27] V. T. Rathod, "A review of electric impedance matching techniques for piezoelectric sensors, actuators and transducers," *Electron.*, vol. 8, no. 2, 2019, doi: 10.3390/electronics8020169.
- [28] E. A. Kosmatos, N. D. Tselikas, and A. C. Boucouvalas, "Integrating RFIDs and Smart Objects into a Unified Internet of Things Architecture," *Adv. Internet Things*, vol. 01, no. 01, pp. 5–12, 2011, doi: 10.4236/ait.2011.11002.
- [29] P. Tan, H. Wu, P. Li, and H. Xu, "Teaching management system with applications of RFID and IoT technology," *Educ. Sci.*, vol. 8, no. 1, 2018, doi: 10.3390/educsci8010026.
- [30] H. Ghayvat, S. Mukhopadhyay, X. Gui, and N. Suryadevara, "WSN- and IOT-based smart homes and their extension to smart buildings," *Sensors (Switzerland)*, vol. 15, no. 5, pp. 10350–10379, 2015, doi: 10.3390/s150510350.
- [31] D. Dutta, *IEEE 802.15.4 as the MAC protocol for internet of things (IoT) applications for achieving QoS and energy efficiency*, vol. 31, no. June 2019. Springer Singapore, 2019.
- [32] J. Gubbi, R. Buyya, S. Marusic, and M. Palaniswami, "Internet of Things (IoT): A vision, architectural elements, and future directions," *Futur. Gener. Comput. Syst.*, vol. 29, no. 7, pp. 1645–1660, 2013, doi: 10.1016/j.future.2013.01.010.
- [33] B. M. Kumar Gandhi and M. Kameswara Rao, "A prototype for IoT based car parking management system for smart cities," *Indian J. Sci. Technol.*, vol. 9, no. 17, 2016, doi: 10.17485/ijst/2016/v9i17/92973.
- [34] T. Savolainen, J. Soininen, and B. Silverajan, "IPv6 addressing strategies for IoT," *IEEE Sens. J.*, vol. 13, no. 10, pp. 3511–3519, 2013, doi: 10.1109/JSEN.2013.2259691.
- [35] J. Gubbi, R. Buyya, and S. Marusic, "1207.0203," *Atmos. Environ.*, no. 1, pp. 1–19, 2013, doi: 10.1016/j.future.2013.01.010.
- [36] J. Tournier, F. Lesueur, F. Le Mouël, L. Guyon, and H. Ben-Hassine, "A survey of IoT protocols and their security issues through the lens of a generic IoT stack," *Internet of Things*, p. 100264, 2020, doi: 10.1016/j.iot.2020.100264.
- [37] J. Yang, K. Sandstrom, T. Nolte, and M. Behnam, "Data distribution service for industrial automation," *IEEE Int. Conf. Emerg. Technol. Fact. Autom. ETFA*, 2012, doi: 10.1109/ETFA.2012.6489544.
- [38] D. Soni and A. Makwana, "A survey on mqtt: a protocol of internet of things(IoT)," *Int. Conf. Telecommun. Power Anal. Comput. Tech. (Ictpact - 2017)*, no. April, pp. 0–5, 2017, [Online]. Available: [https://www.researchgate.net/publication/316018571\\_A\\_SURVEY\\_ON\\_MQTT\\_A\\_PROTOCOL\\_OF\\_INTERNET\\_OF\\_THINGSIOT](https://www.researchgate.net/publication/316018571_A_SURVEY_ON_MQTT_A_PROTOCOL_OF_INTERNET_OF_THINGSIOT).
- [39] B. H. Çorak, F. Y. Okay, M. Güzel, Ş. Murt, and S. Ozdemir, "Comparative Analysis of IoT Communication Protocols," *2018 Int. Symp. Networks, Comput. Commun. ISNCC 2018*, no. June, 2018, doi: 10.1109/ISNCC.2018.8530963.
- [40] N. Naik, "Choice of effective messaging protocols for IoT systems: MQTT, CoAP, AMQP and HTTPNaik, N. (2017). Choice of effective messaging protocols for IoT systems: MQTT, CoAP, AMQP and HTTP. In 2017 IEEE International Symposium on Systems Engineering, ISSE 2017 - , " *2017 IEEE Int. Symp. Syst. Eng. ISSE 2017 - Proc.*, pp. 1–7, 2017, [Online]. Available: <http://ieeexplore.ieee.org/document/8088251/>.
- [41] A. Al-Fuqaha, "AL-FA-Internet of Things: A Survey on Enabling Technologies, Protocols, and Applications," *IEEE Commun. Surv. Tutorials (Accepted Publ.)*, vol. 1, no. 2, pp. 78–95, 2013, doi: 10.5752/P.2316-9451.2013v1n2p78.
- [42] V. Hassija, V. Chamola, V. Saxena, D. Jain, P. Goyal, and B. Sikdar, "A Survey on IoT Security: Application Areas, Security Threats, and Solution Architectures," *IEEE Access*, vol. 7, pp. 82721–82743, 2019, doi: 10.1109/ACCESS.2019.2924045.
- [43] B. N. Mohapatra and P. P. Panda, "Machine learning applications to smart city," *Accent. Trans. Image Process. Comput. Vis.*, vol. 5, no. 14, pp. 1–6, 2019, doi: 10.19101/tipcv.2018.412004.
- [44] H. Arasteh *et al.*, "Iot-based smart cities: A survey," *EEEIC 2016 - Int. Conf. Environ. Electr.*

- Eng.*, no. May, 2016, doi: 10.1109/EEEIC.2016.7555867.
- [45] A. Zanella, N. Bui, A. Castellani, L. Vangelista, and M. Zorzi, "Internet of things for smart cities," *IEEE Internet Things J.*, vol. 1, no. 1, pp. 22–32, 2014, doi: 10.1109/JIOT.2014.2306328.
- [46] M. H. Mir and D. Ravindran, "Role of IoT in Smart City Applications : A Review," *Int. J. Adv. Res. Comput. Eng. Technol.*, vol. 6, no. 7, pp. 1099–1104, 2017.
- [47] S. T. Saarika P S, Sandhya K, "6Pduw 7Udqvsruwdwlrq 6\Vwhp Xvlqj ,R7," 978-1-5386-0569-1\$31.00 c?2017 IEEE, vol. 6, pp. 1104–1107, 2017.
- [48] Redhat, "Intelligent Systems for the Transportation Industry," *Technol. Overv.*, pp. 1–7, 2016, [Online]. Available: <https://www.redhat.com/cms/managed-files/iot-transportation-technology-overview-201608-en.pdf>.
- [49] S. Muthuramalingam, A. Bharathi, S. Rakesh kumar, N. Gayathri, R. Sathiyaraj, and B. Balamurugan, "Iot based intelligent transportation system (iot-its) for global perspective: a case study," *Intell. Syst. Ref. Libr.*, vol. 154, pp. 279–300, 2019, doi: 10.1007/978-3-030-04203-5\_13.
- [50] N. Gondchawar and R. S. Kawitkar, "IoT based smart agriculture," *Int. J. Adv. Res. Comput. Commun. Eng.*, vol. 5, no. 6, pp. 838–842, 2016, doi: 10.17148/IJARCCE.2016.56188.
- [51] C. Salim and N. Mitton, "Machine Learning Based Data Reduction in WSN for Smart Agriculture," *Adv. Intell. Syst. Comput.*, vol. 1151 AISC, pp. 127–138, 2020, doi: 10.1007/978-3-030-44041-1\_12.
- [52] L. Klerkx, E. Jakku, and P. Labarthe, "A review of social science on digital agriculture, smart farming and agriculture 4.0: New contributions and a future research agenda," *NJAS - Wageningen J. Life Sci.*, vol. 90–91, no. November, p. 100315, 2019, doi: 10.1016/j.njas.2019.100315.
- [53] O. Access, "We are IntechOpen , the world ' s leading publisher of Open Access books Built by scientists , for scientists TOP 1 % Smart Home Systems Based on Internet of Things," pp. 0–13.
- [54] M. Vaezi and Y. Zhang, "Radio Access Network Evolution," no. November, pp. 67–86, 2017, doi: 10.1007/978-3-319-54496-0\_6.
- [55] I. Machorro-Cano, G. Alor-Hernández, M. A. Paredes-Valverde, L. Rodríguez-Mazahua, J. L. Sánchez-Cervantes, and J. O. Olmedo-Aguirre, "HEMS-IoT: A big data and machine learning-based smart home system for energy saving," *Energies*, vol. 13, no. 5, 2020, doi: 10.3390/en13051097.
- [56] H. Ahmadi, G. Arji, L. Shahmoradi, R. Safdari, M. Nilashi, and M. Alizadeh, *The application of internet of things in healthcare: a systematic literature review and classification*, vol. 18, no. 4. Springer Berlin Heidelberg, 2019.
- [57] S. Tuli *et al.*, "Next generation technologies for smart healthcare: challenges, vision, model, trends and future directions," *Internet Technol. Lett.*, vol. 3, no. 2, p. e145, 2020, doi: 10.1002/itl2.145.
- [58] W. Li *et al.*, "A Comprehensive Survey on Machine Learning-Based Big Data Analytics for IoT-Enabled Smart Healthcare System," *Mob. Networks Appl.*, 2021, doi: 10.1007/s11036-020-01700-6.
- [59] Gartner, "Gartner Internet Of Things (iot)," <https://www.gartner.com/en/information-technology/glossary/internet-of-things>.
- [60] M. Hassanalieragh *et al.*, "Health Monitoring and Management Using Internet-of-Things (IoT) Sensing with Cloud-Based Processing: Opportunities and Challenges," *Proc. - 2015 IEEE Int. Conf. Serv. Comput. SCC 2015*, pp. 285–292, 2015, doi: 10.1109/SCC.2015.47.
- [61] I. Yaqoob *et al.*, "Internet of Things Architecture: Recent Advances, Taxonomy, Requirements, and Open Challenges," *IEEE Wirel. Commun.*, vol. 24, no. 3, pp. 10–16, 2017, doi: 10.1109/MWC.2017.1600421.
- [62] K. Patel and Keyur, "Internet of Things-IOT: Definition, Characteristics, Architecture, Enabling Technologies, Application & Future Challenges.,," *Univ. Iberoam. Ciudad México*, no. May, 2016.
- [63] IoTsf, "Internet of Things Security Foundation Set for Global Launch," <https://www.iotsecurityfoundation.org/donec-at-mauris-enim-duis-nisi-tellus/#:~:text=The%20Internet%20of%20Things%20Security,security%20excellence%20in%20IoT%20systems>.
- [64] K. Alieyan, A. Almomani, R. Abdullah, B. Almutairi, and M. Alauthman, "Botnet and Internet of Things (IoTs)," no. January, pp. 304–316, 2019, doi: 10.4018/978-1-5225-9742-1.ch013.
- [65] C. and F. D. Internet of Robotic Things: Current Technologies, Applications, "Internet of Robotic Things: Current Technologies, Applications, Challenges and Future Directions," 2021, [Online]. Available: <http://arxiv.org/abs/2101.06256>.
- [66] S. A. Kumar, T. Vealey, and H. Srivastava, "Security in internet of things: Challenges, solutions and future directions," *Proc. Annu. Hawaii Int. Conf. Syst. Sci.*, vol. 2016-March, pp. 5772–5781, 2016, doi: 10.1109/HICSS.2016.714.

# **IoT Based Remote Monitoring System for Quality Control of Drinking Water at Unmanned Water Stations**

**Tarun Ojha, Jayashri Vajpai and Vinit Mehta**

**Abstract** Water borne diseases are among the biggest problems of the developing countries all over the world. Water pollution is the largest cause of morbidity worldwide. This paper proposes a system for autonomous remote monitoring of Total Dissolved Solids (TDS), pH & temperature of water. This is expected to be very useful for both rural and urban unmanned drinking water stations. The main aim of this system is to assess and control quality of water using internet of things. The proposed system for monitoring the water quality operates through three sensors and includes microcontroller, LCD and Global System for Mobile (GSM) module. The microcontroller processes the data which is captured by using sensors. This data is collected in the adafruit MQTT cloud. If the water quality is not within permissible range, then an alert message is sent to control station using GSM module. Water quality monitoring systems need to quickly identify any changes in the quality of water and report the same to the officials for immediate action. The system is designed for continuous onsite sensing and real time reporting of water quality data where the officials can access this data on the smart phone/Computer through Internet.

**Keywords-** Water quality, Micro-controller (Arduino nano, NodeMCU), Temperature sensor, pH sensor, Total dissolved substance (TDS) sensor, Internet of things, GSM module.

## **1. Introduction**

The quality of drinking water affects the quality of human life loss of quality is associated not only with cleanliness but also with its mineral content. Its effect is visible in the form of electrolyte imbalance leading to neurological & neuro motor control disorders and even morphological malformation. These are rampant in all developing countries including the landlocked areas of our country. The population of western Rajasthan is greatly challenged due to high TDS & harmful chemicals, because the drinking water in these regions comes primarily from underground sources that are depleting and getting contaminated day by day. It is expected that the proposed monitoring system will ultimately lead to better quality control of drinking water in a variety of applications. These include not only urban facilities like commercial establishments, railways, offices etc.

Many factors affect the quality of available drinking water, such as the use of land (agriculture, forest, urban, etc.), the number of people living in a watershed, and the everyday behaviour of the population.

---

Tarun Ojha

Department of Electrical Engineering MBM Engineering College of Engineering  
Jodhpur, India

Email Address : tarunojha710@gmail.com

Jayashri Vajpai

Department of Electrical Engineering MBM Engineering College of Engineering  
Jodhpur, India  
Email Address : jvajpai@gmail.com

Vinit Mehta

Department of Electrical Engineering MBM Engineering College of Engineering  
Jodhpur, India  
Email Address : vinit741@gmail.com

The monitoring system proposed in this paper will continuously check the quality and temperature of drinking water for ensuring health of users.

Using three sensors, the system collects water quality parameter such as temperature, TDS and pH etc. The data collected from sensors is compared with the pre-set values. If the monitored data is not within the range, i.e. water is not suitable for drinking, the GSM module sends the alert message to the supervisor and at the same time operates buzzer and control relay.

This system is expected to be useful for remote monitoring the quality of drinking water. This system is automatic and operating staff can interact with the system easily. The size of the remote system is small enough to be useful for home appliances, office & commercial water stations. Multiple such system can be connected to the Central Control Station.

The major objectives for design and development of the proposed system are as follow:

1. To develop an automatic device for keeping a check on level of demineralization of water in offices, homes & other water stations.
2. To control the pH and TDS level of water within acceptable limit so as to avoid harmful impact of these.
3. To control temperature of water within range so that consumption of electricity can be reduced.
4. To transfer the measuring data to control station for automatic monitoring purpose.
5. To control the quality of water from the remote-control station and design an alarm and alert system for the same.

The proposed system employs multiple sensors to measure the parameters of quality of water in real-time for effective action, and is economical, accurate, and conserves manpower. In this paper section 2 presents literature survey on water quality monitoring while section 3 explains the proposed system. Section 4 discusses components needed for this system while section 5 discusses hardware design part of water quality monitoring system. Finally, the result obtained through the system are discussed in section 6. Section 7 concludes the project.

## 2. Literature Survey

Several researchers have proposed different models to check water quality by analyzing the parameters such as temperature, pH and TDS. But seldom do we find a complete quality control system.

N. R. Moparthi, Ch. Mukesh, P. V. Sagar [1] have developed “Water Quality Monitoring System Using IOT” for municipal water tanks and drinking water reservoirs. They used Arduino for finding pH value and GSM module to send message to control station. The IOT based smart water monitoring system proposed here can perform the monitoring of several parameter and sends the sensor data to the cloud for processing purpose and on the basis of these data conclude the quality of water.

P. Srivastava, M. Bajaj, A. S. Rana, [2] have developed “ESP8266 Wi-Fi module based Smart Irrigation System using IoT” they have proposed a system for efficient use of Internet of Things for agriculture. By employing pH sensor, water flow sensor, temperature sensor and soil moisture sensor and by evaluating data from sensors microcontroller to operate the servo motor and pump. Micro-controller collects information and transmit with ESP8266 WiFi module wirelessly to cloud by using internet. [2]

Shruti Sridharan, [3] has designed “Water Quality Monitoring System Using Zigbee Based Wireless Sensor Network”. In this paper they discussed about Zigbee based technology for wireless network. They choose ZigBee technology due to its features that fulfill the requirement for a low cost, easy to use, minimal power consumption and reliable data communication between sensor nodes. They have developed a graphical user interface for the monitoring purposes.[3]

Manish Kumar Jha, Rajni Kumari Sah, Rashmitha M. S., has designed “Smart Water Monitoring System for Real-time water quality and usage monitoring”. The objective of this paper is to design a Smart Water Quantity Meter to ensure water conservation by monitoring the amount of water consumed by a household, and notifying the same to the consumer and the authority. They used an online monitoring system to provide sensors data to the cloud in real-time.[4]

## 3. Proposed System

The proposed water quality monitoring system is illustrated in below figure 1. This system has three parts: data monitoring nodes, data comparison with predetermined range of values, transmission of

information. Three sensors have their own nodes which are dipped in water and collect the parameters such as pH, total dissolved solids and Temperature.

The analog data captured by all the sensors installed at water station will be sent to the microcontroller through, Analog to Digital converter. After processing the digital information in the micro controller based central monitoring system where analysis is done and the water quality is identified, these parameters are sent to the supervisor. The same will be displayed in the LCD display unit of the microcontroller and transmitted through the Wi-Fi module to the control station web page that linked with the microcontroller. The central monitoring system at the control station receives the measured value. Based on the received data, the supervisor will take necessary action for control of parameters. Alternatively, if the supervisor does not attend to the alert, the emergency control system at the control station will take over to switch off the system through the Wi Fi system.

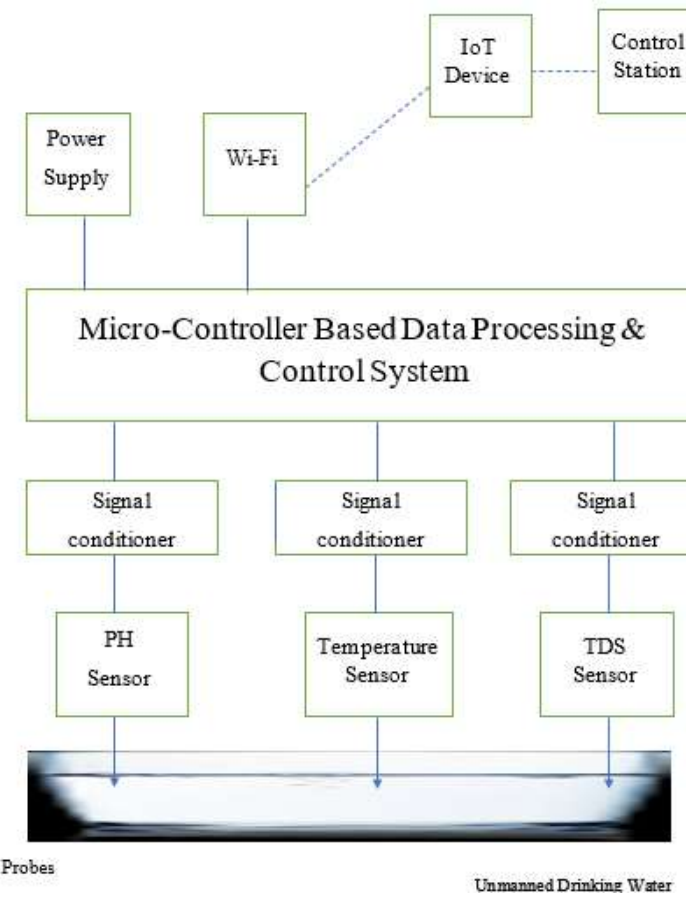


Fig. 1. Scheme of the Proposed System

#### **Alert System & Communication**

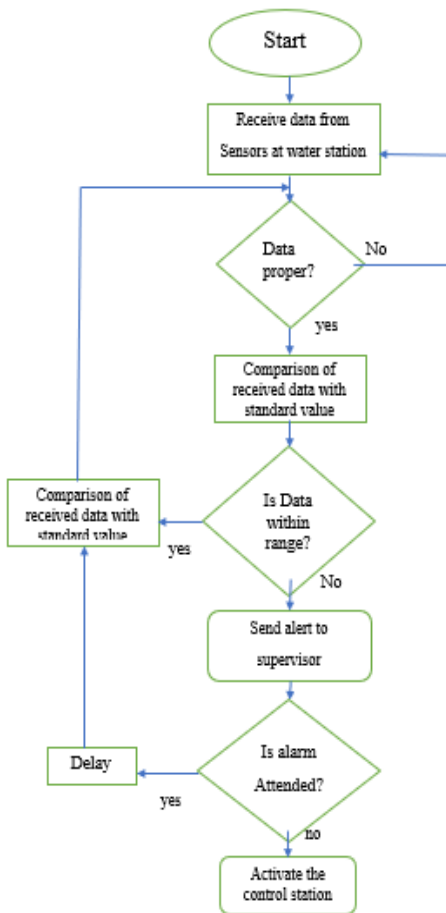


Fig. 2. Real time functioning of the Proposed System

After data is been measured, if any of the three parameters deviates from desired value, then microcontroller sends an alert command to supervisor. In addition to that particular parameter all other parameter values are also sent so that every little deflection in other sensor can also be supervised.

If the alarm is not attended by the supervisor, the alert message is also given to the control station. Figure 2 shows flow chart of the complete process.

#### 4. Component Description

The propose system can be divided into five categories on the basis of type of component used. These are Sensor unit, controller unit, Alert system unit, internet of things system, Angular concepts.

Brief discussion of the components of each of these categories along with their role and specification is given below

##### 4.1 Sensor Unit

The sensor is a device that measures the physical quantity (i.e. Heat, light, sound, etc.) into an easily readable signal (voltage, current etc.). It gives accurate readings after calibration. The sensors to be used in this project are as follow

###### 4.1.1 pH Sensor

The pH level of drinking water reflects how acidic it is. pH stands for “potential of hydrogen,” referring to the amount of hydrogen found in a substance. Generally, pH is measured on a scale that runs from 0 to 14. Seven is neutral, meaning there is a balance between acid and alkalinity. A measurement below 7 means acid is present and a measurement above 7 is basic (or alkaline). But here we used pH sensor for measuring pH of water which map the received voltages into related pH value.

#### Key Points

pH sensor used in this project is calibrated at 24°C (room temperature).

The calibrated Values are:

- pH4 = 1.5V
- pH7 = 1.2V
- pH9 = 2.5V

This is an Analog pH sensor kit and requires the  
Module Power: at DC 9.00V and has rating of 1A

Range: 0-14 pH

Analog output value from the sensor is in the range of 0.5V to 3V.

#### **4.1.2 TDS Sensor**

All elements dissolved in water have some electrical charge. Therefore, it is possible to estimate the quantity of total dissolved solids (TDS) by determining the electrical conductivity (EC) of the water by passing a small current through it.

TDS in parts per million (PPM) or milligrams per liter (mg/l) is calculated from the electrical conductivity of a fluid by multiplying EC reading with a conversion factor. EC is the inverse of the electrical resistance of the fluid between two probes measuring when the plug is submerged in the liquid of interest.

#### **4.1.3 Temperature Sensor**

The DS18B20 digital thermometer used for this project this is a water resistance temperature sensor which provides 9-bit to 12-bit Celsius temperature measurements. this sensor communicates over a 1-Wire bus so that here requires only one data line for communication with a microprocessor. the DS18B20 can derive power directly from the data line.

The major features of DS18B20 are as follows:

Sensor Tip Temperature Range: -67° F to 257° F (-55° C to +125° C)

Cable Temperature Range: -4° F to 185° F (-20° C to +85° C)

Accuracy: ±0.5° C (from -10° C to +85° C)

Type: Digital 1-Wire (Maxim Semiconductor DS18B20)

Rating: IP66 (Dust tight, water spray)

Extend cable length up to 600 feet in length (comes standard with 4 meters/12-foot cable)

2-inch-long Stainless-Steel probe

Weather resistance.

### **4.2 Controller Unit**

The controller unit integrates the data obtain from the sensors to estimates the quality of drinking water at the water station and communicates it to the central monitoring station and concerned authority. For this purpose, it is necessary to use two microcontrollers, one as NodeMCU and the other as remote terminal unit, as follows:

#### **4.2.1 ESP8266 NodeMCU**

The ESP8266 is the name of a micro controller designed by Espressif Systems. The ESP8266 itself is a self-contained WiFi networking solution offering as a bridge from existing micro controller to WiFi and is also capable of running self-contained applications. This module comes with a built in USB connector and a rich assortment of pin-outs, for connection to central processing unit. [5]

Figure 3 shows the basic structure of NodeMCU.



Fig. 3 Basic structure of NodeMCU

The major features of Node MCU ESP8266 are as follows:

- WIFI module: ESP-12E, Power supply: 5V, Logic level: 3.3V
- Processor: ESP8266, CP2102 chip
- Built-in Flash: 32Mbit
- Peripheral interface: UART/SPI/I2C/SDIO/GPIO/ADC/PWM
- WiFi protocol: IEEE 802.11 b/g/n
- Frequency range: 2.4G~2.5G(2400 M~2483.5M)

The major advantages of NodeMCU platform are

- Low cost
- Integrated support for WIFI network
- Reduced size of the board
- Low energy consumption

#### 4.2.2 Arduino Nano

Since there is a limitation of number of analog pins in NodeMCU so there is need for another microcontroller for collecting data from sensors. Arduino nano is used for this purpose.

It is a Microcontroller board developed by Arduino.cc and based on Atmega328. Arduino Nano is a small, compatible. It comes with exactly the same functionality as in Arduino UNO but quite in small size. It comes with an operating voltage of 5V, however, the input voltage can vary from 7 to 12V. Arduino Nano Pinout contains 14 digital pins, 8 analog Pins, 2 Reset Pins & 6 Power Pins. The analog pins come with a total resolution of 10bits which measure the value from zero to 5V. Arduino Nano operates with a crystal oscillator of frequency 16 MHz It is used to produce a clock of precise frequency using constant voltage. Flash memory is 16KB or 32KB that all depends on the Atmega board i.e. Atmega168 comes with 16KB of flash memory while Atmega328 is interfaced with flash memory of 32KB. Flash memory is used for storing code. The 2KB of memory out of total flash memory is used for a bootloader.

#### 4.3 Alert System Unit

If the parameters which determine water quality are not within predefined range then the alert devices operate. There are three alert devices connected to the system as follows:

##### 4.3.1 GSM Module SIM800L

SIM800L GSM/GPRS module is a miniature GSM modem, which can be integrated into the IoT projects module to send SMS text messages. At the heart of the module is a SIM800L GSM cellular chip from SimCom. The operating voltage of the chip is from 3.4V to 4.4V, which can be directly connected to the LiPo battery supply within small space. All the necessary data pins of SIM800L GSM chip are broken out to 0.1" pitch headers. This includes pins required for communication with a microcontroller over UART. The module supports baud rate from 1200bps to 115200bps with Auto-Baud detection.

#### **4.3.2 Relay (5V)**

An electromagnetic relay Leone SC5-S-DC5V is used to operate the pump motor circuit as the requirement

#### **4.3.3 Buzzer**

A magnetic buzzer, is used to produce sound by the movement of the ferromagnetic disk in a speaker. A magnetic buzzer is a current driven device, but the power source is typically a voltage.

### **4.4 Internet of Things System**

Internet of Things module links physical devices, i.e. sensors and actuators through the internet. The sensors will be allotted with an Internet Protocol address to gather and transfer the data over a system without physical help or involvement. The embedded technology used in the system makes all devices and sensors to work together from the water station.

The deployment of IoT system achieves deeper automation, analysis, and integration within this system. This IoT based system exploits recent advances in software, falling hardware prices, and modern attitudes towards technology.[6]

#### **4.4.1 Adafruit IO (Cloud)**

Adafruit IO is a platform designed to display, respond, and interact with our project's data. They also keep our data private (data feeds are private by default) for us. It's the internet of things - for everyone!

##### **Features**

Adafruit IO Displays the several parameters in real-time and provides internet connectivity so that user can control the process by observing collected data in easy way. Adafruit IO provides facility to Connect projects to web services like Twitter, RSS feeds, weather services, etc. and other internet-enabled devices without any need of payment.

### **4.5 Angular Concepts**

Angular is a platform and framework for building single-page client applications using HTML and TypeScript. Angular is written in TypeScript. It implements core and optional functionality as a set of TypeScript libraries that we import into our apps.

The architecture of an Angular application relies on certain fundamental concepts. The basic building blocks are NgModules, which provide a compilation context for components. NgModules collect related code into functional sets; an Angular app is defined by a set of NgModules. An app always has at least a root module that enables bootstrapping, and typically has many more feature modules. Angular framework components define views, which are sets of screen elements that Angular can choose among and modify according to your program logic and data. Its components use services, which provide specific functionality not directly related to views. Service providers can be injected into components as dependencies, making your code modular, reusable, and efficient.

## **5. System Architecture**

This project uses three sensors for collecting data, as shown in figure 4. These are connected to microprocessor NodeMCU and Arduino nano. The stability and regulation of Power supply plays an important role for operating the proposed system. Hence, voltage regulators IC 7805 provides power supply to microcontroller. SIM800L GSM module operates on 3.4V-4.4V. Hence, a buck converter is used for providing power supply to GSM module. Voltage regulator IC 7809 is used for supplying power to the PH sensor. Buzzer and relay are connected to NodeMCU which operates when alert signals are generated. NodeMCU contains an inbuilt wi-fi which sends collected sensor data to MQTT server.

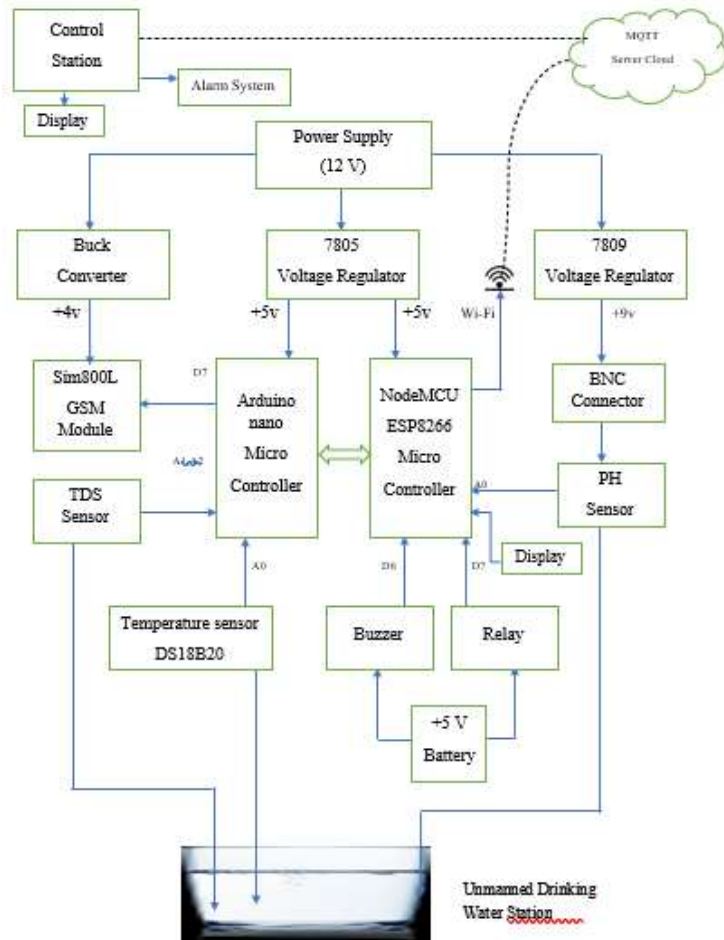


Fig. 4. Hardware Module

## 6. Results and Discussion

The proposed system for quality control of drinking water through remote monitoring was designed and implemented using hardware as shown in figure 5. The same was tested by placing it in a water cooler located at electrical department of MBM engineering college.

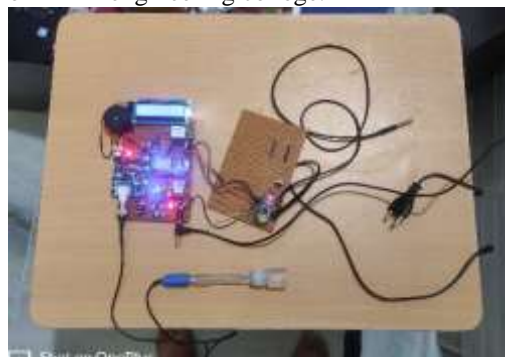


Fig 5. Hardware Module

Its performance was verified and it was observed that the sensors send correct data to the IoT cloud which further transfer to central control station by using angular framework of java script. the data received at the control station was also proper and followed the program designed for this purpose. On the basis of the observations, the assessment of quality water is carried out into four categories. These are

- Excellent

- Good
- fair
- Poor

The corresponding ranges of TDS and pH for these are given in table 1.

Table 1. Classification of data at control station are observed in a way given below

TDS Level of Drinking Water	pH Level of Drinking Water			
	PH<4 or PH>10	4=<PH<5 or 9<PH=<10	5=<PH<6.5 or 7.5<PH=<9	6.5=<PH=<7.5
TDS<300	Poor	Fair	Good	Excellent
300=<TDS<600	Poor	Fair	Good	Good
600=<TDS<900	Poor	Fair	Fair	Fair
TDS>=900	Poor	Poor	Poor	Poor

The testing results for some samples of data are shown in the following sub sections

### **6.1 Data at Cloud**

Fig 6 shows data sent by microcontroller at the Adafruit cloud. Three feeds named as Temp, pH1 and TDS have been created for saving sensor data.



Fig 6. Data at cloud

### **6.2 Alert Messages Sent to the User or Operator**

Figure 7 shows screen view of alert messages sent to the user and operator under the following situations:

If

1. Temperature >30 OR <22
2. PH >7.5 OR <6.5
3. TDS >800 OR <50

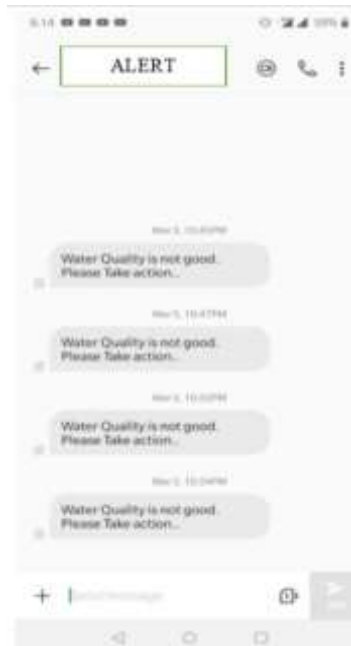


Fig. 7 Alert Message

### 6.3 Data at Control Station

The sensor data is classified according to table 1 and the quality of water is indicated at the control station as shown in figure 8.

Date	Time	pH	Temp	TDS	Quality
Jun 4, 2020	3:56:48 PM	7.15	19.81	223	Excellent
Jun 4, 2020	3:56:25 PM	7.27	19.81	223	Excellent
Jun 4, 2020	3:55:03 PM	7.22	19.75	221	Excellent
Jun 4, 2020	3:55:45 PM	6.85	19.78	221	Excellent
Jun 4, 2020	3:55:25 PM	7.19	19.63	222	Excellent
Jun 4, 2020	3:55:05 PM	7.28	19.56	223	Excellent
Jun 4, 2020	3:54:45 PM	6.98	19.58	223	Excellent
Jun 4, 2020	3:54:25 PM	6.95	19.44	223	Excellent
Jun 4, 2020	3:54:05 PM	6.96	19.37	225	Excellent
Jun 4, 2020	3:53:45 PM	7.06	19.25	224	Excellent
Jun 4, 2020	3:53:25 PM	7.07	19.28	226	Excellent
Jun 4, 2020	3:53:05 PM	7.08	19.37	226	Excellent

Fig. 8 Display of Result

This was verified with the help of ground truth and known quality parameters of sample waters. Hence it can be concluded that proposed and implemented system is working effectively to the satisfaction of the researchers.

## 7. Conclusion

IoT based remote monitoring system for quality control of drinking water system was designed and implemented in this paper. The Monitoring of pH, Temperature and level of Total dissolved solid in water IoT is based on transferring the unique advantage of remote monitoring to existing sensors-based quality control water supply system. This system is low in cost and does not require people on continuous duty at the water station. It also safeguards against the missing of alarms by the operating personnel. So, the water quality testing is likely to be more economical, convenient and fast. This system has good flexibility. Only by replacing the corresponding sensors and changing the relevant software programs, this system can be

used to monitor other water quality parameters such as. This system can be expanded to monitor hydrologic, air pollution, industrial and agricultural production and so on. It has widespread application and value.

## **Future Scope**

It is visualised that the following additions will be make the system even more useful in future.

- Display can be added to water station to give right to quality drinking water and right to information to whole users who depend on water supply by utility services.
- Modification for rural supply system by monitoring the more parameters such as turbidity.
- This project can also be used at hospitals or big organisations where large numbers of filters with water coolers are in use and require server-based monitoring for safeguarding all stakeholders.
- Machine learning technology can be added to this system for predicting the life of filters, motors used in water cooler.
- Fuzzy logic system can be added for making system more reliable.

## **Acknowledgment**

This project is funded by the technical education quality improvement program (TEQIP-III) under the scheme of student project. This paper and the research behind it would not have been possible without the exceptional support of Mr. Mani Ram (director at Sense Techno Solutions).

## **References**

- [ 1.] N. R. Moparthi, Ch. Mukesh, P. V. Sagar “Water Quality Monitoring System Using IOT” Fourth International Conference on Advances in Electrical, Electronics, Information, Communication and Bioinformatics (AEEICB) Page s: 1 - 5 Feb 2018
- [ 2.] P. Srivastava, M. Bajaj, A. S. Rana, “Overview of ESP8266 Wi-Fi module based Smart Irrigation System using IoT” Fourth International Conference on Advances in Electrical, Electronics, Information, Communication and Bio-Informatics (AEEICB) Page s: 1 - 5 Feb 2018.
- [ 3.] Shruti Sridharan, “Water Quality Monitoring System Using Zigbee Based Wireless Sensor Network” JEST-M, Vol 3, Issue 2, July-2014
- [ 4.] Manish Kumar Jha, Rajni Kumari Sah, Rashmitha M. S., has designed “Smart Water Monitoring System for Real-time water quality and usage monitoring”, Proceedings of the International Conference on Inventive Research in Computing Applications (ICIRCA 2018). IEEE Xplore Compliant Part Number:CFP18N67-ART; ISBN:978-1-5386-2456-2
- [ 5.] Sandy Suryo Prayogo, Yulisdin Mukhlis, Bayu Kumoro Yakti, “The Use and Performance of MQTT and CoAP as Internet of Things Application Protocol using NodeMCU ESP8266” 2019 Fourth International Conference on Informatics and Computing (ICIC), 16-17 Oct. 2019.
- [ 6.] O. Vermesan and F. Peter, "Internet of Things: Converging Technologies for Smart Environment and Integrated Ecosystems," in River Publisher. ISBN 978-87-92982-96-4, Denmark, 2013.
- [ 7.] Ravi Kishore Kodali, Sasweth C.Rajanarayanan, Naga Raja Sai Ashish Peddada, “IoT based Consumer-Centric Packaged Drinking Water Quality Monitoring System” , 2018 Tenth International Conference on Advanced Computing (ICoAC), 13-15 Dec. 2018.

# DESIGN OF COHERENT DIGITAL RECEIVER

Jainendra Kumar and Sanjeev Kumar

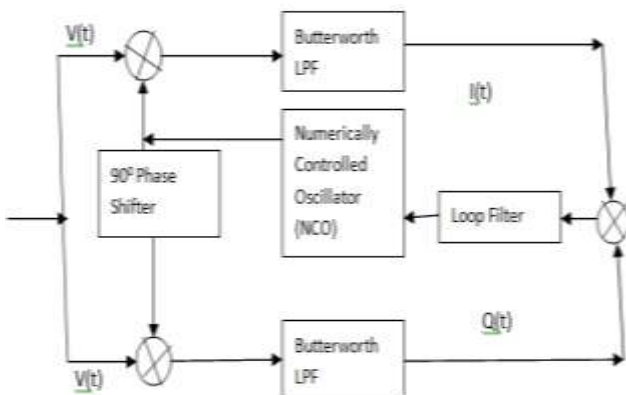
**Abstract** Digital demodulator is the one of the major functional blocks in the design of digital communication system. The Design of demodulator involves numerous design complexities to detect the original data in the channel. The major challenges in the design are phase error, efficiency, area & power consumption. So this paper have some parameters improvement, which is based on the analysis of the speed, synchronization, efficiency based on the in this research paper, it represent a solution to the saving of chip area, which depends on simulation. For synchronous recovery of binary phase shift keying signal. The design which is proposed having aim to saving of area with the ordinary Costas receiver. The modified receiver is suitable for saving of area, very efficient which result the ending of angle equivocal. The simulation results show that the proposed design can reduced phase error, area & power consumption and improve efficiency.

**Keywords-** BPSK, Costas loop receiver, Simulink, Phase ambiguity.

## 1. Introduction

The Costas receiver is a phase locked loop based circuit which is used for carrier frequency recovery from binary phase modulation signal, such as BPSK and QPSK. At small deviation the Costas receiver loop error voltages is twice the sinusoidal as compared to half of twice of sinusoidal. This translates to double the sensitivity and also makes the Costas receiver loop. Uniquely switched for tracking Doppler shifted carrier especially in OFDM and GPS receivers. In this paper, SIMULINK model of proposed Costas loop is presented. So the result of simulation are received and characteristics of receiver can be changed as per the model. In this network every block of the diagram having knowledge based on the carrier recovery, which is having meaningful task [3].

## 2. Carrier Recovery in Costas Receiver



---

Jainendra Kumar,  
PhD Scholar, EEE Department, SITE, SVSU Meerut, India-250005

Email Address : jk1229ster@gmail.com

Sanjeev Kumar  
Associate Professor, EEE Department, SITE, SVSU, Meerut, India-250005

The classical Costas receiver eliminates the phase information is shown in the Fig. 1. In this system, two coherent detectors, each of these detectors is supplied by in coming signal. Since binary phase shift keying does not have carry in its own, so we have to generate this local oscillator at the receiver side. This diagram of receiver is very powerful tools for the synchronization of the receiving signals without any phase ambiguity. Signal coming from the outside have same phase and frequency available within voltage control oscillators, which the main block for the synchronous receiver. In the above block diagram, the incoming voltage signal is divided into two paths, in the path they find demodulators or synchronous detectors, which receive the signal and extract the necessary information from those incoming signals. After extracting the information, the signal is then passed to the low pass filter which then passes only the low signal and blocks the high frequency signals. After this process, the incoming signal is fed to the summing point which then adds these voltages and fed to the loop filter. The function of loop filter is to serve the purpose and send the signal to the numerically controlled oscillator [4-5].

In the first rotation which is known as the in-phase arm, work accurately as in phase locked loop and was very efficient too in this circuit, the second arm i.e., quadrature phase arm, in this case a 90-degree phase shift is obtained in the voltage-controlled oscillator [6]. The in-phase arm and quadrature phase arm mixers having filtered output by low pass filter. So, the output of in phase and quadrature phase multiplied together and the loop filter get the differences or error [7].

### 3. PROPOSED COSTAS LOOP

The Proposed Model is developed with the help of Simulink. In this proposed model, a block diagram, for proposed Costas receiver for carrier recovery has been given in Fig. 2. The Random Number, give designated block generates normally, distributed random numbers, that is fed to FIR Interpolator. In this case, FIR Interpolation block, resamples, discrete time taken input at rate L times growing faster than, input sample rate, in which the integer L, specified by Interpolation factor, parameter. The FIR Interpolator has function as scope of, interpolated output, the discrete time eye diagram, and scope having modulated input.

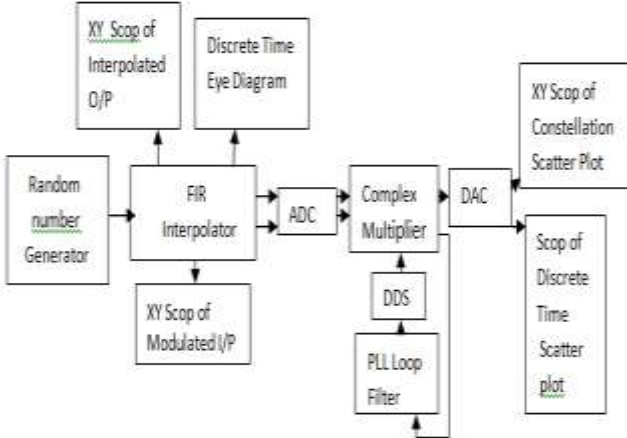


Fig. 2: Modified design of Costas loop

The function, of this scope of interpolated response is useful of examining; limit cycles their and other two-state data. Data outside this specified range are not displayed. So, discrete time, eye diagram Scope design block displays multiple and repetitive traces of modulated signal for produce this eye diagram. The Discrete Time, Eye Diagram design Scope block have one input port. The block accepts, signal of type, which are of double, single, Boolean or base integer, and also fixed-point data type of forgiven input, but we will cast it as double. The FIR Interpolator signal has been fed to analog to digital converter (ADC) for convert it into digital form, which is sent for the complex multiplier this design which passes real or imaginary signal in this the DAC and PLL receiver filter. In the direct digital synthesizer or it can be called as (DDS) synthesize, digital signal and it give to complex multiplier, where both the ADC and the DDS signal combined it and give this to DAC, which gives, in phase and Quadrature from phase output from constellation, scatter plot with discrete time, having scatter plot. This proposed Costas receiver gives minimum error, good and efficient synchronization and also

used it for few logic elements in circuits. In new design, the multipliers have been replaced with multiplexers, thus that avoid doing multiplication.

#### 4. SIMULATED OUTPUT RESULTS

The Developed Model is simulated by the help of Simulink. The Simulated results, from this proposed design is described in this below sections.

##### A. Modulated excitation/Input

In this XY plot that measures, values between X-axis and with Y-axis.

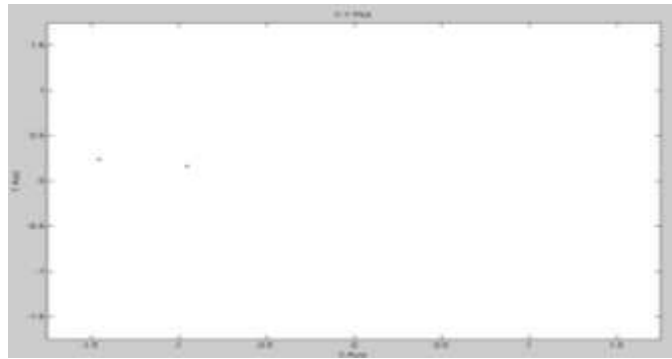


Figure 3: Modulated input

In this value of after modulation, the range of value on this x-axis, vary from different values of modulated excitation. The y-axis is having the same range, of different values. In figure 3, the value, of modulated excitation/input has more the x-axis on y-axis.

##### B. Eye Diagram Scattering

In this Eye diagram, the graph between, In-phase and time and Quadrature with time. In this case, Inter Symbol Interference (ISI) will affect the signal maximum/mostly, at In-phase condition. Figure shows below in fig. 4, more is the eye has been opening in this figure; less will, the affects, of ISI on this signal performance.

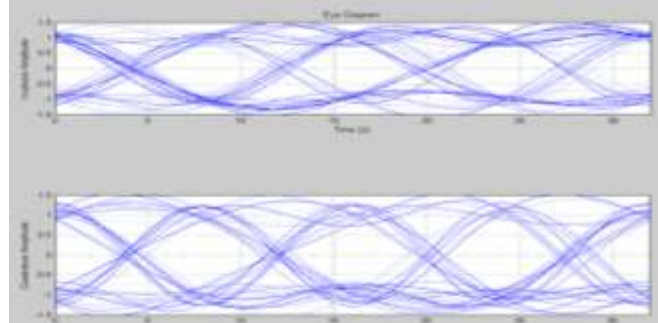


Figure 4: Eye diagram Scattering

##### C. XY Scope with Constellation Scatter plot having different values of different6 values

In this plot, values of response, will be exactly calculated between, x-axis and the y-axis in XY plot. In this, being the plot Y axis, it has minimum value, while on the x-axis which is corresponds to minimum, and maximum different values as in fig. 5.

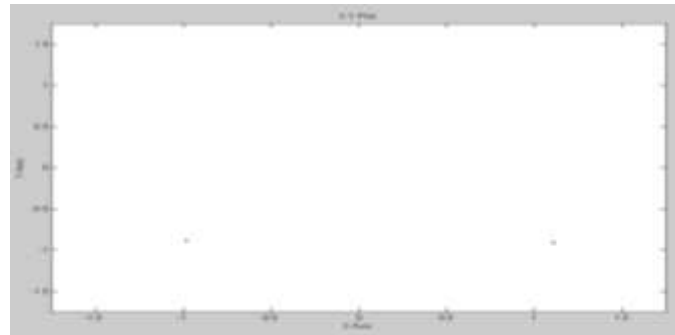


Fig. 5: XY Scope having different values with Constellation Scatter plot

#### D. Scope having different values of Discrete time with Scatter plot

In this Scope having Discrete time with Scatter plot is calculated and measured between In phase, amplitude with Quadrature amplitude, that by which shows different symmetrical response of both the in phase, amplitude with and Quadrature amplitude as given in fig. 6.

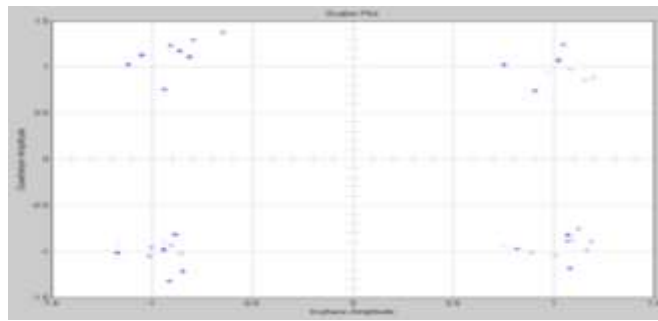


Figure 6: Scope with values having discrete time scattering variable plot

#### E. Scope with different Interpolated output

In this output, it is block, having two scalar inputs. So output block having different plots data with first input (in x direction) versus data with second input (in y direction).

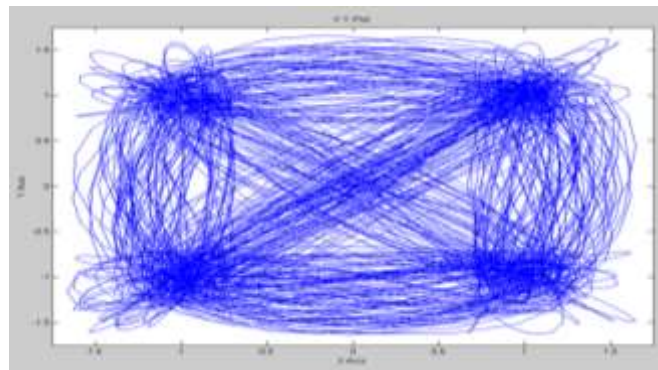


Fig. 7: Scope having different values with Interpolated output

In this parameter/block, it is useful for different examining various limit cycles. So, in this response or output block having the symmetrical values about both, the axis.i.e. x-axis and with y-axis with having with same values, in the x-axis and with y-axis as in figure. 7.

## 4. Results

The modified and achieved structure, is greatly decreases about the resource utilization and consumption with the thermal power utilization/dissipation. In Table I a lists shown the comparison with the ordinary Costas receiver with the modified receiver.

TABLE I: COMPARISON OF DIFFERENT PERFORMANCE

	Area (Logic Elements)	Multiplier having different input and output
Typical and ordinary Costas Loop receiver	106	0
Modified and digital Costas Loop receiver	67	0

From the results obtained from above table, it is found that digital and modified structure minimizes and reduces approximately 39%, of logic elements (LEs). So, Digital receiver needs not with any embedded different multipliers. Besides, this performance with the advanced Costas receiver is highly improved. Finally, the desired results of digital Costas receiver are acquired with the hardware tests.

## Conclusion

The ordinary/modified Costas receiver and digital/improved digital Costas receiver with carrier recovery is implemented and proved for realize on synchronization that is the most complex target/tasks in these digital communication systems.

## Acknowledgments

The Author is thankful to DR. Sanjeev Kumar, Asso. Professor & Head, EEE Department, Subharti Institute of Technology and Engineering, Swami Vivekanand Subharti University, Meerut(UP) and Prof. (Dr.) Manoj Kapil, Principal, Subharti Institute of Technology and Engineering, Swami Vivekanand Subharti University, Meerut (U.P), for providing necessary and required support with guidance during this research work.

## References

- [1] Yao Liu and Wouter A. Serdijn, "Analysis and Design of a Passive Receiver Front-End Using an Inductive Antenna Impedance," IEEE transactions on circuits and systems—I: regular papers, vol. 65, no. 2, pp. 733-744, IEEE, 2018.
- [2] Jose Krause Perin, Anujit Shastri and Joseph M. Kahn "Design of Low Power DSP Free Coherent Receivers for Data Center Links," Journal of lightwave technology, vol. 35, no. 21, pp. 4650-4662, 2017.
- [3] Masafumi Koga, Yusuke Shigeta, Futoshi Shirazawa, Hiroshi Ohta and Akira "Costas Loop Homodyne Detection for 20-Gb/s QPSK Signal on the Optical Frequency Synchronous Network," Journal of lightwave technology, vol. 33, no. 23, pp. 4752-4760, 2015.
- [4] J. Treuttel, L. Gatilova, A. Maestrini et al., "A 520–620-GHz, Schottky Receiver Front End for Planetary Science and Remote Sensing With 1070 K–1500 K DSB Noise Temperature at Room Temperature," IEEE transactions on terahertz science and technology, vol. 6, no. 1, pp. 148-155, 2016.

- [5] Janilson Leao de Souzaa and Karlo Queiroz da Costa, "Broadband Wireless Optical Nanolink Composed by Dipole Loop Nanoantennas," IEEE Photonics Journal, vol. 10, no. 2 pp. 107-111, 2018.
- [6] Hyunwoo Cho, Hyungwoo Lee, Joonsung Bae et al, "A 5.2 mW IEEE 802.15.6 HBC Standard Compatible Transceiver With Power Efficient Delay Locked-Loop Based BPSK Demodulator," IEEE Journal of solid-state circuits, vol. 5, no. 11 pp. 1-11, 2015.
- [7] Masafumi Koga and Akira Mizutori, "Decision-Directed Costas Loop Stable Homodyne Detection for 10-Gb/s BPSK Signal Transmission," IEEE photonics technology letters, vol. 26, no. 4, pp 319-322, 2014.
- [8] Serkan yakut. "The Phase Locked Loop and Costas Loop," International Journal of Contemporary Research and Review, vol. 08, no. 11, pp. 20347- 20351, 2017.
- [9] Liu Zhi, Jiang Zhou, Li Qing and Zeng Xiaoyang, "Efficient Carrier Recovery for High Order QAM," International Conference on Consumer Electronics, pp.1-2, January, IEEE, 2014.
- [10] Alireza Razavi and Dennis M. Akos, "Carrier Loop Architectures for Tracking Weak GPS Signals," IEEE Transactions on Aerospace and Electronic System, Vol. 44, No. 2, pp. 697-710, 2013.

# **Transfer Learning based Feature Fusion Approach for Handwritten Digits Recognition of Devanagari Script**

**Danveer Rajpal and Akhil Ranjan Garg**

**Abstract** Recognizing handwritten alphabets is the field of greater interest for data scientists for a long due to its important role in the automation of various prime services like the postal, judiciary, banking, and academic services. These services demand a robust system for handwritten alphabet recognition due to the huge variation in the writing styles of individuals. The proposed scheme exploits feature extraction capabilities of pre-trained Deep Convolutional Models (DCM) namely DenseNet-121 and ResNet-50, by implementing a transfer learning approach for handwritten digits recognition of Devanagari script. The features collected from these models include minute detailing of given pattern; but suffer from feature redundancy and co-linearity. The proposed model takes the advantage of the Principal Component Analysis (PCA) method to handle these problems effectively. Proposed model is also tested for the features developed by fusion of attributes collected from respective pre-trained models for given handwritten digits. Multi-layer perceptron neural network is used for recognition tasks due to its ability to classify non-linearly separable data. The model has achieved 94.4% recognition-accuracy with feature-vector size of just 20.

**Keywords-** Co-linearity, DenseNet-121, Devanagari script, Feature redundancy, PCA, ResNet-50, Transfer learning. .

## **1. Introduction**

The pattern recognition task becomes more interesting due to the rapid development of Machine Learning (ML) and Deep Learning (DL) algorithms and tools. The proposed scheme is a step in the same direction. The scheme is introducing a transfer learning-based feature fusion approach for the recognition of handwritten Devanagari numerals. The Digit set of the script is given in Fig. 1.1. Devanagari script is selected specifically to support the self-reliant program of the nation India in the field of ML and DL. The scheme utilizes pre-trained DCM; DenseNet-121 and ResNet-50 due to their ability of fine features extraction. The features so obtained are redundant due to co-linearity between them. The PCA method is used to determine the degree of relatedness among the features and to produce new features which will be non-co-linear in nature. The scheme is also experimenting with fusion of features gathered from respective pre-trained models. MLP network is used for digit recognition.



**Fig. 1.1 . Digit set of Devanagari script.**

The following sections will include preliminary, related work, methodology, results & discussions, conclusion and references.

---

Danveer Rajpal  
Electrical Engineering Department, MBM Engineering College, Jai Narain Vyas University Jodhpur, India  
Email Address : danveer.rajpal@rediffmail.com

Akhil Ranjan Garg  
Electrical Engineering Department, MBM Engineering College, Jai Narain Vyas University Jodhpur, India  
e-mail: agarg@jnvu.edu.in

## 2. Preliminary

This section covers a brief theoretical base of pre-trained models and techniques used in the proposed work.

### 2.1 DenseNet-121

Since each layer of DenseNet is directly associated with every other layer of the network, it is named as a Densely connected neural network. For  $N$  number of layers, there exist  $N(N+1)/2$  direct connections. The input of each layer consists of feature maps produced by all the previous layers. This type of architecture makes the DenseNet immensely powerful [1]. DenseNet-121 carries four dense convolutional blocks with 6, 12, 24, and 16 convolutional layers respectively. The other types of layers are pooling, transition, and classification. The network effectively handles the vanishing gradient effect, minimizing the number of parameters, improving feature propagation.

### 2.2 ResNet-50

It is a 50-layer deep convolutional neural network based on residual learning. To solve the complex problem of recognition or classification, the depth of convolutional networks was used to increase; but to some extent, the depth of the network makes neural network training difficult and the network accuracy starts saturating or degrading. The Residual network was designed to counter both problems [2]. The network learns residuals rather than features. Residual is determined by subtracting learned features from the input of the layer.

### 2.3 PCA Method

It is a conventional and effective method to find the degree of relatedness between variables under test. The method generates a new set of variables against highly co-linear variables. The new set of variables carries successive mutual variance. On that basis, one can select a significant number of principal components [3]. The method can be efficiently used for dimensionality reduction.

### 2.4 MLP classifier

MLP network has the tremendous capability of separating non-linearly separable data. It consists of a minimum of three types of layer; namely Input, Hidden, and Output layer. Multiple hidden layers can also be accommodated for solving complex problems of classification [4]. Hidden units carry a nonlinear activation function. The network architecture is displayed in Fig. 2.1.

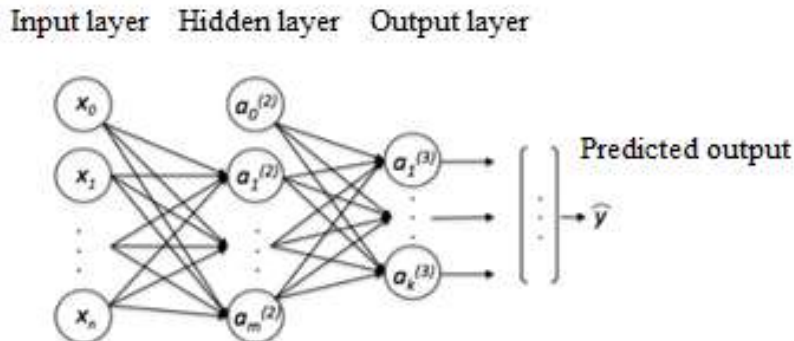


**Fig. 2.1 . Architecture of MLP network.**

## 3. Related work

This section includes an overview of recent work published in the field of handwritten alphabet recognition. Gupta and Bag presented a handwritten digit recognition model based on CNN-SVM. The model was able to distinguish handwritten digits of 8 different scripts[5]. Emily Xiaoxuan Gu analysed the performance of CNN over the Kannad-MNIST (K-MNIST) dataset of digits and compared it with that of logistic regression and Support Vector Machine (SVM) [6]. Zhang, Zhou, and Lin improved the recognition performance of the CNN model for the detection of handwritten digits [7]. Roy and Arif extracted global, local, and geometric features from handwritten Bangla digit set using Radon and Radon cumulative distribution transform and classify them with SVM [8]. Alsobae and Ahmad evaluated the performance of three compression techniques namely Discrete cosine, Discrete sine, and Wavelet transform over MNIST digit dataset using CNN and Pattern-Net [9]. Mohammed and Ahmad implemented a discrete cosine transform with CNN as the classifier for the recognition of handwritten digits [10]. Mane and Kulkarni introduced

customized CNN for automatic feature learning from handwritten Marathi digit set with a k-fold cross-validation scheme [11]. Shifeng Huang investigated the performance of CNN in recognition of MNIST digit set by varying parameters like dropout, epochs, dense layers with variable sizes [12].

#### **4. Methodology**

The design of the proposed model is given in Fig. 4.1.

##### **4.1 Data Set Pre-processing**

The digit dataset of the Devanagari script was compiled from a large number of individuals to have wide variations in it. The handwritten documents were scanned and digits were cropped manually. The complete dataset was prepared by Acharya and pant [13]; they made it available in the public domain. A dataset of size 5000 was selected for the proposed scheme. The individual images were resized into 224 by 224 by 3 as per the need of pre-trained models.

##### **4.2 Feature Extraction**

The proposed model utilized pre-trained DenseNet-121 and Resnet-50 deep CNN models for feature extraction from digit datasets. The models were called into the Python platform with the help of Keras library and the trainable layers were frozen to take benefit of transfer learning.

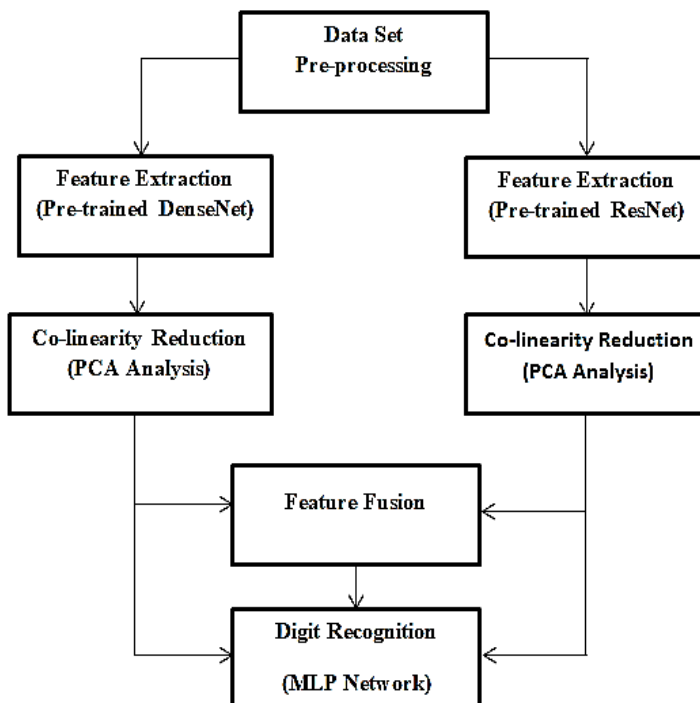


**Fig. 4.1 Design of proposed model.**

Training parameters are summarized in TABLE 4.1. The dataset images were given to the models and features were collected from the final global average pooling layer of respective models. The size of feature maps collected from DenseNet-121 and Resnet-50 were 1024 and 2048 respectively.

**Table-4.1 Summary of Training Parameters of Pre-trained Models.**

Model Name	Total Parameters	Non Trainable Parameters	Trainable Parameters
DenseNet-121	7,039,554	7,039,554	0
Resnet-50	23,591,810	23,591,810	0

##### **4.3 Co-linearity Reduction**

The PCA method was used to reduce co-linearity between features collected from respective models. The method was devised to determine 10 principal components from corresponding feature maps. The PCA method not only handled the co-linearity problem but also minimized feature redundancy. The outcome of

the PCA method was the reduction in feature map sizes from 1024, 2048 to 10, 10 for respective pre-trained models. The cumulative variance carried by the PCA components of respective models is given in TABLE 4.2.

**Table-4.2 Summary of Cumulative Variance.**

No. of PCA Components	Cumulative Variance in Percent	
	DenseNet-121	ResNet-50
1	30.78	28.64
2	52.67	40.33
3	62.39	50.33
4	69.64	56.25
5	74.03	60.24
6	77.39	63.45
7	79.53	66.30
8	81.56	68.59
9	83.17	70.68
10	84.47	72.43

#### 4.4 Feature Extraction

The reduced feature maps from both the pre-trained models for given digit images were integrated into a single map. The size of the fused feature map became 20. The format of the fused feature map is given in Fig. 4.2.

DenseNet-121 Reduced Feature-map of size 10	ResNet-50 Reduced Feature-map of size 10
--	---

**Fig. 4.2 Format of Fused feature map for given digit image.**

#### 4.5 Digit Recognition

Three types of new datasets were created so far; which were summarized in TABLE 4.3.

**Table-4.3 Summary of New Data Sets.**

Dataset Type	Source	No. of samples	Sample size
Dataset-1	DenseNet-121	5000	10
Dataset-2	Resnet-50	5000	10
Dataset-3	Fusion of two	5000	20

The MLP network was trained and tested over three datasets. The individual dataset was broken into a Train and Test set with 70:30 proportions. The MLP network was devised to generate confusion matrixes for respective datasets. With the help of confusion matrixes accuracy, precision, recall, and F1-score were determined in terms of True Positive (TP), True Negative (TN), False Positive (FP), and False Negative (FN) as given in Equations (1) to (4).

$$\text{Accuracy} = \frac{\text{TP} + \text{TN}}{\text{TP} + \text{FP} + \text{FN} + \text{TN}}$$

(1)

$$\text{Precision (P)} = \frac{\text{TP}}{\text{TP} + \text{FP}}$$

(2)

$$\text{Recall (R)} = \frac{\text{TP}}{\text{TP} + \text{FN}}$$

(3)

$$\text{F1 score} = \frac{2 * \text{P} * \text{R}}{\text{P} + \text{R}}$$

(4)

## 5. Results and discussions

### 5.1 Results

The classification reports generated by the MLP classifier for Dataset-1, Dataset-2, and Dataset-3 are summarized in TABLES 5.1, 5.2, and 5.3. The comparative analysis of respective precision, recall, and f1-score are plotted in Fig. 5.1 The related confusion matrixes are given in Fig. 5.2.

**Table 5.1 Results of Dataset-1.**

Digit Class	Precision	Recall	F1-Score	Support
0	0.9877	0.9938	0.9907	161
1	0.8322	0.8322	0.8322	143
2	0.7938	0.8194	0.8063	155
3	0.7500	0.7719	0.7608	171
4	0.8550	0.8615	0.8582	130
5	0.7197	0.7338	0.7267	154
6	0.6806	0.6950	0.6877	141
7	0.8993	0.8645	0.8816	155
8	0.9252	0.9577	0.9412	142
9	0.8092	0.7162	0.7599	148
Accuracy	82.46%			

(Data Set-1 Belongs to DenseNet-121)

**Table 5.2 Results of Dataset-2.**

Digit Class	Precision	Recall	F1-Score	Support
0	0.9821	0.9880	0.9851	167
1	0.9207	0.9321	0.9264	162
2	0.8467	0.8301	0.8383	153
3	0.8552	0.9051	0.8794	137
4	0.9530	0.9045	0.9281	157
5	0.8561	0.9187	0.8863	123
6	0.8707	0.8477	0.8591	151
7	0.9467	0.9161	0.9311	155
8	0.9438	0.9321	0.9379	162
9	0.8815	0.8947	0.8881	133
Accuracy	90.8%			

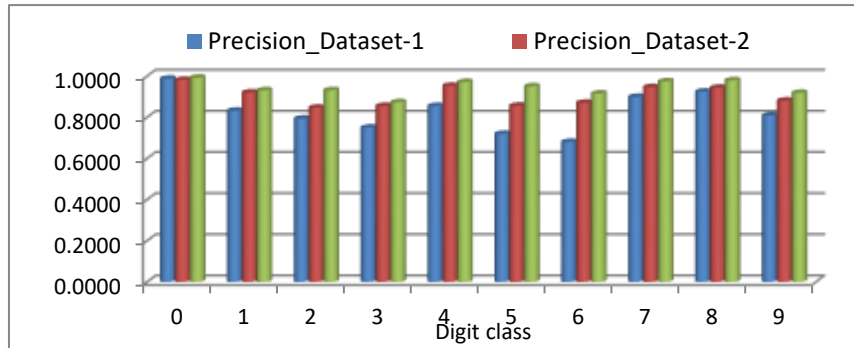
(Data Set-2 Belongs to ResNet-50)

**Table 5.3 Results of Dataset-3**

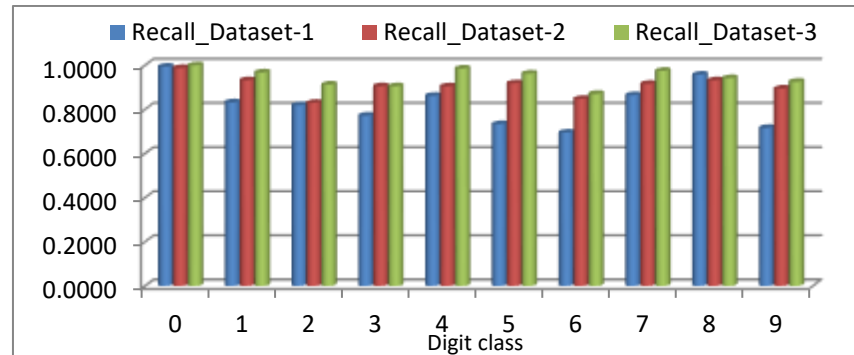
Digit Class	Precision	Recall	F1-Score	Support
0	0.9928	1	0.9964	138
1	0.9313	0.9675	0.9490	154
2	0.9315	0.9128	0.9220	149
3	0.8732	0.9051	0.8889	137
4	0.9716	0.9856	0.9786	139
5	0.9506	0.9625	0.9565	160

6	0.9156	0.8704	0.8924	162
7	0.9748	0.9748	0.9748	159
8	0.9799	0.9419	0.9605	155
9	0.9189	0.9252	0.9220	147
Accuracy	94.4%			

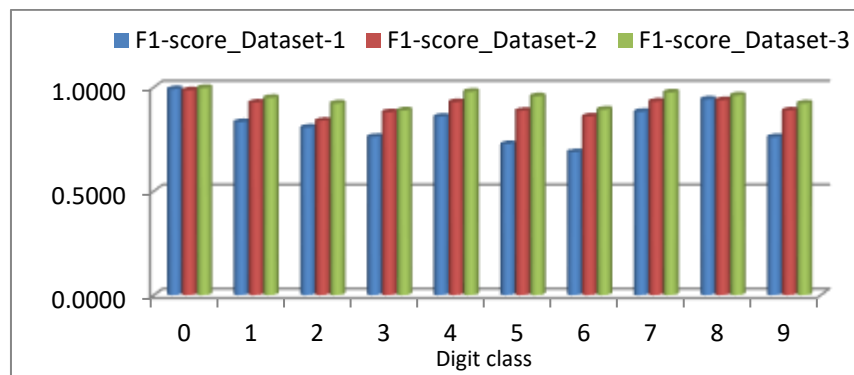
(Data Set-3 Belongs to Fusion of both)



(a)



(b)



(c)

**Fig. 5.1 Comparative analysis of results produced by Datasets-1, 2 and 3.**

**(a) Precision analysis (b) Recall analysis (c) F1-score analysis.**

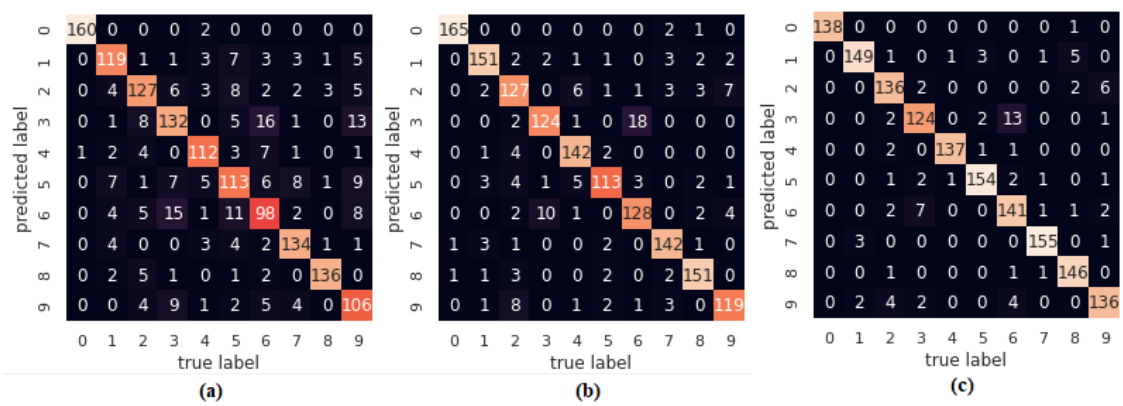


Fig. 5.2 Confusion matrixes generated by Datasets-1, 2, and3.

The overall recognition accuracy achieved by the model for respective datasets was 82.46%, 90.8%, and 94.4%. The graphical representation is given in Fig. 5.3.

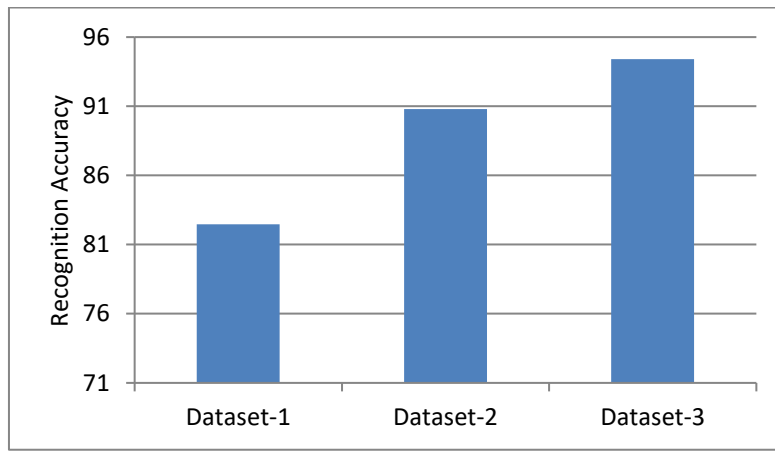


Fig. 5.3 Comparative plots of Recognition accuracy.

## 5.2. Discussions

It has been observed from TABLES 5.1, 5.2, and 5.3 that the proposed model produced comparatively high-performance matrices for digits 0, 7, and 8; when tested over all three datasets. This might be due to the unique shapes of these digits. From the comparative analysis given in Fig. 5.1, it is obvious that fusion-based features (Dataset-3) outperformed the features (Dataset-1 and Dataset-2) collected from individual models. Referring to Fig. 5.3, the features collected from ResNet-50 (Dataset-2) were a step ahead of those collected from DenseNet-121(Dataset-1) for the given problem. The proposed fusion-of -feature approach has boosted the recognition-accuracy of the model up to 94.4%; that has significantly higher than that achieved by the individual features as received from DenseNet-121, and ResNet-50.

## Conclusion

The proposed model took advantage of the PCA method for co-linearity reduction from features extracted by pre-trained deep convolutional models DenseNet-121, ResNet-50; and managed to score high for the fusion-based approach in recognizing handwritten numerals of Devanagari script. In the future, the proposed scheme can be extended by taking more pre-trained models into account for feature integration.

## References

- [1] T. A. O. Li, W. Jiao, L. Wang, and G. Zhong, “Automatic DenseNet Sparsification,” IEEE Access, vol. 8, pp. 62561–62571, 2020, doi: 10.1109/ACCESS.2020.2984130.
- [2] Y. Kaya, “Using ResNet Transfer Deep Learning Methods in Person Identification According to Physical Actions,” vol. 8, 2020, doi: 10.1109/ACCESS.2020.3040649.
- [3] Y. C. Du, W. C. Hu, and L. Y. Shyu, “The effect of data reduction by independent component analysis and principal component analysis in hand motion identification,” Annu. Int. Conf. IEEE Eng. Med. Biol. - Proc., vol. 26 I, pp. 84–86, 2004, doi: 10.1109/imebs.2004.1403096.
- [4] S. Han, G. Kong, and S. Choi, “A Detection Scheme With TMR Estimation Based on Multi-Layer

- Perceptrons for Bit Patterned Media Recording," IEEE Trans. Magn., vol. 55, no. 7, pp. 2019–2022, 2019.
- [5] D. Gupta and S. Bag, "CNN-based multilingual handwritten numeral recognition: A fusion-free approach," Expert Syst. Appl., vol. 165, p. 113784, 2021, doi: 10.1016/j.eswa.2020.113784.
  - [6] E. X. Gu, "Convolutional Neural Network Based Kannada- MNIST Classification," in 2021 IEEE International Conference on Consumer Electronics and Computer Engineering (ICCECE 2021), 2021, no. Iccece, pp. 180–185.
  - [7] C. Zhong, Y. Wang, D. Zhang, and K. Wang, "Handwritten digit recognition based on corner detection and convolutional neural network," in Journal of Physics: Conference Series, 2020, vol. 1651, no. 1, pp. 7384–7388, doi: 10.1088/1742-6596/1651/1/012165.
  - [8] A. R. Roy, A. Shamim, and M. Arif, "Recognizing Bangla Handwritten Numerals : A Hybrid Model," in Proceedings of the Third International Conference on Intelligent Sustainable Systems [ICISS 2020], 2020, pp. 636–643.
  - [9] H. Alsobaie and I. Ahmad, "Compression Techniques for Handwritten Digit Recognition," in 2020 International Conference on Innovation and Intelligence for Informatics, Computing and Technologies (3ICT) Compression, 2021, pp. 1–6, doi: 10.1109/3ict51146.2020.9312005.
  - [10] A. M. Almohammed and I. Ahmad, "Feature Compression Based on Discrete Cosine Transform for Handwritten Digit Recognition," in Proceedings - 2020 1st International Conference of Smart Systems and Emerging Technologies, SMART-TECH 2020, 2020, pp. 13–20, doi: 10.1109/SMArT-TECH49988.2020.00021.
  - [11] D. T. Mane and U. V Kulkarni, "ScienceDirect Visualizing and Understanding Customized Convolutional Neural Network for Recognition of Handwritten Marathi Numerals," Procedia Comput. Sci., vol. 132, no. Iccids, pp. 1123–1137, 2018, doi: 10.1016/j.procs.2018.05.027.
  - [12] G. Huang, Z. Liu, L. Van Der Maaten, and K. Q. Weinberger, "Densely connected convolutional networks," Proc. - 30th IEEE Conf. Comput. Vis. Pattern Recognition, CVPR 2017, vol. 2017-Janua, pp. 2261–2269, 2017, doi: 10.1109/CVPR.2017.243.
  - [13] S. Acharya, A. K. Pant, and P. K. Gyawali, "Deep learning based large scale handwritten Devanagari character recognition," Ski. 2015 - 9th Int. Conf. Software, Knowledge, Inf. Manag. Appl., 2016, doi: 10.1109/SKIMA.2015.7400041.

# Fuzzy Arithmetic Geometric Divergence and its Utility in Pattern Recognition

Sapna Gahlot and R. N. Saraswat

**Abstract** Here, we have discussed bounds on recognized fuzzy information divergence measures in terms of fuzzy arithmetic geometric divergence and found the relations among the recognized measures by convex function, fuzzy new f-divergence, known inequalities and applied to Pattern Recognition. Inequalities are very useful for literature of information theory.

**Keywords-** Fuzzy divergence measures, fuzzy new f-divergence measure, Jensen's inequality, fuzzy information inequalities, pattern recognition.

## 1. Introduction

Entropy is the important concept of information theory and Shannon [1] used entropy to find a grade of uncertainty in a p.d (probability distribution). Let  $\Gamma_n = U = (u_1, u_2, \dots, u_n)$ :  $u_i \geq 0$ ,

$\sum_{i=1}^n u_i = 1$  be a set of complete finite discrete p.d.

$$H(u) = - \sum_{i=1}^n u_i \log u_i$$

Directed divergence (d.d) is a cross entropy measure which provides a distance between the two p.d. K-L [2] developed a measure of d.d among two p.d  $U = (u_1, u_2, \dots, u_n)$  and  $V = (v_1, v_2, \dots, v_n)$  as:

$$D(U | V) = \sum_{i=1}^n u_i \log \frac{u_i}{v_i}$$

Csiszar's f-measure contains divergences used in determining the affinity between two p.d. and Csiszar [3] introduced this by convex function f in  $(0, \infty)$ .

$$C_f\left(\frac{u}{v}\right) = \sum_{i=1}^n v_i f\left(\frac{u_i}{v_i}\right)$$

## 2. Fuzzy sets:-

Fuzziness is a feature of uncertainty, outcomes along the lack of sharp difference of being or not being a member of the set. FS A defined in universe of discourse X is defined by Zadeh [4]

---

Sapna Gahlot  
Department of Mathematics and Statistics, Manipal University Jaipur, Jaipur  
Email Address : sapna1994gahlot@gmail.com

R. N. Saraswat  
Department of Mathematics and Statistics, Manipal University Jaipur, Jaipur  
Email Address : saraswatramn@gmail.com

$$A = \{x, \mu_A(x) / x \in X_i\},$$

Here,  $\mu_A(x) : X \rightarrow [0, 1]$  is the membership degree of A and membership value defines the grade of belongingness of X in A. Fuzzy entropy by Shannon's entropy defined as below:

$$H(U) = - \sum_{i=1}^n (\mu_A(x_i) \log \mu_A(x_i) + (1 - \mu_A(x_i)) \log (1 - \mu_A(x_i)))$$

This idea of divergence measure was extended from probabilistic to fuzzy set theory through fuzzy information measure for discrimination of a FS B among the other FS A. Suppose A and B be FS introduced in  $X = \{x_1, x_2, \dots, x_n\}$  and membership values  $\mu_A(x_i)$  and  $\mu_B(x_i)$  w.r.t  $i = 1, 2, \dots, n$

In next section we present the a few examples of identified information measures by FNf-DM (fuzzy new f-divergence measure).

### 3. FNf-DM and its Cases: -

Here, we present a few properties of FNf-DM [5] and its cases . Here, for convenience,  $\mu_A(x_i)$  and  $\mu_B(x_i)$  denoted by  $\mu_{A_i}$  and  $\mu_{B_i}$  respectively.

$$S_\varphi(A, B) = \sum_{i=1}^n \left[ \mu_{B_i} \varphi \left( \frac{\mu_{A_i} + \mu_{B_i}}{2\mu_{B_i}} \right) + (1 - \mu_{B_i}) \varphi \left( \frac{(2 - \mu_{A_i} - \mu_{B_i})}{2(1 - \mu_{B_i})} \right) \right] \quad (3.1)$$

Where  $\varphi: \mathbb{R}_+ \rightarrow \mathbb{R}_+$  is a convex function,  $A, B \in X_n$

**Proposition 3.1.** Let  $\varphi: (0, \infty) \rightarrow \mathbb{R}$  be convex and  $A, B \in X_n$  then,

$$S_\varphi(A, B) \geq \varphi(1) \quad (3.2)$$

Equality hold iff  $\mu_{A_i} = \mu_{B_i} \quad \forall i = 1, 2, \dots, n$

**Corollary 3.0.1.** Let  $\varphi: (0, \infty) \rightarrow \mathbb{R}$  be convex,  $\varphi(1) = 0$

Then  $\forall A, B \in X_n$  from (3.2) and by  $\varphi(1) = 0$ , we get the inequality

$$S_\varphi(A, B) \geq 0 \quad (3.3)$$

If  $\varphi'' > 0$ , equality holds iff  $\mu_{A_i} = \mu_{B_i} \quad \forall i = 1, 2, \dots, n$

$$S_\varphi(A, B) \geq 0 \text{ and } S_\varphi(A, B) = 0 \text{ iff } A = B \quad (3.4)$$

**Proposition 3.2.** Let  $\varphi_1$  and  $\varphi_2$  are two convex functions and  $g = a\varphi_1 + b\varphi_2$  then  $S_g(A, B) = aS_{\varphi_1}(A, B) + bS_{\varphi_2}(A, B)$  where a and b constants and  $A, B \in X_n$ .

- **Fuzzy chi-square measure (1900) [6] :**

If  $\varphi(y) = (y - 1)^2$  then,

$$S_\varphi(A, B) = \frac{1}{4} \sum_{i=1}^n \left[ \left( \frac{(\mu_{A_i})^2}{\mu_{B_i}} + \frac{(1-\mu_{A_i})^2}{(1-\mu_{B_i})} \right) - 1 \right] = \frac{1}{4} \chi^2(A, B) \quad (3.5)$$

- **Fuzzy relative Jensen-Shannon measure (1999) [7]:**

If  $\varphi(y) = -\log y$  then,

$$S_\varphi(A, B) = \sum_{i=1}^n \mu_{B_i} \log \left( \frac{2\mu_{B_i}}{\mu_{A_i} + \mu_{B_i}} \right) + (1 - \mu_{B_i}) \log \left( \frac{2(1-\mu_{B_i})}{(2-\mu_{A_i}) - \mu_{B_i}} \right) = F(B, A) \quad (3.6)$$

- **Fuzzy arithmetic-geometric measure (FAGM) (1982) [8]:**

If  $\varphi(y) = y \log y$  then

$$S_\varphi(A, B) = \sum_{i=1}^n \left[ \left( \frac{\mu_{A_i} + \mu_{B_i}}{2} \right) \log \left( \frac{\mu_{A_i} + \mu_{B_i}}{2\mu_{B_i}} \right) + \left( \frac{2 - \mu_{A_i} - \mu_{B_i}}{2} \right) \log \left( \frac{(2 - \mu_{A_i} - \mu_{B_i})}{2(1 - \mu_{B_i})} \right) \right] = G(B, A) \quad (3.7)$$

- **Fuzzy Hellinger measure (1977) [9]:**

$\varphi(y) = 1 - \sqrt{y}$  then,

$$S_\varphi(A, B) = \frac{1}{2} \sum_{i=1}^n \left[ \left( \sqrt{\mu_{A_i}} - \sqrt{\mu_{B_i}} \right)^2 + \left( \sqrt{(1-\mu_{A_i})} - \sqrt{(1-\mu_{B_i})} \right)^2 \right] = H(A, B) \quad (3.8)$$

- **Fuzzy triangular measure (2003) [10] :**

If  $\varphi(y) = \frac{(y-1)^2}{y}$ ,  $\forall y > 0$ , then

$$S_\varphi(A, B) = \sum_{i=1}^n \left[ \left( \frac{(\mu_{A_i} - \mu_{B_i})^2}{2(\mu_{A_i} + \mu_{B_i})} \right) + \left( \frac{(\mu_{B_i} - \mu_{A_i})^2}{2(2 - \mu_{A_i} - \mu_{B_i})} \right) \right] = \frac{1}{2} \Delta(A, B) \quad (3.9)$$

- **Fuzzy relative J-divergence measure**

If  $\varphi(y) = (y - 1) \log y$  then,

$$S_\varphi(A, B) = \sum_{i=1}^n \left[ \frac{(\mu_{A_i} - \mu_{B_i})^2}{2} \log \left( \frac{\mu_{A_i} + \mu_{B_i}}{2\mu_{B_i}} \right) + \frac{(2 - \mu_{A_i} - \mu_{B_i})^2}{2} \log \left( \frac{2 - \mu_{A_i} - \mu_{B_i}}{2(1 - \mu_{B_i})} \right) \right] = \frac{1}{2} J_m(A, B) \quad (3.10)$$

#### 4. Inequalities among FNf-DM and FAGM:-

**Theorem 4.1.** Let  $\varphi: (0, \infty) \rightarrow R$  is  $\varphi(1) = 0$  and,

(i).  $\varphi' \geq 0$  on  $(r, R)$ ,  $(0 \leq r \leq 1 \leq R < \infty)$

(ii)  $\exists n, N$  s.t.  $n < N$

$$n \leq y \varphi''(y) \leq N \quad (4.1)$$

if A and B be FS defined in  $X = \{x_1, x_2, \dots, x_n\}$  satisfying the relation

$$r \prec \frac{1}{2} \leq r_i = \sum_{i=1}^n \left[ \frac{\mu_{A_i} + \mu_{B_i}}{2\mu_{B_i}} + \frac{2 - \mu_{A_i} - \mu_{B_i}}{2(1 - \mu_{B_i})} \right] \leq R,$$

here,  $i = 1, 2, \dots, n$

(4.2)

Thus, we obtain the inequality

$$nG(B, A) \leq S_\varphi(A, B) \leq NG(B, A) \quad (4.3)$$

**Proof.** Let  $F_n : (0, \infty) \rightarrow \mathbb{R}$ ,  $F_n(y) = \varphi(y) - ny \log y$ ,

then  $F_n(\cdot)$  is normalized,

$$F_n'' = \frac{1}{y} (\varphi''(y) - n) \geq 0,$$

$\forall y \in (r, R)$ ,  $F_n(\cdot)$  is convex on  $(r, R)$ . Now, by linearity property, then we get the inequality,

$$0 \leq S_{F_n}(A, B) = S_\varphi(A, B) - nS_{y \log y}(A, B) = S_\varphi(A, B) - nG(B, A)$$

$$\Rightarrow 0 \leq S_\varphi(A, B) - nG(B, A) \quad (4.4)$$

Now Again,  $F_N : (0, \infty) \rightarrow \mathbb{R}$ ,  $F_N(y) = Ny \log y - \varphi(y)$ ,  $\forall y \in (r, R)$ , by non-negativity and linearity property, then we get the inequality,

$$\Rightarrow 0 \leq NG(B, A) - S_\varphi(A, B) \quad (4.5)$$

So, By (4.4) and (4.5) we get the result (4.3).

—

## 5. Results on fuzzy f-divergences:-

Here, we present the restrictions of identified measures through fuzzy arithmetic-geometric measure by inequality of (4.3) of Theorem 4.1.

**Result 5.1.** Let  $A, B \in X_n$  be two fuzzy sets then

$$r \prec \frac{1}{2} \leq r_i = \sum_{i=1}^n \left[ \frac{\mu_{A_i} + \mu_{B_i}}{2\mu_{B_i}} + \frac{2 - \mu_{A_i} - \mu_{B_i}}{2(1 - \mu_{B_i})} \right] \leq R,$$

here,  $i = (1, 2, \dots, n)$

Now, we get the inequality

$$\frac{1}{r} G(A, B) \leq F(A, B) \frac{1}{R} G(A, B) \quad (5.1)$$

**Proof.** Let a mapping  $\varphi : (r, R) \rightarrow \mathbb{R}$

$$\phi(y) = -\log y, \phi''(y) = \frac{1}{y^2}, y > 0$$

so, f is convex and

$$g(1) = 0, g(y) = y\phi''(y) = y \cdot \frac{1}{y^2} = \frac{1}{y}$$

so, f is convex and

Then,

$$N = \sup_{y \in [r, R]} g(y) = \frac{1}{r}, n = \inf_{y \in [r, R]} g(y) = \frac{1}{R} \quad (5.2)$$

and  $S_\phi(A, B) = F(B, A)$  (from 3.6)

By inequality (3.6), (4.3) and (5.2),

$$\frac{1}{r} G(A, B) \leq F(A, B) \leq \frac{1}{R} G(A, B) \quad (5.3)$$

Interchange A → B of (5.3), we get of the result (5.1).

**Result 5.2.** Let  $A, B \in X_n$  be two FS and satisfy the (4.2). Then get the next inequality

$$\frac{1}{r^2} G(A, B) \leq \frac{1}{4} \Delta(A, B) \frac{1}{R^2} G(A, B) \quad (5.4)$$

**Proof.** Let a mapping  $\varphi:(r, R) \rightarrow \mathbb{R}$

$$\varphi(y) = \frac{(y-1)^2}{y}, \varphi''(y) = \frac{2}{y^3}, \forall y > 0$$

so, f is convex and  $\varphi(1) = 0$ ,

$$g(y) = y \varphi''(y) = \frac{2}{y^2},$$

Then,

$$N = \sup_{y \in [r, R]} g(y) = \frac{2}{r^2}, n = \inf_{y \in [r, R]} g(y) = \frac{2}{R^2} \quad (5.5)$$

$$\text{and } S_\varphi(A, B) = \frac{1}{4} \Delta(A, B) \quad (\text{from 3.6})$$

$$\frac{1}{r^2} G(B, A) \leq \frac{1}{4} \Delta(A, B) \frac{1}{R^2} G(B, A)$$

(5.6)

By inequality (3.9), (4.3) and (5.5),

Interchange A → B of (5.6), we get of the result (5.4).

**Result 5.3.** Let  $A, B \in X_n$  be two FS and satisfy the (4.2). Then get the following inequality

$$rG(B, A) \leq \frac{1}{8} \chi^2(A, B) \leq RG(B, A) \quad (5.7)$$

**Proof.** Let a mapping  $\varphi:(r, R) \rightarrow \mathbb{R}$

$$\phi(y) = (y^2 - 1), \phi''(y) = 2, \forall y > 0$$

so, f is convex and  $\varphi(1) = 0$ ,

$$g(y) = y\varphi''(y) = 2y$$

Then,

$$N = \sup_{y \in [r, R]} g(y) = 2R, n = \inf_{y \in [r, R]} g(y) = 2r$$

(5.8)

$$\text{and } S_\varphi(A, B) = \frac{1}{8} \chi^2(A, B) \text{ (from 3.6)}$$

$$rG(A, B) \leq \frac{1}{8} \chi^2(A, B) \leq RG(A, B)$$

from relation (3.5), (4.3) and (5.8) we get the result (5.7)

**Result 5.4.** Let  $A, B \in X_n$  be two FS and satisfy the (4.2). Then get the following inequality

$$\frac{r+1}{r} G(A, B) \leq \frac{1}{2} J_m(A, B) \leq \frac{R+1}{R} G(A, B)$$

(5.9)

**Proof.** Let a mapping  $\varphi: (r, R) \rightarrow \mathbb{R}$

$$\varphi(y) = (y-1)\log y, \varphi''(y) = \frac{1+y}{y^2}, \forall y > 0$$

so, f is convex and  $\varphi(1) = 0$ ,

$$g(y) = y \varphi''(y) = \frac{1+y}{y},$$

Then,

$$N = \sup_{y \in [r, R]} g(y) = \frac{R+1}{R}, n = \inf_{y \in [r, R]} g(y) = \frac{r+1}{r}$$

(5.10)

$$\text{and } S_\varphi(A, B) = J_m(A, B) \text{ (from 3.10)}$$

from relation (3.10), (4.3) and (5.10), we get the result (5.9)

$$\frac{r+1}{r} G(A, B) \leq \frac{1}{2} J_m(A, B) \leq \frac{R+1}{R} G(A, B)$$

## 6. Application in Pattern Recognition: -

Now, we will discuss how pattern recognition become simple by demonstrating application of the fuzzy divergence measure defined as below.

Assume, we are have m identified patterns  $P_1, P_2, P_3, \dots, P_m$  having the classification  $D_1, D_2, D_3, \dots, D_m$  individually.

The Pattern are introduced through the FS in the universe of discourse  $T = \{t_1, t_2, \dots, t_n\}$ :

$$P_i = \{t_j, \mu_{P_i}(t_j) / t_j \in T\} \quad (i = 1, 2, \dots, m, j = 1, 2, \dots, n).$$

and unspecified pattern Q denoted through FS

$$Q_i = \{t_j, \mu_{Q_i}(t_j) / t_j \in T\}$$

Our main motive is to analyze Q to the classes D<sub>1</sub>, D<sub>2</sub>, D<sub>3</sub>, ..., D<sub>m</sub>. The procedure of allocating Q to D<sub>x\*</sub> described below is as per the principle of minimum discrimination information among FS.

$$X^* = \arg \min_x \{M(P_x, Q)\}.$$

By above method we can select the best class.

### **Case Study**

Consider a problem having four identified patterns P<sub>1</sub>, P<sub>2</sub> and P<sub>3</sub> having the classifications D<sub>1</sub>, D<sub>2</sub> and D<sub>3</sub> individually. These are denoted through the following FS in T = {t<sub>1</sub>, t<sub>2</sub>, t<sub>3</sub>, t<sub>4</sub>}.

$$P_1 = \{t_1, .5\}, \{t_2, .6\}, \{t_3, .2\}, \{t_4, .3\}$$

$$P_2 = \{t_1, .8\}, \{t_2, .7\}, \{t_3, .3\}, \{t_4, .4\}$$

$$P_3 = \{t_1, .7\}, \{t_2, .5\}, \{t_3, .1\}, \{t_4, .7\}$$

and unspecified pattern Q, denoted by the FS

$$Q = \{t_1, .5\}, \{t_2, .3\}, \{t_3, .4\}, \{t_4, .9\}$$

### **Calculated numerical values of M (P<sub>x</sub>, Q), X = 1, 2, 3**

$$M(P_1, Q) = .1155$$

$$M(P_2, Q) = .1220$$

$$M(P_3, Q) = .0697$$

Our focus to analyse Q to one of the greatest P<sub>1</sub>, P<sub>2</sub> and P<sub>3</sub>. By the formula (3.7), we can find out the M(P<sub>x</sub>, Q), X = {1, 2, 3}.

From these values recognized that P<sub>3</sub> is the greatest value.

## **7. Conclusions**

Here, we reached on a few relations of fuzzy divergence measure through fuzzy new f-divergence measures, discussed the some relations with the help of fuzzy arithmetic divergence measure with pattern recognition. It is very help full of our daily life.

## **Acknowledgment**

The authors would like to thank the referees and Editor-in-Chief for their valuable suggestions and comments for improving this paper.

## **References:-**

- [ 1.] Shannon C.E.. A mathematical theory of communication, The Bell Syst. Tech. Journal 27(3), 379-423 (1948).
- [ 2.] Kullback S. and R.A. Leibler On information and sufficiency, The Annals of Mathematical Statistics 22(1) ,79-86 (1951).
- [ 3.] Csiszar's I. On Topological Properties of f-Divergences. Studia Math. Hungarica, Vol. 2, 329-339 (1967).
- [ 4.] Zadeh and L.A. Toward a generalized theory of uncertainty (GTU): an outline, Information Sciences—Informatics and Computer Science: An International Journal, v.172 n.1-2, p.1-40 (2005).
- [ 5.] Jain K.C. and A. Srivastava On Symmetric Information Divergence Measures of Csiszar's f-Divergence Class, Journal of Applied Mathematics, Statistics and Informatics (JAMSI),3(1),85-102 (2007).
- [ 6.] Pearson K.. On the criterion that a give system of deviations from the probable in the

- case of correlated system of variables in such that it can be reasonable supposed to have arisen from random sampling, Phil. Mag., 50,157-172 (1900).
- [ 7.] Topse F.. Some inequalities for information divergence and related measures of discrimination. Res.Coll. RGMIA2 ,85-98 (1999).
- [ 8.] Burbea J., and C. R. Rao On Convexity of Some Divergence measures based on entropy functions,IEEE Transe.on.inform.theory ,IT-28,489-495 (1982).
- [ 9.] Luca De. A. and Termini S. . A definition of non-probabilistic entropy in the setting of fuzzy sets theory. Information and Control. v20. ,301-312 (1972).
- [ 10.] Dragomir S.S.. Bounds of f-divergences under likelihood Ratio Constraints No.3, 48,205- 223 (2003) .
- [ 11.] Beran R.. Minimum Hellinger distance estimates for parametric models Ann.Statist.5,445-463 (1977).
- [ 12.] Bhattacharyya A.. Some Analogues to the Amount of Information and Their uses in Statistical Estimation, Sankhya, 8, 1-14 (1946).
- [ 13.] Csiszar's I. Information-type measures of difference of probability functions and indirect observations. studia Sci. Math. hungar.2,299-318 (1961).
- [ 14.] Dragomir S.S., J. Sunde and C. Buse. New Inequalities for Jeffreys Divergence measure, Tamusi Oxford Journal of Mathematical Sciences,16(2),295-309 (2000). Dragomir S.S.. Bounds of f-divergences under likelihood Ratio Constraints No.3, 48,205- 223 (2003) .
- [ 15.] Hellinger E. and Neue Begrundung der Theorie der quadratischen Formen von unendlichen vielen Veranderlichen, J. Reine Aug. Math., 136,210-271 (1909).
- [ 16.] Jain K.C. and R. N. Saraswat. Some well-known inequalities and its applications in information theory" Jordan Journal of Mathematics and Statistics. 157-167 (2013).
- [ 17.] Jain K. C. and R. N. Saraswat. Some Bounds of Information Divergence Measures in Terms of Relative-Arithmetic Divergence Measure" International Journal of Applied Mathematics and Statistics, 32 (2) ,48-58 (2013).
- [ 18.] Kaufmann A. Introduction to the Theory of Fuzzy Sets - Fundamental Theoretical Elements. Academic Press, New York., Vol. 1 (1975).
- [ 19.] Loo and S.G.. Measures of fuzziness. Cybernetica. v20., 201-210 (1997).
- [ 20.] Saraswat R. N. and A. Umar. New Fuzzy Divergence Measure and its Applications in Multi Criteria Decision Makin Using New Tool, Springer Proceedings in Mathematics & Statistics Vol 307, pp-191-206 (2020) .
- [ 21.] Saraswat R. N. and Neha Khatod. New Fuzzy Divergence Measures, Series, Its Bounds and Applications in Strategic Decision-Making, Lecture notes in Electrical Engineering (springer) vol 607, pp-641-653 (2020).
- [ 22.] Sibson R.. Information Radius, Z, Wahrs.und verw. geb. (14),149-160 (1969).
- [ 23.] Taneja I.J. and Pranesh Kumar. Relative information of type's, Csiszar's f-divergence, and information inequalities, Information sciences 166 ,105-125 (2004).
- [ 24.] Taneja I.J.. New Developments in generalized information measures, Chapter in: Advances in imaging and Electron Physics, Ed. P.W. Hawkes 91,37-135 (1995) .
- [ 25.] Umar A. and R.N. Saraswat. New generalized intuitionistic fuzzy divergence measure with applications to multi-attribute decision making and pattern recognition, Recent Patents on Computer Science 13 (1) (2020).

# Analysis of Voltage Stability in Power System: A Research Review

Kushketu Kundan Srivastava, Sanjiv Kumar and Ajay Kumar

**Abstract**— This paper aims to analyze the static voltage stability in a power system, it refers to maintain the fluctuations in voltages that occur at all bus bars in the power system from sending voltage end to receiving voltage end. The stability of the power system is to return to its normal or stable conditions after being disturbed. In this scenario, meeting the electrical power demand isn't the sole criteria but also it's the responsibility of the facility system engineers to supply a stable and quality power to the consumers. The main purpose of analysis is to identify and study the sudden voltage change that could be static or dynamic, steady or transient to limit the voltage inaccuracy in the transmission of power supply from one end to another end. The controlling strategy of static voltage stability is analyzed and summarized. Finally, the future development direction in power system stability is prospected. The loads which are generally dependent on voltage have an important role in voltage stability, so the loads that are dependent on static voltage stability are modeled ZIP model. The need for increase thanks to electrical power sensitive industries like information technology, communication, electronics etc.

**Keywords**— Voltage stability, static voltage, voltage stability index, transient voltage, dynamic voltage, power system, bus-bar, rotor angle stability, frequency stability, bus voltage response, power grid.

## 1. Introduction

The analysis of static voltage stability [1], the analysis method has made great progress in recent years, in the field of transmission of power system and it's already been mature [2]. Currently, the static voltage stability analysis methods are supported the facility flow equation or the improved power flow equation, the physical nature which is that the limit operation state of power transmission network because the critical voltage instability point. The difference is that a variety of methods use the diverse characteristics of limit state as the criterion of critical point. The advantages of static voltage stability analysis are a small amount of calculation. It shows the system voltage stability level and gives the power system voltage stability margin and its sensitivity information on the state variables and control variables [3]. The static stability tends towards the steadiness of the system that obtains without the help (benefit) of automatic control devices reliable, stable and quality power is on the like governors and voltage regulators. The Purpose is to watch and optimize the facility system, which is of great practical

---

Kushketu Kundan Srivastava

Department of Electrical & Electronics Engineering, Subharti Institute of Technology and Engineering, Swami Vivekanand Subharti University, Meerut (UP), India

Email Address : [kks4april@gmail.com](mailto:kks4april@gmail.com)

Sanjiv Kumar

Department of Electrical & Electronics Engineering, Subharti Institute of Technology and Engineering, Swami Vivekanand Subharti University, Meerut (UP), India.

Ajay Kumar

Department of Electrical & Electronics Engineering, Subharti Institute of Technology and Engineering, Swami Vivekanand Subharti University, Meerut (UP), India.

significance to the facility system operation and dispatch department. Static voltage stability analysis has been greatly developed as it's simple and practicable, when the system voltage stability index and voltage collapse prevention strategy are needed urgently by electric power operating department [4]. It is one among the foremost important directions within the research of voltage stability at the present.

"Static voltage stability in Power System for stabilization is that the ability of an electrical power grid, for a given initial operating condition, to regain an operating equilibrium stage after being subjected to a physical disturbance, with most system variables bounded, in order that practically the whole system remains intact"[5,6].

The power system is usually designed to be stable under those disturbances which have a high degree of occurrence. The response to a disturbance is extremely complex and involves practically all the equipment of the facility system. For example, a brief circuit resulting in line isolation by circuit breakers will cause variations within the power flows, network bus voltages and generators rotor speeds [7]. The voltage variations for steady state or dynamic voltage stability state will actuate the voltage regulators within the system and generator speed variations will actuate the first cause governors; voltage and frequency variations will affect the system loads [8]. In stable systems, practically all generators and loads remain connected, albeit parts of the system could also be isolated to preserve bulk operations [9]. On the other side, an unstable system condition could lead on to cascading outages and a shutdown of a serious portion of the facility system. For improving the voltage stability; have to identify and allocate the optimal reactive power [10].

## **2. Basic Concept of Power System Stability**

Power system stability is a crucial think about power grid. Static analysis methods might help to analyze voltage stability problems approximately. Several voltage stability indexes derived from static power flow analysis were proposed for a utility power grid [1]. Power system voltage stability has been one among the recent issues in recent years. There are many methods to research the voltage stability, the researchers have studied the voltage stability from different angles, although many progresses are made, there are still many difficulties to be solved. "Power system stability is that the ability of an electrical power grid, for a given initial operating condition, to regain a state of operating equilibrium after being subjected to a physical or any mechanical disturbance, with most of the system variables bounded in order that practically the whole system remains intact" [2,3]. The disturbances listed within the definition might be faults, load changes, generator outages, line outages, voltage collapse or some combination of those. Power system stability is often broadly classified into rotor angle, voltage and frequency stability. Each of those three stabilities are often further classified into large disturbance or small disturbance, short term or future.

## **3. Classification of Power System Stability**

Basically there are three types of stability: Steady state, transient and dynamic stability.

1. Steady state stability.
2. Dynamic stability.
3. Transient stability.

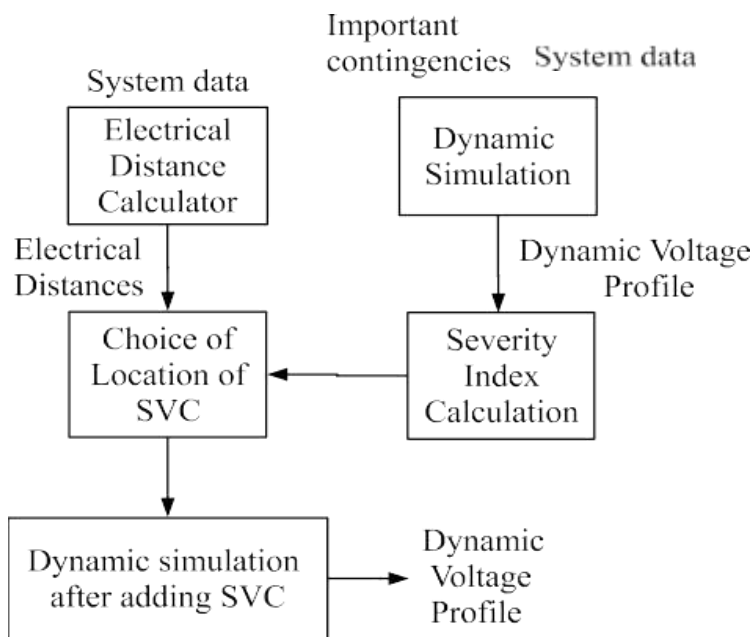


**Fig. 2.1 Work outline: dynamic stability**

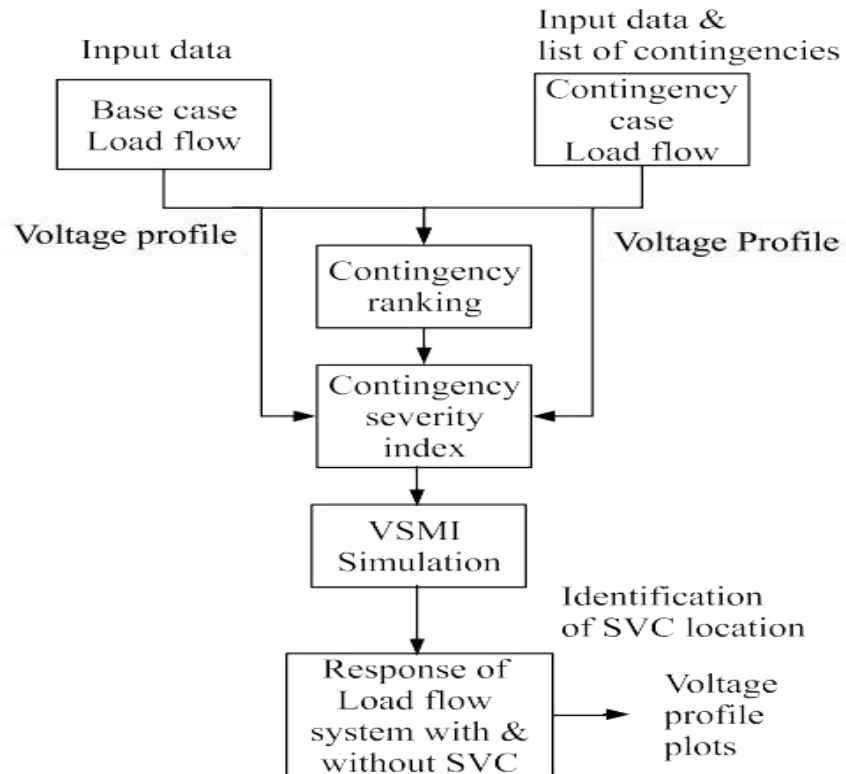


**Fig. 2.2 Work outline: steady-state stability**

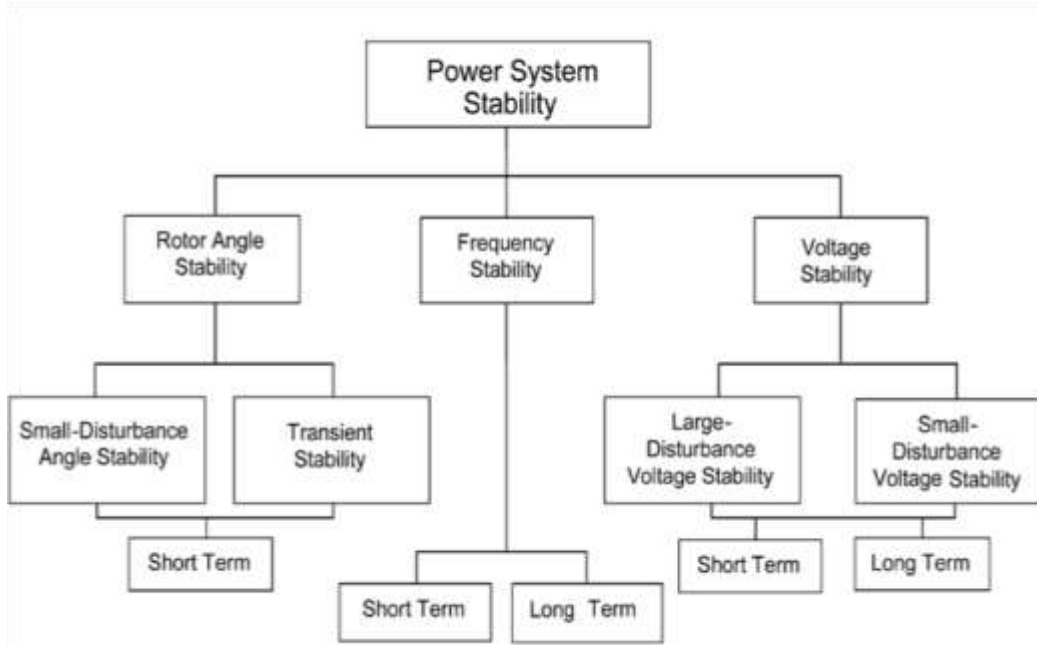


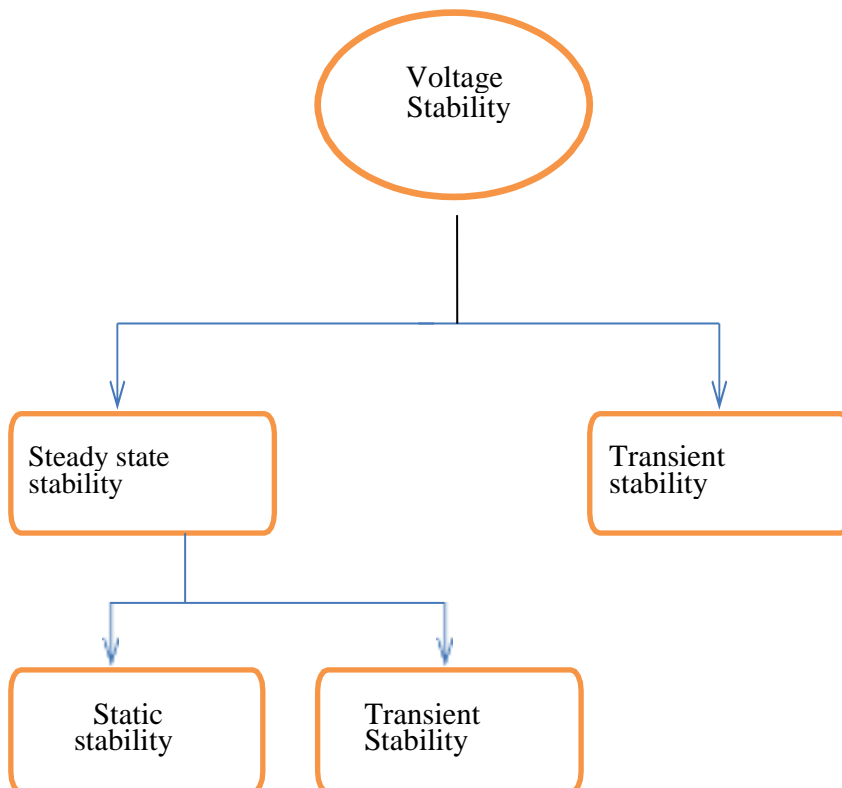
**Fig. 2.3 Classification of power system stability**

### 3.1 Steady state stability

Steady-state stability relates to the response of synchronous machine to a gradually increasing load. It is basically concerned with the determination of the upper limit of machine loading without losing synchronism, provided the loading is increased gradually. The steady-state stability of an influence system is defined because during the ability of the system to bring itself back to its stable configuration following little disturbance within the network (like normal load fluctuation or action of automatic voltage regulator). It can only be considered only during a really gradual and infinitesimally small power change [3,5].

### 3.2 Dynamic Stability

Dynamic stability involves the response to small disturbances that occur on the system, producing oscillations. The system is claimed to be dynamically stable if these oscillations don't acquire quite certain amplitude and die out quickly. If these oscillations continuously grow in amplitude, the system is dynamically unstable. The source of this type of instability is typically an interconnection between control systems.

**Fig. 3.1 Classification of voltage stability**

### 3.3 Transient Stability

Transient stability involves the response to large disturbances, which may cause rather large changes in rotor speeds, power angles and power transfers. Transient stability could also be quick phenomenon usually evident within a couple of second. It actually deals within the working process of the system to retain synchronism following a disturbance sustaining for a reasonably long period and therefore maximum power that's permissible to flow through the network without loss of stability following a sustained period of disturbance is mentioned because the transient stability of the system.

### 3.4 Steady State Voltage Stability

By considering the methodology for steady state voltage stability improvement, we know that the voltage performance can be analyzed by when voltage drop is maximum to the allowed voltage deviation from the nominal voltage. The stable voltage needs the stabilization in power system instruments.

### 3.5 Dynamic State Voltage stability

For the dynamic voltage stability can be considered for same system that has been used for steady state voltage stability [5]. In the dynamic voltage stability, the dynamic simulation can be done by adding exciter data and total contingencies that happened during the normal voltage flow.

### 3.6 Voltage stability

“This is the facility of the system to need care of steady state voltages within the smallest amount the system buses when subjected to a small disturbance. If the disturbance is large then it's called as large-disturbance voltage stability and if the disturbance is little it's called as small disturbance voltage stability”[1,5].

Voltage stability further classified into steady-state stability and Transient stability. Currently the demand for electricity is rising phenomenally specially in developing country like India. This persistent demand is resulting in operation of the facility system at its limit. Unlike angle stability, voltage stability also can be an extended term phenomenon. In case voltage fluctuations occur because of fast acting devices like induction motors, power electronic drive, HVDC etc then the time-frame for understanding the stableness is within the range of 10-20 s and hence are often treated as short term phenomenon. Other hand if voltage variations are due to slow change in load, over loading of lines, generators hitting reactive power limits, tap changing transformers etc then time frame for voltage stability can stretch from 1 minute to many minutes. The difference between voltage stability and angle stability is that voltage stability depends on the balance of reactive power demand and generation within the system where because the angle stability preferably depends on the balance between real power generation and demand [2].

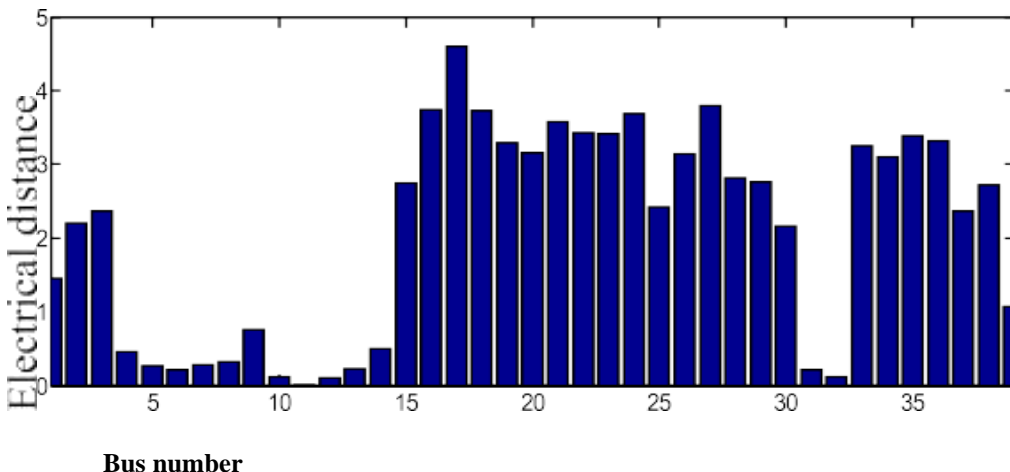


**Fig. 3.2 Electrical distance between bus and line**

### 3.7 Frequency stability

“The facility of an influence system to require care of steady frequency following a severe disturbance between generation and load”.

It depends on the facility to revive equilibrium between system generation and cargo, with minimum loss of load. Frequency instability may cause sustained frequency swings resulting in tripping of generating units or loads. At the time of frequency excursions, the characteristic times of the processes and devices that are activated will range from fraction of seconds like under frequency control to several minutes, like the response of devices like first cause and hence frequency stability could also be a short-term phenomenon or a long-term phenomenon.

Though, stability is assessed into rotor angle, voltage and frequency stability they need not be independent isolated events. A voltage collapse at a bus can cause large excursions in rotor angle and frequency. Similarly, large frequency deviations can cause large changes in voltage magnitude.

### **3.8 Rotor angle stability**

It is the power of the system to stay in synchronism when subjected to a disturbance". The rotor angle of a generator depends on the balance between the electromagnetic torque due to the generator electric power output and mechanical torque due to the input mechanical power through a prime mover [6]. Remaining in synchronism means all the generators electromagnetic 1.2 torque is strictly adequate to the mechanical torque within the other way. If during a generator the balance between electromagnetic and mechanical torque is disturbed, thanks to disturbances within the system, then this may cause oscillations within the rotor angle. Rotor angle stability is further classified into small disturbance angle stability and large disturbance angle stability.

### **3.9 Small-disturbance or small-signal angle stability**

"It is that the power of the system to remain in synchronism when subjected to small disturbances". If a disturbance is little enough in order that the nonlinear power grid is often approximated by a linear system, then the study of rotor angle stability of that specific system is called as small-disturbance angle stability analysis. Small disturbances are often small load changes like switching on or off of small loads, line tripping, small generators tripping etc. Due to small disturbances there are often two sorts of instability: non-oscillatory instability and oscillatory instability.

In this case, the system equation is often literalized round the initial operating point and therefore the stability depends only on the operating point and not on the disturbance.

Instability may result in:

1. A non-oscillatory or a periodic increase of rotor angle.
2. Increasing amplitude of rotor oscillations thanks to insufficient damping.

The first sort of instability is essentially eliminated by modern fast acting voltage regulators and therefore the second sort of instability is more common. In the time-frame of small signal stability is of the order of 10-20 seconds after a disturbance [5].

### **3.10 Large-disturbance or transient angle stability**

"It is that the facility of the system to stay in synchronism when subjected to large disturbances". Large disturbances are often faults, switching on or off of huge loads, large generators tripping etc. When an influence system is subjected to large disturbance, it'll cause large excursions of generator rotor angles. Since there are large rotor angle changes the facility system can't be approximated by a linear representation like within the case of small - disturbance stability. Long term voltage stability involves slower acting equipment like tap changing transformers and generator current limiters. Instability is due to loss of long-term equilibrium.

1. Power system stability mainly concerned with rotor stability analysis [2]. For this various assumptions needed such as:
2. For the stability analysis balanced three phase system and balanced disturbances are considered.
3. The deviations of machine frequencies from synchronous frequency are small.
4. During short circuit in generator, dc offset and high frequency current are present. But for analysis of stability, theses are neglected.
5. Network and impedance loads are at steady state. Hence voltages, currents and powers are often computed from power flow equation.

Step 1: Perform the initial operational load flow (or output of state estimation) to obtain the values of Lindex (voltage stability index) at each load bus and identify the voltage violations in the system.

Step 2: Advance the VAR control iteration count.

Step 3: Compute the column matrices ( $b_{\max}$ ,  $b_{\min}$ ) of the linearized upper and lower limits on the dependent variables.

Step 4: Compute the column matrices ( $x_{\max}$ ,  $x_{\min}$ ) of the linearized upper and lower limits on the control variables.

Step 5: Modify the matrices  $x_{\max}$  and  $x_{\min}$  to reasonably small ranges.

Step 6: Compute the sensitivity matrix ( $S$ ), relating the dependent variables and the control variables.

Step 7: Compute the row matrix ( $C$ ) of the objective function sensitivities with respect to the control variables.

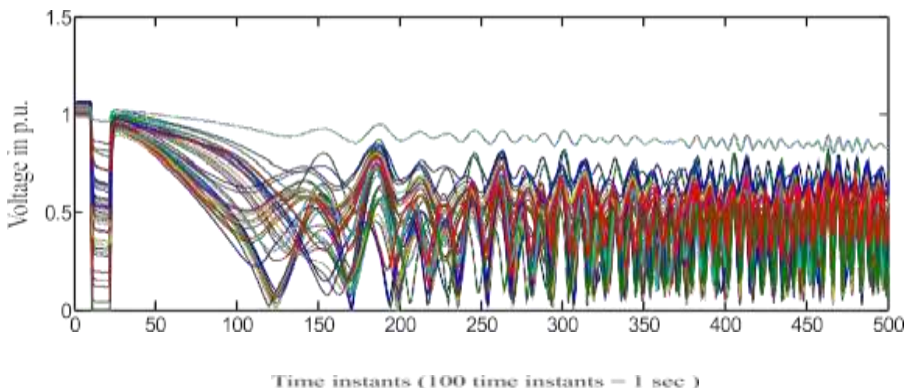
Fig. 6: Bus voltage response due to line

Step 8: Solve the optimization problem using the linear programming technique.

Step 9: Obtain the optimum settings of control variables[9,10].

Step 10: Perform the operational load-flow with the optimum settings of the control variables. Find the L-index for all the load buses in the system.

Step 11: Check for satisfactory limits on the dependent variables [3]. If no, go to step 2.



## Conclusion

The problem of voltage stability is that the basis of a topic within the research field of the facility system stability, the voltage instability is usually not isolated. In the analysis of voltage stability, power angle stability, rotor speed and frequency stability also are considered. The whole theoretical system of the study of power grid stability has not contingency. Nowadays power systems operations for static voltage stability, the following are the steps used to attain the optimal reactive power allocation in the power system for betterment and smooth flow of power in the system for voltage stability. With the event of voltage stability research, the important role of dynamic characteristics of composite load in voltage instability has become a standard consensus. Composite load, thanks to complex, variate, geographical dispersion and nonlinear characteristics, often adopts approximate simplified model within the actual simulation, which greatly affects the reliability of voltage stability analysis results. Therefore, established accurate and practical load model will greatly promote the event of voltage stability analysis. This paper is a relative study on static voltage stability that determines the causes of power loss in power system and voltage fluctuations in power supply so with the help of vast study on voltage stability.

## References

- [1] Eleonor Stoenescu, Jenica Ileana Corcău, Teodor Lucian Grigorie, Static Voltage Stability Analysis of a Power System, Proceedings of the 4<sup>th</sup> Iasme / Wseas International Conference on Energy & Environment (EE'09), ISBN:978-960474-055-0, ISSN:1790-5095, year 2009.
- [2] Janakrani Wadhawan, Mala Yadav, Updesh Pandey, Amit Kumar Kesarwani, A Review on Power Quality Problems and Improvement Techniques, International Journal of Engineering Research & Technology (IJERT), ISSN:22780181, July 2020.
- [3] Rohan Prakash, S.P. Singh, International Journal of Engineering Research & Technology (IJERT), ISSN:2278-0181, April 2018.

- [4] Loiy Rashed Almobasher, Ibrahim Omar A Habiballah, Review of Power System Faults, International Journal of Engineering Research&Technology (IJERT), ISSN:22780181, November 2020.
- [5] Mohammed Mynuddin<sup>1</sup>, K. M. Roknuzzaman<sup>2</sup>, Prodip Biswas<sup>3</sup>, Mohammad Tanjimuddin, International Journal of Energy and Power Engineering, ISSN:2326-957, November 2020.
- [6] Pinki Yadav, P. R. Sharma, S. K. Gupta, Enhancement of Voltage Stability in A Power System Using Static Var System, International Journal of Engineering Research & Technology (IJERT) Vol. 2 Issue 12, December – 2013, ISSN:2278-0181, December 2013.
- [7] Manish Kumar Saini, Naresh Kumar Yadav, Naveen Mehra, Transient Stability Analysis of Multimachine Power System with FACT Devices using MATLAB/Simulink Environment, IJCEM International Journal of Computational Engineering & Management, Vol. 16 Issue 1, January 2013 ISSN (Online):2230-7893, April 2020.
- [8] Youjie Ma, ShaofengLv, Xuesong Zhou and Zhiqiang Gao, Review Analysis of Voltage Stability in Power System, International Conference on Mechatronics and Automation, Tokyo, Japan, 2017.
- [9] M. V. Reddy , Yemula Pradeep, S. K. Murthy Balijepalli , S. A. Khaparde, Improvement of Voltage Stability Based on Static and Dynamic Criteria, 16th National Power Systems Conference, 15th-17th December, 2010.
- [10] A.S.Ravi, Ashutosh Dwivedi, Bhuvan Sharma, Voltage Stability Analysis, International Journal of Scientific & Engineering Research, Volume 4, Issue 6, June-2013.
- [11] Javad Modarresi, Eskandar Gholipour, Amin Khodabakhshian, A comprehensive review of the voltage stability indices, Renewable and Sustainable Energy Reviews 63(2016) 1–12, 3 May 2016.
- [12] Mohamed K. Jalboub, Haile S. Rajamani, Darwin T.W. Liang, Raed A. Abd-Alhameed, and Abdulbassat M. Ihbal, Investigation of Voltage Stability Indices to Identify Weakest Bus (TBC), J. Rodriguez, R. Tafazolli, C. Verikoukis (Eds.): MOBIMEDIA 2010, LNICST 77, pp. 682–687, 2012

# **Energy conservation in educational institution and reduction of electricity bill by using IOT.**

**M. Veerasundaram, K. Narmadha and S. Snega**

**Abstract** It is well known truth that energy requires adequate of time to regenerate. This energy must be preserved in order to decrease the extent of toxic gases freed by the power plants and the effect of famine in future. Energy saving is also protect the earth's natural treasure and shield ecosystems from destruction. Sustaining and consuming the energy at the exact proportion ends in the progress of public and environment. A definite person's small effort to support energy can create a lot of value for the society. Not only how the energy is sufficiently used but also conserved proficiently is illustrated in this case study. The approach used here reduces the use of Energy to a requirable amount. By altering lights to ecofriendly bulbs can save electricity and money.

**Keywords:**LED lights; Sensors; ordinary tube light; energy; switches.

## **1. Objectives**

The vital sources in our earth is electricity.so its not yours, its not mine, its our duty to save the electricity for the environment. But we are wasting electricity in many times mainly in educational institutions. To overwhelm this issue in our institution, we make a step to prevent the waste of electricity. In order to save electricity we replace ordinary fluorescent lamp(Tube light) by conventional bulbs in classroom. The power consumption of conservative bulb is very less and has extremely high efficiency then to the normal bulbs. Another obstacle is that many persons forget to turn the fan off later they finished use up it. This can be regulated by automatic turn on/off of switches by

---

M. Veerasundaram  
Dept of EEE, Sri Sairam Institute of Technology, Chennai, India  
Email Address : [veerasundaram.eee@sairamit.edu.in](mailto:veerasundaram.eee@sairamit.edu.in)

K. Narmadha.  
Dept of EEE, Sri Sairam Institute of Technology, Chennai, India  
Email Address : [Sit19ee015@sairamtap.edu.in](mailto:Sit19ee015@sairamtap.edu.in)

S. Snega.  
Dept of EEE, Sri Sairam Institute of Technology, Chennai, India  
Email Address : [Sit19ee041@sairamtap.edu.in](mailto:Sit19ee041@sairamtap.edu.in)

sensors. The key thought behind this case study statement is helps to saving electricity by energy reduction consumption.

## 2. Introduction

In the recent years people are looking towards the automation in their day to day life(1). And some of the people are also excited to save the energy paid everyday, but they are simply becoming lazy to turn off the light switches while exit the room(2). This occurs due to casualness or we forget to turn off the light and fan switch when we are in rush(3). The wastage of excess electricity is one of the main problem which we are facing now a days(4). In our home, college, school or industry we are seeing that fan or light are kept ON even if there is nobody in the classroom or passage(5). To avoid such situations we created a way for Automatic room light and fan regulator. In this case study report there are two modules. The first one shows the conservation of electricity by Light Emitting Diode(LED) showed in "figure 1"and the second module shows the automatic room light and fan regulator with the Arduino based device. Using this automation in switching the lightning system afford more energy to conserve which in turn save money for the institutions.



Figure1. Light Emitting Diode

## 3. Motivation

We always looking forward to smart and automation even in all the simple tasks and also we are aiming to lower human efforts. The automatic switching of the lighting system reduces the human efforts. By using this automatic room fan and light regulator, the person will not give certain care for turning OFF the lights while he/she leaving the room. This system also helpful in reduce the power wasted by all the electrical appliances and home appliances. This also helpful in the pandemic situation to count the no of people entered in the room and so crowding of people get avoided. The cost of the device is also less and it can installed even in houses, hospitals, government offices and industry. We use this device for nearly 20 classrooms in our institution.

## **4. Description**

### **4.1Module 1**

We can save electricity by using LED light in its place of using usual tube lights. “Figure. 2” On comparing the LED light with ordinary tube light the LED has high efficiency. The LED is composed by nonharmful substances and so it is safe for everyone. But our normal tube light is made by mercury and lead which is harmful to health. The LED lights are reusable! so there is no disposal problems. The energy core LED lights last far longer than the ordinary fluorescent tubes. The current LED specification measurements state our LED light can withstand 80,000 hour of testing. This means an LED lights will compensate for itself all over a time. On standard, the electrical consumption cost is 27% of an institution budget. LED light can slash costs down drastically with its efficiency. The LED light needs 26 watts(W) and the turnout is about 3334lumens(lm) thus, transmuting in to nearly 130 lumens per watt! There is a plenty of light for such small voltage. But the normal fluorescent tubes can gives about 50-100 lumens per watt. As the ordinary tube light produce a lot of energy but it get transformed in to heat instead of light and so much more energy is wasted in the form of heat. The LED tube relics pretty cool, so extreme amount of light beams can be produced, while there is a slight to no lavish heat produced. The moststrong change you notice with the LED is how strictly it be like with the natural light. This is for the reason that all continuum of color are signified in LED chips and so it can produce such a bright light.



Figure2. LED Tube light Vs Fluorescent Tube light

## 4.2 Module 2

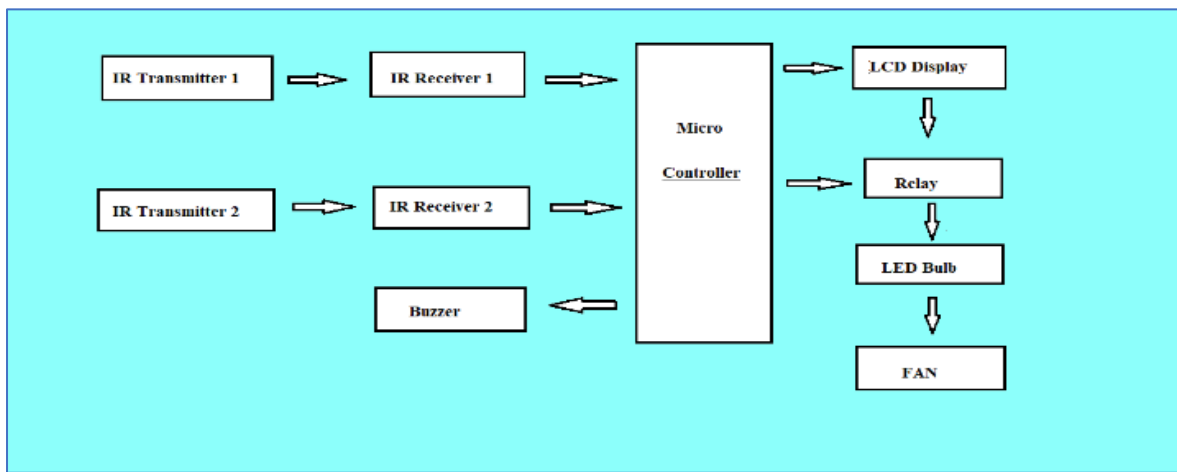


Figure3. Process Description

In the modern world we want every portable thing around as to be mechanized which eases human efforts. There are multiplying electrical circuits that create today's lifespan easier. Similarly we create a work that valuable for the students neglect to turn off fan and light while leaving the room. The Automated room light and fan regulator has the elements like two transmitters, two receivers, one microcontroller, relay and LCD display. The "Figure 3" and "Figure 4" displayed the block diagram of the automatic room light and fan regulator.

### 4.2.1 Components

**A) Infrared Transmitters:** There are two infrared sensors having infrared transmitters and infrared receivers. The aim behind selecting this infrared transmitters is, the infrared beams are not detectable to human eyes and are not simply actuated by exterior resources. The Infrared transmitter 1 senses the number of people go into the room and Infrared transmitter 2 senses the number of people departing the room. These two transmitters use the Infrared LED, helps for detecting to object which cuts the light radiated by the diode and then the light recoils in to return from the object to the transmitters.

**B) Infrared Receiver:** There are two Infrared sensors works as a receiver. It can effectively act as a low device, which means it hands low turnout when it accepts infrared rays. When an infrared rays are disrupted by any one, then the microcontroller will sensing a extreme pulse from the IR receiver.

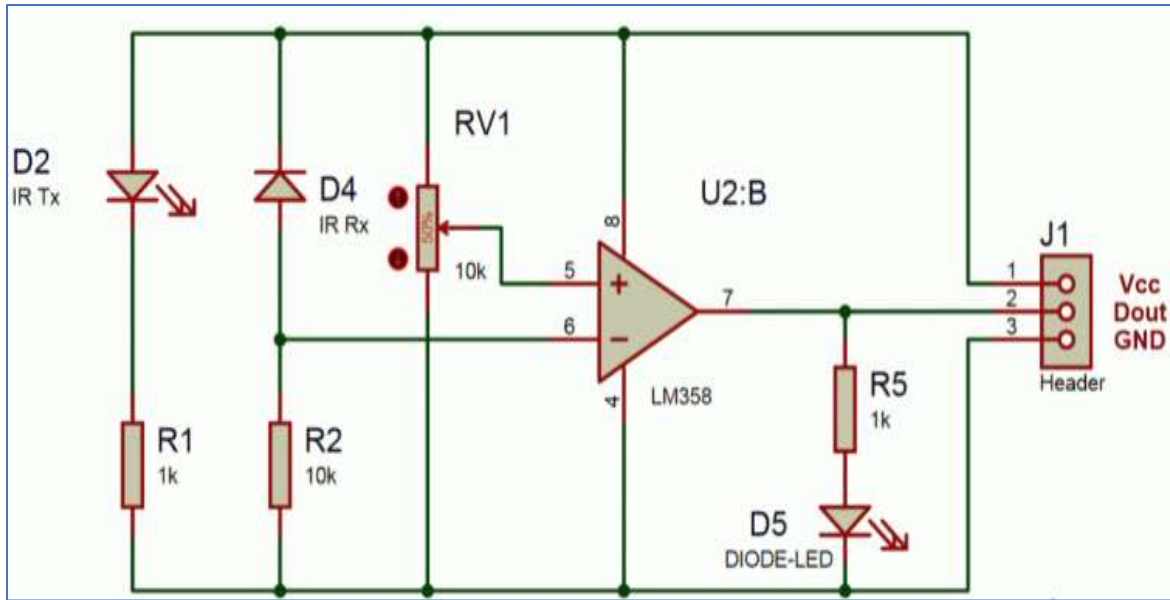


Figure4. Circuit Diagram

**C) LCD display:** An alphanumerical Liquid Crystal Display(LCD) is sourced and it fixed in outdoor of the classroom. It shows the implication like “People Counter Incremented”, “People Counter Decrement”, “No of people in the classroom=ABC” where ABC is the actual person count.

**D) Microcontroller:** The microcontroller 89s51 taken from the microcontroller category. These microcontrollers find response from the two Infrared receivers and then estimate the number of persons. The microcontroller sent the reading values of person count to the LCD display. The microcontroller turning on the light when person count up is greater than or equal to one. When the person count up is equal to zero means microcontroller just turn off the lights.

**E) Relay:** The microcontroller couldn't on directly, we have to connect a relay circuit. This circuit contains a transistor that helps to turn on the relay circuit through the microcontroller. Here a (SPDT)single pole double throw relay is utilized.

## 5. Code explanation

This Arduino based device used here are coded with the C programming for the working of the standard libraries. The Arduino core functions are generally a set of C classes and libraries that can be easily include in our devices. Library is included here for LCD. We have designed the input pin and the output pin for relay and also for the sensors. Direction is given to input pin and output pin and LCD is initialized here in set up loop. Loop function is included here where input is read. The counting can be incremented or decremented which is based on whether the operation should be entered or exited. Zero condition is also checked whether it is true or false. If the zero condition is true then then bulb is turned off. This is done by the Arduino. Arduino deactivates the relay by the transistor. The “figure 5” shows the coding for this device.

On the begin of the code a header file named as standard liquid crystal. Then the liquid crystal library is included for the LCD and then pin also defined to the same. The function named with the liquid crystal LCD is defined for the relay network and the sensors. For the IN variable, the value fourteen is assigned and for the OUT variable the value nineteen is assigned. The relay value is designated as 2. The integer variable initially assigned to zero. The first function void IN() with loops gives the direction to the output pin and initialized LCD in the setup loop.

In this loop functions the input value is defined with the detection of the persons entering the room. The input value get incremented or decremented based on the enter or the exit operation. Initially the lcd remains clear and people entering means the function set the cursor of LCD display with(0,1) and it shows the person count for the time delay of every 1 minutes and 10 seconds. If the counting value greater than or equals to ten means the input value get started to increment. Secondly the function defined with void OUT() under loop for counting the people leaving the room under the exit operation. If the counted value is equal to or less than zero means the value get decremented and the LCD displays the person counts at that time. Here, the time delay is also same as the input function. Thirdly the function shows the entire operation of the device. The function is named with void setup(). This function only decides to the which function get executed from both the conditions. If the count tends to zero means this Arduino based devices turns off its light thus the second function get executed and if this zero conditions fails that is false means the Arduino turn on the LED light by considering the first function in the program

When person enters in room means the Infrared signal bounces back its signal and get received by the IR receiver. By this entry the count is incremented and if the person leaving means the count get decremented. When the person's count is greater than zero means the relay get turned high, then the fan and room light get turned ON automatically. Likewise when persons count is less than or equal to zero means the turned to zero means the relay gets low and thus the fan and light in rooms get turned off automatically. This takes place in the arduino based device and the output also verified correctly.



The screenshot shows a code editor interface with the following components:

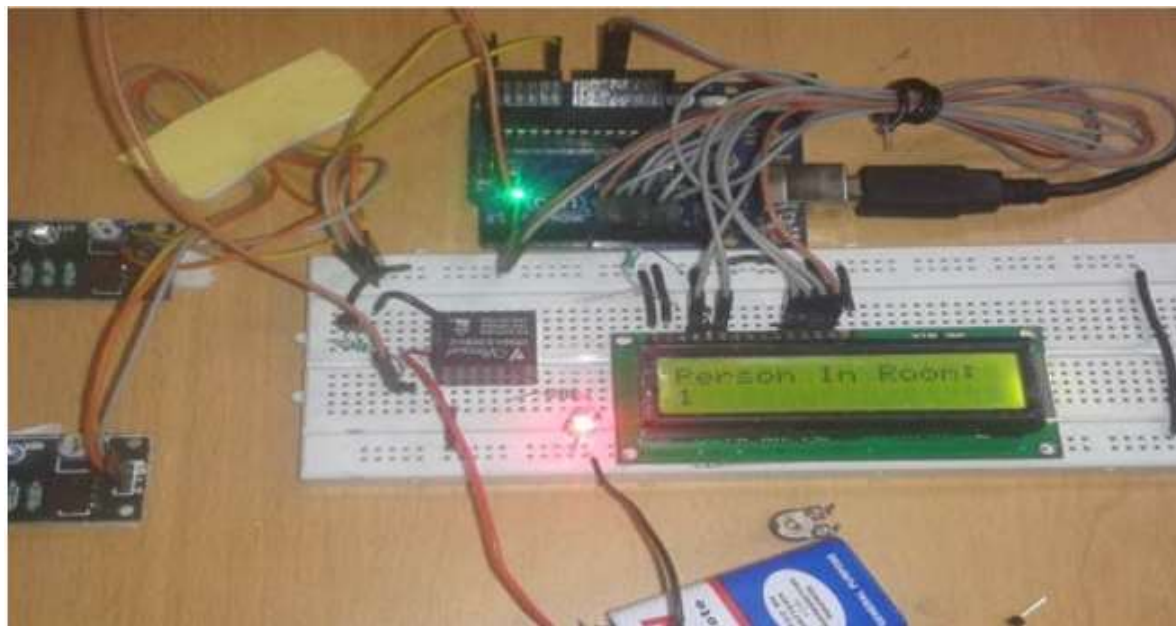
- Top bar: "Ardu" (dropdown), "C (gcc 8.4)" (dropdown), and "Select" button.
- Code area:

```
#include<LiquidCrystal.h>
LiquidCrystal lcd(13,12,11,10,9,8);
#define in 14
#define out 19
#define relay 2
int count=0;
void IN()
{
    count++;
    if(count>=10)
    {
        count=10;
    }
    lcd.clear();
    lcd.print("Person In Room:");
    lcd.setCursor(0,1);
    lcd.print(count);
    delay(1000);
}
void OUT()
{
    count--;
    if(count<=0)
    {
        count=0;
    }
    lcd.clear();
    lcd.print("Person In Room:");
    lcd.setCursor(0,1);
    lcd.print(count);
    delay(1000);
}
void setup()
{
    lcd.begin(16,2);
    lcd.print("Visitor Counter");
    delay(2000);
    pinMode(in, INPUT);
    pinMode(out, INPUT);
    pinMode(relay, OUTPUT);
    lcd.clear();
    lcd.print("Person In Room:");
    lcd.setCursor(0,1);
    lcd.print(count);
}
void loop()
{
    if(digitalRead(in))
        IN();
    if(digitalRead(out))
        OUT();

    if(count<=0)
    {
        lcd.clear();
        digitalWrite(relay, LOW);
        lcd.clear();
        lcd.print("Nobody In Room");
        lcd.setCursor(0,1);
        lcd.print("Light Is Off");
        delay(200);
    }

    else
        digitalWrite(relay, HIGH);
}
```

Figure 5. Sample code



The automated room light and fan regulator controls the switches of room lights and the fans shown in the "Figure 6". When an individual goes into a classroom means the counter get counted to one and only one light in the room will be switched ON and when the individual exit the classroom, then counter will get decounted to one. when the numbers of individual is greater than five means, two lights will be switched ON and the fan also get switched ON. When an individual in the room is more than ten, three lights will be switched ON. Likewise on increases of every five individuals one more fan will be switched ON. Light will turn OFF when all the individuals go out off the classroom. The total students present inside a room is also displayed on the LCD. The microcontroller and the IR sensors have done all this jobs. When the numbers of person inside the room is equal to zero means lights and fans inside the room get turned off. This results in reduction of unnecessary power wastage.

Realistically speaking, both of the sensors must be placed on either side of the door or at the entrance of the classroom. This can able to save the electricity and avoiding wastage. The key benefit of this automated system is energy maintenance and it can also utilized as home automation system. It also avoids the problem of short circuit and circuit breakage. The cost of this project is nearly 4000-4500 and circuit can be designed certainly. The sensors used here should not get disrupted by atmospheric conditions. Here the only shortcoming is one person can cut the rays of sensors and then it receives correct input. Since it cannot be used for two or more people crosses the door region simultaneously. When anyone is inside the room and we need to switch off the power means then we have do it by manually

## 6. Case study report

This Table 1 shows the complete power usage of all our loads. In our college we almost use nearly 351550.8 units for an year. For educational institutions the energy charges is 6.35 Rupees (Rs) per unit and the demand charges 350 Rs/kVA/month. The sanctioned

load is nearly 70 kW/h. The average annual electricity charge of our institutions is Rs 5,25,757 per year. This indicates that we are consuming more electricity in our college. The average amount we are spending for two months is Rs 87626. So it is essential for us to save energy in our college. The “Figure 7” shows the different types of components using in our institutions.

Name of the load	No of components	Rating of the equipment(w)	Connected loads[w]	Hours used per day	No of days in year	energy consumption per day in watt hour	energy consumption per day in (KW\h)	Energy consumption per year in watt hour	consumption
Tube light	740	40	29600	8	215	236800	236.8	50912000	50912
Fan	602	60	36120	8	215	288960	288.96	62126400	62126.4
Projector	4	165	660	4	215	2640	2.64	567600	567.6
Computers in lab	175	150	26250	6	215	157500	157.5	33862500	33862.5
Exhaust fan	8	50	400	8	215	3200	3.2	688000	688
Photo stat machine	2	900	1800	2	215	3600	3.6	774000	774
Power sockets	27	1000	27000	6	215	162000	162	34830000	34830
Ordinary sockets	417	100	41700	6	215	250200	250.2	53793000	53793
Water Cooler	2	200	400	6	215	2400	2.4	516000	516
Overall load in EEE labs			64400	6	215	386400	386.4	83076000	83076
overall load in Mechanical labs			23570	6	215	141420	141.42	30405300	30405.3
						Total units	1635.12	351550800	351550.8

#### (A) Energy consumption without using sensors

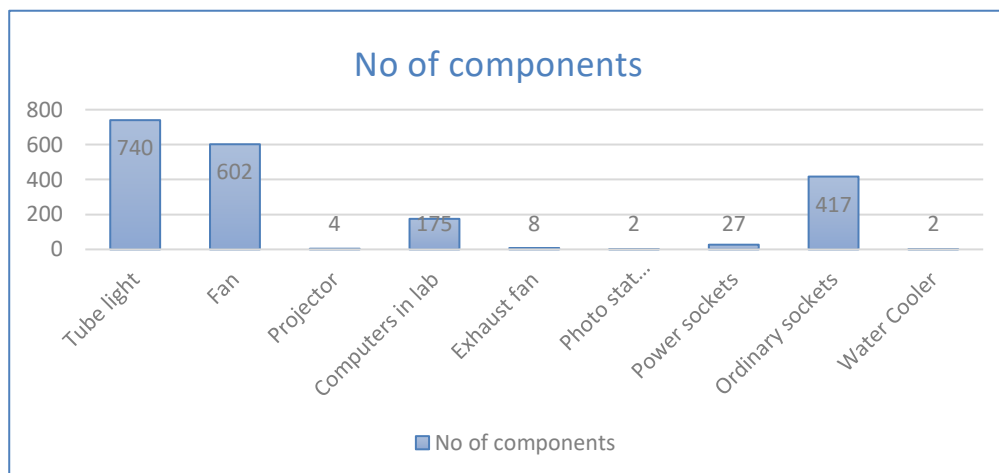


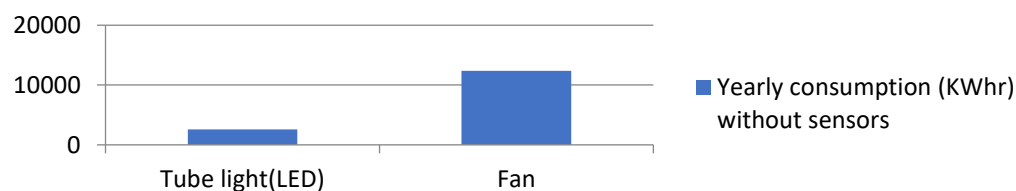
Figure 6. Types of components

For saving energy we are take 20 classroom and in every classroom we replace the ordinary fluorescent tube by LED tube light with 25 watts. The ordinary tube light we are using in our college is of 36 watts. The little variation can help in saving the usage of electricity consumption. The Table 1 explains the energy conservation in twenty classroom. There are 60 LED tube lights and 120 fans are there in our college. The energy consumed by LED tube light for one day is 12 kilowatt hours. Then the yearly consumption of LED tube light 2580000 hour respectively. Before fixing this Sensors in the classrooms the average annual energy consumption is calculated as totally 2580 units. The “Figure 8” explains the energy consumed by the tube light and fan without using sensors.

Name Of the load	Tube Light(LED)	Fan
No of components	60	120
Watts Rating	25	60
Total consumption in watts	1500	7200
Hours of usage	8	8
Days of usage in a year	215	215
Energy consumption per day(Whr)	12000	57600
Energy consumption per day(Kwhr)	12	57.6
Yearly consumption(Whr)	2580000	12384000
Yearly consumption (KWhr) without sensors	2580	12384
<b>TOTAL</b>		14964

For an individual classroom we use 3 tube lights and for 20 classroom we are using nearly 60 tube lights. The price of single LED tube light is about 350. The price for sixty bulbs in twenty classroom is Rs 21000. This installation cost of LED tube light is high when compared to the ordinary tube light, but the efficiency of LED light is appropriate high. The total units for LED light consumption is nearly 2580 kilowatts per year which is very low as compared with the units carry over by electricity. The LED bulb can saves up to the unit of 1135.2kw/ This definitely helps in decreasing the electricity bill. For light bulbs led bulbs used and for the fan we are go our automatic room fan regulator. Before using automatic systems the fan alone consumes nearly 57.6 kwhr for a day and 12384000 for an hour. The average energy consumption before using this sensors is 12384 KWhr.

### Yearly consumption (KWhr) without Sensors



The LED bulb saves the energy a lot similarly, we fix the automatic room light and fan system in the twenty classrooms. This device supports in saving the energy and money.

### **(B) Energy consumption with sensors**

Next, after fixing this device in every classroom we did a report for the same 60 lights and 120 fans. The electricity wastage is prevented and we regularly monitor the devices and also reduced the usage hours from eight to six

Name Of the load	Tube Light(LED)	Fan
No of components	60	120
Watts Rating	25	60
Total consumption in watts	1500	7200
Hours of usage	6	6
Days of usage in a year	215	215
Energy consumption per day(Whr)	9000	43200
Energy consumption per day(KWhr)	9	43.2
Yearly consumption(Whr)	1935000	9288000
Yearly consumption (KWhr) with sensors	1935	9288
<b>TOTAL</b>		11223

The second table shows the energy conservation of the LED tube light and Fan after the installation of the sensor based device. The energy consumed by the LED lights and fan of one day is reduced greatly of about 9KWhr and 43.2KWhr. Then the yearly consumption of the LED and fan are also reduced from 1935000watt and 9288watt hours which is very much less than the previous calculation. Thus the energy saved and utilized successfully. The “Figure 9” is the graph plotted for the tube light and fan to depicts its consumption.

The “Figure 10” and “Figure 11” shows the average of energy difference of the LED tube light and fan in the classroom by with and without using the sensor devices.

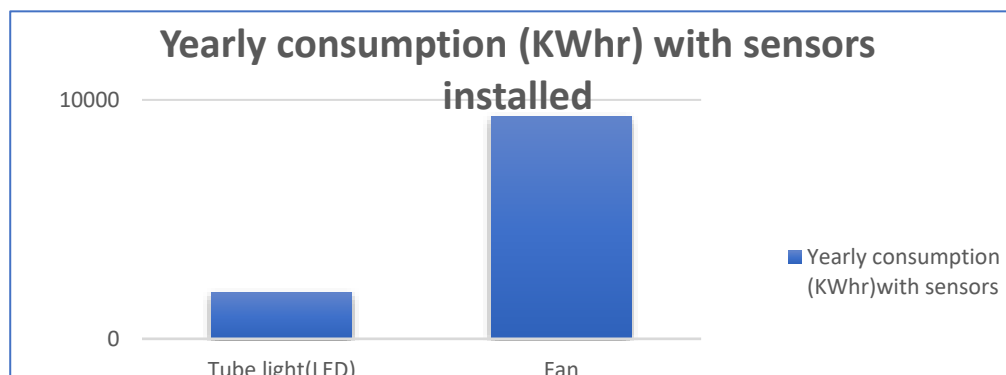


Figure 9. Energy consumption with sensors

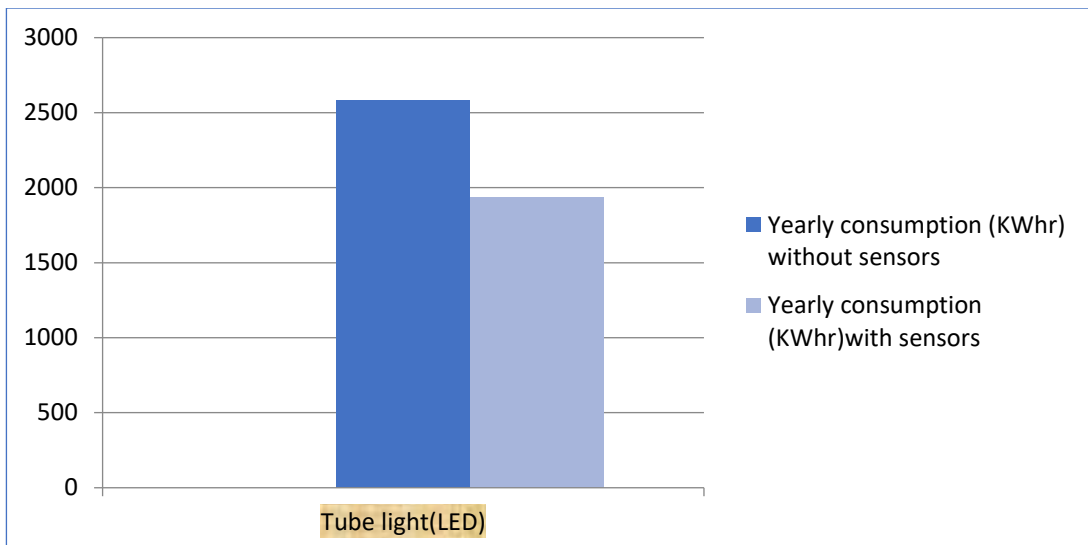


Figure7. Energy utilized by LED tube lights

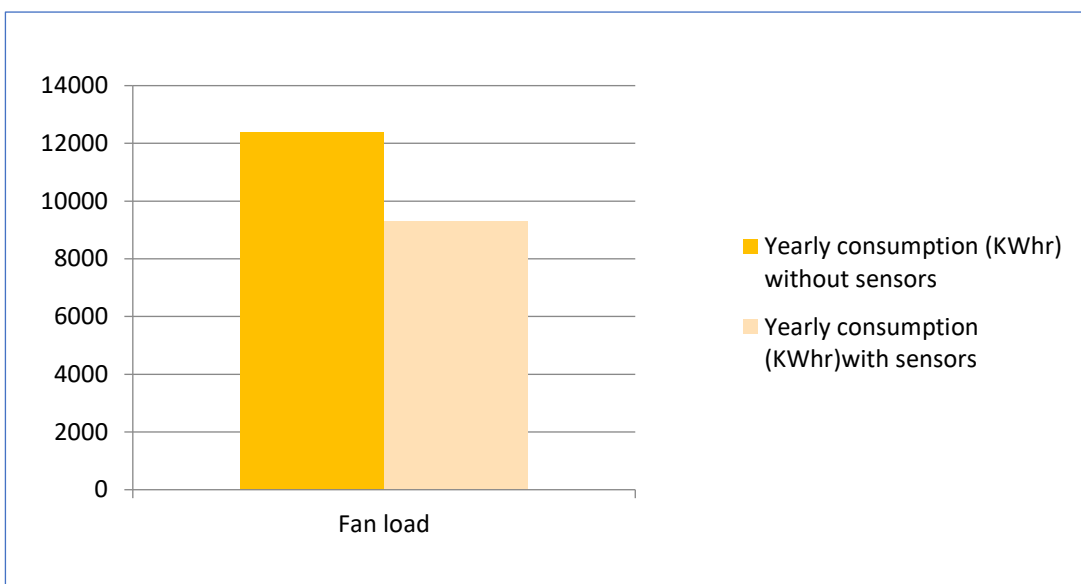


Figure 11. Energy utilized by fan

Our college spend nearly Rs 40000 for installing this automatic room light and fan controller. This device monitor and exactly turn off the switches in the room when students leave the classes. The net unit saved after few months of installation of device is about 235000 kw/h. This surely reduce the electricity consumption. This sensorbased circuit will also help to find the count of students in the classroom and it is necessary in the pandemic situation. Now we are decided to used it in various rooms like meeting hall seminar hall and conference hall, where the capacity of rooms is limited

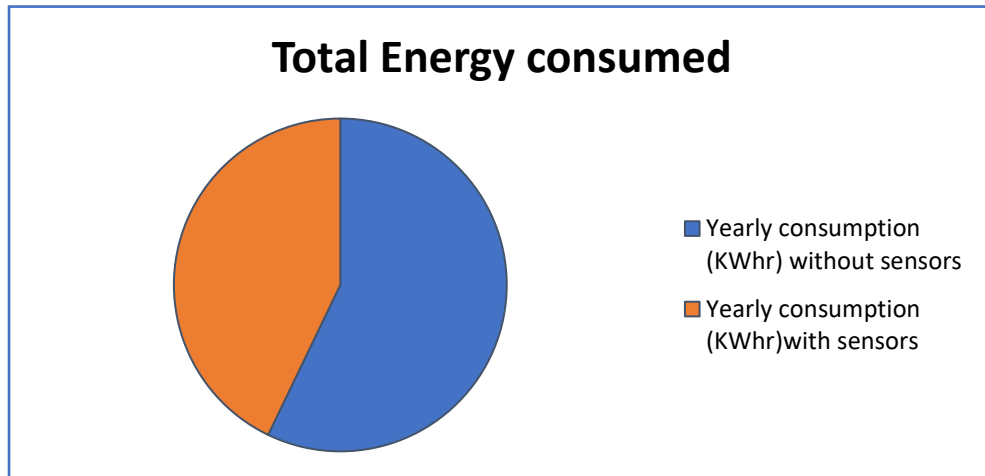


Figure8. Annual Energy consumption

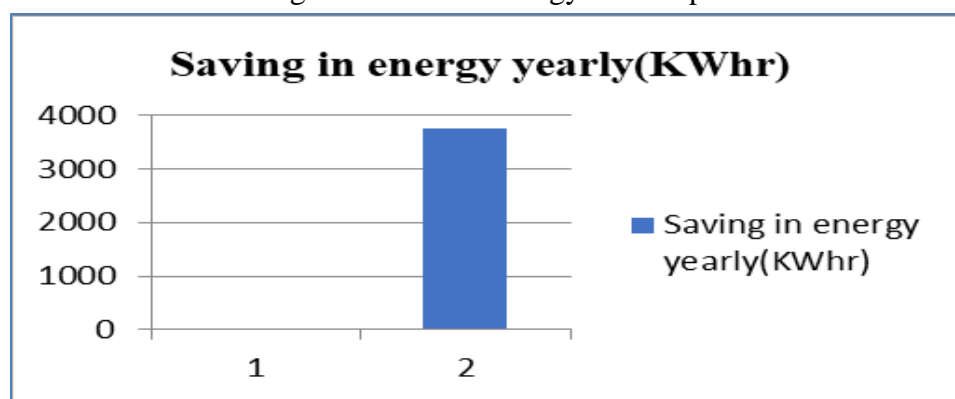


Figure 13. Saved energy results

The average annual unit calculated in our college is 3435094.56 kwh for an year which shown in the pie chart labelled with “Figure 12”. By taking difference between this units we saved up to 3785 kwh for an year. This savings are shown in the “Figure 13”. The costs can also reduced up to Rs 87626 to Rs 85574 for a month. The saving is about Rs 2052. By using this circuit with proper power supply we can implement for various applications in home. We can also insert voice alarm inside the room to indicate that the room is filled. Through using this automatic room light and fan controller can helps in saves the electricity bill yet we also have to provide some measures to prevent the wastage of electricity.

## Conclusion

Electricity is very precious. We have to avoid wasting it by knowingly or unknowingly. Saving electricity will be very useful in our future life. Many researches is being done on generating electricity from various sources. Researchers do research on saving electricity since it is very important now a days In this project, research is done on automatic room light and fan controller in classrooms. This method saves much electricity. It is well known that generating electricity is a very difficult thing. So these energy must be conserved properly. People will be able to save power in an adequate amount. This

method also reduces the tension of people. They need not worry whether they have turned off the fan and light switches in their living place.

## References

- [ 1.] V. Soldatkin, V. Tuev, Y. Yulaeva, K. Afonin, A. Vilisov and V. Kamenkova, "Operation Characteristics of LED Filament Bulbs," 2018 XIV International Scientific-Technical Conference on Actual Problems of Electronics Instrument Engineering (APEIE), 2018, pp. 376-379, doi: 10.1109/APEIE.2018.8545675.
- [ 2.] A. Yadav, R. K. Pachauri and Y. K. Chauhan, "Power quality improvement using PFC SEPIC converter for LED bulb adaptable for universal input voltage," 2016 IEEE 1st International Conference on Power Electronics, Intelligent Control and Energy Systems (ICPEICES), 2016, pp. 1-6, doi: 10.1109/ICPEICES.2016.7853725.
- [ 3.] D. Xing and J. Li, "Circuit Switch Automatic Shutoff Technique for Electrical Equipment Based on Big Data Analysis," 2020 IEEE Conference on Telecommunications, Optics and Computer Science (TOCS), 2020, pp. 109-112, doi: 10.1109/TOCS50858.2020.9339753.
- [ 4.] S. H. Kim and S. Lee, "A new high-performance led converter with separation of the ac and dc driving parts for a t8 led tube," in IEEE Access, vol. 7, pp. 61433-61441, 2019, doi: 10.1109/ACCESS.2019.2904524.
- [ 5.] A.W. Louw and C. Neethling, "Digital LED lighting solutions," pp. 1-4, Proceedings of the 21st Domestic Use of Energy Conference, Cape Town, 2013.
- [ 6.] L. Lei, Z. Wang and Y. Li, "Analysis on the effectiveness of detection and alarm of cable corridor," ICFSFPE chengdu, china, pp. 1-7, doi: 10.1109/ICFSFPE48751.2019.9055788. [9th international conference on fire science and fire protection engineering.

# **Design of Experiment for IoT Based Condition Monitoring and Detection of Hot Spots in Tank of Oil- Immersed Transformers**

**Vinit Mehta, Jayashri Vajpai and Tarun Ojha**

**Abstract** Oil- immersed power or distribution transformers play a key role in the interconnection of power systems at different voltage levels. Therefore, it is very important for these transformers to operate within the safe limits prescribed by the power system designers. The safe operation and loading limit of these transformers is decided by the thermal limits of the insulation used in the design of these transformers. The heat transfer takes place within and across oil- immersed transformer tank walls. However, there may be some heat accumulation in certain areas inside oil- immersed transformers that may result in development of high stress points or hot spots under critical or abnormal operating conditions. Therefore, continuous monitoring of interior temperatures of oil- immersed transformers becomes essential for keeping a check on the development of hotspots and in order to localise the position of the hot spots. This paper presents an IoT based design of experiment for monitoring of temperature for identification of hot spots. This is based on a scaled down hardware model fitted with temperature sensors working along with a decision making module for localisation. This is implemented with the help of four temperature sensors placed in a cubical tank which is filled with transformer oil. The location of these hot spots is sent to the control room before any unprecedent rise that may lead to damage or failure. The proposed experiment is expected to be useful to design a condition monitoring system that can be scaled and implemented in the oil- immersed power or distribution transformers in order to exactly locate the position of hot spots inside the transformer tank.

**Keywords-** Oil- immersed power or distribution transformers, heat transfer, hot spots, condition monitoring, Internet of Things (IoT).

## **1. Introduction**

Oil- immersed power and distribution transformers play a vital role in the safe and reliable operation of power system for maintaining continuous and reliable electrical supply right from generating end to the consumer end. These are popularly known as oil natural air natural (ONAN) class of transformers. With the increase in the demand at the utility end, these transformers are often operated at rated or overloaded conditions. This may result in the failure of the winding insulation inside the transformers caused by development of high stress points or hot spots under abnormal or critical operating conditions. Therefore, it is very important to continuously monitor the temperature at several critical positions inside the transformer tank to identify the development and location of these hot spots inside the oil-immersed transformers. This requires modification in design and proper prognosis measures to be taken by the operating staff and field engineers in order to operate the transformer within the safe limits. Further, the operator has to ensure that the loading on the transformer is controlled within prescribed operating limits to avoid the rise of interior temperatures beyond the tolerance thresholds. In either case,

---

Vinit Mehta

Research Scholar, Department of Electrical Engineering, M.B.M. Engineering College, Jodhpur, India  
Email Address : vinit741@gmail.com

Jayashri Vajpai

Professor, Department of Electrical Engineering, M.B.M. Engineering College, Jodhpur, India

Tarun Ojha

Department of Electrical Engineering, M.B.M. Engineering College, Jodhpur, India

continuous monitoring of interior temperatures of a transformer along with loading condition is essential for localization of the hot spots.

In the conventional design of oil- immersed power and distribution transformers, winding temperature indicator (WTI) and oil temperature indicator (OTI) are used to indicate the winding temperature and top oil temperature of the transformer respectively. These indicators consist of a thermocouple based sensor bulb, a capacity tube, and a dial thermometer. The sensor bulb and capacity tube are fitted with evaporation liquid. The vapor pressure varies with temperature and is transmitted to a bourdon tube inside the dial thermometer, which moves in accordance with the changes in pressure that is proportional to the temperature. However, this type of measuring system only measures the temperature at two or three specific locations inside the power and distribution transformer. Therefore, the hot spots developed at some other places inside the transformer cannot be monitored with the help of these indicators. Such hot spots may develop over the core, windings or inside the transformer tank along different surfaces, whenever the heat dissipation is not uniform or effective. These hot spots may also get formed, if undesirable material or dust enters the transformer tank during the regular maintenance procedures. Occasionally, these hot spot areas may become severe if the insulating oil does not reach or circulate properly or somehow the heat is not dissipated properly, or heat dissipation is slow (or less) in comparison to heat generation. Such heat accumulation results in high temperature, which reduces the life of the oil- immersed power and distribution transformer drastically or may even damage the transformers permanently.

The main reason for the increase in the temperature inside an oil- immersed power transformer is the power losses that occur in the windings and core. In addition to this, losses occur in transformer tank walls and end plates on account of eddy currents. All these losses are converted into heat energy and the temperature of certain parts of the transformer rises above the temperature of the ambient medium. The heat thus generated in an oil- immersed transformer is dissipated to the surrounding ambient medium through one or more of the possible modes of heat transfer- conduction, convection and radiation as shown in Fig.1.

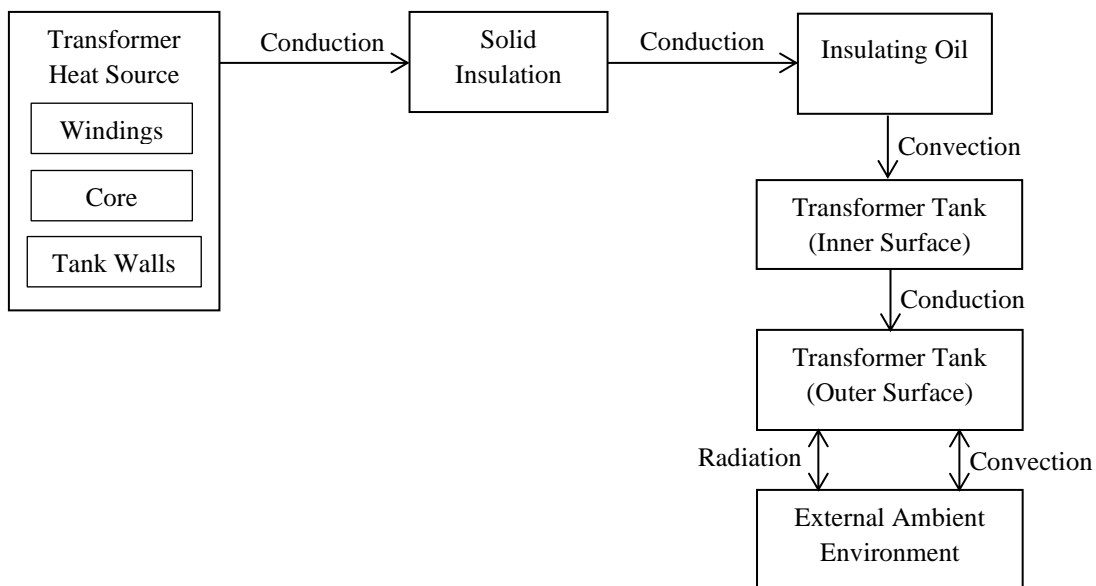


**Fig.1. Heat Transfer Process in Power Transformer**

The insulating oil circulating inside an oil- immersed transformer absorbs heat from the windings and core through conduction. The heat carried by the solid insulation and insulating oil is transferred to the transformer tank inner surface by convection and further to outer surface through conduction, and finally from the outer surface to the external ambient environment by convection and radiation. This heat is dissipated to the ambience through natural means or by forced cooling methods by using suitable coolants. The various mediums used for the cooling purpose in the oil- immersed transformer are air, synthetic oils, mineral oils, gas and water. Different cooling methods with suitably designed heat exchangers are used depending upon the quantity of heat to be handled for proper heat exchange inside an oil- immersed transformer. There may also be some external or surrounding conditions too that affect the inner temperature of oil- immersed transformer significantly. These conditions that impact on the heat dissipation process may include natural conditions as well as built- in conditions. The natural conditions include the effect of solar radiation, wind, rain, dust, natural landscape and humidity and the

built-in conditions include transformer external layout, sheds, buildings, abstractions and design of enclosures, etc.

Therefore, a distributed multi sensor temperature monitoring system that covers the entire exposed areas of the windings and core in all dimensions is an essential part of condition monitoring system. This paper presents an IoT based design of experiment to build a scaled down hardware model (as shown in Fig.2.) for tank of transformer that may be useful to develop a system for monitoring the temperature at all the exposed surfaces inside the oil-immersed power and distribution transformers. The system is suitable for surveillance of development of hot spots in order to take corrective measures and timely action for control of damage to the transformer and the associated power system.

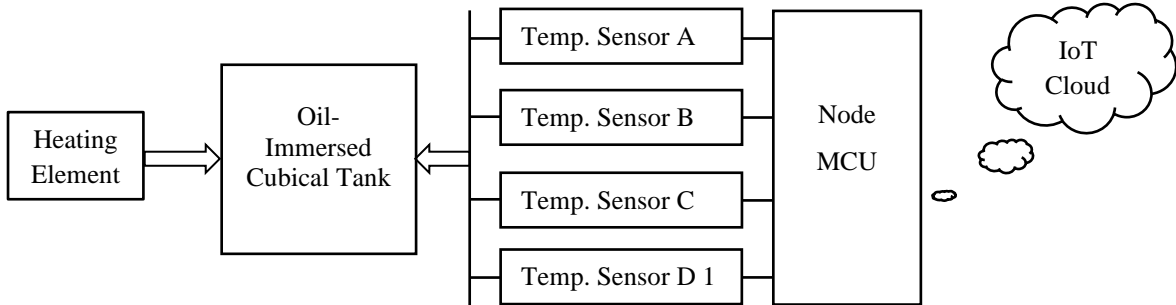


**Fig.2. Block Diagram of IoT Based Design for Monitoring Hot spots**

The proposed model comprises of a heating element inside a cubical tank fitted with four temperature sensors. It acquires the data from the sensors and applies a decision making process to identify the location of the hottest area and also sends the information of that area to the remote control centre using Internet of Things (IoT) for corrective measures.

This paper is divided into 5 sections. After introduction, the paper includes five more sections that present the literature survey, proposed methodology, system architecture, results and discussions followed by conclusions.

## 2. Literature Survey

A literature survey was conducted for creating background for research on hot spot monitoring and protection of oil-immersed power and distribution transformers in order to support prognosis of faults and abnormal operating conditions. IoT based methods for monitoring the temperature inside the transformers have been proposed by many authors.

Rohit R. Pawar et. al. [1] have developed an embedded system for monitoring the current, temperature, oil level, vibration and humidity of a distribution transformer. The system sends the alarm message to the mobile phones about the abnormality with the help of microcontroller. Rohit R. Pawar et. al. [2] have also developed a remote terminal unit for analysing different parameters of the distribution transformer using GSM/ GPRS modules. T. K. Roy et. al. [3] have designed IoT based real time and periodic monitoring system for distribution transformers located at far places from the central control room. They have concluded that IoT based system is economical as compared to the GSM based monitoring system that offers comparatively less control for periodic maintenance. D. Srivastava and M.M. Tripathi [4] have employed IoT for monitoring the temperature, voltage and current values of the distribution transformer for acquiring the real time conditions so that necessary action may be taken to avoid the outage of the electricity supply in case of any fault. R. De. Giorgi et. al.[5] have modeled heat transfer phenomena during the charge or the discharge of a tank for complex circuit simulation and for the identification of instantaneous mass flow rate.

L. Thangiah et. al. [6] have combined the key aspects of edge computing and intelligent agents for experimental condition monitoring of distribution transformers. H. Jamal et. al. [7] have developed IoT based thermal modeling and protection system for distribution transformer under residential loads for monitoring the overloading and internal hydration that may result in overheating and short circuit. The collected data from the distribution transformer is send to ThingSpeak server for real time monitoring, analysis and control. W.K.A. Hasan et. al. [8] have developed an IoT based protection system for the power transformer that can disconnect the less essential loads while keeping the more essential loads in service during the maintenance period. In case of more severe conditions, the system can disconnect all the loads from the power transformer automatically. M. Bagheri et. al. [9] have discussed an analytical approach for the precise measurements of vibration signals occurring in the power transformer and have developed an IoT based prognosis model for measuring vibration signals in the power transformer. Real time information is then transferred to the cloud system for further processing and decision making. S. T. Chacko and V. Deshmukh [10] have designed and developed an online system for power

consumption monitoring by loads from a distribution transformer using IoT server. This monitoring system detects faults in distribution transformer by verifying and maintaining records of the internal parameters of the distribution transformer.

R. Basak et. al. [11] have developed a surveillance unit to monitor the temperature of distribution transformers along with the current drawn from it using thermal camera and current measuring device. The system is also used to monitor any illegal connections in distribution transformer by following the electrical route using GPS module. N Mussin et. al. [12] have studied and implemented the real time diagnosis technique for power transformer based on the analysis of the vibrational signal spectrum that is transferred and processed over the cloud environment using IoT and then the prognosis algorithm is executed over portable device. A.K. Al Mhdawi and H.S. Al Raweshidy [13] have proposed an IoT based remote condition monitoring and fault prediction system that is based on a distributed software. This approach is a transition to smart grid implementation by fusing the power grid with efficient and real-time wireless communication architecture.

In general, there is some published literature in the field but directly implementable solution to the problem of developing IoT based techniques for the continuous monitoring of parameters of the oil-immersed power or distribution transformers is not yet available. The objective of this paper is to design an experiment to develop a scaled down model for IoT based monitoring of hot spots in power and distribution transformers.

### 3. Proposed Methodology

#### 3.1 Heat Transfer Studies in Oil- Immersed Transformers

The locations where the high temperature develops inside an oil- immersed transformer are known as hot spots. These are the major cause for the loss of life of power transformer. The loading capacity of an oil- immersed transformer is defined in terms of the normal operation hot spot temperature (HST). The HST in a power transformer winding consists of three components: the ambient temperature rise, the top oil temperature (TOT) rise and the hot spot temperature rise over the top oil temperature. The temperature distribution along the height of the oil- immersed transformer tank is shown in Fig.3.

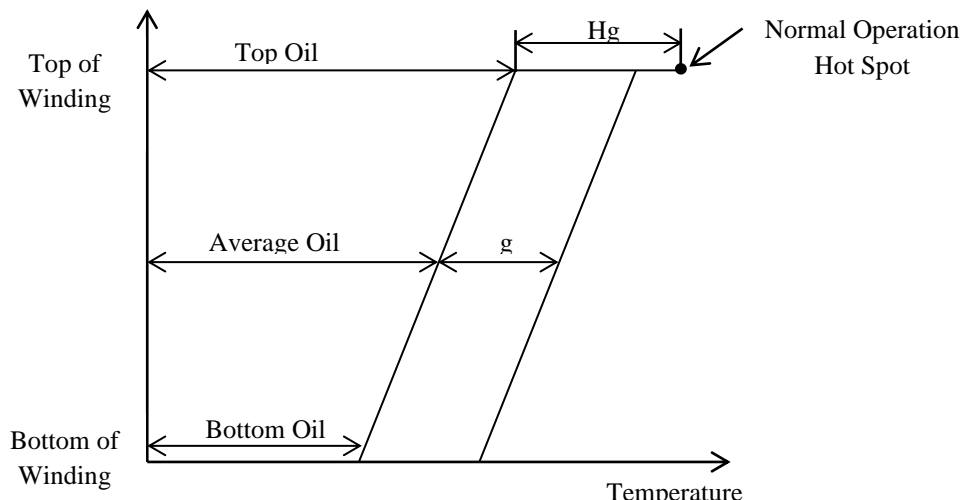


**Fig.3. Temperature distribution along the height of the power transformer tank**

Generally, under normal operation, the temperature of insulating oil increases linearly from bottom to top of the winding inside the transformer tank. Also, the temperature rise of the conductor along the winding increases linearly, parallel to the oil temperature rise, while maintaining a constant difference  $g$  from the average oil temperature rise.

The HST rise is higher than the temperature rise of the conductor at the top of the winding as shown in Fig.3. because of the allowance that has to be made for the increase in stray losses. To take account of these nonlinearities, the differences in temperature between the hot spot and the oil at the top of the winding is made equal to  $Hg$ . The factor  $H$  may vary from 1.1 to 1.5 depending on transformer size,

short-circuit impedance and winding design. A value of 1.1 has been used for distribution transformers and 1.3 for medium and large power transformers.

An empty transformer tank is shown in Fig.4. The scaled down hardware model in this paper can be helpful in continuous monitoring of the temperature at different locations inside the transformer tank by fitting the temperature sensors at each wall of the tank such that any hot spot developed over the core-winding assembly during the operation gets exposed to the temperature sensors and the respective data can be read by microcontroller board. The WiFi competence of the NodeMCU along with ease of IoT helps in real time monitoring of the hot spots inside the transformer tank.



**Fig.4. Empty Transformer Tank**

Thus, the design of experiment develops a scaled down hardware that can continuously monitor the temperature inside the cubical tank at four different locations and helps in locating the exact position of heating element. The design description of the proposed work is now discussed.

### 3.2 Design Description

The proposed design contains various components for its appropriate working. For instance, a heating element is used for incorporating mock hot spots at nine different locations inside a chamber containing transformer insulating oil, four temperature sensors for measuring temperature at four different locations, a microcontroller board for controlling and wireless communication using Wi-Fi built-in feature, a timer circuit for controlling the duty cycle for operating heating element. Brief discussion of the components of each of these categories along with their role and specification is given below:

#### 3.2.1 Heating Element

The heating element used in this work is a tube-shaped element that can be inserted into drilled holes. It consists of resistance coil wound around a ceramic core that is surrounded by dielectric and encased in a metal sheath. Powered heat transferred through the coil to the sheath causes the sheath to heat up. This heat is then transferred to the liquid in which it the element is immersed for heat transfer. Fig.5 shows the 230V, 350W heating element that is used in this design for heating purpose.



**Fig.5. 230V, 350W Heating Element**

#### 3.2.2. Temperature Sensors

The sensor used in this work is a DS18B20 programmable temperature sensor widely used to measure temperature in hard environments like chemical solutions, mines or soil etc. It is a water resistant sensor which provides 9-bit to 12-bit Celsius temperature measurements. This sensor communicates over a 1-wire bus so that it requires only one data line for communication with a microcontroller by deriving power directly from the data line.



**Fig.6. DS18B20 Programmable Temperature Sensor**

It has three pin, namely, Vcc, Data and Ground as shown in Fig.6. It can measure a wide range of temperature from  $-55^{\circ}\text{C}$  to  $+125^{\circ}\text{C}$  with a good accuracy of  $\pm 0.5^{\circ}\text{C}$ . Each sensor has a unique address and requires only one pin of the microcontroller to transfer data so it is a very good choice for measuring temperature at multiple points without compromising much of the digital pins on the microcontroller. The temperature value measured by the sensor is stored in a 2-byte register inside the sensor. This data can be read by the using the 1-wire method by sending in a sequence of data.

### 3.2.3. Microcontroller Board

The microcontroller board used in this work is NodeMCU (ESP8266) which is a self-contained WiFi networking solution offering as a bridge from existing microcontroller to WiFi and is also capable of running self-contained applications. This module comes with a built in USB connector and a rich assortment of pin-outs, for connection to central processing unit. Fig.7. shows the basic structure of NodeMCU microcontroller board.



**Fig.7. Basic Structure of NodeMCU**

The major features of Node MCU ESP8266 are as follows:

- WIFI module: ESP-12E, Power supply: 5V, Logic level: 3.3V
- Processor: ESP8266, CP2102 chip
- Built-in Flash: 32Mbit
- Peripheral interface: UART/SPI/I2C/SDIO/GPIO/ADC/PWM
- WiFi protocol: IEEE 802.11 b/g/n
- Frequency range: 2.4G~2.5G(2400 M~2483.5M)

The major advantages of NodeMCU platform are

- Low cost
- Integrated support for WIFI network
- Reduced size of the board
- Low energy consumption

### 3.3. Internet of Things System

The Internet of things (IoT) system provides deeper automation, analysis and integration within the system. IoT based system not only exploits recent advances in software but also reduces the hardware prices and provides better attitude towards technology by displaying the data in more user friendly manner. It works on connected things. It has four basic building blocks, sensors, IoT gateway/framework, cloud server and mobile apps/ display. The sensors sense the data which is carried by IoT

gateway/framework to the cloud server. This is generally done by the help of WiFi competence with the microcontroller. All the decision rules are applied at cloud server. The data collected at cloud server is then send to the recipient in the form of alarming signal or indication on mobile app/ display boards carried with the field engineers.

In this way, IoT links physical devices, i.e. sensors and actuators through the internet by allotting an internet protocol address to gather and transfer the data over a system without physical help or involvement.

#### **4. System Architecture**

The proposed design of experiment consists of a cubical tank made up of iron sheet coated with lead oxide and painted with grey colour on its inner and outer surfaces. The dimensions of the cubical tank are 50cm\*50cm\*15cm with the tank sheet having thickness of 0.2cm, the 3D design model of which is shown in Fig.8.

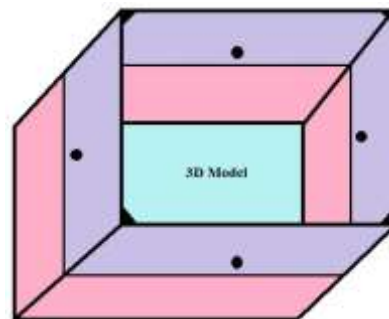


**Fig.8. 3D Design Model of the proposed design**

The four temperature sensors are mounted at a height of 9cm from the bottom of the tank and the side and top view of the design is as shown in Fig.9(a) and Fig.9(b). The four temperature sensors are marked as A, B, C and D and there is provision of mounting the heating element in the cubical tank at 9 different locations as shown in Fig.9(b).

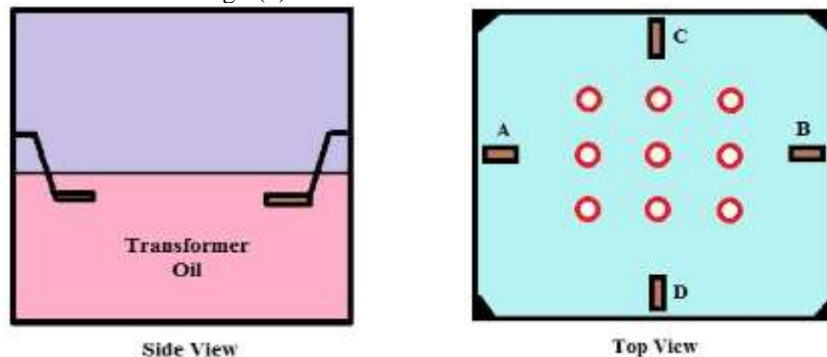


**Fig.9(a). and 9(b). Side and Top View of the Design**

The heating element is fitted on an acrylic sheet of thickness 0.2cm and dimensions 50cm\*50cm that is fixed on the upper corner supports provided at the top corner edges of the cubical tank. The heating element is energised with 230V, 50Hz ac supply along with the help of a timer circuit in order to control the heating duty cycle. Also, microcontroller NodeMCU- ESP8266 is used for sensing the temperature data measured with the help of four temperature sensors.

The cubical tank is filled with the transformer oil upto a height of 10 to 12cm. The cubical tank is containing four temperature sensors at four sides of the tank and which are mounted at a height of 9cm so that the sensors get immersed in the transformer oil. This can be easily predicted as shown in Fig.10.



**Fig.10. Cubical tank filled with transformer oil and containing 4 temperature sensors**

The heating element is placed at one of the 9 locations provided in the design and is suspended inside the cubical tank with the support of acrylic sheet at the top such that the heating part of the element gets completely immersed in the transformer oil filled in the tank. Now, the power supplies to the heating element as well as to the microcontroller board are given and after an interval of 15 seconds, the sensor values are recorded using NodeMCU. Depending upon the location of the heating element in the 3\*3 array positions, the temperature values measured by the sensors will be different. For an instance (as shown in Fig.11.), if the heating element is placed at position 'P11', the temperature values measured by the sensors A and C will be more as compared to the temperature values read by sensors B and D, as these sensors get distant from the heating element in this particular position.

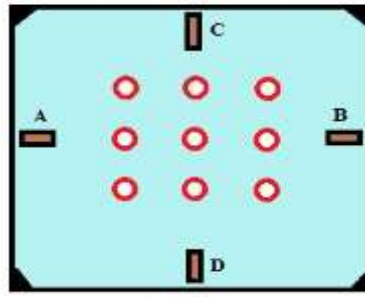


**Fig.11. Location 'P11' and 'P12' for the heating element**

Similarly, if the heating element is allowed to place at position 'P12', the temperature reading of sensor C will be maximum because the heating element is nearest to the sensor C. In this way, the temperature values of the sensors at all the different position of the heating element are recorded. This results in the development of 9 different patterns of the temperature profiles as predicted by the 4 temperature sensors. This allows the user to generate a programming procedure to identify the exact location of the heating element inside the cubical tank for 9 different positions P11 to P33. Further, the system has a provision to send the exact location of the heating element to the control room with the help of IoT using WiFi competence of NodeMCU. The procedural steps for positioning the exact location of the heating element in the cubical tank with the aid of IoT technology is shown in the flow chart (Fig.12). The temperature readings sensed by the four temperature sensor are read by microcontroller NodeMCU and compared with a threshold temperature ( $T_{th}$ ). The control room will receive all of the temperature readings (TA, TB, TC, TD) on the display at computer moniter until the readings are less than this threshold temperature. As soon as any of the temperature readings exceeds the threshold temperature, the system will execute a logical program to identify the location of the heating element.

First of all, the temperature readings TA and TB are compared in order to identify the column in the 3\*3 array position and then the temperature readings TC and TD are compared to identify the row. In this way, the location of the heating element is identified, the information of which is carried by the IoT gateway/framework to the cloud server with the help of in-built WiFi competence of NodeMCU. The data collected at cloud server is then send to the recipient in the form of alarming signal or indication on mobile app/ display boards carried with the field engineers.

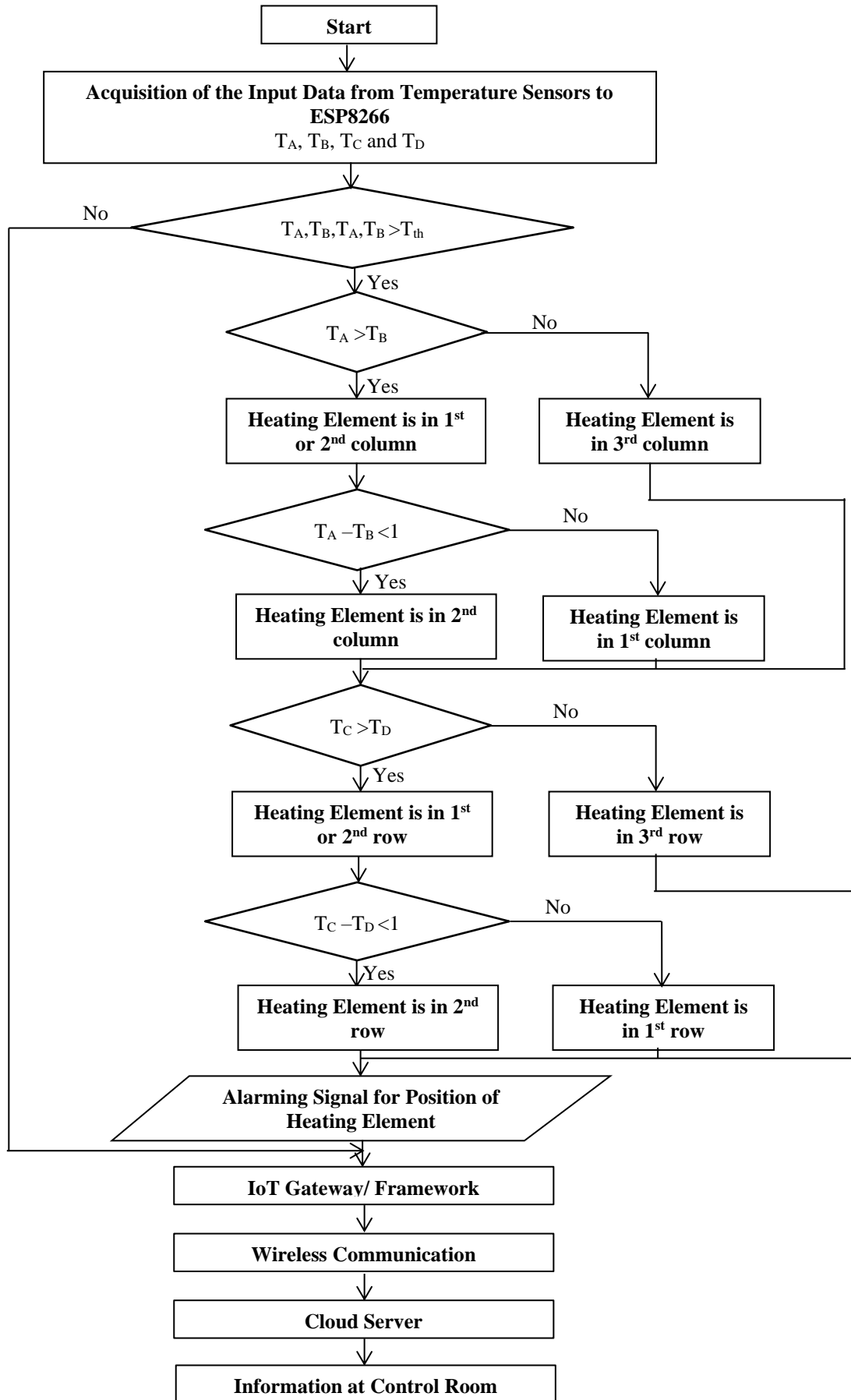


Fig.12. Flow chart for showing the procedural steps for localising hot spots in the cubical tank

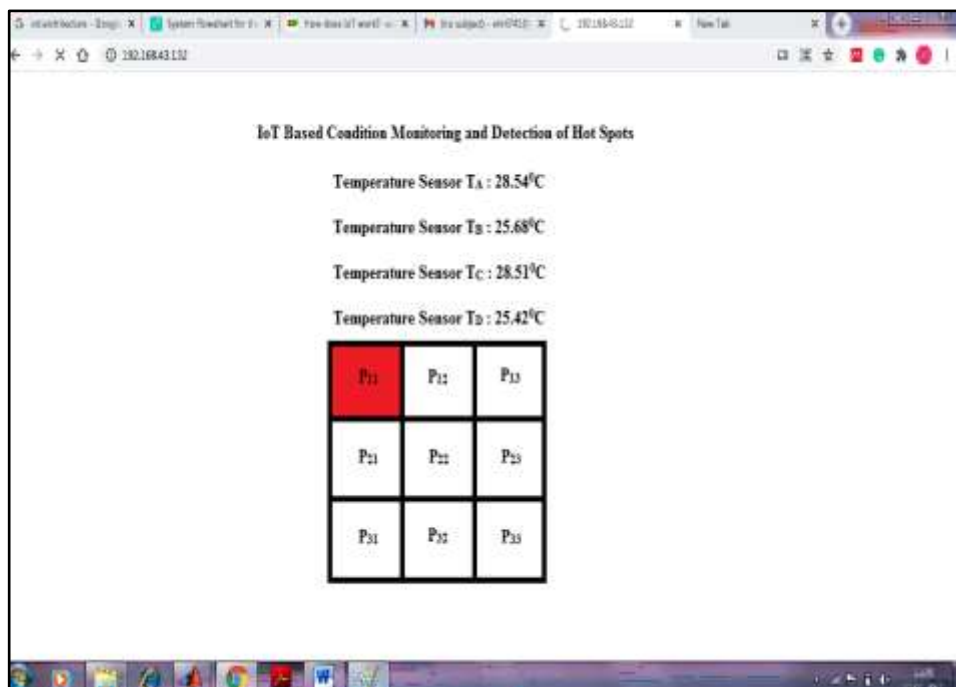
## 5. Results and Discussion

The temperature values from the four temperature sensors at 9 different position of heating element are recorded and a program burned in NodeMCU module is then executed to identify the location of the heating element among the different position. Table 1. shows the readings of temperature read by the four temperature sensors and the obtained position (P<sub>11</sub> to P<sub>33</sub>) of the heating element as determined by the logical programming.

**Table 1. Temperature readings by the four temperature sensors at nine different positions**

S. No.	Temperature Readings (°C)				Position of Heating Element
	Sensor A	Sensor B	Sensor C	Sensor D	
1	28.54	25.68	28.51	25.42	P <sub>11</sub>
2	24.29	23.54	30.17	24.09	P <sub>12</sub>
3	22.15	28.95	28.51	20.18	P <sub>13</sub>
4	30.54	24.28	24.98	23.17	P <sub>21</sub>
5	25.18	24.69	26.85	25.93	P <sub>22</sub>
6	24.19	31.25	25.93	25.19	P <sub>23</sub>
7	28.55	22.19	23.54	27.96	P <sub>31</sub>
8	22.21	21.58	21.53	28.63	P <sub>32</sub>
9	23.10	27.65	23.45	27.11	P <sub>33</sub>

The continuous monitoring of the temperature at four locations is done with the help of IoT platform by displaying the data on the server in the control room. Fig.13(a) and Fig.13(b) shows the location of heating element at position P<sub>11</sub> and P<sub>12</sub> respectively.



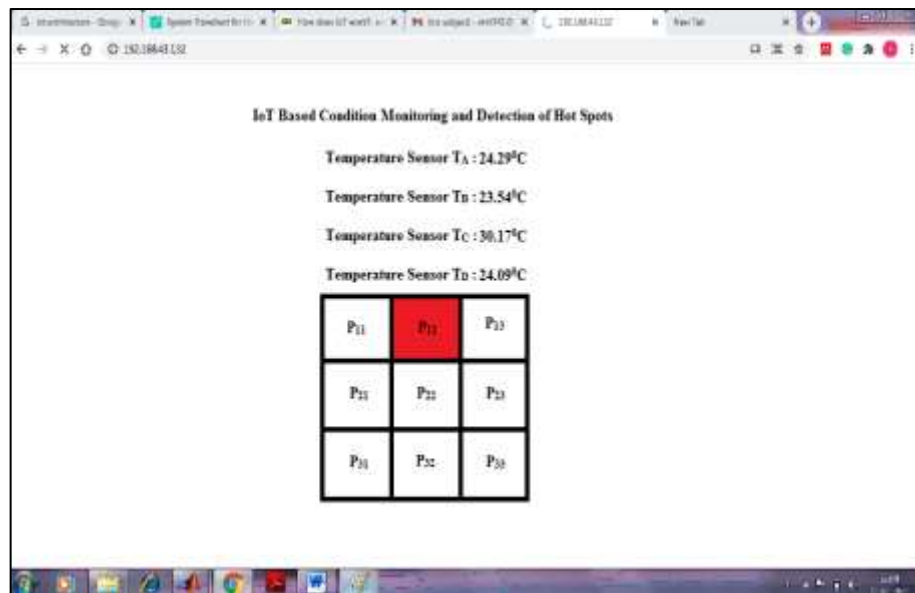


**Fig.13(a) and (b): Server in control room showing location of heating element at position P<sub>11</sub> and P<sub>12</sub> respectively**

In this way, the location of the heating element can be detected using sensing technique incorporated with the microcontroller with an edge of IoT for sending these locations to the control room for taking the prognosis action before any accidental affair. This design is therefore can be useful if their procedural technique is implemented in the oil immersed power or distribution transformer in order to exactly locate the position of hot spots inside the transformer tank.

## 6. Conclusion

The results obtained with the help of programming in microcontroller board ESP8266 are in agreement with the real position of the heating element during the experiment. The results are shown graphically in Fig.14 which shows that this experimental design is useful in localising the position of hot spots in a cubical tank. Thus, it can be concluded that the concept used in the proposed design can also be implemented in the oil- immersed transformers so that the position of the hot spots can be easily located during real time operation. Further, the involvement of IoT aids new feature in the design that can not only be used in sending the information to remote control room but also helps in the thermal protection of the transformers.

Future directions for extension of this work can be focus on improvement of this experiment by considering the effect of evolved gases during the heat dissipation phenomenon by the use of the respective sensors so that more accurate and precise results can be achieved. However, further research and development is required to enhance the prevailing monitoring systems and introduce new designs and applications that include better thermal modeling. This design will allow the manufacturers to provide better specifications and users to operate the transformers on appropriate loading.

## References

- [1] R. R. Pawar and D. S. B. Deosarkar, "Health Condition Monitoring System For Distribution Transformer Using Internet of Things ( IoT )," in Proceedings of the IEEE 2017 International Conference on Computing Methodologies and Communication, 2017, no. ICCMC, pp. 117–122.
- [2] R. R. Pawar, P. A. Wagh, and S. B. D. I. Member, "Distribution Transformer Monitoring System Using Internet of Things ( IoT )," pp. 1–4, 2017.
- [3] T. K. Roy and T. K. Roy, "Implementation of IoT: Smart Maintenance for Distribution Transformer using MQTT," pp. 5–8.
- [4] D. Srivastava, "Transformer Health Monitoring System Using Internet of Things," 2018 2nd IEEE Int. Conf. Power Electron. Intell. Control Energy Syst., pp. 903–908, 2018.

- [5] R. De Giorgi, N. Kobbi, S. Sesmat, and E. Bideaux, "Thermal Model of a Tank for Simulation and Mass Flow Rate Characterization Purposes," Proc. 7th JFPS Int. Symp. Fluid Power, pp. 225–230, 2008, doi: 10.5739/isfp.2008.225.
- [6] L. Thangiah, "Distribution Transformer Condition Monitoring based on Edge Intelligence for Industrial IoT," 2019 IEEE 5th World Forum Internet Things, pp. 733–736, 2019.
- [7] H. Jamal, M. F. N. Khan, A. Anjum, and M. K. Janjua, "Thermal Monitoring and Protection for Distribution Transformer Under Residential Loading Using Internet of Things," 2018 IEEE Glob. Conf. Internet Things, no. January, pp. 1–6, 2019, doi: 10.1109/GCIoT.2018.8620135.
- [8] W. K. A. H. et. Al., "Design and Implementation Smart Transformer based on IoT," 2019 Int. Conf. Comput. Electron. Commun. Eng., pp. 16–21, 2019.
- [9] M. Bagheri and A. Zollanvari, "Transformer Fault Condition Prognosis Using Vibration Signals Over Cloud Environment," IEEE Access, vol. 6, pp. 9862–9874, 2018, doi: 10.1109/ACCESS.2018.2809436.
- [10] S. T. Chacko and V. Deshmukh, "IoT based Online Power Consumption Monitoring of a Distribution transformer feeding Domestic / Commercial Consumer loads," 2019 4th Int. Conf. Inf. Syst. Comput. Networks, pp. 441–445, 2019.
- [11] R. Basak, "IOT Based Drone Operated Monitoring Of Distribution Transformers and Terminating Illegal Power Connections," pp. 1–5, 2019.
- [12] N. Mussin and A. Suleimen, "Transformer Active Part Fault Assessment Using Internet of Things," 2018 Int. Conf. Comput. Netw. Commun., pp. 1–6, 2018.
- [13] A. K. Al Mhdawi, H. S. Al-raweshidy, and S. Member, "A Smart Optimization of Fault Diagnosis in Electrical Grid Using Distributed Software-Defined IoT System," IEEE Syst. J., vol. PP, pp. 1–11, 2019, doi: 10.1109/JYST.2019.2921867.

# **Application of Deep Learning in Health Informatics: A Review**

**Vinit Mehta and Noopur Srivastava**

**Abstract** Today a variety of health care practices have been evolved to maintain and restore health by the latest prevention and best treatment. This implements biomedical sciences, biomedical research, genetics and medical technology to diagnose, treat, and prevent injury and disease, typically through pharmaceuticals or surgery, therapies as diverse as psychotherapy, external splints and traction, medical devices, biologics, and ionizing radiation. With advances in technology, the health sciences are constantly pushing toward more effective treatments and cures. With a massive influx of multimodality data, the role of data analytics in health informatics has grown rapidly in the last decade. This has also provoked increasing interests in the generation of analytical, data driven models based on machine learning in health informatics. Deep learning, a technique with its foundation in artificial neural networks, is emerging in recent years as a powerful tool for machine learning, promising to reform the future of artificial intelligence. Rapid improvements in computational power, fast data storage, and parallelization have also contributed to the rapid uptake of the technology in addition to its predictive power and ability to generate automatically optimized high-level features and semantic interpretation from the input data. This paper presents a comprehensive review of research employing deep learning in health informatics, providing a critical analysis of the relative merit, and potential pitfalls of the technique as well as its future outlook. The paper mainly focuses on key applications of deep learning in the fields of translational bioinformatics, medical imaging, pervasive sensing, medical informatics, and public health. Finally the limitations and challenges of deep learning in the field of health informatics have been discussed.

**Keywords-** machine learning, deep learning, health informatics, translational bioinformatics, medical imaging, pervasive sensing, medical informatics, and public health.

## **1. Introduction**

Deep learning has become a new trend in machine learning since recent years. The background foundations of deep learning are well rooted in the classical neural network (NN) theory. But unlike traditional NNs, deep learning algorithm uses many hidden neurons and layers, typically more than two that contribute an architectural advantage combined with new training paradigms. Deep learning is based on a set of algorithms that model high level abstractions in data. In a simple case, there might be two sets of neurons: one set that receives an input signal and one that sends an output signal. When the input layer receives an input it passes on a modified version of the input to the next layer. In a deep network, there are many layers between the input and the output, that allows the algorithm to use multiple processing layers, composed of multiple linear and non-linear transformations. Fig. 1 shows that each successive layer in a neural network uses features from the previous layer to learn more complex features. In this manner a deep neural network is capable of composing features of increasing complexity in each of its successive layers.

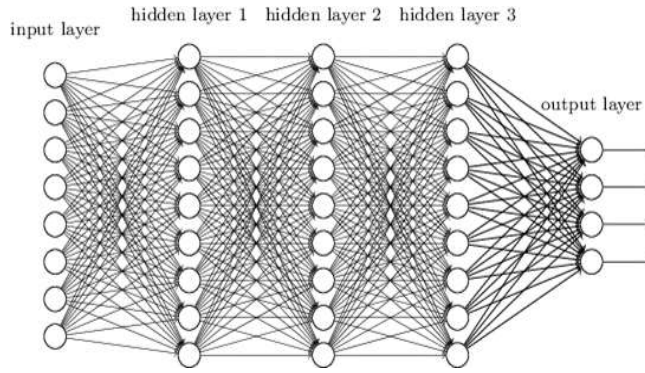
---

Vinit Mehta

Research Scholar, Department of Electrical Engineering, M.B.M. Engineering College, Jodhpur, India  
Email Address : vinit741@gmail.com

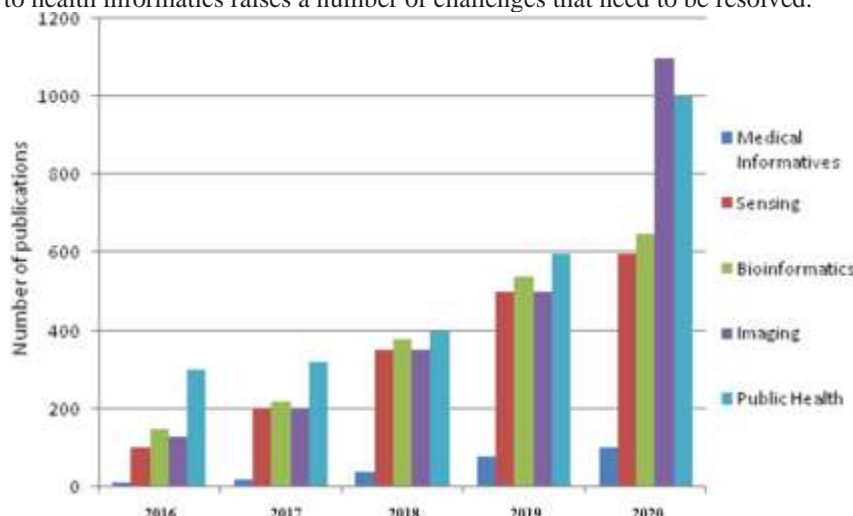
Noopur Srivastava

Department of Electrical Engineering Anand International College of Engineering Jaipur, India

**Fig.1. Block diagram of Deep Neural Network**

Also the layer-by-layer pipeline of nonlinear combination of their outputs generates a lower dimensional projection of the input space. Every lower-dimensional projection corresponds to a higher perceptual level. This results in an effective high-level abstraction of the raw data or images if the network is optimally weighted.

In the past few years, deep learning has become an immediate tool to solve applications in computer vision, speech recognition, natural language processing, and other application areas of commercial interest. In areas such as health informatics, the generation of the deep learning feature set without human intervention has many advantages. In medical imaging, it can generate features that are more sophisticated and difficult to elaborate in descriptive means. Implicit features could determine fibroids and polyps [1], and characterize irregularities in tissue morphology such as tumors [2]. In translational bioinformatics, such algorithms may also determine nucleotide sequences that could bind a DNA or RNA strand to a protein [3]. Fig. 2 outlines a quick rush of interest in deep learning in recent years in terms of the number of papers published in sub-fields in health informatics including bioinformatics, medical imaging, pervasive sensing, medical informatics, and public health. The publication statistics have obtained from Google Scholar; the search phrase is defined as the subfield name with the exact phrase deep learning. A excess of experimental works have implemented deep learning models for heath informatics, reaching similar performance or in many cases exceeding that of alternative techniques. Nevertheless, the application of deep learning to health informatics raises a number of challenges that need to be resolved.

**Fig.2. Number of published papers that use deep learning in health informatic applications**

In addition, deep learning requires extensive computational resources, without which training could become excessively time-consuming. Attaining an optimal definition of the network's free parameters can become a particularly laborious task to solve. Eventually, deep learning models can be affected by convergence issues as well as overfitting, hence supplementary learning strategies are required to address these problems [4]. In this paper, a review of recent health informatics studies has been done that employ deep learning to discuss its relative strength and potential pitfalls. Furthermore, their schemas and operational frameworks are described in detail to clarify their practical implementations, as well as expected performance.

## 2. From Perceptron to Deep Learning

Perceptron is a bio inspired algorithm for binary classification and consist of an input layer directly connected to an output node, emulate this biochemical process through an activation function (also referred to as a transfer function) and a few weights. Specifically, it can learn to classify linearly separable patterns by adjusting these weights accordingly.

To solve more complex problems, NNs with one or more hidden layers of perceptrons have been introduced [5]. To train these NNs, many stages or epochs are usually performed where each time the network is presented with a new input sample and the weights of each neuron are adjusted based on a learning process called delta rule. The delta rule is used by the most common class of supervised NNs during the training and is usually implemented by exploiting the back-propagation routine [6]. Specifically, without any prior knowledge, random values are assigned to the network weights. Through an iterative training process, the network weights are adjusted to minimize the difference between the network outputs and the desired outputs. The most common iterative training method uses the gradient descent method where the network is optimized to find the minimum along the error surface. This method requires the activation functions to be always differentiable.

Adding more hidden layers to the network allows a deep architecture to be built that can express more complex hypothesis as the hidden layers confine the nonlinear relationships. These NNs are known as Deep Neural Networks (DNN). Deep learning has provided new sophisticated approaches to train DNN architectures. In general, DNNs can be trained with unsupervised and supervised learning methodologies. In supervised learning, labeled data are used to train the DNNs and learn the weights that minimize the error to predict a target value for classification or regression, whereas in unsupervised learning, the training is performed without requiring labeled data. Unsupervised learning is usually used for clustering, feature extraction or dimensionality reduction. For some applications it is common to combine an initial training procedure of the DNN with an unsupervised learning step to extract the most relevant features and then use those features for classification by exploiting a supervised learning step.

For many years, hardware limitations have made DNNs impractical due to high computational demands for both training and processing, especially for applications that require real-time processing. Recently, these limitations have been partially overcome and have enabled DNNs to be recognized as a significant breakthrough in artificial intelligence.

## 3. Applications

### 3.1. Medical Informatics

Medical Informatics focus on the analysis of large, aggregated data in healthcare fields with the aim to enhance and develop clinical decision support systems or assess medical data both for quality assurance and accessibility of health care services. Deep learning approaches have been designed to scale up well with big and distributed datasets. The success of DNNs is largely due to their ability to learn novel features/patterns and understand data representation in both an unsupervised and supervised hierarchical manners. DNNs have also proven to be efficient in handling multi information since they can combine several DNN architectural components. Therefore, it is unsurprising that deep learning has quickly been adopted in medical informatics research. In the field of medical informatics, many authors have made several documentations. Shin et al. [7] have presented a combined text image CNN to identify semantic information that links radiology images and reports from a typical picture archiving and communication system. Liang et al. [8] have used a modified version of DNN as an effective training method for large scale datasets on hypertension. Putin et al. [9] have applied DNNs for identifying markers that predict human chronological age based on simple blood tests. Nie et al. [10] have proposed a deep learning network for automatic disease inference, which requires manual gathering the key symptoms or questions related to the disease.

In another study, Mioto et al. [11] have showed that a stack of autoencoders can be used to automatically infer features from a large scale EHR database and represent patients without requiring additional human effort. The authors demonstrated the ability of their system to predict the probability of a patient developing specific diseases, such as diabetes, schizophrenia and cancer. Furthermore, Futoma et al. [12] have compared different models in their ability to predict hospital readmissions based on a large EHR database. DNNs have significantly higher prediction accuracies than conventional approaches, such as penalized logistic regression, though training of the DNN models were not straightforward. Mehrabi et al. [13] have proposed the use of DBN to discover common temporal patterns and characterize disease progression. The authors have highlighted the ability to interpret the newly discovered patterns requires further investigation.

The motivations behind these studies are to develop general purpose systems to accurately predict length of stay, future illness, readmission, and mortality with the view to improve clinical decision making and

optimize clinical pathways. Early prediction in health care is directly related to saving patient's lives. Furthermore, the discovery of novel patterns can result in new hypotheses and research questions. In computational phenotype research, the goal is to discover meaningful data-driven features and disease characteristics. For example, Che et al. [14] have highlighted that although DNNs outperform conventional machine learning approaches in their ability to predict and classify clinical events, they suffer from the issue of model interpretability, which is important for clinical adaptation. They pointed out that interpreting individual units can be misleading and the behavior of DNNs are more complex than originally thought. They suggested that once a DNN is trained with big data, a simpler model can be used to distil knowledge and mimic the prediction performance of the DNN.

Deep learning has paved the way for personalized health care by offering an unprecedented power and efficiency in mining large multimodal unstructured information stored in hospitals, cloud providers and research organization. Although, it has the potential to outperform traditional machine learning approaches, appropriate initialization and tuning is important to avoid overfitting. Noisy and sparse datasets result in considerable fall of performance indicating that there are several challenges to be addressed. Furthermore, adopting these systems into clinical practice requires the ability to track and interpret the extracted features and patterns.

### **3.2. Sensing**

Pervasive sensors, such as wearable, implantable, and ambient sensors have [15] allowed continuous monitoring of health and wellbeing. An accurate estimation of food intake and energy expenditure throughout the day can help tackle obesity and improve personal wellbeing. For elderly patients with chronic diseases, wearable and ambient sensors can be utilized to improve quality of care by enabling patients to continue living independently in their own homes. The care of patients with disabilities and patients undergoing rehabilitation can also be improved through the use of wearable and implantable assistive devices and human activity recognition. For patients in critical care, continuous monitoring of vital signs, such as blood pressure, respiration rate, and body temperature, are important for improving treatment outcomes by closely analyzing the patient's condition [16].

Wulsin et al. [17] proposed a DBN approach to detect anomalies in EEG waveforms. EEG is used to record electrical activity of the brain. Interpreting the waveforms from brain activity is challenging due to the high dimensionality of the input signal and the limited understanding of the brain operations. Jia et al. [18] have used a deep learning method based on RBM to recognize affective state of EEG. Although the sample sets are small and noisy, the proposed method achieves greater accuracy. A DBN was also used for detecting arrhythmias from electrocardiography (ECG) signals. The main purpose of the system is identifying arrhythmias which are a complex pattern recognition problem. Yan et al. have attained classification accuracies of 98% using a two-lead ECG dataset. For low power wearable and implantable EEG sensors, where energy consumption and efficiency are major concerns, Wang et al. [19] have designed a DBN to compress the signal. This results in more than 50% of energy savings while retaining accuracy for neural decoding. The introduction of deep learning has increased the utility of pervasive sensing across a range of health applications by improving the accuracy of sensors that measure food calorie intake, energy expenditure, activity recognition, sign language interpretation, and detection of anomalous events in vital signs. Many applications use deep learning to achieve greater efficiency and performance for real-time processing on low-power devices; however, a greater focus should be placed upon implementations on neuromorphic hardware platforms designed for low-power parallel processing. The most significant improvements in performance have been achieved where the data has high dimensionality as seen in the EEG datasets. Most current research has focused on the recognition of activities of daily living and brain activity. Many opportunities for other applications and diseases remain, and many currently studies still rely upon relatively small datasets that may not fully capture the variability of the real world.

### **3.3. Bioinformatics**

Bioinformatics aim to investigate and understand biological processes at a molecular level. Advances in biotechnology have helped reduce the cost of genome sequencing and steered the focus on prognostic, diagnostic and treatment of diseases by analyzing genes and proteins. This can be illustrated by the fact that sequencing the first human genome cost billions of dollars, whereas today it is affordable [20]. Further motivated by P4 (predictive, personalized, preventive, participatory) medicine [21], bioinformatics aim to predict and prevent diseases by involving patients in the development of more efficient and personalized treatments. The application of machine learning in bioinformatics can be divided into three areas: prediction of biological processes, prevention of diseases and personalized treatment. These areas are found in genomics, pharmacogenomics and epigenomics. Genomics explores the function and information structures encoded in the DNA sequences of a living cell [22]: it analyzes genes responsible for the creation of protein

sequences and the expression of phenotypes. A goal of genomics is to identify gene alleles and environmental factors that contribute to diseases such as cancer. Pharmacogenomics evaluates variations in an individual's drug response to treatment brought about by differences in genes. It aims to design more efficient drugs for personalized treatment. Finally, epigenomics aims to investigate protein interactions and understand higher level processes, such as transcriptome (mRNA count), proteome, and metabolome, which lead to modification in the gene's expression. Understanding how environmental factors affect protein formation and their interactions is a goal of epigenomics.

The ability of deep learning to abstract large, complex, and unstructured data offers a powerful way of analyzing heterogeneous data such as gene alleles, proteins occurrences, and environmental factors [23]. In deep learning approaches, feature extraction and model fitting takes place in a unified step. Multilayer feature representation can capture nonlinear dependencies at multiple scales of transcriptional and epigenetic interactions and can model molecular structure and properties in a data driven way. These nonlinear features are invariant to small input changes which results in eliminating noise and increasing the robustness of the technique.

Several works have demonstrated that deep learning features outperformed methods relying on visual descriptors in the recognition and classification of cancer cells. For example, Ibrahim et al. [24] have proposed a DBN with an active learning approach to find features in genes and microRNA that resulted in the best classification performance of various cancer diseases such as hepatocellular carcinoma, lung cancer and breast cancer. For breast cancer genetic detection, Khademi et al. [25] have overcame missing attributes and noise by combining a DBN and Bayesian network to extract features from microarray data. Deep learning approaches have also outperformed SVM in predicting splicing code and understanding how gene expression changes by genetic variants [26]. Angermueller et al. [27] have used DNN to predict DNA methylation states from DNA sequences and incomplete methylation profiles. After applying to 32 embryonic mice stem cells, the baseline model was compared with the results. This method can be used for genome-wide downstream analyses.

Deep learning not only outperforms conventional approaches but also opens the door to more efficient methods to be developed. Kearnes et al. [28] have described how deep learning based on graph convolutions can encode molecular structural features, physical properties, and activities in other assays. This allows a rich representation of possible interactions beyond the molecular structural information encoded in standard databases. Similarly, multitask DNNs provides an intuitive model of correlation between molecule compounds and targets because information can be shared among different nodes. This increases robustness, reduces chances to miss information, and usually outperforms other methods that process large datasets [29].

### 3.4. Medical Imaging

Automatic medical imaging analysis is crucial in modern medicine. Diagnosis based on the interpretation of images can be highly subjective. Computer-aided diagnosis can provide an objective assessment of the underlying disease processes. Modeling of disease progression, common in several neurological conditions, such as Alzheimer's, multiple sclerosis, and stroke, requires analysis of brain scans based on multimodal data and detailed maps of brain regions. In recent years, CNNs have been adapted rapidly by the medical imaging research community because of their outstanding performance demonstrated in computer. The fact that CNNs in medical imaging have yielded promising results have also been highlighted in a recent survey of CNN approaches in brain pathology segmentation [30] and in an editorial of deep learning techniques in computer aided detection, segmentation, and shape analysis [31].

Among the biggest challenges in CAD are the differences in shape and intensity of tumors/lesions and the variations in imaging protocol even within the same imaging modality. In several cases, the intensity range of pathological tissue may overlap with that of healthy samples. Furthermore, Rician noise, non isotropic resolution, and bias field effects in magnetic resonance images (MRI) cannot be handled automatically using simpler machine learning approaches. To deal with this data complexity, hand-designed features are extracted and conventional machine learning approaches are trained to classify them in a completely separate step.

Deep learning provides the possibility to automate and merge the extraction of relevant features with the classification procedure. CNNs inherently learn a hierarchy of increasingly more complex features and, thus, they can operate directly on a patch of images centered on the abnormal tissue. Example applications of CNNs in medical imaging include the classification of interstitial lung diseases based on computed tomography (CT) images, the classification of tuberculosis manifestation based on X-ray images, the classification of neural progenitor cells from somatic cell source , the detection of haemorrhages in color fundus images and the organ or body-part-specific anatomical classification of CT images. A multistage deep learning framework based on CNNs extracts both the patches with the most as well as least discriminative local patches in the pretraining stage. Subsequently, a boosting stage exploits this local information to improve performance. The authors point out that training based on discriminative local

appearances are more accurate compared to the usage of global image context. Although CNNs have dominated medical image analysis applications, other deep learning approaches/architectures have also been applied successfully. In a recent paper, a stacked denoising autoencoder was proposed for the diagnosis of benign malignant breast lesions in ultrasound images and pulmonary nodules in CT scans [32]. The method outperforms classical CAD approaches, largely due to the automatic feature extraction and noise tolerance. Furthermore, it eliminates the image segmentation process to obtain a lesion boundary. Shan et al. [33] presented a stacked sparse autoencoder for microaneurysms detection in fundus images as an instance of a diabetic retinopathy strategy. The proposed method learns high-level distinguishing features based only on pixel intensities. Various autoencoder-based learning approaches have also been applied to the automatic extraction of biomarkers from brain images and the diagnosis of neurological diseases. These methods often use available public domain brain image databases such as the Alzheimer's disease neuroimaging initiative database. For example, a deep Autoencoder combined with a softmax output layer for regression is proposed for the diagnosis of Alzheimer's disease.

Low level image processing, such as image segmentation and registration can also benefit from deep learning models. Brosch et al. [34] described a manifold learning approach of 3-D brain images based on DBN. It is different than other methods because it does not require a locally linear manifold space. Mansoor et al. [35] developed a fully automated shape model segmentation mechanism for the analysis of cranial nerve systems. The deep learning approach outperforms conventional methods particularly in regions with low contrast, such as optic tracts and areas with pathology. A pipeline is proposed for object detection and segmentation in the context of automatically processing volumetric images. A novel framework called marginal space deep learning implements an object parameterization in hierarchical marginal spaces combined with automatic feature detection based on deep learning. A DNN architecture called input–output deep architecture is described to solve the image labelling problem. A single NN forward step is used to assign a label to each pixel. This method avoids the handcrafted subjective design of a model with a deep learning mechanism, which automatically extracts the dependencies between labels. Deep learning is also used for processing hyperspectral images. Spectral and spatial learned features are combined together in a hierarchical model to characterize tissues or materials.

In general, deep learning in medical imaging provides automatic discovery of object features and automatic exploration of feature hierarch and interaction. In this way, a relatively simple training process and a systematic performance tuning can be used, making deep learning approaches improve over the state-of-the art. However, in medical imaging analysis, their potentials have not been unfolded fully. To be successful in disease detection and classification approaches, deep learning requires the availability of large labeled datasets. Annotating imaging datasets is an extremely time-consuming and costly process that is normally undertaken by medical doctors. Currently, there is a lot of debate on whether to increase the number of annotated datasets with the help of non-experts (crowd- sourcing) and how to standardize the available images to allow objective assessment of the deep learning approaches.

### **3.5. Public Health**

Public health aims to prevent disease, prolong life, and promote healthcare by analyzing the spread of disease and social behaviors in relation to environmental factors. Public health studies consider small localized populations to large populations that encompass several continents such as in the case of epidemics and pandemics. Applications involve epidemic surveillance, modeling lifestyle diseases, such as obesity, with relation to geographical areas, monitoring and predicting air quality, drug safety surveillance, etc. The conventional predictive models scale exponentially with the size of the data and use complex models derived from physics, chemistry, and biology. Nevertheless, existing computational methods are able to accurately model several phenomena, including the progression of diseases or the spread of air pollution. However, they have limited abilities in incorporating real time information, which could be crucial in controlling an epidemic or the adverse effects of a newly approved medicine. In contrast, deep learning approaches have a powerful generalization ability. They are data-driven methods that automatically build a hierarchical model and encode the information within their structure. Most deep learning algorithm designs are based on online machine learning and, thus, optimization of the cost function takes place sequentially as new training datasets become available. One of the simplest online optimization algorithms applied in DNNs is stochastic gradient descent. For these reasons, deep learning, along with recommendation systems and network analysis, are suggested as the key analysis methods for public health studies [36].

Another interesting application is tracking outbreaks with social media for epidemiology and lifestyle diseases. Social media can provide rich information about the progression of diseases, such as Influenza and Ebola, in real time. Zhao et al. [37] used the microblogging social media service, Twitter, to continuously track health states from the public. DNN is used to mine epidemic features that are then combined into a simulated environment to model the progression of disease. Text from Twitter messages can also be used to gain insight into antibiotics and infectious intestinal diseases. DBN is used to categorize antibiotic- related

Twitter posts into nine classes (side effects, wanting/need, advertisement, advice/information, animals, general use, resistance, misuse, and other). To obtain the classifier, Twitter messages were randomly selected for manual labeling and categorization. They used a training set of 412 manually labeled and 150 000 unlabeled examples. A deep learning approach based on RBMs was pretrained in a layer-by-layer procedure. Fine-tuning was based on standard back propagation and the labeled data. Deep learning is used to create a topical vocabulary of keywords related to three types of infectious intestinal disease—campylobacter, norovirus, and food poisoning. When compared to officially documented cases, their results show that social media can be a good predictor of intestinal diseases.

For tracking certain stigmatized behaviors, social media can also provide information that is often undocumented; Garimella et al. [38] used geographically-tagged images from Instagram to track lifestyle diseases, such as obesity, drinking, and smoking, and compare the self-categorization of images from the user against annotations obtained using a deep learning algorithm.

Furthermore, mining food and drug records to identify adverse events could provide vital large scale alert mechanisms. We have presented a few examples that use deep learning for early identification and modeling the spread of epidemics and public health risks. However, strict regulation that protects data privacy limits the access and aggregation of the relevant information. For example, Twitter messages or Facebook posts could be used to identify new mothers at risk from postpartum depression. Although, this is positive, there is controversy associated with whether this information should become available, since it stigmatizes specific individuals. Therefore, it has become evident that we need to strike a balance between ensuring individuals can control access to their private medical information and providing pathways on how to make information available for public health studies [39]. The complexity and limited interpretability of deep learning models constitute an obstacle in allowing an informed decision about the precise operation of a DNN, which may limit its application in sensitive data.

#### 4. Deep Learning in Healthcare: Limitations and Challenges

Although for different artificial intelligence tasks, deep learning techniques can deliver substantial improvements in comparison to traditional machine learning approaches, many researchers and scientists remain sceptical of their use where medical applications are involved. These scepticisms arise since deep learning theories have not yet provided complete solutions and many questions remain unanswered. The following four aspects summarize some of the potential issues associated with deep learning:

- 1) Despite some recent work on visualizing high level features by using the weight filters in a CNN, the entire deep learning model is often not interpretable. Consequently, most researchers use deep learning approaches as a black box without the possibility to explain why it provides good results or without the ability to apply modifications in the case of misclassification issues.
- 2) To train a reliable and effective model, large sets of training data are required for the expression of new concepts. Although an explosion of available healthcare data with many organizations is often limited. Therefore, not all applications, particularly rare diseases or events are well suited to deep learning. A common problem that can arise during the training of a DNN (especially in the case of small datasets) is overfitting, which may occur when the number of parameters in the network is proportional to the total number of samples in the training set. Therefore, although the error on the training set is driven to a very small value, the errors for new data will be high. To avoid the overfitting problem and improve generalization, regularization methods, such as the dropout [40], are usually exploited during training.
- 3) Another important aspect to take into account when deep learning tools are employed, is that for many applications the raw data cannot be directly used as input for the DNN. Thus, preprocessing, normalization or change of input domain is often required before the training. Finding the correct preprocessing of the data and the optimal set of hyperparameters can be challenging, since it makes the training process even longer, requiring significant training resources and human expertise, without which is not possible to obtain an effective classification model.
- 4) The last aspect is that many DNNs can be easily fooled. For example, it is possible to add small changes to the input samples (such as imperceptible noise in an image) to cause samples to be misclassified. However, it is important to note that almost all machine learning algorithms are susceptible to such issues. Values of particular features can be deliberately set very high or very low to induce misclassification in logistic regression. Similarly, for decision trees, a single binary feature can be used to direct a sample along the wrong partition by simply switching it at the final layer. Hence in general, any machine learning models are susceptible to such manipulations. On the other hand, the work in [41] discusses the opposite problem.

To conclude, the healthcare informatics today is a human machine collaboration that may ultimately become a symbiosis in the future. As more data becomes available, deep learning systems can evolve and deliver where human interpretation is difficult. This can make diagnoses of diseases faster and smarter and reduce uncertainty in the decision making process. Finally, the last boundary of deep learning could be the

feasibility of integrating data across disciplines of health informatics to support the future of precision medicine.

## 5. Conclusion

Deep learning has gained a central position in recent years in machine learning and pattern recognition. It has enabled the development of more data driven solutions in health informatics by allowing automatic generation of features that reduce the amount of human intervention in this process. This is advantageous for many problems in health informatics and has eventually supported a great leap forward for unstructured data such as those arising from medical imaging, medical informatics, and bioinformatics. Until now, most applications of deep learning to health informatics have involved processing health data as an unstructured source. A significant amount of information is equally encoded in structured data such as EHRs, which provide a detailed picture of the patient's history, pathology, treatment, diagnosis, outcome, and the like. In the case of medical imaging, the cytological notes of a tumor diagnosis may include compelling information like its stage and spread. This information is beneficial to acquire a holistic view of a patient condition or disease and then be able to improve the quality of the obtained inference. In fact, robust inference through deep learning combined with artificial intelligence could ameliorate the reliability of clinical decision support systems.

Therefore, methodological aspects of NNs need to be revisited in this regard. Another concern is that deep learning predominantly depends on large amounts of training data. Many researchers have been encouraged to apply deep learning to any data-mining and pattern recognition problem related to health informatics in light of the wide availability of free packages to support this research. In practice, it is still questionable whether the large amount of training data and computational resources needed to run deep learning at full performance is worthwhile, considering other fast learning algorithms that may produce close performance with fewer resources, less parameterization, tuning, and higher interpretability.

Therefore, deep learning has provided a positive revival of NNs and connectionism from the genuine integration of the latest advances in parallel processing enabled by coprocessors. Nevertheless, a sustained concentration of health informatics research exclusively around deep learning could slow down the development of new machine learning algorithms with a more conscious use of computational resources and interpretability.

## References

- [1] H. R. Roth et al., Improving computer-aided detection using convolutional neural networks and random view aggregation, in IEEE Trans. Med. Imag., vol. 35, no. 5, pp. 1170–1181, May 2016.
- [2] R. Fakoor, F. Ladhak, A. Nazi, and M. Huber, Using deep learning to enhance cancer diagnosis and classification, in Proc. Int. Conf. Mach. Learn., 2013, pp. 1–7.
- [3] B. Alipanahi, A. Delong, M. T. Weirauch, and B. J. Frey, —Predicting the sequence specificities of DNA-and RNA-binding proteins by deep learning, in Nature Biotechnol., vol. 33, pp. 831–838, 2015.
- [4] Y. LeCun, Y. Bengio, and G. Hinton, Deep learning, in Nature, vol. 521, no. 7553, pp. 436–444, 2015.
- [5] J. L. McClelland et al., Parallel distributed processing. Cambridge, MA, USA: MIT Press, vol. 2, 1987.
- [6] D. E. Rumelhart, G. E. Hinton, and R. J. Williams, Learning representations by back-propagating errors, in Neurocomputing: Foundations of Research, J. A. Anderson and E. Rosenfeld, Eds. Cambridge, MA, USA: MIT Press, 1988, pp. 696–699. [Online]. Available: <http://dl.acm.org/citation.cfm?id=65669.104451>
- [7] H. Shin, L. Lu, L. Kim, A. Seff, J. Yao, and R. M. Summers, Interleaved text/image deep mining on a large-scale radiology database for automated image interpretation, vol. abs/1505.00670, 2015. Also available: <http://arxiv.org/abs/1505.00670>
- [8] Z. Liang, G. Zhang, J. X. Huang, and Q. V. Hu, Deep learning for healthcare decision making with emrs, in Proc. Int. Conf. Bioinformat. Biomed., Nov 2014, pp. 556–559.
- [9] E. Putin et al., Deep biomarkers of human aging: Application of deep neural networks to biomarker development, in Aging, vol. 8, no. 5, pp. 1–021, 2016.
- [10] L. Nie, M. Wang, L. Zhang, S. Yan, B. Zhang, and T. S. Chua, Disease inference from health-related questions via sparse deep learning, in IEEE Trans. Knowl. Data Eng., vol. 27, no. 8, pp. 2107–2119, Aug. 2015.
- [11] R. Miotto, L. Li, B. A. Kidd, and J. T. Dudley, Deep patient: An unsupervised representation to predict the future of patients from the electronic health records, in Sci. Rep., vol. 6, pp. 1–10, 2016.
- [12] J. Futoma, J. Morris, and J. Lucas, A comparison of models for predicting early hospital readmissions, in J. Biomed. Informat., vol. 56, pp. 229–238, 2015.
- [13] S. Mehrabi et al., Temporal pattern and association discovery of diagnosis codes using deep

- learning,|| in Proc. Int. Conf. Healthcare Informat., Oct. 2015, pp. 408–416.
- [14] Z. Che, S. Purushotham, R. Khemani, and Y. Liu, Distilling knowledge from deep networks with applications to healthcare domain,|| ArXiv e-prints, Dec. 2015.
- [15] G.-Z. Yang, Body Sensor Networks, 2nd ed. New York, NY, USA: Springer, 2014.
- [16] A. E. W. Johnson, M. M. Ghassemi, S. Nemati, K. E. Niehaus, D. A. Clifton, and G. D. Clifford, Machine learning and decision support in critical care,|| Proc. IEEE, vol. 104, no. 2, pp. 444–466, Feb. 2016.
- [17] D. Wulsin, J. Blanco, R. Mani, and B. Litt, Semi-supervised anomaly detection for eeg waveforms using deep belief nets,|| in Proc. 9th Int. Conf. Mach. Learn. Appl., Dec. 2010, pp. 436–441.
- [18] X. Jia, K. Li, X. Li, and A. Zhang, A novel semi-supervised deep learning framework for affective state recognition on eeg signals,|| in Proc. Int. Conf. Bioinformat. Bioeng., 2014, pp. 30–37.
- [19] A. Wang, C. Song, X. Xu, F. Lin, Z. Jin, and W. Xu, Selective and compressive sensing for energy-efficient implantable neural decoding,|| in Proc. Biomed. Circuits Syst. Conf., Oct. 2015, pp. 1–4.
- [20] L. A. Pastur-Romay, F. Cedr' n, A. Pazos, and A. B. Porto-Pazos, Deep oartificial neural networks and neuromorphic chips for big data analysis: Pharmaceutical and bioinformatics applications,|| Int. J. Molecular Sci., vol. 17, no. 8, 2016, Art. no. 1313.
- [21] L. Hood and S. H. Friend, Predictive, personalized, preventive, participatory (p4) cancer medicine,|| Nature Rev. Clin. Oncol., vol. 8, no. 3, pp. 184–187, 2011.
- [22] M. K. Leung, A. Delong, B. Alipanahi, and B. J. Frey, Machine learning in genomic medicine: A review of computational problems and data sets,|| Proc. IEEE, vol. 104, no. 1, pp. 176–197, Jan. 2016.
- [23] V. Marx, —Biology: The big challenges of big data,|| Nature, vol. 498, no. 7453, pp. 255–260, 2013.
- [24] R. Ibrahim, N. A. Yousri, M. A. Ismail, and N. M. El-Makky, Multi- level gene/mirna feature selection using deep belief nets and active learning,|| in Proc. Eng. Med. Biol. Soc., 2014, pp. 3957–3960.
- [25] M. Khademi and N. S. Nedialkov, Probabilistic graphical models and deep belief networks for prognosis of breast cancer,|| in Proc. IEEE 14th Int. Conf. Mach. Learn. Appl., 2015, pp. 727–732.
- [26] D. Quang, Y. Chen, and X. Xie, Dann: A deep learning approach for annotating the pathogenicity of genetic variants,|| Bioinformatics, vol. 31, p. 761–763, 2014.
- [27] C. Angermueller, H. Lee, W. Reik, and O. Stegle, Accurate prediction of single-cell dna methylation states using deep learning,|| bioRxiv, 2016, Art. no. 055715.
- [28] S. Kearnes, K. McCloskey, M. Berndl, V. Pande, and P. Riley, Molecular graph convolutions: moving beyond fingerprints,|| J. Comput. Aided Mol. Des., vol. 30, no. 8, pp. 595–608, 2016.
- [29] B. Ramsundar, S. Kearnes, P. Riley, D. Webster, D. Konerding, and V. Pande, —Massively multitask networks for drug discovery,|| ArXiv e-prints, Feb. 2015.
- [30] M. Havaei, N. Guizard, H. Larochelle, and P. Jodoin, Deep learning trends for focal brain pathology segmentation in MRI,|| CoRR, vol. abs/1607.05258,2016.. Available: <http://arxiv.org/abs/1607.05258>
- [31] H. Greenspan, B. van Ginneken, and R. M. Summers, Guest editorial deep learning in medical imaging: Overview and future promise of an exciting new technique,|| IEEE Trans. Med. Imag., vol. 35, no. 5, pp. 1153–1159, May 2016.
- [32] J.-Z. Cheng et al., Computer-aided diagnosis with deep learning architecture: Applications to breast lesions in us images and pulmonary nodules in ct scans,|| Sci. Rep., vol. 6, 2016, Art. no. 24454.
- [33] J. Shan and L. Li, A deep learning method for microaneurysm detection in fundus images,|| in Proc. IEEE Connected Health, Appl., Syst. Eng. Technol., 2016, pp. 357–358.
- [34] T. Brosch et al., Manifold learning of brain mrис by deep learning,|| in Proc. MICCAI, 2013, pp. 633–640.
- [35] A. Mansoor et al., Deep learning guided partitioned shape model for anterior visual pathway segmentation,|| IEEE Trans. Med. Imag., vol. 35, no. 8, pp. 1856–1865, Aug. 2016.
- [36] T. Huang, L. Lan, X. Fang, P. An, J. Min, and F. Wang, Promises and challenges of big data computing in health sciences,|| Big Data Res., vol. 2, no. 1, pp. 2–11, 2015.
- [37] L. Zhao, J. Chen, F. Chen, W. Wang, C.-T. Lu, and N. Ramakrishnan, Simnest: Social media nested epidemic simulation via online semi- supervised deep learning,|| in Proc. IEEE Int. Conf. Data Mining, 2015, pp. 639–648.
- [38] V. R. K. Garimella, A. Alfayad, and I. Weber, Social media image analysis for public health,|| in Proc. CHIConf. Human Factors Comput. Syst., 2016, pp. 5543–5547.
- [39] E. Horvitz and D. Mulligan, Data, privacy, and the greater good,|| Science, vol. 349, no. 6245, pp. 253–255, 2015.
- [40] N. Srivastava, G. E. Hinton, A. Krizhevsky, I. Sutskever, and R. Salakhutdinov, Dropout: a simple way to prevent neural networks from overfitting,|| J. Mach. Learn. Res., vol. 15, no. 1, pp. 1929–1958, 2014.

# **Application of TOPSIS Optimization Technique in TIG Welding of Mild Steel Plates**

**Prashant Kumar and Bhavana Mathur**

**Abstract:** The present study focused on the Technique for order preference by similarity to ideal solution method. This mathematical method was applied by taking the output of the tensile testing, and micro-hardness testing of the samples prepared by TIG welding method [11]. The experiment was designed according to Taguchi's L9 orthogonal arrays [6]. The nine experiments were ranked taking both the tensile strength value and micro-hardness value. The nine experiments were ranked taking the positive ideal solution. The ranking was done in descending order of the obtained values which are near to the positive ideal solution. Finally, the welding parameters were optimized to get the better tensile strength, and microhardness value and also each sample were ranked taking both tensile strength and microhardness values in consideration by a technique for order preference by similarity to the ideal solution.

**Keywords-**TIG (Tungsten inert gas welding); TOPSIS (technique for order preference by similarity to ideal solution); UTS (Ultimate tensile strength)

## **1. Introduction**

TOPSIS focus on the positive and negative ideal solutions and work with the concept that the alternative that has been selected should have a close distance to the positive-solution taken. With the help of this concept, the rankings were given. This method consists of generating a matrix which shows the various alternatives and the criteria. Ideal alternatives or ideal positive solutions which have the best level of all attributes are considered. In TOPSIS method the alternatives that are close to the positive ideal solution is selected. For carrying out the TOPSIS analysis tensile strength and Micro hardness value were taken as the criteria. The aim was to do the ranking of the nine samples prepared by TIG welding using Taguchi's L9 orthogonal array design [3]. Three different parameters were taken while welding the samples the parameters were welding current, welding speed and gas flow rate [10]. The welding current was taken as 80, 100, 120 amperes and welding speed was taken as 3, 3.5, 4 mm/sec while gas flow rate was taken as 10,12,14 l/min. The present experimental work focuses on getting a sample which has optimized tensile strength and hardness properties. TOPSIS mathematical analysis is used to obtain the ranking of various samples so that the best among them can be identified which has optimized values of both tensile strength and micro hardness values [23].

---

Prashant Kumar

Department of Mechanical Engineering, Anand International College of Engineering, Jaipur (India)

Email Address : Prashant.kumar@anandice.ac.in

Bhavana Mathur

Department of Mechanical Engineering, Anand International College of Engineering, Jaipur (India)

Email Address : Bhavana.mathur@anandice.ac.in

## 2. Experimental Work

The experimental work for the present work includes preparation of specimens for checking both tensile strength and microhardness. This chapter includes description of the machine set up experimental design, preparation of the specimens and finally testing of the samples for tensile strength and microhardness.

### 2.1 TIG Welding Setup

The TIG welding was done with a constant voltage of 12 V with direct current straight polarity. The inert atmosphere during the welding was provided by argon gas.



**Fig.2.1 TIG Welding Setup**

### 2.2 Taguchi's experimental design

Taguchi's L9 orthogonal array was used for designing the experiments which will give the optimal result. Nine specimens were butt welded by using three levels of current, three levels of welding speed and three levels of gas flow rate.

**Table-2.1 Welding parameters and their levels (Domain of Experimentation) for L9 Taguchi's Orthogonal Array Design of Experiment.**

<b>FACTORS</b>	<b>UNITS</b>	<b>LEVELS</b>		
		1	2	3
Welding current	Ampere (A)	80	100	120
Welding speed	mm/sec	3	3.5	4
Gas flow rate	L/min	10	12	14

**Table-2.2 Design matrix based on Taguchi's L9 array design of experiment**

SAMPLE NO	WELDING PARAMETERS		
	Welding current (Ampere)	Welding speed (mm/sec)	Gas flowrate (L/min)
1	80	3	10
2	80	3.5	12
3	80	4	14
4	100	3	12
5	100	3.5	14
6	100	4	10
7	120	3	14
8	120	3.5	10
9	120	4	12

### 2.3 Preparation of welding samples

Mild steel plates of  $(50 \times 25) \text{ mm}^2$  in dimension were butt using TIG welding process to get a welded joint of  $(100 \times 25) \text{ mm}^2$  in dimension. Mild steel plate of thickness 2 mm was selected as working material for the present experiment. Automatic hacksaw cutter was used to cut the mild steel plates of dimensions  $(50 \times 25) \text{ mm}^2$ . Grinding was done at the edges to smooth the surfaces. After the sample's preparation was done, it was cleaned and was welded according to the various process parameters as discussed in the Taguchi's L9 orthogonal array.

**Fig.2.2 Tungsten inert gas welded specimens**

### 2.4 Testing of welded specimen

The tensile testing of the welded samples was done on UTM (30 kN). For tensile testing, the specimens were cleaned to remove any dust particles. After that, the specimens were given a standard form for tensile testing.



**Fig.2.3 Tensile testing of the specimen on UTM machine**

#### **2.4 Microhardness testing**

The microhardness testing was carried out on the welded specimens. Indentation hardness was measured for every nine specimens. TIG welded nine specimens were taken after that the surface of the rectangular samples were rubbed by emery papers of different grades. Finally, acetone solution was applied to the surface. The testing was done on Vicker's hardness testing machine.



**Fig. 2.4. Vicker's microhardness tester**

### 3. Result Analysis and Discussion

#### 3.1 Analysis of variance for tensile testing

ANOVA is a statistical tool which helps in analyzing differences among group means. ANOVA is a handy tool when it is required to find the significant parameters which can affect the experiment. Through ANOVA it is easier to obtain the contribution of each parameter in percentage which gives the optimal result and also the errors.

##### 3.1.1 Calculation of S/N ratio for tensile strength

S/N ratio was calculated from the software MINITAB by UTS values. The Taguchi's L9 orthogonal array was used for taking the input factor i.e. the tensile strength values which obtained from different parameters values. UTS value was taken as the response factor. The larger is better concept was used for calculating S/N ratio.

**Table-3.1 S/N ratio for tensile strength**

S.NO	Welding current (a)	Welding speed (mm/sec)	Gas flow rate (l/min)	UTS (ultimate tensile strength) Mpa	S/N Ratio
1	80	3	10	309.90	49.8244
2	80	3.5	12	335	50.5009
3	80	4	14	368.33	51.3247
4	100	3	12	452	53.0256
5	100	3.5	14	565	55.0870
6	100	4	10	570.31	55.1222
7	120	3	14	445	52.9672
8	120	3.5	10	498.92	53.9606
9	120	4	12	469	53.4235

##### 3.1.2 Main effect plot for S/N ratio

The main effect plot was plotted between the S/N ratio and the various process parameters in the present work the parameters are welding current, welding speed, and gas flow rate. The higher is better criteria was used for the interpretation of the main effect plot. From the fig.5 , it can be seen that the welding current of 100 A, welding speed of 4 mm/sec and gas flow rate of 14 L/min gives the higher values.

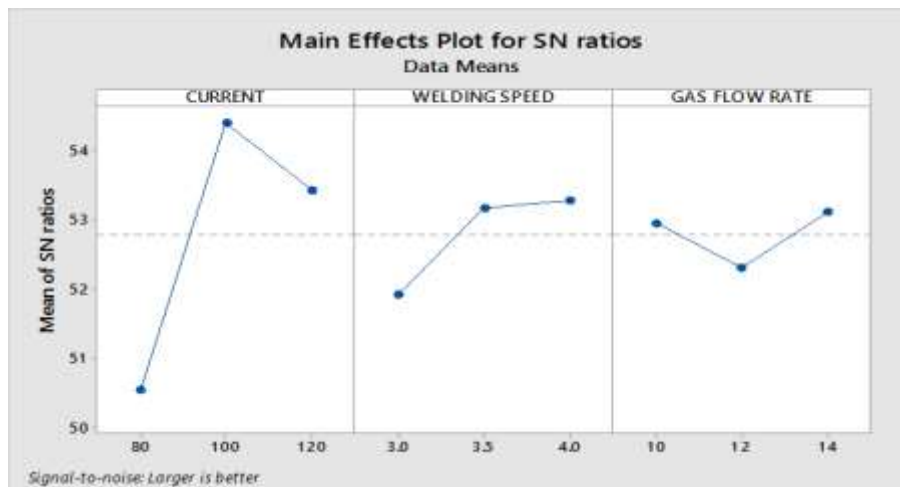


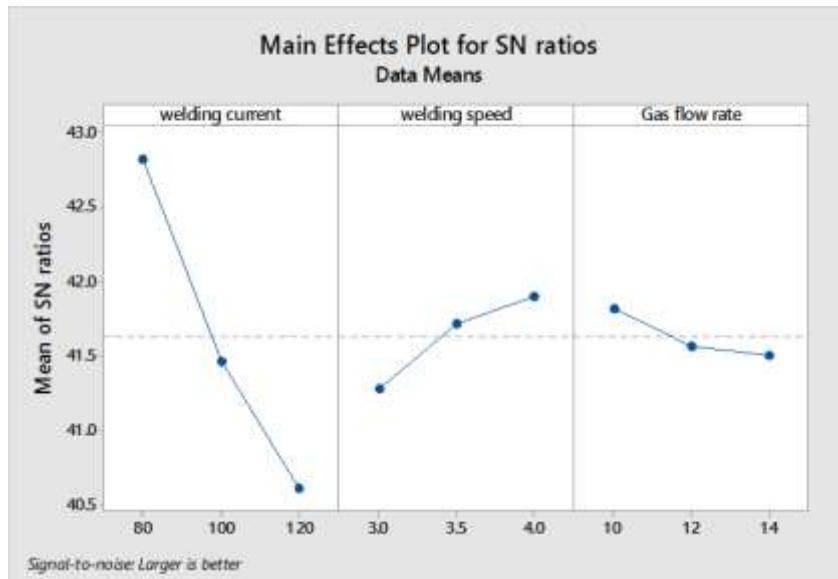
**Fig.3.1 Main effect plot for S/N ratio (Tensile strength)**

**Table-3.2 Calculation of S/N ratio for microhardness**

S.NO	Welding current (A)	Welding speed (mm/sec)	Gas flow rate (L/min)	Microhardness (vicker's hardness) HV	S/N ratio
1	80	3	10	136.0	42.6708
2	80	3.5	12	138.0	42.7976
3	80	4	14	141.0	42.9844
4	100	3	12	113.0	41.0616
5	100	3.5	14	118.0	41.4376
6	100	4	10	124.0	41.8684
7	120	3	14	101.1	40.0950
8	120	3.5	10	111.0	40.9065
9	120	4	12	110.0	40.8279

### 3.1.3 Main effect plot for S/N ratio

The main effect plot for S/N ratio is plotted between the various welding parameters here it is welding current, welding speed and gas flow rate and S/N ratio.

**Fig.3.2 Main effect plot for S/N ratio (Micro hardness)**

The plot is based on higher the better criteria. Here welding current of 80 A, welding speed of 4 mm/sec and gas flow rate of 10 L/min is associated with highest mean microhardness values.

## 4. Technique for order Preference by Similarity to Ideal Solution (TOPSIS)

TOPSIS focus on the positive and negative ideal solutions and work with the concept that the alternative that has been selected should have a close distance to the positive solution taken. With the help of this concept, the rankings were given. This method consists of generating a matrix which shows the various alternatives and the criteria. Ideal alternatives or ideal positive solutions which have the best level of all attributes are considered. In TOPSIS method the alternatives that are close to the positive ideal solution is selected.

**Table-4.1 Experimental data of various mechanical properties**

S.NO	Tensile Strength (MPa)	Hardness (Vicker's) HV
1	309.90	136.0
2	335	138.0
3	368.33	141.0
4	452	113.0
5	565	118.0
6	570.31	124.0
7	445	101.1
8	498.92	111.0
9	469	110.0

#### 4.1 Formation of decision matrix

First, of all performance defining criterion and alternatives of the problem are identified, and a decision matrix is created. In the decision, matrix alternatives are represented by M and criteria are represented by N

#### 4.2 The normalized decision matrix

The decision matrix is normalized to make all the values of the decision matrix comparable. The normalized matrix R= [ ] and the normalized value are calculated as below.

$$r_{ij} = \frac{a_{ij}}{\left[ \sum_{i=1}^M (a_{ij}^2) \right]^{1/2}}$$

$$D_{M \times N} = \begin{pmatrix} a_{11} & a_{12} & \dots & a_{1N} \\ a_{21} & a_{22} & \dots & a_{2N} \\ \vdots & \vdots & & \vdots \\ a_{M1} & a_{M2} & \dots & a_{MN} \end{pmatrix}$$

Where i= 1, 2, 3 ....M and j=1, 2, 3.....N

**Table-4.2 The normalized decision matrix**

S.No	Tensile Strength (MPa)	Hardness (Vicker's) HV
1	0.2272	0.3713
2	0.2456	0.3768
3	0.2701	0.3849
4	0.3314	0.3085
5	0.4143	0.3221
6	0.4182	0.3385
7	0.3263	0.2760
8	0.3658	0.3030
9	0.3439	0.3003

#### 4.3 Positive and negative ideal solution

The positive ideal solution and the negative ideal solution found out as follows.

Ideal positive solution is given by  $A^+ = (r^+_1, r^+_2, r^+_3, \dots, r^+_n)$

Where  $A^+ = (0.4182, 0.3849)$

Ideal negative solution is given by  $A^- = (r^-_1, r^-_2, r^-_3, \dots, r^-_n)$

Where  $A^- = (0.2272, 0.2760)$

#### 4.4 Calculating closeness index and ranking

It is crucial to find the closeness index. From the closeness index ranking of the various experiments are given. For finding the closeness index, the Euclidian distances are required. It is calculated by

$$D_i^+ = \sqrt{\sum_j^N (r_i^+ - r_{ij}^+)^2} \quad D_i^- = \sqrt{\sum_j^N (r_{ij}^- - r_i^-)^2}$$

Where for  $i=1, 2, 3, \dots, M$

Finally, the closeness index of the alternatives is calculated by the equation mentioned below.

Where

$$CI_i = \frac{D_i^-}{D_i^+ + D_i^-}$$

**Table-4.3 Calculation of closeness index and ranking**

S.No	Di+	Di-	CI	Ranking
1	0.1914	0.0953	0.3324	9
2	0.1727	0.1024	0.3722	8
3	0.1481	0.1170	0.4413	6
4	0.1156	0.1091	0.4855	5
5	0.0629	0.1926	0.7538	2
6	0.0464	0.2009	0.8123	1
7	0.1424	0.0991	0.4103	7
8	0.0972	0.1412	0.5922	3
9	0.1125	0.1192	0.5144	4

Finally, the ranking is given to the various results which have the highest CI values in descending order as shown in table 4.3.

#### 4.5 Result of technique for order preference by similarity to ideal solution (TOPSIS)

From the TOPSIS analysis, each sample is ranked. Table 4.23 shows the different welding parameters and the values of the ultimate tensile testing (UTS) and microhardness testing (Vicker's microhardness) for the nine specimens. The TOPSIS analysis gives the combined results of both the testing and finds out which process was best and is close to positive ideal solutions. The nine samples were ranked keeping the benefit criteria.

**Table-4.4 Result of Topsis analysis**

S.N O	Current (ampere)	Welding speed (mm/min )	Gas flow rate (l/min)	UTS ( MPa )	Micro-hardness (vicker's) HV	Topsis Ranking
1	80	3	10	309.90	136.0	9
2	80	3.5	12	335	138.0	8
3	80	4	14	368.33	141.0	6
4	100	3	12	452	113.0	5
5	100	3.5	14	565	118.0	2
6	100	4	10	570.31	124.0	1
7	120	3	14	445	101.1	7
8	120	3.5	10	498.92	111.0	3
9	120	4	12	469	110.0	4

## Conclusions

From the study, it can be concluded that

1. The optimum welding condition obtained by Taguchi method for tensile strength is current = 100 A, welding speed 4mm/sec and gas flow rate = 14L/min[17].
2. The optimum welding condition obtained by Taguchi method for hardness is current = 80A, welding speed 4mm/sec and gas flow rate = 12 L/min.
3. From the analysis of TOPSIS, each sample was ranked, and a welding current of 100 A, welding speed of 4 mm/min and gas flow rate of 10 L/minwas given rank one.

## References

- [1] M. Chellappan, K. Lingadurai, and P. Sathiya, "Characterization and Optimization of TIG welded supermartensitic stainless steel using TOPSIS," *Mater. Today Proc.*, vol. 4, no. 2, pp. 1662–1669, 2017.
- [2] G. Magudeeswaran, S. R. Nair, L. Sundar, and N. Harikannan, "Optimization of process parameters of the activated tungsten inert gas welding for aspect ratio of UNS S32205 duplex stainless steel welds," *Def. Technol.*, vol. 10, no. 3, pp. 251–260, 2014.
- [3] L. S. Patel, T. C. Patel, A. Professor, and M. E. Student, "Optimization Of Welding Parameters For TIG Welding Of 304 L Stainless Steel Using Taguchi Approach," *Int. J. Eng. Dev. Res.*, vol. 2, no. 1, pp. 2321–9939, 2014.
- [4] S. C. Juang and Y. S. Tarn, "Process parameter selection for optimizing the weld pool geometry in the tungsten inert gas welding of stainless steel," *J. Mater. Process. Technol.*, vol. 122, no. 1, pp. 33–37, 2002.
- [5] S. Srivastava and R. K. Garg, "Process parameter optimization of gas metal arc welding on IS:2062 mild steel using response surface methodology," *J. Manuf. Process.*, vol. 25, pp. 296–305, 2017.
- [6] P. Bharath, V. G. Sridhar, and M. Senthil Kumar, "Optimization of 316 stainless steel weld joint characteristics using taguchi technique," *Procedia Eng.*, vol. 97, pp. 881–891, 2014.
- [7] N. Kiaee and M. Aghaei-Khafri, "Optimization of gas tungsten arc welding process by response surface methodology," *Mater. Des.*, vol. 54, pp. 25–31, 2014.
- [8] A. Razal Rose, K. Manisekar, V. Balasubramanian, and S. Rajakumar, "Prediction and optimization of pulsed current tungsten inert gas welding parameters to attain maximum tensile strength in AZ61A magnesium alloy," *Mater. Des.*, vol. 37, pp. 334–348, 2012.
- [9] K. Nandagopal and C. Kailasanathan, "Analysis of mechanical properties and optimization of gas tungsten Arc welding (GTAW) parameters on dissimilar metal titanium (6Al-4V) and aluminium 7075 by Taguchi and ANOVA techniques," *J. Alloys Compd.*, vol. 682, pp. 503–516, 2016.

- [10] J. Pasupathy and V. Ravisankar, "PARAMETRIC OPTIMIZATION OF TIG WELDING PARAMETERS USING TAGUCHI METHOD FOR DISSIMILAR JOINT (Low carbon steel with AA1050)," vol. 4, no. 1, pp. 25–28, 2013.
- [11] S. Rajendra and R. R. Arakerimath, "Parameter Optimization of Tig Welding Using Austenitic Stainless Steel," vol. 2, no. 1, pp. 120– 124, 2015.
- [12] V. Anand Rao and R. Deivanathan, "Experimental investigation for welding aspects of stainless steel 310 for the process of TIG welding," *Procedia Eng.*, vol. 97, pp. 902–908, 2014.
- [13] N. Moslemi, N. Redzuan, N. Ahmad, and T. N. Hor, "Effect of current on characteristic for 316 stainless steel welded joint including microstructure and mechanical properties," *Procedia CIRP*, vol. 26, pp. 560–564, 2015.
- [14] R. Kumar, S. Chattopadhyaya, and S. Kumar, "Influence of Welding Current on Bead Shape, Mechanical and Structural Property of Tungsten Inert Gas Welded Stainless Steel Plate," *Mater. Today Proc.*, vol. 2, no. 4–5, pp. 3342–3349, 2015.
- [15] Q. Wang, D. L. Sun, Y. Na, Y. Zhou, X. L. Han, and J. Wang, "Effects of TIG welding parameters on morphology and mechanical properties of welded joint of Ni-base superalloy," *Procedia Eng.*, vol. 10, pp. 37–41, 2011.
- [16] S. P. Gadewar, P. Swaminadhan, M. G. Harkare, and S. H. Gawande, "Experimental Investigations of Weld Characteristics for a Single Pass Tig Welding With Ss304 Experimental Investigations of Weld Characteristics for a Single Pass Tig Welding With," no. September 2016, 2010.
- [17] V. Subravel, G. Padmanaban, and V. Balasubramanian, "Effect of welding speed on microstructural characteristics and tensile roperties of GTA welded AZ31B magnesium alloy," *Trans. Nonferrous Met. Soc. China (English Ed.)*, vol. 24, no. 9, pp. 2776– 2784, 2014.
- [18] T. Senthil Kumar, V. Balasubramanian, and M. Y. Sanavullah, "Influences of pulsed current tungsten inert gas welding parameters on the tensile properties of AA 6061 aluminium alloy," *Mater. Des.*, vol. 28, no. 7, pp. 2080–2092, 2007.
- [19] W. B. L. and R. F. K.C. Winco Yung, Ralph, "An investigation into welding parameters affecting the tensile properties oftitanium welds," *J. ofMaterials Process. Technol.*, vol. 63, no. 96, pp. 759– 764, 1997.
- [20] W. Chuaiphan and L. Srijaroenpramong, "Effect of welding speed on microstructures, mechanical properties and corrosion behavior of GTA-welded AISI 201 stainless steel sheets," *J. Mater. Process. Technol.*, vol. 214, no. 2, pp. 402–408, 2014.
- [21] C. Balaji, S. V. A. Kumar, S. A. Kumar, R. Sathish, and T. Nadu, "Evaluation of Mechanical Properties of SS 316 L Weldments Using Tungsten Inert Gas Welding," vol. 4, no. 5, pp. 2053–2057, 2012.
- [22] K. D. Ramkumar *et al.*, "Comparative studies on the weldability, microstructure and tensile properties of autogeneous TIG welded AISI 430 ferritic stainless steel with and without flux," *J. Manuf. Process.*, vol. 20, pp. 54–69, 2015.
- [23] H. Li, J. Zou, J. Yao, and H. Peng, "The effect of TIG welding techniques on microstructure, properties and porosity of the welded joint of 2219 aluminum alloy," *J. Alloys Compd.*, vol. 727, pp. 531– 539, 2017.
- [24] L. Srinivasan, S. J. Jakka, and P. Sathiya, "Microstructure and mechanical properties of Gas tungsten arc welded High Strength Low Alloy (15CDV6) steel joints," *Mater. Today Proc.*, vol. 4, no. 8, pp. 8874– 8882, 2017.
- [25] S. Kumar and A. S. Shahi, "Effect of heat input on the microstructure and mechanical properties of gas tungsten arc weldedAISI 304 stainless steel joints," *Mater. Des.*, vol. 32, no. 6, pp. 3617–3623, 2011.
- [26] A. Kumar *et al.*, "Experimental Process of Tungsten Inert Gas Welding of a Stainless Steel Plate," *Mater. Today Proc.*, vol. 2, no. 4–5, pp. 3260–3267, 2015.
- [27] Q. Zhu, Y. C. Lei, X. Z. Chen, W. J. Ren, X. Ju, and Y. M. Ye, "Microstructure and mechanical properties in TIG welding of CLAM steel," *Fusion Eng. Des.*, vol. 86, no. 4–5, pp. 407–411, 2011.
- [28] T. Wen, S. Y. Liu, S. Chen, L. T. Liu, and C. Yang, "Influence of high frequency vibration on microstructure and mechanical properties of TIG welding joints of AZ31 magnesium alloy," *Trans. Nonferrous Met. Soc. China (English Ed.)*, vol. 25, no. 2, pp. 397– 404, 2015.
- [29] H. Lin, L. Ying, L. Jun, and L. Binghong, "Microstructure and Mechanical Properties for TIG Welding Joint of High Boron Fe-Ti- B Alloy," *Rare Met. Mater. Eng.*, vol. 43, no. 2, pp. 283–286, 2014.

# **Application of Deep Learning in Health Informatics: A Review**

**Vinit Mehta and Noopur Srivastava**

**Abstract** Today a variety of health care practices have been evolved to maintain and restore health by the latest prevention and best treatment. This implements biomedical sciences, biomedical research, genetics and medical technology to diagnose, treat, and prevent injury and disease, typically through pharmaceuticals or surgery, therapies as diverse as psychotherapy, external splints and traction, medical devices, biologics, and ionizing radiation. With advances in technology, the health sciences are constantly pushing toward more effective treatments and cures. With a massive influx of multimodality data, the role of data analytics in health informatics has grown rapidly in the last decade. This has also provoked increasing interests in the generation of analytical, data driven models based on machine learning in health informatics. Deep learning, a technique with its foundation in artificial neural networks, is emerging in recent years as a powerful tool for machine learning, promising to reform the future of artificial intelligence. Rapid improvements in computational power, fast data storage, and parallelization have also contributed to the rapid uptake of the technology in addition to its predictive power and ability to generate automatically optimized high-level features and semantic interpretation from the input data. This paper presents a comprehensive review of research employing deep learning in health informatics, providing a critical analysis of the relative merit, and potential pitfalls of the technique as well as its future outlook. The paper mainly focuses on key applications of deep learning in the fields of translational bioinformatics, medical imaging, pervasive sensing, medical informatics, and public health. Finally the limitations and challenges of deep learning in the field of health informatics have been discussed.

**Keywords-** machine learning, deep learning, health informatics, translational bioinformatics, medical imaging, pervasive sensing, medical informatics, and public health.

## **1. Introduction**

Deep learning has become a new trend in machine learning since recent years. The background foundations of deep learning are well rooted in the classical neural network (NN) theory. But unlike traditional NNs, deep learning algorithm uses many hidden neurons and layers, typically more than two that contribute an architectural advantage combined with new training paradigms. Deep learning is based on a set of algorithms that model high level abstractions in data. In a simple case, there might be two sets of neurons: one set that receives an input signal and one that sends an output signal. When the input layer receives an input it passes on a modified version of the input to the next layer. In a deep network, there are many layers between the input and the output, that allows the algorithm to use multiple processing layers, composed of multiple linear and non-linear transformations. Fig. 1 shows that each successive layer in a neural network uses features from the previous layer to learn more complex features. In this manner a deep neural network is capable of composing features of increasing complexity in each of its successive layers.

---

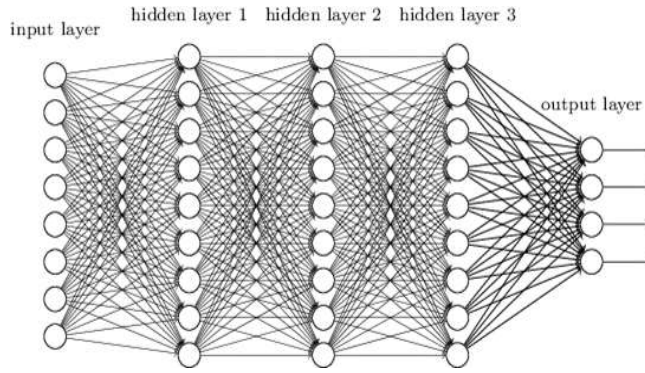
Vinit Mehta

Research Scholar, Department of Electrical Engineering, M.B.M. Engineering College, Jodhpur, India  
e-mail: vinit741@gmail.com

Noopur Srivastava

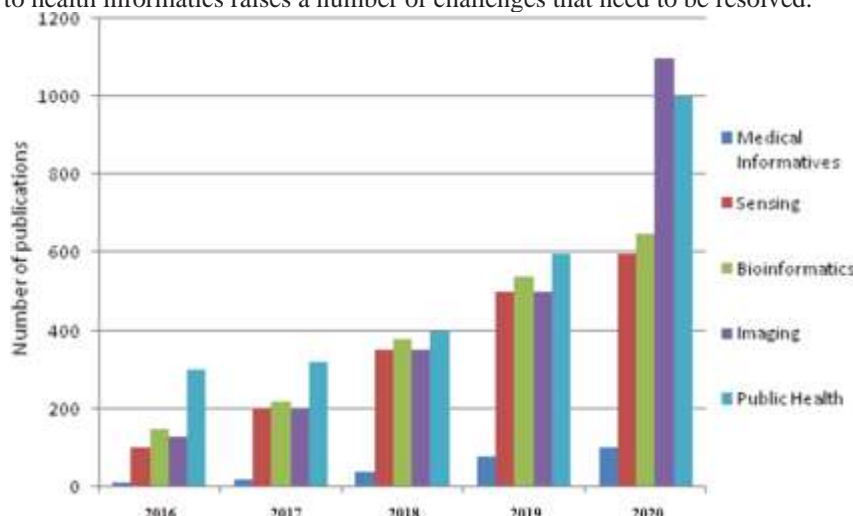
Centre of Excellence Electric Vehicle, Department of Mechanical Engineering,  
Anand International College of Engineering Jaipur, India

**P. Agarwal et al. (eds.), Recent Developments in Engineering & Technology**  
**September 14-15, 2019, AICE, Jaipur, India**

**Fig.1. Block diagram of Deep Neural Network**

Also the layer-by-layer pipeline of nonlinear combination of their outputs generates a lower dimensional projection of the input space. Every lower-dimensional projection corresponds to a higher perceptual level. This results in an effective high-level abstraction of the raw data or images if the network is optimally weighted.

In the past few years, deep learning has become an immediate tool to solve applications in computer vision, speech recognition, natural language processing, and other application areas of commercial interest. In areas such as health informatics, the generation of the deep learning feature set without human intervention has many advantages. In medical imaging, it can generate features that are more sophisticated and difficult to elaborate in descriptive means. Implicit features could determine fibroids and polyps [1], and characterize irregularities in tissue morphology such as tumors [2]. In translational bioinformatics, such algorithms may also determine nucleotide sequences that could bind a DNA or RNA strand to a protein [3]. Fig. 2 outlines a quick rush of interest in deep learning in recent years in terms of the number of papers published in sub-fields in health informatics including bioinformatics, medical imaging, pervasive sensing, medical informatics, and public health. The publication statistics have obtained from Google Scholar; the search phrase is defined as the subfield name with the exact phrase deep learning. A excess of experimental works have implemented deep learning models for heath informatics, reaching similar performance or in many cases exceeding that of alternative techniques. Nevertheless, the application of deep learning to health informatics raises a number of challenges that need to be resolved.

**Fig.2. Number of published papers that use deep learning in health informatic applications**

In addition, deep learning requires extensive computational resources, without which training could become excessively time-consuming. Attaining an optimal definition of the network's free parameters can become a particularly laborious task to solve. Eventually, deep learning models can be affected by convergence issues as well as overfitting, hence supplementary learning strategies are required to address these problems [4]. In this paper, a review of recent health informatics studies has been done that employ deep learning to discuss its relative strength and potential pitfalls. Furthermore, their schemas and operational frameworks are described in detail to clarify their practical implementations, as well as expected performance.

## 2. From Perceptron to Deep Learning

Perceptron is a bio inspired algorithm for binary classification and consist of an input layer directly connected to an output node, emulate this biochemical process through an activation function (also referred to as a transfer function) and a few weights. Specifically, it can learn to classify linearly separable patterns by adjusting these weights accordingly.

To solve more complex problems, NNs with one or more hidden layers of perceptrons have been introduced [5]. To train these NNs, many stages or epochs are usually performed where each time the network is presented with a new input sample and the weights of each neuron are adjusted based on a learning process called delta rule. The delta rule is used by the most common class of supervised NNs during the training and is usually implemented by exploiting the back-propagation routine [6]. Specifically, without any prior knowledge, random values are assigned to the network weights. Through an iterative training process, the network weights are adjusted to minimize the difference between the network outputs and the desired outputs. The most common iterative training method uses the gradient descent method where the network is optimized to find the minimum along the error surface. This method requires the activation functions to be always differentiable.

Adding more hidden layers to the network allows a deep architecture to be built that can express more complex hypothesis as the hidden layers confine the nonlinear relationships. These NNs are known as Deep Neural Networks (DNN). Deep learning has provided new sophisticated approaches to train DNN architectures. In general, DNNs can be trained with unsupervised and supervised learning methodologies. In supervised learning, labeled data are used to train the DNNs and learn the weights that minimize the error to predict a target value for classification or regression, whereas in unsupervised learning, the training is performed without requiring labeled data. Unsupervised learning is usually used for clustering, feature extraction or dimensionality reduction. For some applications it is common to combine an initial training procedure of the DNN with an unsupervised learning step to extract the most relevant features and then use those features for classification by exploiting a supervised learning step.

For many years, hardware limitations have made DNNs impractical due to high computational demands for both training and processing, especially for applications that require real-time processing. Recently, these limitations have been partially overcome and have enabled DNNs to be recognized as a significant breakthrough in artificial intelligence.

## 3. Applications

### 3.1. Medical Informatics

Medical Informatics focus on the analysis of large, aggregated data in healthcare fields with the aim to enhance and develop clinical decision support systems or assess medical data both for quality assurance and accessibility of health care services. Deep learning approaches have been designed to scale up well with big and distributed datasets. The success of DNNs is largely due to their ability to learn novel features/patterns and understand data representation in both an unsupervised and supervised hierarchical manners. DNNs have also proven to be efficient in handling multi information since they can combine several DNN architectural components. Therefore, it is unsurprising that deep learning has quickly been adopted in medical informatics research. In the field of medical informatics, many authors have made several documentations. Shin et al. [7] have presented a combined text image CNN to identify semantic information that links radiology images and reports from a typical picture archiving and communication system. Liang et al. [8] have used a modified version of DNN as an effective training method for large scale datasets on hypertension. Putin et al. [9] have applied DNNs for identifying markers that predict human chronological age based on simple blood tests. Nie et al. [10] have proposed a deep learning network for automatic disease inference, which requires manual gathering the key symptoms or questions related to the disease.

In another study, Mioto et al. [11] have showed that a stack of autoencoders can be used to automatically infer features from a large scale EHR database and represent patients without requiring additional human effort. The authors demonstrated the ability of their system to predict the probability of a patient developing specific diseases, such as diabetes, schizophrenia and cancer. Furthermore, Futoma et al. [12] have compared different models in their ability to predict hospital readmissions based on a large EHR database. DNNs have significantly higher prediction accuracies than conventional approaches, such as penalized logistic regression, though training of the DNN models were not straightforward. Mehrabi et al. [13] have proposed the use of DBN to discover common temporal patterns and characterize disease progression. The authors have highlighted the ability to interpret the newly discovered patterns requires further investigation.

The motivations behind these studies are to develop general purpose systems to accurately predict length of stay, future illness, readmission, and mortality with the view to improve clinical decision making and

optimize clinical pathways. Early prediction in health care is directly related to saving patient's lives. Furthermore, the discovery of novel patterns can result in new hypotheses and research questions. In computational phenotype research, the goal is to discover meaningful data-driven features and disease characteristics. For example, Che et al. [14] have highlighted that although DNNs outperform conventional machine learning approaches in their ability to predict and classify clinical events, they suffer from the issue of model interpretability, which is important for clinical adaptation. They pointed out that interpreting individual units can be misleading and the behavior of DNNs are more complex than originally thought. They suggested that once a DNN is trained with big data, a simpler model can be used to distil knowledge and mimic the prediction performance of the DNN.

Deep learning has paved the way for personalized health care by offering an unprecedented power and efficiency in mining large multimodal unstructured information stored in hospitals, cloud providers and research organization. Although, it has the potential to outperform traditional machine learning approaches, appropriate initialization and tuning is important to avoid overfitting. Noisy and sparse datasets result in considerable fall of performance indicating that there are several challenges to be addressed. Furthermore, adopting these systems into clinical practice requires the ability to track and interpret the extracted features and patterns.

### **3.2. Sensing**

Pervasive sensors, such as wearable, implantable, and ambient sensors have [15] allowed continuous monitoring of health and wellbeing. An accurate estimation of food intake and energy expenditure throughout the day can help tackle obesity and improve personal wellbeing. For elderly patients with chronic diseases, wearable and ambient sensors can be utilized to improve quality of care by enabling patients to continue living independently in their own homes. The care of patients with disabilities and patients undergoing rehabilitation can also be improved through the use of wearable and implantable assistive devices and human activity recognition. For patients in critical care, continuous monitoring of vital signs, such as blood pressure, respiration rate, and body temperature, are important for improving treatment outcomes by closely analyzing the patient's condition [16].

Wulsin et al. [17] proposed a DBN approach to detect anomalies in EEG waveforms. EEG is used to record electrical activity of the brain. Interpreting the waveforms from brain activity is challenging due to the high dimensionality of the input signal and the limited understanding of the brain operations. Jia et al. [18] have used a deep learning method based on RBM to recognize affective state of EEG. Although the sample sets are small and noisy, the proposed method achieves greater accuracy. A DBN was also used for detecting arrhythmias from electrocardiography (ECG) signals. The main purpose of the system is identifying arrhythmias which are a complex pattern recognition problem. Yan et al. have attained classification accuracies of 98% using a two-lead ECG dataset. For low power wearable and implantable EEG sensors, where energy consumption and efficiency are major concerns, Wang et al. [19] have designed a DBN to compress the signal. This results in more than 50% of energy savings while retaining accuracy for neural decoding. The introduction of deep learning has increased the utility of pervasive sensing across a range of health applications by improving the accuracy of sensors that measure food calorie intake, energy expenditure, activity recognition, sign language interpretation, and detection of anomalous events in vital signs. Many applications use deep learning to achieve greater efficiency and performance for real-time processing on low-power devices; however, a greater focus should be placed upon implementations on neuromorphic hardware platforms designed for low-power parallel processing. The most significant improvements in performance have been achieved where the data has high dimensionality as seen in the EEG datasets. Most current research has focused on the recognition of activities of daily living and brain activity. Many opportunities for other applications and diseases remain, and many currently studies still rely upon relatively small datasets that may not fully capture the variability of the real world.

### **3.3. Bioinformatics**

Bioinformatics aim to investigate and understand biological processes at a molecular level. Advances in biotechnology have helped reduce the cost of genome sequencing and steered the focus on prognostic, diagnostic and treatment of diseases by analyzing genes and proteins. This can be illustrated by the fact that sequencing the first human genome cost billions of dollars, whereas today it is affordable [20]. Further motivated by P4 (predictive, personalized, preventive, participatory) medicine [21], bioinformatics aim to predict and prevent diseases by involving patients in the development of more efficient and personalized treatments. The application of machine learning in bioinformatics can be divided into three areas: prediction of biological processes, prevention of diseases and personalized treatment. These areas are found in genomics, pharmacogenomics and epigenomics. Genomics explores the function and information structures encoded in the DNA sequences of a living cell [22]: it analyzes genes responsible for the creation of protein

sequences and the expression of phenotypes. A goal of genomics is to identify gene alleles and environmental factors that contribute to diseases such as cancer. Pharmacogenomics evaluates variations in an individual's drug response to treatment brought about by differences in genes. It aims to design more efficient drugs for personalized treatment. Finally, epigenomics aims to investigate protein interactions and understand higher level processes, such as transcriptome (mRNA count), proteome, and metabolome, which lead to modification in the gene's expression. Understanding how environmental factors affect protein formation and their interactions is a goal of epigenomics.

The ability of deep learning to abstract large, complex, and unstructured data offers a powerful way of analyzing heterogeneous data such as gene alleles, proteins occurrences, and environmental factors [23]. In deep learning approaches, feature extraction and model fitting takes place in a unified step. Multilayer feature representation can capture nonlinear dependencies at multiple scales of transcriptional and epigenetic interactions and can model molecular structure and properties in a data driven way. These nonlinear features are invariant to small input changes which results in eliminating noise and increasing the robustness of the technique.

Several works have demonstrated that deep learning features outperformed methods relying on visual descriptors in the recognition and classification of cancer cells. For example, Ibrahim et al. [24] have proposed a DBN with an active learning approach to find features in genes and microRNA that resulted in the best classification performance of various cancer diseases such as hepatocellular carcinoma, lung cancer and breast cancer. For breast cancer genetic detection, Khademi et al. [25] have overcame missing attributes and noise by combining a DBN and Bayesian network to extract features from microarray data. Deep learning approaches have also outperformed SVM in predicting splicing code and understanding how gene expression changes by genetic variants [26]. Angermueller et al. [27] have used DNN to predict DNA methylation states from DNA sequences and incomplete methylation profiles. After applying to 32 embryonic mice stem cells, the baseline model was compared with the results. This method can be used for genome-wide downstream analyses.

Deep learning not only outperforms conventional approaches but also opens the door to more efficient methods to be developed. Kearnes et al. [28] have described how deep learning based on graph convolutions can encode molecular structural features, physical properties, and activities in other assays. This allows a rich representation of possible interactions beyond the molecular structural information encoded in standard databases. Similarly, multitask DNNs provides an intuitive model of correlation between molecule compounds and targets because information can be shared among different nodes. This increases robustness, reduces chances to miss information, and usually outperforms other methods that process large datasets [29].

### 3.4. Medical Imaging

Automatic medical imaging analysis is crucial in modern medicine. Diagnosis based on the interpretation of images can be highly subjective. Computer-aided diagnosis can provide an objective assessment of the underlying disease processes. Modeling of disease progression, common in several neurological conditions, such as Alzheimer's, multiple sclerosis, and stroke, requires analysis of brain scans based on multimodal data and detailed maps of brain regions. In recent years, CNNs have been adapted rapidly by the medical imaging research community because of their outstanding performance demonstrated in computer. The fact that CNNs in medical imaging have yielded promising results have also been highlighted in a recent survey of CNN approaches in brain pathology segmentation [30] and in an editorial of deep learning techniques in computer aided detection, segmentation, and shape analysis [31].

Among the biggest challenges in CAD are the differences in shape and intensity of tumors/lesions and the variations in imaging protocol even within the same imaging modality. In several cases, the intensity range of pathological tissue may overlap with that of healthy samples. Furthermore, Rician noise, non isotropic resolution, and bias field effects in magnetic resonance images (MRI) cannot be handled automatically using simpler machine learning approaches. To deal with this data complexity, hand-designed features are extracted and conventional machine learning approaches are trained to classify them in a completely separate step.

Deep learning provides the possibility to automate and merge the extraction of relevant features with the classification procedure. CNNs inherently learn a hierarchy of increasingly more complex features and, thus, they can operate directly on a patch of images centered on the abnormal tissue. Example applications of CNNs in medical imaging include the classification of interstitial lung diseases based on computed tomography (CT) images, the classification of tuberculosis manifestation based on X-ray images, the classification of neural progenitor cells from somatic cell source , the detection of haemorrhages in color fundus images and the organ or body-part-specific anatomical classification of CT images. A multistage deep learning framework based on CNNs extracts both the patches with the most as well as least discriminative local patches in the pretraining stage. Subsequently, a boosting stage exploits this local information to improve performance. The authors point out that training based on discriminative local

appearances are more accurate compared to the usage of global image context. Although CNNs have dominated medical image analysis applications, other deep learning approaches/architectures have also been applied successfully. In a recent paper, a stacked denoising autoencoder was proposed for the diagnosis of benign malignant breast lesions in ultrasound images and pulmonary nodules in CT scans [32]. The method outperforms classical CAD approaches, largely due to the automatic feature extraction and noise tolerance. Furthermore, it eliminates the image segmentation process to obtain a lesion boundary. Shan et al. [33] presented a stacked sparse autoencoder for microaneurysms detection in fundus images as an instance of a diabetic retinopathy strategy. The proposed method learns high-level distinguishing features based only on pixel intensities. Various autoencoder-based learning approaches have also been applied to the automatic extraction of biomarkers from brain images and the diagnosis of neurological diseases. These methods often use available public domain brain image databases such as the Alzheimer's disease neuroimaging initiative database. For example, a deep Autoencoder combined with a softmax output layer for regression is proposed for the diagnosis of Alzheimer's disease.

Low level image processing, such as image segmentation and registration can also benefit from deep learning models. Brosch et al. [34] described a manifold learning approach of 3-D brain images based on DBN. It is different than other methods because it does not require a locally linear manifold space. Mansoor et al. [35] developed a fully automated shape model segmentation mechanism for the analysis of cranial nerve systems. The deep learning approach outperforms conventional methods particularly in regions with low contrast, such as optic tracts and areas with pathology. A pipeline is proposed for object detection and segmentation in the context of automatically processing volumetric images. A novel framework called marginal space deep learning implements an object parameterization in hierarchical marginal spaces combined with automatic feature detection based on deep learning. A DNN architecture called input–output deep architecture is described to solve the image labelling problem. A single NN forward step is used to assign a label to each pixel. This method avoids the handcrafted subjective design of a model with a deep learning mechanism, which automatically extracts the dependencies between labels. Deep learning is also used for processing hyperspectral images. Spectral and spatial learned features are combined together in a hierarchical model to characterize tissues or materials.

In general, deep learning in medical imaging provides automatic discovery of object features and automatic exploration of feature hierarch and interaction. In this way, a relatively simple training process and a systematic performance tuning can be used, making deep learning approaches improve over the state-of-the art. However, in medical imaging analysis, their potentials have not been unfolded fully. To be successful in disease detection and classification approaches, deep learning requires the availability of large labeled datasets. Annotating imaging datasets is an extremely time-consuming and costly process that is normally undertaken by medical doctors. Currently, there is a lot of debate on whether to increase the number of annotated datasets with the help of non-experts (crowd- sourcing) and how to standardize the available images to allow objective assessment of the deep learning approaches.

### **3.5. Public Health**

Public health aims to prevent disease, prolong life, and promote healthcare by analyzing the spread of disease and social behaviors in relation to environmental factors. Public health studies consider small localized populations to large populations that encompass several continents such as in the case of epidemics and pandemics. Applications involve epidemic surveillance, modeling lifestyle diseases, such as obesity, with relation to geographical areas, monitoring and predicting air quality, drug safety surveillance, etc. The conventional predictive models scale exponentially with the size of the data and use complex models derived from physics, chemistry, and biology. Nevertheless, existing computational methods are able to accurately model several phenomena, including the progression of diseases or the spread of air pollution. However, they have limited abilities in incorporating real time information, which could be crucial in controlling an epidemic or the adverse effects of a newly approved medicine. In contrast, deep learning approaches have a powerful generalization ability. They are data-driven methods that automatically build a hierarchical model and encode the information within their structure. Most deep learning algorithm designs are based on online machine learning and, thus, optimization of the cost function takes place sequentially as new training datasets become available. One of the simplest online optimization algorithms applied in DNNs is stochastic gradient descent. For these reasons, deep learning, along with recommendation systems and network analysis, are suggested as the key analysis methods for public health studies [36].

Another interesting application is tracking outbreaks with social media for epidemiology and lifestyle diseases. Social media can provide rich information about the progression of diseases, such as Influenza and Ebola, in real time. Zhao et al. [37] used the microblogging social media service, Twitter, to continuously track health states from the public. DNN is used to mine epidemic features that are then combined into a simulated environment to model the progression of disease. Text from Twitter messages can also be used to gain insight into antibiotics and infectious intestinal diseases. DBN is used to categorize antibiotic- related

Twitter posts into nine classes (side effects, wanting/need, advertisement, advice/information, animals, general use, resistance, misuse, and other). To obtain the classifier, Twitter messages were randomly selected for manual labeling and categorization. They used a training set of 412 manually labeled and 150 000 unlabeled examples. A deep learning approach based on RBMs was pretrained in a layer-by-layer procedure. Fine-tuning was based on standard back propagation and the labeled data. Deep learning is used to create a topical vocabulary of keywords related to three types of infectious intestinal disease—campylobacter, norovirus, and food poisoning. When compared to officially documented cases, their results show that social media can be a good predictor of intestinal diseases.

For tracking certain stigmatized behaviors, social media can also provide information that is often undocumented; Garimella et al. [38] used geographically-tagged images from Instagram to track lifestyle diseases, such as obesity, drinking, and smoking, and compare the self-categorization of images from the user against annotations obtained using a deep learning algorithm.

Furthermore, mining food and drug records to identify adverse events could provide vital large scale alert mechanisms. We have presented a few examples that use deep learning for early identification and modeling the spread of epidemics and public health risks. However, strict regulation that protects data privacy limits the access and aggregation of the relevant information. For example, Twitter messages or Facebook posts could be used to identify new mothers at risk from postpartum depression. Although, this is positive, there is controversy associated with whether this information should become available, since it stigmatizes specific individuals. Therefore, it has become evident that we need to strike a balance between ensuring individuals can control access to their private medical information and providing pathways on how to make information available for public health studies [39]. The complexity and limited interpretability of deep learning models constitute an obstacle in allowing an informed decision about the precise operation of a DNN, which may limit its application in sensitive data.

#### 4. Deep Learning in Healthcare: Limitations and Challenges

Although for different artificial intelligence tasks, deep learning techniques can deliver substantial improvements in comparison to traditional machine learning approaches, many researchers and scientists remain sceptical of their use where medical applications are involved. These scepticisms arise since deep learning theories have not yet provided complete solutions and many questions remain unanswered. The following four aspects summarize some of the potential issues associated with deep learning:

- 1) Despite some recent work on visualizing high level features by using the weight filters in a CNN, the entire deep learning model is often not interpretable. Consequently, most researchers use deep learning approaches as a black box without the possibility to explain why it provides good results or without the ability to apply modifications in the case of misclassification issues.
- 2) To train a reliable and effective model, large sets of training data are required for the expression of new concepts. Although an explosion of available healthcare data with many organizations is often limited. Therefore, not all applications, particularly rare diseases or events are well suited to deep learning. A common problem that can arise during the training of a DNN (especially in the case of small datasets) is overfitting, which may occur when the number of parameters in the network is proportional to the total number of samples in the training set. Therefore, although the error on the training set is driven to a very small value, the errors for new data will be high. To avoid the overfitting problem and improve generalization, regularization methods, such as the dropout [40], are usually exploited during training.
- 3) Another important aspect to take into account when deep learning tools are employed, is that for many applications the raw data cannot be directly used as input for the DNN. Thus, preprocessing, normalization or change of input domain is often required before the training. Finding the correct preprocessing of the data and the optimal set of hyperparameters can be challenging, since it makes the training process even longer, requiring significant training resources and human expertise, without which is not possible to obtain an effective classification model.
- 4) The last aspect is that many DNNs can be easily fooled. For example, it is possible to add small changes to the input samples (such as imperceptible noise in an image) to cause samples to be misclassified. However, it is important to note that almost all machine learning algorithms are susceptible to such issues. Values of particular features can be deliberately set very high or very low to induce misclassification in logistic regression. Similarly, for decision trees, a single binary feature can be used to direct a sample along the wrong partition by simply switching it at the final layer. Hence in general, any machine learning models are susceptible to such manipulations. On the other hand, the work in [41] discusses the opposite problem.

To conclude, the healthcare informatics today is a human machine collaboration that may ultimately become a symbiosis in the future. As more data becomes available, deep learning systems can evolve and deliver where human interpretation is difficult. This can make diagnoses of diseases faster and smarter and reduce uncertainty in the decision making process. Finally, the last boundary of deep learning could be the

feasibility of integrating data across disciplines of health informatics to support the future of precision medicine.

## 5. Conclusion

Deep learning has gained a central position in recent years in machine learning and pattern recognition. It has enabled the development of more data driven solutions in health informatics by allowing automatic generation of features that reduce the amount of human intervention in this process. This is advantageous for many problems in health informatics and has eventually supported a great leap forward for unstructured data such as those arising from medical imaging, medical informatics, and bioinformatics. Until now, most applications of deep learning to health informatics have involved processing health data as an unstructured source. A significant amount of information is equally encoded in structured data such as EHRs, which provide a detailed picture of the patient's history, pathology, treatment, diagnosis, outcome, and the like. In the case of medical imaging, the cytological notes of a tumor diagnosis may include compelling information like its stage and spread. This information is beneficial to acquire a holistic view of a patient condition or disease and then be able to improve the quality of the obtained inference. In fact, robust inference through deep learning combined with artificial intelligence could ameliorate the reliability of clinical decision support systems.

Therefore, methodological aspects of NNs need to be revisited in this regard. Another concern is that deep learning predominantly depends on large amounts of training data. Many researchers have been encouraged to apply deep learning to any data-mining and pattern recognition problem related to health informatics in light of the wide availability of free packages to support this research. In practice, it is still questionable whether the large amount of training data and computational resources needed to run deep learning at full performance is worthwhile, considering other fast learning algorithms that may produce close performance with fewer resources, less parameterization, tuning, and higher interpretability.

Therefore, deep learning has provided a positive revival of NNs and connectionism from the genuine integration of the latest advances in parallel processing enabled by coprocessors. Nevertheless, a sustained concentration of health informatics research exclusively around deep learning could slow down the development of new machine learning algorithms with a more conscious use of computational resources and interpretability.

## References

- [1] H. R. Roth et al., Improving computer-aided detection using convolutional neural networks and random view aggregation, in IEEE Trans. Med. Imag., vol. 35, no. 5, pp. 1170–1181, May 2016.
- [2] R. Fakoor, F. Ladhak, A. Nazi, and M. Huber, Using deep learning to enhance cancer diagnosis and classification, in Proc. Int. Conf. Mach. Learn., 2013, pp. 1–7.
- [3] B. Alipanahi, A. Delong, M. T. Weirauch, and B. J. Frey, —Predicting the sequence specificities of DNA-and RNA-binding proteins by deep learning, in Nature Biotechnol., vol. 33, pp. 831–838, 2015.
- [4] Y. LeCun, Y. Bengio, and G. Hinton, Deep learning, in Nature, vol. 521, no. 7553, pp. 436–444, 2015.
- [5] J. L. McClelland et al., Parallel distributed processing. Cambridge, MA, USA: MIT Press, vol. 2, 1987.
- [6] D. E. Rumelhart, G. E. Hinton, and R. J. Williams, Learning representations by back-propagating errors, in Neurocomputing: Foundations of Research, J. A. Anderson and E. Rosenfeld, Eds. Cambridge, MA, USA: MIT Press, 1988, pp. 696–699. [Online]. Available: <http://dl.acm.org/citation.cfm?id=65669.104451>
- [7] H. Shin, L. Lu, L. Kim, A. Seff, J. Yao, and R. M. Summers, Interleaved text/image deep mining on a large-scale radiology database for automated image interpretation, vol. abs/1505.00670, 2015. Also available: <http://arxiv.org/abs/1505.00670>
- [8] Z. Liang, G. Zhang, J. X. Huang, and Q. V. Hu, Deep learning for healthcare decision making with emrs, in Proc. Int. Conf. Bioinformat. Biomed., Nov 2014, pp. 556–559.
- [9] E. Putin et al., Deep biomarkers of human aging: Application of deep neural networks to biomarker development, in Aging, vol. 8, no. 5, pp. 1–021, 2016.
- [10] L. Nie, M. Wang, L. Zhang, S. Yan, B. Zhang, and T. S. Chua, Disease inference from health-related questions via sparse deep learning, in IEEE Trans. Knowl. Data Eng., vol. 27, no. 8, pp. 2107–2119, Aug. 2015.
- [11] R. Miotto, L. Li, B. A. Kidd, and J. T. Dudley, Deep patient: An unsupervised representation to predict the future of patients from the electronic health records, in Sci. Rep., vol. 6, pp. 1–10, 2016.
- [12] J. Futoma, J. Morris, and J. Lucas, A comparison of models for predicting early hospital readmissions, in J. Biomed. Informat., vol. 56, pp. 229–238, 2015.
- [13] S. Mehrabi et al., Temporal pattern and association discovery of diagnosis codes using deep

- learning,|| in Proc. Int. Conf. Healthcare Informat., Oct. 2015, pp. 408–416.
- [14] Z. Che, S. Purushotham, R. Khemani, and Y. Liu, Distilling knowledge from deep networks with applications to healthcare domain,|| ArXiv e-prints, Dec. 2015.
- [15] G.-Z. Yang, Body Sensor Networks, 2nd ed. New York, NY, USA: Springer, 2014.
- [16] A. E. W. Johnson, M. M. Ghassemi, S. Nemati, K. E. Niehaus, D. A. Clifton, and G. D. Clifford, Machine learning and decision support in critical care,|| Proc. IEEE, vol. 104, no. 2, pp. 444–466, Feb. 2016.
- [17] D. Wulsin, J. Blanco, R. Mani, and B. Litt, Semi-supervised anomaly detection for eeg waveforms using deep belief nets,|| in Proc. 9th Int. Conf. Mach. Learn. Appl., Dec. 2010, pp. 436–441.
- [18] X. Jia, K. Li, X. Li, and A. Zhang, A novel semi-supervised deep learning framework for affective state recognition on eeg signals,|| in Proc. Int. Conf. Bioinformat. Bioeng., 2014, pp. 30–37.
- [19] A. Wang, C. Song, X. Xu, F. Lin, Z. Jin, and W. Xu, Selective and compressive sensing for energy-efficient implantable neural decoding,|| in Proc. Biomed. Circuits Syst. Conf., Oct. 2015, pp. 1–4.
- [20] L. A. Pastur-Romay, F. Cedr' n, A. Pazos, and A. B. Porto-Pazos, Deep oartificial neural networks and neuromorphic chips for big data analysis: Pharmaceutical and bioinformatics applications,|| Int. J. Molecular Sci., vol. 17, no. 8, 2016, Art. no. 1313.
- [21] L. Hood and S. H. Friend, Predictive, personalized, preventive, participatory (p4) cancer medicine,|| Nature Rev. Clin. Oncol., vol. 8, no. 3, pp. 184–187, 2011.
- [22] M. K. Leung, A. Delong, B. Alipanahi, and B. J. Frey, Machine learning in genomic medicine: A review of computational problems and data sets,|| Proc. IEEE, vol. 104, no. 1, pp. 176–197, Jan. 2016.
- [23] V. Marx, —Biology: The big challenges of big data,|| Nature, vol. 498, no. 7453, pp. 255–260, 2013.
- [24] R. Ibrahim, N. A. Yousri, M. A. Ismail, and N. M. El-Makky, Multi- level gene/mirna feature selection using deep belief nets and active learning,|| in Proc. Eng. Med. Biol. Soc., 2014, pp. 3957–3960.
- [25] M. Khademi and N. S. Nedialkov, Probabilistic graphical models and deep belief networks for prognosis of breast cancer,|| in Proc. IEEE 14th Int. Conf. Mach. Learn. Appl., 2015, pp. 727–732.
- [26] D. Quang, Y. Chen, and X. Xie, Dann: A deep learning approach for annotating the pathogenicity of genetic variants,|| Bioinformatics, vol. 31, p. 761–763, 2014.
- [27] C. Angermueller, H. Lee, W. Reik, and O. Stegle, Accurate prediction of single-cell dna methylation states using deep learning,|| bioRxiv, 2016, Art. no. 055715.
- [28] S. Kearnes, K. McCloskey, M. Berndl, V. Pande, and P. Riley, Molecular graph convolutions: moving beyond fingerprints,|| J. Comput. Aided Mol. Des., vol. 30, no. 8, pp. 595–608, 2016.
- [29] B. Ramsundar, S. Kearnes, P. Riley, D. Webster, D. Konerding, and V. Pande, —Massively multitask networks for drug discovery,|| ArXiv e-prints, Feb. 2015.
- [30] M. Havaei, N. Guizard, H. Larochelle, and P. Jodoin, Deep learning trends for focal brain pathology segmentation in MRI,|| CoRR, vol. abs/1607.05258,2016.. Available: <http://arxiv.org/abs/1607.05258>
- [31] H. Greenspan, B. van Ginneken, and R. M. Summers, Guest editorial deep learning in medical imaging: Overview and future promise of an exciting new technique,|| IEEE Trans. Med. Imag., vol. 35, no. 5, pp. 1153–1159, May 2016.
- [32] J.-Z. Cheng et al., Computer-aided diagnosis with deep learning architecture: Applications to breast lesions in us images and pulmonary nodules in ct scans,|| Sci. Rep., vol. 6, 2016, Art. no. 24454.
- [33] J. Shan and L. Li, A deep learning method for microaneurysm detection in fundus images,|| in Proc. IEEE Connected Health, Appl., Syst. Eng. Technol., 2016, pp. 357–358.
- [34] T. Brosch et al., Manifold learning of brain mrис by deep learning,|| in Proc. MICCAI, 2013, pp. 633–640.
- [35] A. Mansoor et al., Deep learning guided partitioned shape model for anterior visual pathway segmentation,|| IEEE Trans. Med. Imag., vol. 35, no. 8, pp. 1856–1865, Aug. 2016.
- [36] T. Huang, L. Lan, X. Fang, P. An, J. Min, and F. Wang, Promises and challenges of big data computing in health sciences,|| Big Data Res., vol. 2, no. 1, pp. 2–11, 2015.
- [37] L. Zhao, J. Chen, F. Chen, W. Wang, C.-T. Lu, and N. Ramakrishnan, Simnest: Social media nested epidemic simulation via online semi- supervised deep learning,|| in Proc. IEEE Int. Conf. Data Mining, 2015, pp. 639–648.
- [38] V. R. K. Garimella, A. Alfayad, and I. Weber, Social media image analysis for public health,|| in Proc. CHIConf. Human Factors Comput. Syst., 2016, pp. 5543–5547.
- [39] E. Horvitz and D. Mulligan, Data, privacy, and the greater good,|| Science, vol. 349, no. 6245, pp. 253–255, 2015.
- [40] N. Srivastava, G. E. Hinton, A. Krizhevsky, I. Sutskever, and R. Salakhutdinov, Dropout: a simple way to prevent neural networks from overfitting,|| J. Mach. Learn. Res., vol. 15, no. 1, pp. 1929–1958, 2014.

# Application of TOPSIS Optimization Technique in TIG Welding of Mild Steel Plates

Prashant Kumar, Bhavana Mathur

**Abstract:** The present study focused on the Technique for order preference by similarity to ideal solution method. This mathematical method was applied by taking the output of the tensile testing, and micro-hardness testing of the samples prepared by TIG welding method [11]. The experiment was designed according to Taguchi's L9 orthogonal arrays [6]. The nine experiments were ranked taking both the tensile strength value and micro-hardness value. The nine experiments were ranked taking the positive ideal solution. The ranking was done in descending order of the obtained values which are near to the positive ideal solution. Finally, the welding parameters were optimized to get the better tensile strength, and microhardness value and also each sample were ranked taking both tensile strength and microhardness values in consideration by a technique for order preference by similarity to the ideal solution.

**Keywords-**TIG (Tungsten inert gas welding); TOPSIS (technique for order preference by similarity to ideal solution); UTS (Ultimate tensile strength)

## 1. Introduction

TOPSIS focus on the positive and negative ideal solutions and work with the concept that the alternative that has been selected should have a close distance to the positive-solution taken. With the help of this concept, the rankings were given. This method consists of generating a matrix which shows the various alternatives and the criteria. Ideal alternatives or ideal positive solutions which have the best level of all attributes are considered. In TOPSIS method the alternatives that are close to the positive ideal solution is selected. For carrying out the TOPSIS analysis tensile strength and Micro hardness value were taken as the criteria. The aim was to do the ranking of the nine samples prepared by TIG welding using Taguchi's L9 orthogonal array design [3]. Three different parameters were taken while welding the samples the parameters were welding current, welding speed and gas flow rate [10]. The welding current was taken as 80, 100, 120 amperes and welding speed was taken as 3, 3.5, 4 mm/sec while gas flow rate was taken as 10,12,14 l/min. The present experimental work focuses on getting a sample which has optimized tensile strength and hardness properties. TOPSIS mathematical analysis is used to obtain the ranking of various samples so that the best among them can be identified which has optimized values of both tensile strength and micro hardness values [23].

---

Prashant Kumar  
Centre of Excellence Material Engineering, Department of Mechanical Engineering,  
Anand International College of Engineering, Jaipur (India)  
Prashant.kumar@anandice.ac.in

Bhavana Mathur  
Centre of Excellence Material Engineering, Department of Mechanical Engineering,  
Anand International College of Engineering, Jaipur (India)  
Bhavana.mathur@anandice.ac.in

## 2. Experimental Work

The experimental work for the present work includes preparation of specimens for checking both tensile strength and microhardness. This chapter includes description of the machine set up experimental design, preparation of the specimens and finally testing of the samples for tensile strength and microhardness.

### 2.1 TIG Welding Setup

The TIG welding was done with a constant voltage of 12 V with direct current straight polarity. The inert atmosphere during the welding was provided by argon gas.



**Fig.2.1 TIG Welding Setup**

### 2.2 Taguchi's experimental design

Taguchi's L9 orthogonal array was used for designing the experiments which will give the optimal result. Nine specimens were butt welded by using three levels of current, three levels of welding speed and three levels of gas flow rate.

**Table-2.1 Welding parameters and their levels (Domain of Experimentation) for L9 Taguchi's Orthogonal Array Design of Experiment.**

<b>FACTORS</b>	<b>UNITS</b>	<b>LEVELS</b>		
		1	2	3
Welding current	Ampere (A)	80	100	120
Welding speed	mm/sec	3	3.5	4
Gas flow rate	L/min	10	12	14

**Table-2.2 Design matrix based on Taguchi's L9 array design of experiment**

SAMPLE NO	WELDING PARAMETERS		
	Welding current (Ampere)	Welding speed (mm/sec)	Gas flowrate (L/min)
1	80	3	10
2	80	3.5	12
3	80	4	14
4	100	3	12
5	100	3.5	14
6	100	4	10
7	120	3	14
8	120	3.5	10
9	120	4	12

### 2.3 Preparation of welding samples

Mild steel plates of  $(50 \times 25) \text{ mm}^2$  in dimension were butt using TIG welding process to get a welded joint of  $(100 \times 25) \text{ mm}^2$  in dimension. Mild steel plate of thickness 2 mm was selected as working material for the present experiment. Automatic hacksaw cutter was used to cut the mild steel plates of dimensions  $(50 \times 25) \text{ mm}^2$ . Grinding was done at the edges to smooth the surfaces. After the sample's preparation was done, it was cleaned and was welded according to the various process parameters as discussed in the Taguchi's L9 orthogonal array.

**Fig.2.2 Tungsten inert gas welded specimens**

### 2.4 Testing of welded specimen

The tensile testing of the welded samples was done on UTM (30 kN). For tensile testing, the specimens were cleaned to remove any dust particles. After that, the specimens were given a standard form for tensile testing.



**Fig.2.3 Tensile testing of the specimen on UTM machine**

#### **2.4 Microhardness testing**

The microhardness testing was carried out on the welded specimens. Indentation hardness was measured for every nine specimens. TIG welded nine specimens were taken after that the surface of the rectangular samples were rubbed by emery papers of different grades. Finally, acetone solution was applied to the surface. The testing was done on Vicker's hardness testing machine.



**Fig. 2.4. Vicker's microhardness tester**

### 3. Result Analysis and Discussion

#### 3.1 Analysis of variance for tensile testing

ANOVA is a statistical tool which helps in analyzing differences among group means. ANOVA is a handy tool when it is required to find the significant parameters which can affect the experiment. Through ANOVA it is easier to obtain the contribution of each parameter in percentage which gives the optimal result and also the errors.

##### 3.1.1 Calculation of S/N ratio for tensile strength

S/N ratio was calculated from the software MINITAB by UTS values. The Taguchi's L9 orthogonal array was used for taking the input factor i.e. the tensile strength values which obtained from different parameters values. UTS value was taken as the response factor. The larger is better concept was used for calculating S/N ratio.

**Table-3.1 S/N ratio for tensile strength**

S.NO	Welding current (a)	Welding speed (mm/sec)	Gas flow rate (l/min)	UTS (ultimate tensile strength) Mpa	S/N Ratio
1	80	3	10	309.90	49.8244
2	80	3.5	12	335	50.5009
3	80	4	14	368.33	51.3247
4	100	3	12	452	53.0256
5	100	3.5	14	565	55.0870
6	100	4	10	570.31	55.1222
7	120	3	14	445	52.9672
8	120	3.5	10	498.92	53.9606
9	120	4	12	469	53.4235

##### 3.1.2 Main effect plot for S/N ratio

The main effect plot was plotted between the S/N ratio and the various process parameters in the present work the parameters are welding current, welding speed, and gas flow rate. The higher is better criteria was used for the interpretation of the main effect plot. From the fig.5 , it can be seen that the welding current of 100 A, welding speed of 4 mm/sec and gas flow rate of 14 L/min gives the higher values.

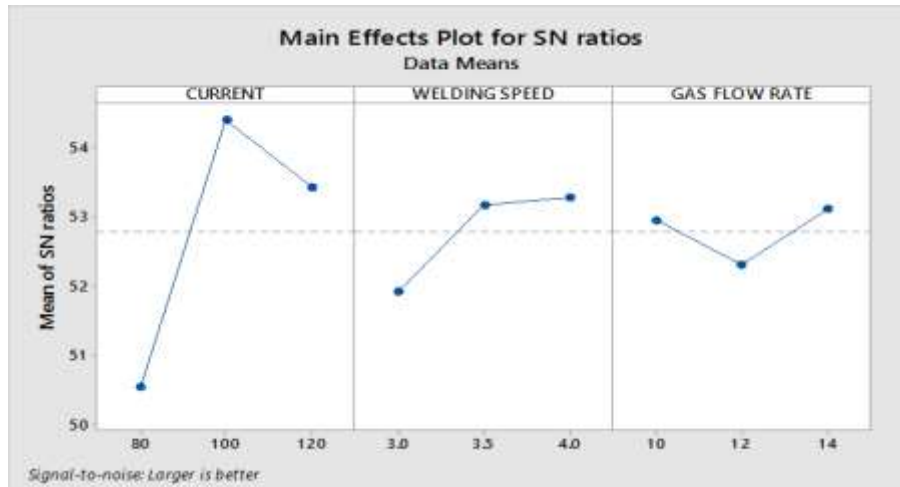


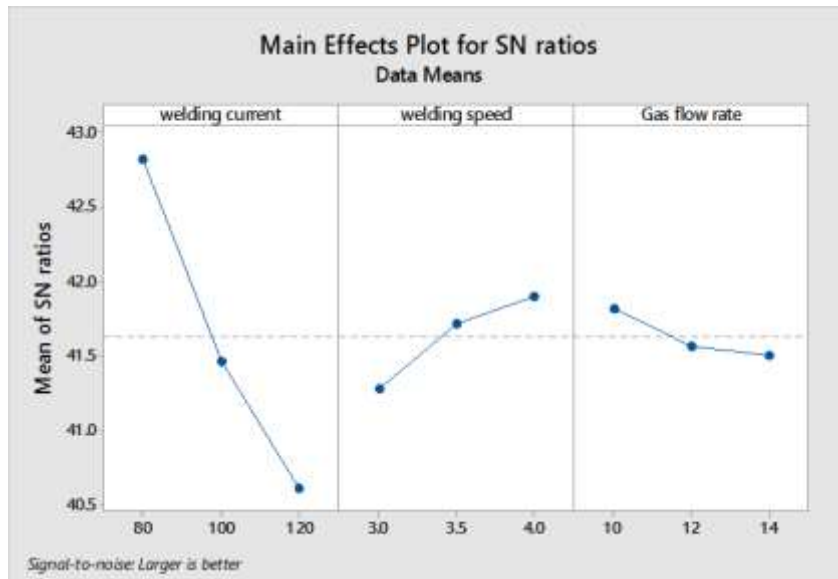
**Fig.3.1 Main effect plot for S/N ratio (Tensile strength)**

**Table-3.2 Calculation of S/N ratio for microhardness**

S.NO	Welding current (A)	Welding speed (mm/sec)	Gas flow rate (L/min)	Microhardness (vicker's hardness) HV	S/N ratio
1	80	3	10	136.0	42.6708
2	80	3.5	12	138.0	42.7976
3	80	4	14	141.0	42.9844
4	100	3	12	113.0	41.0616
5	100	3.5	14	118.0	41.4376
6	100	4	10	124.0	41.8684
7	120	3	14	101.1	40.0950
8	120	3.5	10	111.0	40.9065
9	120	4	12	110.0	40.8279

### 3.1.3 Main effect plot for S/N ratio

The main effect plot for S/N ratio is plotted between the various welding parameters here it is welding current, welding speed and gas flow rate and S/N ratio.

**Fig.3.2 Main effect plot for S/N ratio (Micro hardness)**

The plot is based on higher the better criteria. Here welding current of 80 A, welding speed of 4 mm/sec and gas flow rate of 10 L/min is associated with highest mean microhardness values.

## 4. Technique for order Preference by Similarity to Ideal Solution (TOPSIS)

TOPSIS focus on the positive and negative ideal solutions and work with the concept that the alternative that has been selected should have a close distance to the positive-solution taken. With the help of this concept, the rankings were given. This method consists of generating a matrix which shows the various alternatives and the criteria. Ideal alternatives or ideal positive solutions which have the best level of all attributes are considered. In TOPSIS method the alternatives that are close to the positive ideal solution is selected.

**Table-4.1 Experimental data of various mechanical properties**

S.NO	Tensile Strength (MPa)	Hardness (Vicker's) HV
1	309.90	136.0
2	335	138.0
3	368.33	141.0
4	452	113.0
5	565	118.0
6	570.31	124.0
7	445	101.1
8	498.92	111.0
9	469	110.0

#### 4.1 Formation of decision matrix

First, of all performance defining criterion and alternatives of the problem are identified, and a decision matrix is created. In the decision, matrix alternatives are represented by M and criteria are represented by N

#### 4.2 The normalized decision matrix

The decision matrix is normalized to make all the values of the decision matrix comparable. The normalized matrix R= [ ] and the normalized value are calculated as below.

$$r_{ij} = \frac{a_{ij}}{\left[ \sum_{i=1}^M (a_{ij}^2) \right]^{1/2}}$$

$$D_{M \times N} = \begin{pmatrix} a_{11} & a_{12} & \dots & a_{1N} \\ a_{21} & a_{22} & \dots & a_{2N} \\ \vdots & \vdots & & \vdots \\ a_{M1} & a_{M2} & \dots & a_{MN} \end{pmatrix}$$

Where i= 1, 2, 3 ....M and j=1, 2, 3.....N

**Table-4.2 The normalized decision matrix**

S.No	Tensile Strength (MPa)	Hardness (Vicker's) HV
1	0.2272	0.3713
2	0.2456	0.3768
3	0.2701	0.3849
4	0.3314	0.3085
5	0.4143	0.3221
6	0.4182	0.3385
7	0.3263	0.2760
8	0.3658	0.3030
9	0.3439	0.3003

#### 4.3 Positive and negative ideal solution

The positive ideal solution and the negative ideal solution found out as follows.

Ideal positive solution is given by  $A^+ = (r^+_1, r^+_2, r^+_3, \dots, r^+_n)$

Where  $A^+ = (0.4182, 0.3849)$

Ideal negative solution is given by  $A^- = (r^-_1, r^-_2, r^-_3, \dots, r^-_n)$

Where  $A^- = (0.2272, 0.2760)$

#### 4.4 Calculating closeness index and ranking

It is crucial to find the closeness index. From the closeness index ranking of the various experiments are given. For finding the closeness index, the Euclidian distances are required. It is calculated by

$$D_i^+ = \sqrt{\sum_j^N (r_i^+ - r_{ij}^+)^2} \quad D_i^- = \sqrt{\sum_j^N (r_{ij}^- - r_i^-)^2}$$

Where for  $i=1, 2, 3, \dots, M$

Finally, the closeness index of the alternatives is calculated by the equation mentioned below.

Where

$$CI_i = \frac{D_i^-}{D_i^+ + D_i^-}$$

**Table-4.3 Calculation of closeness index and ranking**

S.No	Di+	Di-	CI	Ranking
1	0.1914	0.0953	0.3324	9
2	0.1727	0.1024	0.3722	8
3	0.1481	0.1170	0.4413	6
4	0.1156	0.1091	0.4855	5
5	0.0629	0.1926	0.7538	2
6	0.0464	0.2009	0.8123	1
7	0.1424	0.0991	0.4103	7
8	0.0972	0.1412	0.5922	3
9	0.1125	0.1192	0.5144	4

Finally, the ranking is given to the various results which have the highest CI values in descending order as shown in table 4.3.

#### 4.5 Result of technique for order preference by similarity to ideal solution (TOPSIS)

From the TOPSIS analysis, each sample is ranked. Table 4.23 shows the different welding parameters and the values of the ultimate tensile testing (UTS) and microhardness testing (Vicker's microhardness) for the nine specimens. The TOPSIS analysis gives the combined results of both the testing and finds out which process was best and is close to positive ideal solutions. The nine samples were ranked keeping the benefit criteria.

**Table-4.4 Result of Topsis analysis**

S.N O	Current (ampere)	Welding speed (mm/min )	Gas flow rate (l/min)	UTS ( MPa )	Micro-hardness (vicker's) HV	Topsis Ranking
1	80	3	10	309.90	136.0	9
2	80	3.5	12	335	138.0	8
3	80	4	14	368.33	141.0	6
4	100	3	12	452	113.0	5
5	100	3.5	14	565	118.0	2
6	100	4	10	570.31	124.0	1
7	120	3	14	445	101.1	7
8	120	3.5	10	498.92	111.0	3
9	120	4	12	469	110.0	4

## Conclusions

From the study, it can be concluded that

1. The optimum welding condition obtained by Taguchi method for tensile strength is current = 100 A, welding speed 4mm/sec and gas flow rate = 14L/min[17].
2. The optimum welding condition obtained by Taguchi method for hardness is current = 80A, welding speed 4mm/sec and gas flow rate = 12 L/min.
3. From the analysis of TOPSIS, each sample was ranked, and a welding current of 100 A, welding speed of 4 mm/min and gas flow rate of 10 L/minwas given rank one.

## References

- [1] M. Chellappan, K. Lingadurai, and P. Sathiya, "Characterization and Optimization of TIG welded supermartensitic stainless steel using TOPSIS," *Mater. Today Proc.*, vol. 4, no. 2, pp. 1662–1669, 2017.
- [2] G. Magudeeswaran, S. R. Nair, L. Sundar, and N. Harikannan, "Optimization of process parameters of the activated tungsten inert gas welding for aspect ratio of UNS S32205 duplex stainless steel welds," *Def. Technol.*, vol. 10, no. 3, pp. 251–260, 2014.
- [3] L. S. Patel, T. C. Patel, A. Professor, and M. E. Student, "Optimization Of Welding Parameters For TIG Welding Of 304 L Stainless Steel Using Taguchi Approach," *Int. J. Eng. Dev. Res.*, vol. 2, no. 1, pp. 2321–9939, 2014.
- [4] S. C. Juang and Y. S. Tarn, "Process parameter selection for optimizing the weld pool geometry in the tungsten inert gas welding of stainless steel," *J. Mater. Process. Technol.*, vol. 122, no. 1, pp. 33–37, 2002.
- [5] S. Srivastava and R. K. Garg, "Process parameter optimization of gas metal arc welding on IS:2062 mild steel using response surface methodology," *J. Manuf. Process.*, vol. 25, pp. 296–305, 2017.
- [6] P. Bharath, V. G. Sridhar, and M. Senthil Kumar, "Optimization of 316 stainless steel weld joint characteristics using taguchi technique," *Procedia Eng.*, vol. 97, pp. 881–891, 2014.
- [7] N. Kiaee and M. Aghaei-Khafri, "Optimization of gas tungsten arc welding process by response surface methodology," *Mater. Des.*, vol. 54, pp. 25–31, 2014.
- [8] A. Razal Rose, K. Manisekar, V. Balasubramanian, and S. Rajakumar, "Prediction and optimization of pulsed current tungsten inert gas welding parameters to attain maximum tensile strength in AZ61A magnesium alloy," *Mater. Des.*, vol. 37, pp. 334–348, 2012.
- [9] K. Nandagopal and C. Kailasanathan, "Analysis of mechanical properties and optimization of gas tungsten Arc welding (GTAW) parameters on dissimilar metal titanium (6Al-4V) and aluminium 7075 by Taguchi and ANOVA techniques," *J. Alloys Compd.*, vol. 682, pp. 503–516, 2016.

- [10] J. Pasupathy and V. Ravisankar, "PARAMETRIC OPTIMIZATION OF TIG WELDING PARAMETERS USING TAGUCHI METHOD FOR DISSIMILAR JOINT (Low carbon steel with AA1050)," vol. 4, no. 1, pp. 25–28, 2013.
- [11] S. Rajendra and R. R. Arakerimath, "Parameter Optimization of Tig Welding Using Austenitic Stainless Steel," vol. 2, no. 1, pp. 120– 124, 2015.
- [12] V. Anand Rao and R. Deivanathan, "Experimental investigation for welding aspects of stainless steel 310 for the process of TIG welding," *Procedia Eng.*, vol. 97, pp. 902–908, 2014.
- [13] N. Moslemi, N. Redzuan, N. Ahmad, and T. N. Hor, "Effect of current on characteristic for 316 stainless steel welded joint including microstructure and mechanical properties," *Procedia CIRP*, vol. 26, pp. 560–564, 2015.
- [14] R. Kumar, S. Chattopadhyaya, and S. Kumar, "Influence of Welding Current on Bead Shape, Mechanical and Structural Property of Tungsten Inert Gas Welded Stainless Steel Plate," *Mater. Today Proc.*, vol. 2, no. 4–5, pp. 3342–3349, 2015.
- [15] Q. Wang, D. L. Sun, Y. Na, Y. Zhou, X. L. Han, and J. Wang, "Effects of TIG welding parameters on morphology and mechanical properties of welded joint of Ni-base superalloy," *Procedia Eng.*, vol. 10, pp. 37–41, 2011.
- [16] S. P. Gadewar, P. Swaminadhan, M. G. Harkare, and S. H. Gawande, "Experimental Investigations of Weld Characteristics for a Single Pass Tig Welding With Ss304 Experimental Investigations of Weld Characteristics for a Single Pass Tig Welding With," no. September 2016, 2010.
- [17] V. Subravel, G. Padmanaban, and V. Balasubramanian, "Effect of welding speed on microstructural characteristics and tensile roperties of GTA welded AZ31B magnesium alloy," *Trans. Nonferrous Met. Soc. China (English Ed.)*, vol. 24, no. 9, pp. 2776– 2784, 2014.
- [18] T. Senthil Kumar, V. Balasubramanian, and M. Y. Sanavullah, "Influences of pulsed current tungsten inert gas welding parameters on the tensile properties of AA 6061 aluminium alloy," *Mater. Des.*, vol. 28, no. 7, pp. 2080–2092, 2007.
- [19] W. B. L. and R. F. K.C. Winco Yung, Ralph, "An investigation into welding parameters affecting the tensile properties oftitanium welds," *J. ofMaterials Process. Technol.*, vol. 63, no. 96, pp. 759– 764, 1997.
- [20] W. Chuaiphan and L. Srijaroenpramong, "Effect of welding speed on microstructures, mechanical properties and corrosion behavior of GTA-welded AISI 201 stainless steel sheets," *J. Mater. Process. Technol.*, vol. 214, no. 2, pp. 402–408, 2014.
- [21] C. Balaji, S. V. A. Kumar, S. A. Kumar, R. Sathish, and T. Nadu, "Evaluation of Mechanical Properties of SS 316 L Weldments Using Tungsten Inert Gas Welding," vol. 4, no. 5, pp. 2053–2057, 2012.
- [22] K. D. Ramkumar *et al.*, "Comparative studies on the weldability, microstructure and tensile properties of autogeneous TIG welded AISI 430 ferritic stainless steel with and without flux," *J. Manuf. Process.*, vol. 20, pp. 54–69, 2015.
- [23] H. Li, J. Zou, J. Yao, and H. Peng, "The effect of TIG welding techniques on microstructure, properties and porosity of the welded joint of 2219 aluminum alloy," *J. Alloys Compd.*, vol. 727, pp. 531– 539, 2017.
- [24] L. Srinivasan, S. J. Jakka, and P. Sathiya, "Microstructure and mechanical properties of Gas tungsten arc welded High Strength Low Alloy (15CDV6) steel joints," *Mater. Today Proc.*, vol. 4, no. 8, pp. 8874– 8882, 2017.
- [25] S. Kumar and A. S. Shahi, "Effect of heat input on the microstructure and mechanical properties of gas tungsten arc weldedAISI 304 stainless steel joints," *Mater. Des.*, vol. 32, no. 6, pp. 3617–3623, 2011.
- [26] A. Kumar *et al.*, "Experimental Process of Tungsten Inert Gas Welding of a Stainless Steel Plate," *Mater. Today Proc.*, vol. 2, no. 4–5, pp. 3260–3267, 2015.
- [27] Q. Zhu, Y. C. Lei, X. Z. Chen, W. J. Ren, X. Ju, and Y. M. Ye, "Microstructure and mechanical properties in TIG welding of CLAM steel," *Fusion Eng. Des.*, vol. 86, no. 4–5, pp. 407–411, 2011.
- [28] T. Wen, S. Y. Liu, S. Chen, L. T. Liu, and C. Yang, "Influence of high frequency vibration on microstructure and mechanical properties of TIG welding joints of AZ31 magnesium alloy," *Trans. Nonferrous Met. Soc. China (English Ed.)*, vol. 25, no. 2, pp. 397– 404, 2015.
- [29] H. Lin, L. Ying, L. Jun, and L. Binghong, "Microstructure and Mechanical Properties for TIG Welding Joint of High Boron Fe-Ti- B Alloy," *Rare Met. Mater. Eng.*, vol. 43, no. 2, pp. 283–286, 2014.



**ANAND**  
INTERNATIONAL COLLEGE  
OF ENGINEERING



# Recent Developments in Engineering & Technology-1

---

Edited by Praveen Agarwal. & Bhavana Mathur.

ISBN 978-81-953996-3-5



**ANAND**  
INTERNATIONAL COLLEGE  
OF ENGINEERING

Near Kanota, Agra Road, Jaipur-303012, Rajasthan, India

Tel.: 9928755552, 53 | [www.anandice.ac.in](http://www.anandice.ac.in)